

Neural circuit mechanisms of early life stress induced olfactory perceptual deficits in mice

A thesis

submitted in partial fulfillment of the requirements

for the degree of
Doctor of Philosophy

by

Meenakshi Pardasani
20152004



INDIAN INSTITUTE OF SCIENCE, EDUCATION AND RESEARCH,
PUNE
2022

Dedicated to...

My late Grandparents

Mr. AD Hirani and Mrs. Meena Hirani

*whose unconditional love, support and strength would stay forever with
me.*

Declaration

I declare that this written submission represents my ideas in my own words. Wherever contributions of others are involved, effort has been made to indicate it clearly, with due reference to the literature and original sources. I also declare that I have followed principles of academic honesty and integrity and have not misinterpreted, fabricated, or falsified any thought, data, fact or source in my submission. I understand that the failure to comply with the above will result in disciplinary action by the Institute, and can also evoke penal action from the sources that have not been properly cited or from whom proper permission has not been taken when needed.

Date:14-04-2022



Meenakshi Pardasani

20152004

Certificate

This is to certify that the work incorporated in the thesis entitled '**Neural circuit mechanisms of early life stress induced olfactory perceptual deficits in mice**', submitted by **Meenakshi Pardasani** was carried out by the candidate, under my supervision. This work presented here or any part of it has not been included in any other thesis submitted previously for the award of any degree or diploma from any other University or Institute.



Dr. Nixon M. Abraham

Date: 14-04-2022

Acknowledgements

I would like to thank my esteemed supervisor and mentor, Dr Nixon M. Abraham for providing an intellectually stimulating laboratory environment, invaluable insights and tutelage during the course of my Master's and PhD term at IISER Pune. I have been inspired by his scientific temper & the principles that he follows. His spirit of aiming high motivates me a lot. I am also indebted to Prof. Dr Sanjeev Galande and Dr Aurnab Ghose, my research advisory committee members for their valuable inputs during my yearly presentations. I extend my gratitude to Prof. N.K. Subedhar, Dr. Raghav Rajan, Dr. Collins Assisi and Dr. Suhita Nadkarni for their guidance, inputs and fruitful scientific interactions during the Neuroscience Interest Group and No-garland neuroscience meetings.

Further, the ever-friendly and supportive members of Laboratory of Neural circuits and behavior provided an enriching environment poised for growth! I thank Sarang, Priya, Shruti, Ananthi, Karishma, Susobhan, Rajdeep, Sanyukta, Madhupriya, Anantu and Arpan to keep the laboratory environment a fun place to work in. I found my best buddies, Sarang, Sasank and Anindya in this lab. Their support and critical evaluation on my work meant a lot. I dearly miss Sasank who was my batchmate too, and his pep talks had a zealous effect on me. Whenever it would come to a point of troubleshooting the instruments or asking for statistics related help, Anindya & Sarang were always ready to help. Three of us made a great tripartite synapse! ☺ I am also grateful to Shruti and Priya who have been great friends apart from being extremely helpful lab mates. I also take the opportunity to thank Ananthi for teaching me the basics of electrophysiology. Discussing science and life outside science with the Masters students of the laboratory, especially, with Meher, Eleanor, Suhel, Kaushik, Atharva and Felix, was a lot of fun. I learnt a lot while mentoring the BS and MS students as well as interns including Urvashi, Nidhi, Meher, Archana, Eleanor, Maitreyee, Madhupriya, Nihali, Sneha, Chinmay, Shreshth, Omika, Vibha and Saanchi, during my course of PhD in this laboratory. They were a great bunch of quick learners and I wish them best for their future endeavours. I also thank Divya, Shikha and Dhriti who mentored me during my Masters' laboratory rotations in other neuroscience labs at IISER Pune. My tryst with neuroscience would not have been possible if I would not have gotten the chance to learn and interact with Dr. Vatsala Thirumalai and her lab members, especially, Lena, Sriram and Abhishek who introduced me to 'life in a neuroscience lab' when I was a summer intern in their laboratory at NCBS, Bangalore. I cannot thank Lena enough for patiently teaching me

techniques as well as help me improve my scientific writing skills. Outside of the laboratory, I had a great time with my integrated-PhD batchmates. Special thanks to Sushmitha and Aparna with whom I did not just attend classes, but also, discussed life in general, played badminton, had multiple coffee breaks and what not. I am very grateful to find Sonashree, my tennis partner and a best friend. She has been my constant motivator, whether it was to do with science or maintaining a healthy, sporty life-style. Her zealous spirit and child-like wonderment inspires me! I enjoyed working and learnt a lot while working on a collaborative project with Mehak and Sonashree. I am grateful to Surya who taught me bit of electronics and helped me to learn coding which are the much needed skills to survive in the field of neuroscience.

I thank IISER Pune for providing fellowship during the course of my Integrated PhD tenure. I thank the biology department at IISER Pune for the remarkable facilities including the microscopy as well as competent personnel to provide a harmonious research environment. I take this opportunity to thank Dr. Suraj, Dr. Mahesh, Dr. Sachin, Dr. Krishnaveni, Vinay, Anubha, Pradnya, Arun and others of the National facility of gene function in health and disease (NFGFHD) at IISER Pune for seamlessly maintaining the animal facility.

Finally, none of what I achieved till now could have been possible without the utmost support and blessings of my parents. Their guidance in treading through life and also putting their faith in me and my decisions has allowed me to maintain a seamless research life.

-Meenakshi

Table of Contents

List of figures	1-3
List of tables	3
Synopsis	4
Chapter 1: <u>Early life environment alterations affect olfactory learning and memory in mice</u>	
1.1. Abstract	7
1.2. Introduction	8
1.2.1. Early life Stress	8
1.2.1.1. Diverse effects of early life stress on brain and physiology	8
1.2.1.2. Models of early life stress in rodents and their effects	9
1.2.1.3. Early life events induced alterations in sensory perception	12
1.2.2. Olfactory bulb	15
1.2.2.1. Adult Neurogenesis in Sub-ventricular zone/Olfactory bulb	17
1.2.2.2. OB as a center of extensive modulation by intrinsic and extrinsic factors	18
1.2.2.3. Olfactory cortical regions	20
1.2.3. Environment enrichment	21
1.2.3.1. Therapeutic effects of EE in animal models	21
1.3. Materials and methods	23
1.3.1. Subjects	23
1.3.2. Early life stress through early weaning	23
1.3.3. Tests for assessing anxiety and depression	24
1.3.4. Olfactory detection, discrimination learning and memory behaviors	25
1.3.4.1. Go/No-go olfactory learning paradigm in freely moving condition	25
1.3.4.2. Olfactometer (freely moving apparatus)	25
1.3.4.3. Task habituation training (pre-training)	27
1.3.4.4. Odors	28
1.3.4.5. Olfactory discrimination learning training paradigm	29
1.3.4.6. Assessment of olfactory learning	30
1.3.4.7. Assessment of olfactory memory	30
1.3.5. Buried food pellet test	31
1.3.6. Environment Enrichment (EE) paradigm	32
1.3.7. Transcriptomic analysis of control and early weaned mice	33

1.4. Results	35
1.4.1. Behavioral characterization of early weaned mice on the anxiety tests	35
1.4.2. Olfactory food detection ability is not perturbed by early life stress	40
1.4.3. Early weaning causes changes in the learning ability but not the threshold of discriminating the odors	41
1.4.4. Early life stress induces olfactory learning and memory impairments in mice	43
1.4.5. Environment enrichment rescues the anxiety responses of early weaned mice	49
1.4.6. Environmental enriched housing ameliorates olfactory deficits in early weaned mice	51
1.5. Discussion	57
1.5.1. Early life stress can induce varied strain-specific responses	57
1.5.2. Early life stress alters sensory-cognitive perception	59
1.5.3. Environment enrichment is effective in ameliorating sensory deficits	61
1.6. Future directions	64
1.6.1. Differential gene expression analysis in control, early weaned and enriched mice using Transcriptomics	64
1.6.2. Gender-dependent effects of ELS on olfactory behavior of mice	65

Chapter 2: Involvement of Somatostatin releasing interneurons of Olfactory bulb in mediating ELS induced learning deficits

2.1. Abstract	66
2.2. Introduction	67
2.2.1. Neuro-modulatory changes by early life stress	67
2.2.1.1. Impact of early life environmental changes on neuropeptides and neurotransmitters	67
2.2.1.2. Somatostatinergic pathways are modulated by stress and enrichment	69
2.2.2. Optogenetics: A tool to study neural circuitry dynamics and functioning	71
2.3. Materials and methods	74
2.3.1. Subjects	74
2.3.2. Genotype and Phenotype details	75
2.3.3. <i>Ex vivo</i> Olfactory bulb slice preparation to quantify neuropeptide release	77
2.3.3.1. Fabrication of multi-LED assembly	78
2.3.3.2. Photo-stimulation paradigm and ELISA	78
2.3.4. Surgical procedures for optogenetic modulation	79

2.3.4.1. Headpost implantation for carrying out olfactory behavior under mouse head restrained (MHR) condition	79
2.3.4.2. Cranial window and LED implantation	80
2.3.5. Olfactory learning and memory behaviors under MHR conditions	81
2.3.5.1. Olfactometer	81
2.3.5.2. Olfactory learning and memory paradigm	82
2.3.5.3. Odors	83
2.3.5.4. Data analysis	83
2.3.6. Morphological quantification of Somatostatin-positive interneurons	83
2.3.7. Micro-endoscopic calcium imaging	84
2.4. Results	86
2.4.1. Ex-vivo optogenetic characterization of somatostatin peptide release by OB neurons	86
2.4.2. Olfactory discrimination learning of simple odor pair under MHR condition	87
2.4.3. Optogenetic activation of OB SST-interneurons improved perceptual learning of EW mice	89
2.4.4. Opposing behavioral manifestations upon optogenetic inhibition of OB SST-interneurons	91
2.4.5. Olfactory memory remained unaffected by the optogenetic manipulation of bulbar circuitry	95
2.5. Discussion	98
2.5.1. Optogenetic activation of inter-neuron population of Olfactory bulb	98
2.5.2. Neuropeptides are released upon optogenetic modulation	99
2.6. Future directions	100
2.6.1. Morphological quantification of SST-releasing inhibitory interneurons of OB	100
2.6.2. Imaging of SST-interneurons and recording of Olfactory bulb projection neurons in early weaned and control mice	101
Chapter 3: <u>Involvement of multiple sensory systems in learning of pheromone locations</u>	
3.1. Abstract	104
3.2. Introduction	105
3.2.1. Social odors in rodent world	105
3.2.1.1. Scent-marking in rodents	105
3.2.1.2. Pheromone guided information processing	106

3.2.1.3. Modulation of social communication strategies by internal and external factors	108
3.2.2. Whisking the odors	110
3.2.2.1. Multisensory strategies for learning and memory	111
3.2.3. Immediate early genes as a tool to assess brain region specific activation profiles	113
3.3. Materials and methods	117
3.3.1. Subjects	117
3.3.2. Multimodal Pheromonal Learning apparatus	119
3.3.3. Multimodal Pheromonal Learning paradigm	119
3.3.4. Behavior quantification	121
3.3.5. Sniffing behavior towards pheromones	121
3.3.6. Arc protein immunohistochemistry	122
3.3.7. Adult neurogenesis quantification	123
3.3.8. Go/No-go odor discrimination	124
3.3.8.1. Odors	124
3.3.8.2. Apparatus	125
3.3.9. Vaginal smear collection & visualization	125
3.3.10. Statistical analyses	125
3.4. Results	126
3.4.1. Paradigm of multimodal learning results in memory for pheromone location in female mice	126
3.4.2. Olfactory and whisker systems are involved in the formation of multimodal pheromonal location memory	131
3.4.3. Sampling strategies of mice are similar under whisker intact and deprived conditions	134
3.4.4. Arc activation in olfactory bulb, somatosensory cortex and hippocampus is enhanced in whisker intact mice displaying multimodal memory	135
3.4.5. Naïve female mice and female mice trained for same sex pheromones display significantly lower Arc activation than the ones trained for opposite sex pheromones	139
3.4.6. Female mice are unable to recall multimodal memory on Day 30 th post training	141

3.4.7. Early weaned female mice exhibit poor multimodal pheromonal memory but their sensory detection is intact	143
3.5. Discussion	146
3.5.1. Olfactory and whisker systems facilitate memory of the socio-sexual encounters in murine world	146
3.5.2. Multi-sensory associations can be differently weighted by different cues	148
3.5.3. Immediate early gene Arc reliably encodes activation of multiple sensory systems during recall of pheromonal location memory	149
3.5.4. Social cognitive behavior is compromised in early weaned female mice	150
3.6. Future directions	151
3.6.1. Multimodal pheromonal learning and adult neurogenesis	151
3.6.2. Estrous cyclicity does not influence odor discrimination learning and memory in female mice	153
Publications	155
Appendix	156
References	157

List of Figures

Figure 1-1: Influence of different factors on the effect of ELS in an organism	10
Figure 1-2: Main olfactory system of mouse and the underlying neural circuits	15
Figure 1-3: Major players of pre-cortical olfactory processing are under massive neuromodulation	18
Figure 1-4: Early weaning in mice	23
Figure 1-5: Parameters utilized in battery of tests conducted to assess anxiety and depression	24
Figure 1-6: Go/No-go olfactory paradigm using a custom-made olfactometer	27
Figure 1-7: Licking criterion and evolution of licking probability with training in the Go/No-go olfactory paradigm	29
Figure 1-8: Buried food pellet test to assess olfactory detection of appetitive stimulus	31
Figure 1-9: A novel Environmental Enrichment paradigm designed in our laboratory	32
Figure 1-10: Anxiety-like responses of early weaned mice on open field test	35
Figure 1-11: Anxiety-like responses of early weaned mice on elevated plus maze test	36
Figure 1-12: Anxiety-like responses were not observed in open field test in aged early weaned mice	38
Figure 1-13: Early weaned mice do not exhibit behavioral despair in forced swim test	39
Figure 1-14: Food olfactory detection ability is normal in early weaned mice	40
Figure 1-15: Odor discrimination threshold is not perturbed by early life stress	42
Figure 1-16: Assessment of olfactory learning capabilities	44
Figure 1-17: Early life stress induces poor olfactory learning and memory in mice	46
Figure 1-18: Effect of early life stress persists in the aged mice	48
Figure 1-19: Odor discrimination learning is not dependent on other sensory cues originating from the olfactometer	49
Figure 1-20: Environmental enriched housing rescues anxiety-like responses of early weaned mice	50
Figure 1-21: Environmental enrichment ameliorates olfactory learning deficits in early weaned mice	52
Figure 1-22: Environment enrichment improves olfactory discrimination learning abilities	54
Figure 1-23: Environment enrichment does not improve olfactory memory	56
Figure 1-24: Differential gene expression in OB of early weaned mice	64

Figure 2-1: Light-activated channels for optogenetic control of cells	72
Figure 2-2: Cre-Lox strategy for obtaining desired transgenic mice	74
Figure 2-3: Specific expression of transgenes in SST-positive neurons of Olfactory Bulb	76
Figure 2-4: Surgical procedure for optogenetic modification of OB micro-circuitry	81
Figure 2-5: Olfactory training paradigm under MHR conditions	82
Figure 2-6: Somatostatin peptidergic release upon optogenetic modulation of OB interneurons	87
Figure 2-7: Slower olfactory discrimination learning in EW mice under MHR condition	88
Figure 2-8: Optogenetic activation of SST-releasing bulbar interneurons leads to faster olfactory discrimination learning in EW mice	90
Figure 2-9: Optogenetic inhibition of Somatostatinergic pathway of OB circuitry results in behavioral impairments	91
Figure 2-10: Optogenetic inhibition of bulbar SST-releasing interneurons in NW mice mimics ELS induced learning deficit	93
Figure 2-11: Learning on a complex odor without optogenetic manipulation of bulbar circuitry	94
Figure 2-12: Olfactory memory remains poor in EW mice irrespective of any optogenetic modulations	96
Figure 2-13: Morphological analysis SST releasing interneurons population of OB	100
Figure 2-14: Response of SST releasing GABAergic interneurons under anesthetized and awake conditions	102
Figure 3-1: Processing of pheromones by olfactory subsystems	107
Figure 3-2: Simultaneously occurring multi-sensory cues in natural surroundings	112
Figure 3-3: Activation of Immediate Early Genes (IEGs)	114
Figure 3-4: Multimodal Pheromonal Learning paradigm and apparatus	120
Figure 3-5: Decayed preference towards opposite sex pheromones location when exposed to a choice of urine and water	128
Figure 3-6: Multimodal learning causes formation of pheromone location memory in female mice	130
Figure 3-7: Whisker deprivation during training period hampers multimodal pheromonal location memory	132
Figure 3-8: Olfactory and whisker systems govern the formation of pheromonal location memory	133
Figure 3-9: Sniffing frequency remains unchanged in whisker deprived condition	135

Figure 3-10: Immediate early gene product activation as a correlate of pheromonal location memory in the Multimodal pheromonal learning paradigm	136
Figure 3-11: Arc activation changes from training to memory phase of multimodal pheromonal learning paradigm	138
Figure 3-12: Lowered Arc expression in naïve female mice	140
Figure 3-13: Lowered Arc expression in FBU trained female mice on Memory Day 15 th	141
Figure 3-14: Absence of multimodal memory on Day 30 th post training phase in whisker intact female mice	143
Figure 3-15: EW female mice show poor multimodal memory and lower Arc immunoreactivity	145
Figure 3-16: Effect of the multimodal training on the OB neurogenesis of female mice	152
Figure 3-17: Estrous cycle induction and synchronization does not alter non-pheromonal volatiles discrimination learning and memory performance	154

List of Tables

Table 1-1: Relevant information about the odors used in the study	28
Table 1-2: Types of enrichment & the required items provided for housing mice	33
Table 2-1: Chemicals used in ACSF preparation for maintaining acute OB slices	77
Table 3-1: Relevant information about the odors used in the study	124

Synopsis

Animals utilize their sensory systems to receive inputs and cues from their environment. They possess neural circuits that control sensation, information processing, decision-making which leads to generation of accurate responses towards specific sensory stimuli. The circuitry can undergo changes, either adaptive or maladaptive, depending on the affective state of an animal¹. Human as well as rodent studies that have focussed on stress mediated neural impairments indicated the associations between the sensory systems and the limbic system. Owing to their neuroanatomical closeness and the top-down neuromodulation that they receive, sensory brain areas are vulnerable to external stressors². A nuanced understanding of how stressors modulate decision-making processes of the brain requires extensive study using model organisms. Modifying the circuits while an animal is behaving, such as using optogenetics, offers an effective tool for investigating the alterations in the circuits that govern complex behavioral responses³.

We aimed to study the effect of Early Life Stress (ELS) on the olfactory perception using mouse as our model system. Adversity in early life can be detrimental, which depends on the nature, severity and the duration of its experience. We carried out Early Weaning (EW) at Postnatal day (P) 14 of the mouse pups, a well-known, established paradigm to induce ELS⁴. Exposure to novel stressors during the stress hyper-responsive period of their postnatal life (i.e P12 to P 14) leads to hyper-active Hypothalamic Pituitary Adrenal (HPA) axis and release of stress hormone⁵. Olfactory Bulb (OB) receives massive neuro-modulatory projections from different areas of the brain which can directly or indirectly affect decision-making processes⁶⁻⁹. This region in the pre-cortical pathway of olfactory processing poised to be modulated by the affective states of the animal allowed us to design paradigms that can probe for OB-mediated behavioral phenotypes upon ELS induction. Thus, we took a behavior-to-circuits approach to probe this. Upon carrying out Go/No-go olfactory discrimination learning paradigm for a wide range of complexities across varying physio-chemical properties of odors¹⁰, we found that the EW mice were poor olfactory learners. Further, we also found out impairment in their olfactory memory. To elucidate if their odor discrimination thresholds were affected, we carried out discrimination learning at different concentrations, starting from the least dilution level to 1% (v/v). We observed that EW mice started to discriminate at the same dilution level as the control mice, however, they learnt the task at a slower pace. This suggested that their concentration threshold of discriminating the

odors remained comparable to normally weaned mice. The latency of finding buried food pellets under food-restricted conditions showed that EW mice could find the pellet as quickly as the control mice. This indicated that their food detection capabilities were indeed normal. When tested on standard battery of tests of anxiety, i.e, Open Field test and Elevated plus maze test, EW mice exhibited anxious responses, during their young adulthood.

In an attempt to rescue olfactory deficits in EW mice, we implemented the approach of Environment Enrichment (EE) (This part of work was carried out along with Eleanor McGowan, MSc student). EE has been shown to induce ameliorating effects on mouse models of various neurodegenerative, depressive disorders and accelerates recovery from acute conditions¹¹. It also promotes neurogenesis, synaptic functioning and circuit maturation which underlies the EE mediated positive behavioral outcomes^{12,13}. Improvement in cognitive flexibility, temporal sensory rule learning, and spatial learning are often observed in rodents reared in EE conditions¹⁴. Our multimodal enrichment cage in which the ELS induced mice were raised, allowed for increased social contact, a stimulating environment consisting of running wheels, saucers, tunnels, nesting materials, textured surfaces, mazes and natural odors. We found out the sensory learning deficits along with the anxiety-like responses were ameliorated in the EW mice reared in EE cage. Overall, we concluded, that the olfactory learning and memory impairments induced by ELS can be rescued by providing an enriched environment.

Thus far, we found out that ELS led to olfactory discrimination learning and memory impairments in mice. To unravel the neural underpinnings of ELS dependent olfactory learning changes, we employed bi-directional optogenetic modulation of a specific sub-population of GABAergic interneurons releasing somatostatin (SST) neuropeptide of OB. Somatostatin neuropeptide has been shown to have anxiolytic effects¹⁵. Controlled activity of SST neurons in other brain regions are also shown to play an important role in learning and working memory^{16,17}. Their functionality in pre-cortical brain regions remains unknown. In OB, these neurons are mainly present in the external plexiform layer (EPL) and are sparsely located in the granule cell layer (GCL)¹⁸. Finally, as the SST levels are known to be affected by conditions that result in cognitive impairments, we began to study their role in ELS mediated olfactory learning impairments¹⁹. Using *ex-vivo* olfactory bulb slices stimulation, we confirmed the release of the neuropeptide on carrying out optogenetic activation of channelrhodopsin-2 (ChR2). Upon photoactivating these interneurons *in vivo*, EW mice

exhibited improved complex odor discrimination learning. Photo-inhibiting these neurons using Archaeorhodopsin (Arch) in control mice resulted in the learning deficit similar to what was observed in ELS mice. This optogenetic modulation, however, did not lead to improvement in the olfactory memory suggesting the neural substrates of olfactory memory which are affected by ELS are beyond this OB micro-circuitry that we probed. We are currently testing the molecular and physiological correlates of the behavioral changes that we observed upon modulating this circuitry using optogenetics. To this end, we are carrying out calcium imaging using micro-endoscopy in anesthetized and behaving mice as well as the opto-electrophysiological recordings of the projection neurons of the OB upon optically modulating the bulbar SST releasing GABAergic neurons.

Finally, we employed a yet another custom-built paradigm to probe for olfactory mediated social learning and memory behavior in EW mice. Social communication and cognition are important for carrying out mate choice. Animals employ both sensory and cognitive skills to find the scent marks, learn its location and return back to it for a successful mating experience^{20,21}. We created a novel ‘Multimodal Pheromonal Learning’ (MPL) paradigm that permitted for depicting the role of olfactory and whisker subsystems, together, in governing the memory of pheromonal location in female mice²². We found out that the OB, somatosensory barrel cortical layers and the Dentate gyrus regions were activated when the whisker-intact animal displayed multimodal memory for the opposite sex pheromones. This was shown by probing for activation of an immediate early gene called Activity regulated cytoskeleton (Arc) and labelling its product using immunohistochemistry. Arc was indeed decreased in mice that were deprived of whiskers during their training on the MPL paradigm. These mice did not show pheromonal memory suggesting the concerted role of both olfactory and whisker subsystems in mediating the memory. We employed this method in EW female mice as well. They could not establish the associations between the two sensory systems, i.e, olfaction and whisking as displayed by poor pheromonal memory and a concomitant decrease in Arc immunoreactivity in the corresponding brain regions. As male pheromones found in urine activated the Main OB circuitry, we were also interested in assessing the role of activated circuit in mediating non-pheromonal volatiles discrimination. We did not find any alterations in the olfactory learning and memory behaviors of the Whitten effect induced female mice. To investigate gender-dependent effects of ELS, we are currently assessing non-pheromonal discrimination learning and memory in early weaned female mice.

Chapter 1

Early life environment alterations affect olfactory learning and memory in mice

1.1 Abstract

Different environmental exposures during early postnatal period can have long-lasting impact on the physiology of an animal. Adversity in early life can be detrimental, which depends on the nature, severity and the duration of its experience. It is one of the leading causes of development of affective disorders in humans. Such maladaptive outcomes are a result of changes in the gene expression patterns, remodeling of the brain circuits and the consequent dysfunctions in behavior. Apart from the emotional disturbances that it can cause, early life stress can also lead to alterations in sensory perception which can negatively affect daily activities of an animal. For investigating the link between the altered neural circuits and the sensory behavioral deficits, well-mapped mouse olfactory system offered an ideal experimental model. Primary research interest involved understanding the effect of early life stress in modulating sensory information processing by Olfactory bulb circuitry. To investigate this, we followed a behavior-to-circuits approach. Induction of early life stress by early weaning of pups at postnatal day 14 led to alterations in their olfactory performance. Slower olfactory learning on a Go/No-go odor discrimination paradigm and impaired olfactory memory with a concomitant increase in the anxiety-like responses were found. To evaluate if the impairments were reversible in nature, we improved the conditions of early life environment of early weaned mice by implementing the approach of environment enrichment housing. Reversal of olfactory learning deficits but not of memory were observed in mice reared in an enriched setting. These mice also had lowered anxiety-like responses. To gain an integrated understanding of the environment induced transformations, an ongoing investigation of mapping transcriptomic changes to circuit-level dysfunctions is underway.

1.2 Introduction

1.2.1 Early life stress

Study of Early life stress (ELS) provides a window into investigating how a sequelae of negative events can lead to adaptive and maladaptive changes in the organism causing either development of resilience or disturbances in emotional and cognitive abilities. Examples of states and conditions that lead to ELS in humans include exposure to impoverished environment, parental neglect, abuse from care-givers, institutionalization, poverty etc^{23–25}. Such conditions during the early period of life can bring about either transient or sustained changes. To probe the circuitries involved and assess the effect of therapeutic interventions, robust animal models are utilized²⁶. Mammalian studies for determining neural correlates of behavioral dysfunctions range from rodents to non-human primates models^{27–29}. Diverse effects on brain and body such as alteration of Hypothalamic-Pituitary-Adrenal (HPA) axis, morphological and functional changes in stress sensitive areas of brain etc. are explained below^{30,31}.

1.2.1.1 *Diverse effects of early life stress on brain and physiology*

Occurrence of psycho-pathological disorders in human patients have often been retrospectively linked with facing adversities during childhood³². Longitudinal studies in humans have found out a positive correlation between the Adverse Childhood Experiences (ACEs) with severity of depression in adulthood, time to remission as well as the chances of depressive recurrences³³. Strong associations between prevalence of anxiety disorders, susceptibility to disease development and illicit substance abuse with ACEs have been found in meta-analysis studies³⁴. Punitive parenting, a form of childhood stress has shown to cause increased negative deflection of event related potentials (ERP) using electroencephalogram, in regions corresponding to error-related activity in a Go/No-go task performed in 6 year old children. These alterations were found to be contemporaneous with increased anxiety levels in children³⁵. Indeed, ELS is a strong contributor to ‘allostatic load’ of an individual, which is the inability of the bodily systems to cope up with the stressful experiences^{36–38}.

Volumetric and morphometric transformations in medial Pre-Frontal Cortex (mPFC), Anterior Cingulate Cortex (ACC) with reduced functional connectivity between ventral mPFC and ACC have been observed in ELA suffered patients³⁹. Heightened amygdalar

activity is seen in patients with history of childhood maltreatment⁴⁰. Regulatory changes in the brain-body signaling are also being investigated for. One of the studies showed lowered interoceptive accuracy after application of acute stressor in patients with Early Life Adversity (ELA)⁴¹. Sociality during adolescence is also shown to be negatively affected in students who suffered ELS and this was reflected in their overall general health status⁴². Indeed, induction of psychosocial stressors during adulthood induce pronounced inflammatory responses in childhood maltreated individuals. In general, the plasma inflammatory markers such as C-reactive protein and fibrinogen are also elevated during their adulthood⁴³. To uncover such system-wide changes ranging from neurobiological to immunological insults as a result of early life stress⁴⁴, model systems are being thoroughly studied.

Peer-rearing (PR), an established model of ELS in rhesus monkeys which deregulates the HPA axis and the serotonin system, has shown to cause enlargement of stress-sensitive brain regions (dorsal ACC and mPFC)^{45,46}. On the other hand, brief intermittent separation from mother, a milder type of ELS, can cause increased measures of white matter in ventromedial prefrontal area assessed using fractional anisotropy. This is indicative of increased myelination of connections emerging from prefrontal area, a sign of improved signal conduction. These monkeys also had improved cognitive performance on the novel object recognition task as compared to mother-reared ones⁴⁷. Such studies indicate how different models of inducing ELA can have differential behavioral and neural morphometric outcomes. To further probe the circuit-level functional changes, rodent models are popularly studied.

1.2.1.2 *Models of early life stress in rodents and their effects*

Variations in maternal care bring about neuro-endocrine changes in pups. The early days of life are crucial in terms of maternal investment such as tactile stimulation in the form of licking, temperature regulation, olfactory cues in addition to providing nutritional enrichment⁴⁸. Programming of HPA axis by the mother keeps the response of pups to threatening conditions under control which can have an adaptive value during adulthood. In fact, mother acts as a 'social buffer' keeping the stress hormones levels at basal level⁴⁹⁻⁵¹.

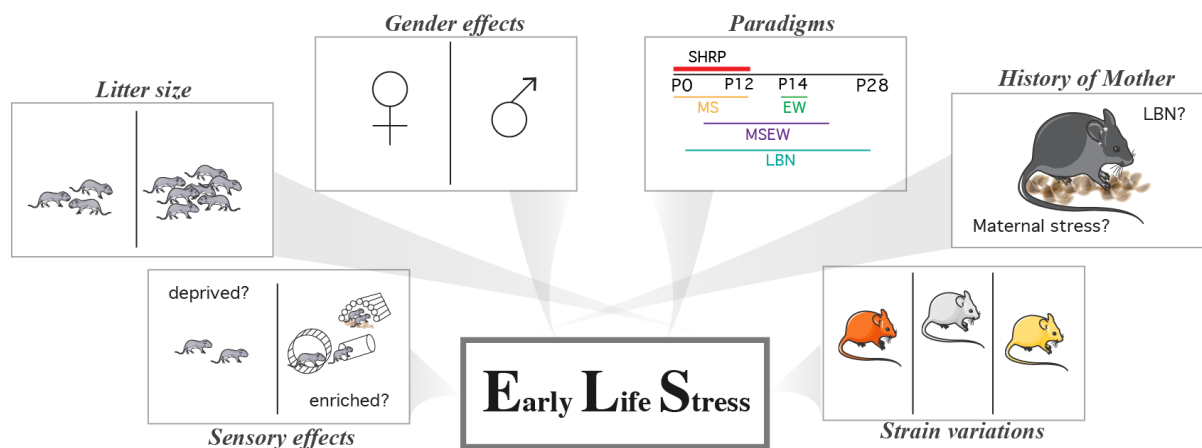


Figure 1-1: Influence of different factors on the effect of ELS in an organism

Illustration summarizes various factors that can influence the extent of ELS mediated deficits in an organism. Such factors include the amount of sensory information that pups receive during their early postnatal life (in addition to being maternally deprived), the number of pups a litter can carry which influences the maternal care & nutritional investment, variations arising as a result of gender, the varied paradigms that are carried out, history of the mother (transgenerational effects of ELS/ maternal stress due to pups handling etc.) and the variations as a result of the strain-specific differences (differential genetic background) SHRP: Stress hypo-responsive period, MS: Maternal Separation, EW: Early Weaning, MSEW: Maternal Separation through Early Weaning, LBN: Low-bedding and nesting (adapted from Murthy and Gould, 2018)²⁸.

Early post-natal life in mice is till Postnatal day (P)21/24, when they are weaned. The stress system remains at basal level during P1 to P12 in mice, referred to as Stress hypo-responsive period (SHRP)⁵². Existence of such a period when corticosterone remains at basal level and does not increase through a mild stressor was first shown in rats, which ranges from P2 to P14⁵. A marked increase in circulating corticosterone and Adrenal corticotrophic hormone (ACTH) is observed at P12 in mice and becomes almost two-fold at P14. Glucocorticoid receptor (GR) in hippocampus and Ucn3 (an activator of corticotrophic releasing hormone receptor 2) in hypothalamus reach their highest expression at P12⁵. In fact, exposure during this crucial time-window to a novel stress causes HPA axis hyperactivity leading to increased corticosterone levels⁵³. Various different paradigms of ELS, including separation of dam and/or reduction in the provision of nesting material are prevalent in the field which are listed below. These paradigms, owing to their differences in the duration and type of separation can cause varied pathophysiological consequences which can also be dependent on the sex of the

animal²⁸. Most of the studies are thus carried out in male rats and mice as they seem to display pronounced negative effects of ELA.

- Prolonged Maternal separation- 60-180 minutes from P1 or P2-P14^{54,55}.
- Maternal deprivation- Depriving pups for 24 hours from P9 onwards⁵⁶.
- Early weaning- Separating pups from dam at P14 in contrast to normal weaning at P21-24⁴.
- Maternal separation with Early weaning- Separation for 180 minutes from P2-P17 followed by early weaning at P17⁵⁷.
- Limited bedding and nesting (LBN) to dam and pups between P2-P9⁵⁸.

One study depicted the partial role of forebrain corticotropin releasing hormone receptor-1 inactivation in attenuating the anxiogenic effects of reducing the quality of maternal care and extent of peer-interaction during the early postnatal days, i.e from P2-P9 by using the LBN paradigm⁵⁹. However, other neuroendocrine systems as well as the regional variation in mediating the anxiogenic effects are to be considered to have a holistic understanding. Another study that carried out Maternal Separation (MS) of rat pups for 180 minutes from P2 to P14 found out transcriptional alterations of genes expressed in mPFC. Repressor element-1 silencing transcription factor 4 was found to be over-expressed in mPFC which partially led to vulnerability to acute stressors. This TF, in turn, regulates the transcription of 'repressor element-1' sites containing genes such as *bdnf*, *crh* and *5ht1a*⁶⁰. Blocking the Serotonin type-2 receptor in the MS rats prevents the pathophysiological sequelae that follows after ELS. It indeed prevents triggering dysregulated transcriptomic changes that occur in the mPFC of adult MS rats⁶¹. Epigenetic basis of ELS induced neuroendocrine changes are also being studied. Proopiomelanocortin (*Pomc*) gene, a pro-hormone of ACTH mRNA expression is upregulated as a result of decreased DNA methylation, after some delay of separating from the dam between P1-10 in mice⁶². Neuropeptides also play a modulatory role in mediating the pathophysiology of ELS. In case of MS rats, Neuropeptide Y and Corticotropin releasing hormone-like immunoreactivity were increased in hypothalamus while it was found to be decreased in the hippocampus and striatum⁶³.

To uncover the molecular underpinnings of stress induced learning and memory behavioral deficits, alterations directly at the level of neuronal turnover and morphology are also being observed. Lower number of GRs were found in the hippocampus of handled mice, receiving

lesser maternal care thus, impairing the negative feedback control on the HPA axis of the pups. In fact, decreased dendritic length of golgi-stained CA1 pyramidal neurons of hippocampus with significantly lesser spine density were found in the lower licked and groomed rats. These structural alterations also caused impairments in the functional consequences, causing lower synaptic potentiation of schaffer collaterals after tetanic stimulation. They also exhibited longer freezing times in a contextual fear conditioning task as compared to highly groomed rats⁶⁴. Cognitive behavioral impairments such as poor spatial maze learning with a concomitant decrease in the turn-over of adult born neurons of hippocampus have also been shown in MS rodents. However, in a more recent study, it was found out that the males who were raised by ‘stressed mothers’ and subsequently underwent MS in first two weeks of life showed enhancement in maze learning task but were more aggressive and exhibited dysfunctions in social coping learning in a resident-intruder task⁶⁵. This could occur as a result of increased resilience upon ELS induction. ELS can also exert its influence on behaviors involving decision-making undertaken by sensory systems and these are enumerated in the subsequent section.

1.2.1.3 Early life events induced alterations in sensory perception

Sensory decision-making utilizes sense organs which collect the incoming information, the relay centers that process and project this information to the cortical regions where the percept gets completely formed. These processes occur under different contexts and conditions and thus continuously involve the usage of our cognitive faculties. Here, I have described the existing literature linking stress with sensory systems.

Although effect of stress on the limbic system is well-studied, the same is not true for sensory areas. Owing to their neuroanatomical closeness and the top-down neuromodulation that they receive, sensory brain areas are vulnerable to external stressors. In a report that determined the relation between retinal functioning and depression, lower contrast gain was found in the depressed patients on a chess-pattern test when assessed using an electroretinogram. Peripheral visual processing at retina thus seems to be negatively affected due to depression⁶⁶. Nociceptive threshold checked using Von Frey test in mice was found to be lower in ELS mice both during their juvenile stages as well as during adulthood. This behavioral change was concomitant with the increased slope of potential of the layer II/III somatosensory cortical fields. They further found out using multiphoton imaging that the otherwise highly stable mushroom spines of the somatosensory neurons were undergoing a

faster turnover in these mice resulting in lower threshold⁶⁷. They further predicted the possibility of faster microglial movement in the instability of these neuronal spines. Indeed, microglial processes were more motile in the somatosensory cortex of ELS mice after an episode of vibrotactile limb stimulation⁶⁸.

Human and rodent studies focusing on stress mediated neural alterations have indicated an association between olfactory system and the limbic system. Since last two decades, many human studies & clinical reports have indicated reciprocal association between olfactory sensitivity and depression stage². Recent studies showed dysfunction of olfactory abilities in patients suffering from MDD^{2,69}. Olfactory acuity calculated using ERPs showed reduced levels of amplitudes of ERPs during early stages of MDD in patients⁷⁰. This is corroborated by a study showing negative correlation between OB volume and depression score in humans⁷¹. The models explaining loss of olfactory sensitivity in depressed population in previous studies are recently tested by Krusemark and others⁷². They utilized laboratory based anxiety paradigm on human subjects. Upon inducing anxiety, the previously tested neutral odors gained negative valence (unpleasantness) in those subjects. Using fMRI imaging and model based approaches, they proposed an integrated circuitry involving higher cortical structures such as Anterior Piriform Cortex (APC) connectivity to OB being altered under stress⁷².

The underlying neural mechanisms governing a link between stress and olfaction is being investigated in rodent models. For instance, olfactory bulbectomized rat have shown signs of depression^{73,74}. The reciprocity between olfaction and emotion, which exists in humans has also been seen in a transgenic mouse model of *cng2a* deficiency leading to altered peripheral processing. The *cng2a* induced perturbations in the odor-evoked neural activity brought about anxiety-like behavior with a concurrent increase in blood corticosterone levels⁷⁵.

Having established the fact that there is a neuroanatomical closeness between OB and limbic system, researchers are currently focusing on changes in the information processing and the differential contribution of circuits upon stress induction. Importantly, the underlying functional connectivity differs based on the kind of stressor employed. For example, predator odor stress in mice causes activation of a specific cortical region called Amygdala- Piriform transition area (AmPir)⁷⁶ while mild acute stress during odor acquisition task triggers Locus

coeruleus (LC) mediated increase in norepinephrine (NE) resulting in olfactory information processing changes⁷⁷.

ELA itself can have pronounced effects on our smelling abilities, however, the underlying circuit interactions are not yet deciphered. Women suffering from Childhood Maltreatment (CM), a form of early life adversity, exhibited up to 20% decreased Olfactory Bulb (OB) volume and lower olfactory detection thresholds⁷⁸. A mouse model of MDD with elevated levels of corticosterone displayed olfactory impairments. Chronic corticosterone treatment resulted in deficit in discriminating perceptually similar odors. Anti-depressant treatment using Fluoxetine displayed reversal of such a sensory impairment⁷⁹. Maternally separated rats (from P1-P10, 3 hours a day) exhibited olfactory dysfunctions in their early life⁸⁰. Olfactory communication is of utmost importance for the dam to recognize the pups, to lick their anogenital regions, groom them and for the pups to recognize their nest odor and suckle the dam's milk. They found out that the deprived pups took longer to show a preference towards the nest odor as compared to controls in an olfactory memory test. A reduction in β -Tubulin positive cells in hippocampus and OB at early time points (P21 & P7, respectively) was found in deprived pups, indicating decreased number of neuronal cells⁸⁰. Indeed, neurogenesis in hippocampus and OB has been shown to be affected by ELS in many studies^{81,82}. However, the extent and duration of the reduction in neurogenesis varies depending on the ELS paradigm chosen. In a yet another study, a unique odor aversion learning in ELS rats was delicately depicted. It was shown that stress-reared P7 old juvenile mice exhibited odor aversive learning compared to normal-reared mice, with under-developed amygdala responses, that displayed odor preference learning. Their peptide infusion and micro-dialysis experiments suggested that in stress-reared mice, there was increased release of CRH from amygdala induced by enhanced blood corticosterone levels. The CRH afferents from amygdala, in turn, activated NE release from LC directly into the OB over and above the amounts required for odor preference learning during neonatal age⁸³.

Different stressors and paradigms can thus, have distinctive neural circuitry activation. Hence, it is important to fully understand the structural and functional connectivity between the different classes of neurons within the olfactory system, the centrifugal projections reaching OB and neuro-modulatory effects on OB so as to decipher state dependent functional changes.

1.2.2 Olfactory bulb

Sense of smell starts at a peripheral center, the nasal epithelium. Odorants bind to their specific receptors present on the olfactory sensory neurons (OSNs) of the olfactory epithelium. The information is then conveyed to OB as OSNs project onto the neuropil like structure called glomeruli where the dendritic tufts of projection neurons synapses with OSNs⁸⁴. Odor-driven excitatory output at the level of projection neurons is controlled by inhibitory currents generated by the interneurons. Such a processing by inhibitory interneurons at the bulb level leads to increased gain control and signal-to-noise ratio⁸⁵. The information is finally passed onto the olfactory cortical regions which results in complete percept formation. Efferent projections of the M/T cells supply to the cortical areas while the cortical areas themselves provide the feedback projection.

The peripheral organ called olfactory epithelium consists of OSNs, each of which expresses a single type of functional receptor. As an exception, small class of chemosensory receptors MS4A can recognize multiple odors. Around 1000 receptor genes expressed by OSNs have been discovered in mouse epithelium⁸⁶. A particular receptor is capable of detecting multiple odors and a single odor can be detected by multiple receptors. However, most studies suggest that OSNs are narrowly tuned, i.e., they respond to odorants with similar odor quality/structure. However, in addition, few broadly tuned receptors are also found^{87,88}. Such a combinatorial coding at periphery acts as an antecedent for achieving a successful olfactory discriminatory power.

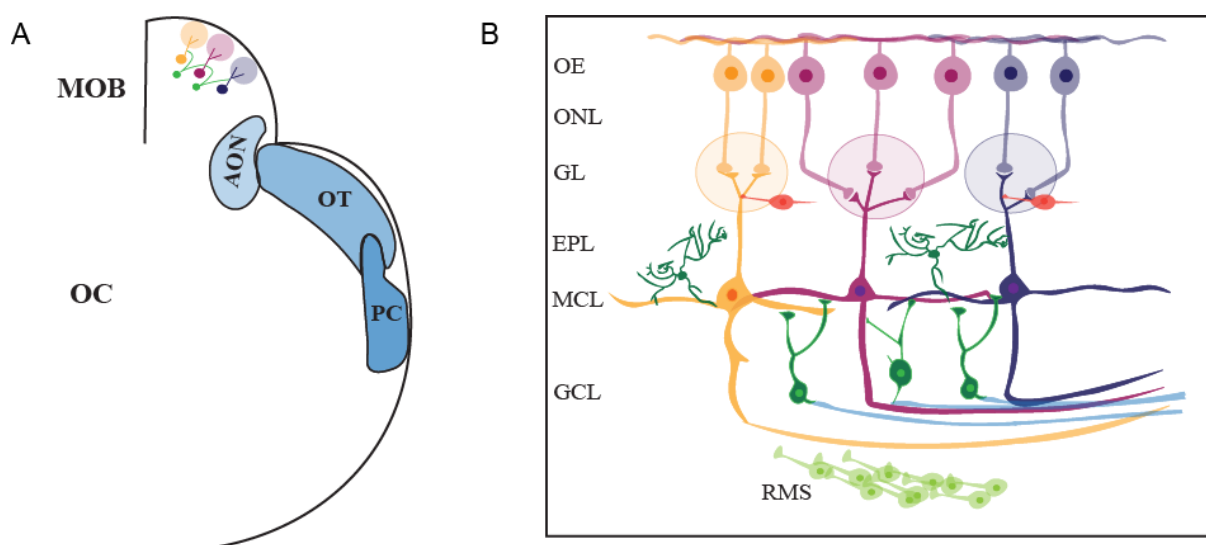


Figure 1-2: Main olfactory system of mouse and the underlying neural circuits

A. Schematic diagram depicting the connectivity in the MOB. The information from MOB is further passed on to the olfactory cortical regions, Anterior olfactory nucleus (AON), Olfactory tubercle (OT) and Piriform Cortex (PC) amongst others.

B. The layered architecture of MOB is depicted in this illustration. The OSNs carrying the same ORs converge onto the glomeruli where they make synaptic connections with the projection neurons (M/T cells). The granule cells (GCs) provide dendro-dendritic inhibition on the distal and lateral dendrites of the projection neurons causing the refinement of the information processing. The peri-glomerular cells present in the GL also provide inhibition to the apical dendrites. The interneurons of External plexiform layer provide the inhibitory and modulatory effects on both the projection neurons and the granule cells. Efferent projections of the M/T cells supply to the cortical areas while the cortical areas themselves provide the feedback projections to the inhibitory interneurons present in the MOB (adapted from D La Rosa-Preito et al. 2015)⁷.

During information processing, OSNs expressing same receptor converge into a single glomerulus making it as a first neural grouping element^{84,89}. These first sensory afferents from epithelium form glutamatergic synapses with the projections from Mitral/Tufted (M/T) cells, in the glomeruli. This results in the formation of a first topographic odorant map in the glomerular layer of the OB during sensory processing⁸⁴. Both excitatory and inhibitory connections are present in the glomerular layer, between OSN outputs to M/T cells, OSN outputs to Juxtglomerular (JG) cells and M/T cells to JG cells. OSNs release glutamate in a glomerulus upon odor stimulation. This, in turn, activates periglomerular cells to inhibit the glutamate release from OSNs so as to avoid excess of glutamate in GL⁹⁰. Connections between PG cells and apical dendrites of M/T cells control the output of the OB. Inhibitory inter-glomerular interactions also exist which fine tune the output further⁹¹.

Synaptic connections existing between the dendrites of M/T cells and the inhibitory interneurons found in Glomerular layer (GL) and granule cell layer, called Granule cells (GC) are responsible for refinement. Release of glutamate from M/T cells activates GCs which in turn release GABA. GABA can either bind to its receptors present on the same M/T cell which activated GCs or to adjacent M/T cells⁹². Spatio-temporal representations of odor start to emerge at OSNs level and gets further refined as a result of inhibition occurring at the level of GL and GCL by interneurons in an activity-dependent manner. This suggests that spatio-temporal representation for each odor is indeed unique. However, it becomes overlapping for perceptually similar odors such as a pair of enantiomers. Such dense bi-

directional connectivity, thus, plays an important role for enhancement of odor contrast⁸⁵. Indeed, overlapping odor-evoked activity in OB is highly dynamic at the level of projection neurons giving rise to separated activity patterns, thus, refining the output⁹³.

Role of neurons present in the External plexiform layer (EPL) in sensory processing is not well understood. Biocytin filling indicates that interneurons present in EPL provide focal inhibition to M/T cells⁹⁴. These interneurons are also positive for different neuropeptides. The functional relevance of neuropeptides in the circuitry, however, remains mostly unknown. Recent report tracing Parvalbumin (PV) positive interneurons in EPL show reciprocal dendro-dendritic connections with Mitral cells. These PV-positive neurons are broadly tuned, i.e., less odor selective. Thus, they are capable of normalizing the output of mitral cells by providing feedback inhibition which is applicable across different levels of sensory inputs⁹⁵.

OB is endowed with a wide variety of interneurons spanning its different layers, especially GCL and EPL. Corticotropin releasing hormone (CRH) positive population of interneurons, constituting around 25% of total EPL interneurons has been recently discovered⁹⁶. These neurons inhibit the mitral cell activity and communicate with GCs through CRH-CRHR1 signaling loop⁹⁷. Modulation of local CRH in OB under stressful conditions is unknown. One study shows that Early life stress can affect aversive learning during adulthood which involves amygdala activation, which in turn, excites locus coeruleus (LC) and norepinephrine in OB⁹⁷. However, role of locally present CRH and other stress-vulnerable neuropeptides during such conditions needs to be deciphered.

1.2.2.1 *Adult Neurogenesis in Sub-ventricular zone / Olfactory bulb*

The adult OB is a highly dynamic structure which undergoes constant renewal of its heterogenous group of interneurons throughout adulthood. This turn-over is maintained by a niche of stem cells present in Sub-ventricular zone (SVZ)⁹⁸. The stem cells form transit-amplifying cells which further give rise to neuroblasts⁹⁸. Neuroblasts traverse through rostral migratory stream to reach OB. Only half of the population finally matures and get integrated into the circuit. The cells present in the niche, like the interneurons of OB, are under activity dependent control⁹⁹. Dopaminergic inputs from substantia nigra and serotonergic inputs from RN have pro-neurogenic effect & promote neuroblast migration^{100,101}.

There have been numerous studies indicating role of adult born interneurons in the well-established circuitry. Ablation using anti-mitotic drugs affects discrimination of perceptually similar odors. Using transgenic technology to specifically ablate adult born GCs led to alteration in odor reward associated memories^{102,103}. Adult neurogenesis levels can change depending on the changes in physiological state of an animal through intrinsic or extrinsic factors¹⁰⁴. Stress has shown to affect Dentate gyrus neurogenesis⁸². Reports on how stressors can affect bulbar neurogenesis, however, are starting to emerge.

1.2.2.2 *OB as a center of extensive modulation by intrinsic and extrinsic factors*

Olfactory system in mammals does not serve only as a sensory feed-forward circuit. Because of its massive top-down regulation and the back & forth communication with cortical regions, it is expected to play a role in various state-dependent behaviors. Modulatory processing mainly happens at the level of interneurons present in OB governing spike timing and synchronization properties, thus, regulating E/I balance¹⁰⁵. These connections are experience-dependent and thus, contribute to plasticity.

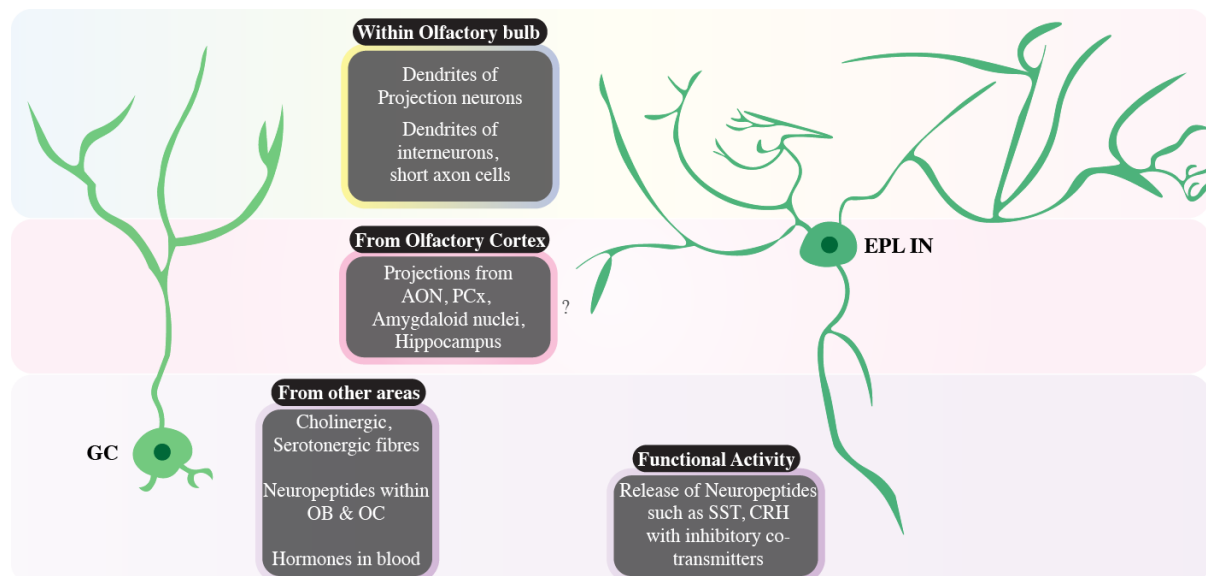


Figure 1-3: Major players of pre-cortical olfactory processing are under massive neuromodulation

Schematic diagram depicting modulation due to massive connectivity of the inhibitory interneurons (Granule cell (GC), EPL interneuron) at different locations across the length of the neuron (color coded). The processing of these interneurons that controls the output of pre-cortical area, OB are modulated by the dendro-dendritic connections with both excitatory and inhibitory connectivity

within and outside of OB. The release of neuropeptides and co-transmitters under certain conditions, for example, by EPL INs could change the circuit activity. Differences in the inputs from other brain areas such as HDB, LC etc. under different contexts can change the activity dynamics of GC functionality.

Cholinergic inputs from basal forebrain:

Interneurons found in GL and GCL and Pyramidal cells present in piriform cortex (PC) receive cholinergic inputs from Horizontal limb of Diagonal band of Broca (HDB) region¹⁰⁶. Both muscarinic and nicotinic receptors are found in the non-overlapping interneuron population in OB¹⁰⁷. Studies involving agonists, antagonists of Acetylcholine (Ach) and Ach esterase enzyme blockers exhibit the importance of these inputs in modulating olfactory perceptual learning^{6,108,109}. For example, local infusion of AchE inhibitor in OB strengthens cholinergic modulation. This results in sharpened response for a particular odor and reduced overlap between the Odorant receptor fields (ORFs) of mitral cells, thereby, increasing odor discrimination⁽³⁹⁾. Electrophysiological data suggests Ach mediated activation of bulbar interneurons resulting in suppressed MC activity¹¹⁰.

Cholinergic modulation is under the control of extrinsic factors. A single stress session is capable of attenuating cholinergic transmission and reducing the available Ach in mice cortical regions¹¹¹. Suppressed cholinergic input to OB and PC may modulate discrimination abilities of animals in a negative manner. However, stress dependent cholinergic modulation of OB has not yet been studied.

Norepinephrine from LC:

Most neuronal types in OB express both α_2 and receptors¹¹². Norepinephrine from LC, however, exerts its effect directly on GCs and Pyr cells in PC¹¹³. The effect is concentration dependent with activation of α_2 receptors on GCs at lower NE levels causing less inhibition of GCs on MCs¹¹⁴. At higher concentrations, it increases the inhibitory drive onto MCs via its action on β receptors.

LC stimulation and thereby, release of NE is state-dependent. A study by Linster group shows that suppression of memory by mild stressors during odor acquisition task is partially dependent on NE. Local delivery of NE antagonists rescued the suppression of odor memory phenotype. In fact, lesion of NE-positive neurons in LC attenuates olfactory memory⁷⁷.

Serotonergic fibers from Raphe Nuclei (RN):

All layers of OB seem to receive serotonergic fibers from RN, however, dorsal GL constitutes the highest density of serotonergic inputs onto PG cells^{8,115}. An *in vivo* study

involving Serotonin release in bulb along with stimulating LC has shown to excite a population of GABAergic PGCs which provide presynaptic inhibition to OSNs¹¹⁶. Projections from RN are also capable of selectively regulating MCs and TCs activation¹¹⁷. The neuromodulators, thus, tend to act in concert with each other, mostly resulting in fine-tuning the output at early olfactory centers.

Serotonergic system originating from RN supplies to whole forebrain, basolateral amygdala (BLA), hippocampus, cortex and striatum. In most anxiety-related issues, mesobasocortical pathway of serotonin is hindered¹¹⁸. ELS suppresses the serotonergic system and reduces receptor expression in various brain regions which receive serotonin from RN¹¹⁹. Indeed, usage of Fluoxetine, a Selective serotonin reuptake inhibitor (SSRI) in mice model of heightened corticosterone (CORT) improved olfactory acuity and restored neurogenesis in OB⁷⁹. However, alteration in the serotonergic circuitry existing between RN and OB upon stress induction remains elusive.

1.2.2.3 *Olfactory cortical regions*

Olfactory cortex (OC) constitutes regions in the forebrain receiving direct inputs from OB projection neurons⁹. While both MCs and TCs project to Anterior Olfactory Nucleus (AON), Anterior Piriform Cortex (APC) and Olfactory tubercle (OT), MCs also reach out to more posterior regions such as Posterior piriform cortex (PPC), Tenia tecta (TT) and amygdaloid nucleus¹²⁰. Such a differential connectivity of MCs and TCs might contribute to deciphering different properties associated with odor information in different cortical regions¹²¹. Although the topography of axonal projections of MCs and the association fibers of AON on the Pyramidal cells of PC is not well understood, the idea of cortical processing is to integrate the bulbar information resulting in complete percept formation.

The organization and role of OC is distinctive. It is not just involved in deciphering the sensory information but due its bi-directional connectivity with limbic areas, the processing is highly state-dependent¹²². Many olfactory cortices project to hypothalamic regions. A recent study characterized the role of a region called Amygdala-piriform transition area using viral tracing and its functional role by chemogenetic activation. This region is present upstream of CRH neurons and is responsible for mediating fear response in presence of predator odor⁷⁶. Olfactory cortical areas connecting to amygdala and lateral hypothalamus which can also mediate stress response^{123,124}. However, how the functioning of olfactory cortex is affected by stress largely remains unknown.

1.2.3 Environment enrichment

While adverse experiences can have negative consequences, enriching experiences are capable of causing positive changes and reversing certain maladies of the brain. Early intervention programs aiming to reverse the ELA mediated neurocognitive ailments in humans is a great example of the same. Head Start program of US Department of Health and Human services started in 1965, aimed at improving the social, nutritional and cognitive “health” of the preschoolers belonging to below-average family backgrounds^{125,126}. An additional Literacy Environmental Enrichment Program (LEEP) built into the Head Start program in New England allowed for the language enhancement and early literacy development of children¹²⁷. In Romania, children at a young age were transferred from institutions to foster parents who were provided with the support from medical practitioners on raising them with utmost care as a part of the Bucharest Early Intervention Project¹²⁸. Institutionalization does not support individualized care-giving with minimal routes of providing sensory and cognitive stimulation to children. Studies have shown delayed neurodevelopmental growth, instances of hyperactivity disorders, increased amygdala volumes in institutionalized children^{40,129}. Fostered kids who were removed from a life of neglect at an early age, on the other hand, displayed higher IQ, more normative growth trajectory of brain’s white matter, lesser chances of suffering from psychological disturbances and overall, a more adaptive functioning on tests assessing social, literacy skills and stress responsiveness^{130–132}. To understand the neural mechanistic aspects, EE has been studied extensively in rodents. In this part of Introduction, I have summarized the positive effects that EE provides in neurodevelopmental and disorder rodent models with a specific emphasis on its modulatory effect on neural function.

1.2.3.1 *Therapeutic effects of EE in animal models*

Multimodal enrichment with increased occurrences of social interactions, stimulatory sensory and motor activities are effective in reducing the behavioral symptoms associated with the neurodevelopmental disorders. The therapeutic effects have been extensively studied in the rat and mice models of Fragile-X syndrome, Autism spectrum disorders and attention deficit hyperactivity disorders (ADHD). Early EE conditions mitigate the hyperactivity and socio-cognitive deficits observed in FMR1-knockout mice¹³³. EE also cause decreased repetitive behaviors with a concomitant increased neural activation and improved dendritic morphology in ADHD model of mice¹³⁴. Effect of EE can be graded, i.e, they can depend on the extent of the enrichment that’s provided to the animals. EE has often been applied in the backdrop of

the deprived, single, small-cage housing of rodents. In contrast to just adding enriching materials to the home-cage, one study made a large arena of EE (super-EE). Effects of super-EE were more enhancing in ameliorating the problems associated with Huntington's disease as compared to those animals which were housed in standard cage provided with EE supplies¹³⁵. Stimulation of repair in models of traumatic brain injury can also be achieved by using EE paradigms. Animals recovering from brain injury when reared in EE showed significantly smaller lesions and improved behavioral manifestation in a Morris water maze task within two weeks of afflicting injury¹³⁶. EE induced betterment is also observed in models of neurodegenerative disorders such as Alzheimer's and Parkinson's. EE can have neuroprotective effects on such progressive disorders. In a rat model of Alzheimer's that had oxidative and memory deficits, different components of EE had varying effects. Enrichment due to social interaction alone only rescued the impairment relating to social recognition memory. Overall EE and anaerobic exercises alone, contrastingly, reversed the cognitive decline as well as the biochemical reaction of Amyloid Beta on lipid peroxidation¹³⁷. So, the different modules of EE may have diverse effects on the behavior of the animal. Most often, all the components, from social to sensory enrichments are applied together to attain most desirable effects of enriching the housing environment. Yet, it is important to note that the inter-animal differences can occur even if EE is provided identically to all cage-mates. This is because each individual is engaging with the environment differently which is their part of the 'non-shared environment'¹². Thus, the individual animal's behavior as well as the circuitry changes upon induction of EE should be analyzed with caution.

1.3 Materials and Methods

1.3.1 Subjects

A total of 85 male mice and 4 pregnant dams (C57Bl/6J) were utilized for this study. Young cohorts of Normal weaned (NW) and Early weaned (EW) mice tested on anxiety tests and olfactory dilution experiment for discrimination threshold included 8 mice per group. For olfactory discrimination training and memory experiments, 17 EW and 21 NW mice were used. Same group of mice were then utilized for carrying out anxiety tests during their late adulthood. 13 EW mice and 12 NW mice were used for testing anxiety and olfactory abilities upon environmental enriched housing. For this a total of 4 pregnant mothers were put in the EE cage and removed at P14 and at P28 for EW and NW groups, respectively (genotype: SST-EYFP pups, details are explained in Chapter 2, section 2.3.2). To carry out transcriptomic analysis of OB, 3 NW and 3 EW male mice were utilized.

1.3.2 Early life stress through Early Weaning

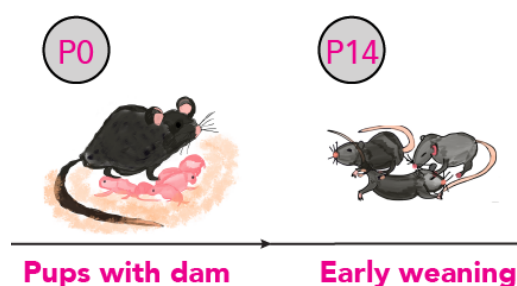


Figure 1-4: Early weaning in mice

Illustration depicts the early weaning protocol. The pups stay with dam from Postnatal day 0 till 13. Enough nesting material is provided. On Postnatal day 14, male pups are separated and added to new cage with bedding but no nesting material.

Experimental groups of C57BL6/J mice were weaned at Postnatal day 14 (P14)^{138,139} and transferred to a cage with new bedding and limited new nesting material. The pre-weaning for all groups was always done in the light period, between 11am-2pm. Food pellets were kept in the form of slurry. Both the slurry and water were provided in petri-dishes, *ad libitum*. Intermittent heating by putting a heating pad below the cage was provided during the first week after pre-weaning to counter hypothermia. This care was restricted to P14-P18 period only.

1.3.3 Tests for assessing anxiety and depression

Standard battery of tests were done to assess if ELS in C57BL6/J mice resulted in changes in the anxiety-like or depressive behavior of the animals. The details of the apparatus used and the parameters assessed are described below.

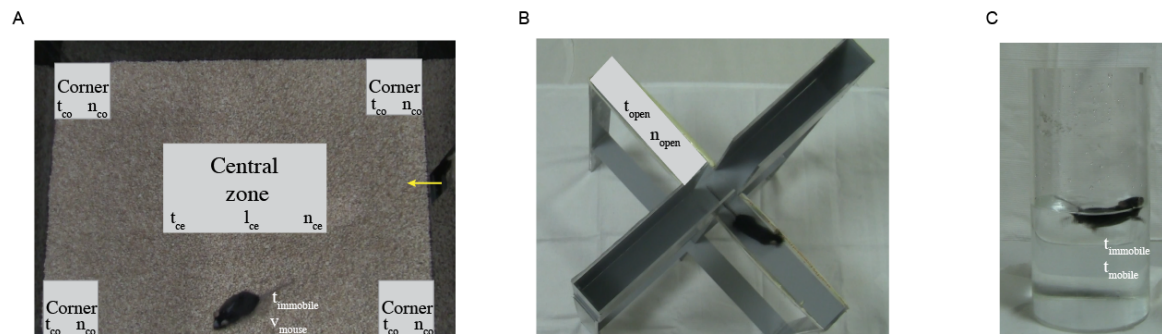


Figure 1-5: Parameters utilized in battery of tests conducted to assess anxiety & depression

A. OFT arena with the laid-out proportioned zones for calculating the time spent and number of entries made in corners (t_{co} , n_{co}) versus center (t_{ce} , n_{ce}) as well as the latency to the center (l_{ce}) from the starting point (yellow arrow). The time spent by mouse immobile in the arena as well as its average moving speed is calculated ($t_{immobile}$, v_{mouse}).

B. EPM test set-up with laid-out proportioned zone for open arm. Time spent and number of entries made into the open arms (t_{open} , n_{open}) are calculated.

C. A mouse carrying out the FST test is shown. The immobility and mobility time of the mouse are calculated ($t_{immobile}$, t_{mobile}).

Open Field test (OFT): It consists of a 60 cm X 45 cm black colored, opaque open arena made out of acrylic sheet. In this test, a mouse is allowed to explore the novel arena for a total of 10 minutes. The exploratory behavior of the mouse is recorded using a video camera mounted on the top using a tripod stand. On the day of testing, all the mice belonging to the same home-cage are put in a black colored, pseudo-cage (same dimensions as that of home cage: 42 cm X 26 cm X 18 cm) and were habituated for 10 minutes. Each mouse was then allowed to singly enter the OFT arena via a small passage. Mouse is tracked using Noldus Ethovision 8.5 software. The time spent in central zones versus the corner zones, number of entries into central zone, latency to the first entry into the central zone and the average velocity were calculated by the software (Figure 1-5, A).

Elevated Plus Maze (EPM) test: It is a plus maze consisting of two oppositely facing open arms and two closed arms. Closed arms have raised walls of 15 cm height. The apparatus was made out of light gray colored acrylic sheet. The maze was raised 50 cm above the ground

and the arms were 55 cm in the length and 5 cm in width. The central zone of the plus maze was of 5 cm X 5 cm dimensions. On the day of testing, mouse was placed in the central zone facing the open arms. It is allowed to explore the arms for a total of 5 minutes. The zones are cleaned with 70% ethanol and then with tissue dampened with distilled water between the testing of mice. Next mouse was put after 5 minutes of cleaning procedure. Times spent in the open versus closed arms are calculated using Noldus Ethovision 8.5 software which tracks the central point of the body of the mouse. Number of entries made into these arms are calculated manually (Figure 1-5, B).

Forced Swim Test (FST): It consisted of a cylinder of 30 cm tall and 15 cm wide made out of acrylic sheet. Ambient temperature (25°C) water was filled up to the depth of 12 cm. This was done to ensure that the mouse neither sank nor jumped out of the apparatus. A mouse was dipped into the water and was then tested for 6 minutes duration. Water was replaced after every animal. The time it spent actively swimming was considered as the time it was mobile. The time mobile versus immobile was calculated manually (Figure 1-5, C). To avoid complications arising due to hypothermia, the animal was kept on dry-towels in an empty cage placed on a heating-pad after the test was completed, before transferring it to the home-cage.

1.3.4 Olfactory detection, discrimination learning and memory behaviors

1.3.4.1 *Go/No-go (GNG) olfactory learning paradigm in freely moving condition*

To assess olfactory discrimination learning and memory in mice, they were trained on a well-known GNG operant conditioning paradigm which has been extensively used in olfactory psychophysical studies^{10,140}. It involved presentation of two odors to the animal, one at a time. Each odor was presented for a fixed duration. One of the odors was paired with a reward (i.e water) while the other was unrewarded. A water-deprived animal was trained on this task to study the rate at which it was able to associate the odors with the reward. This determined the rate of learning of discrimination between the two odors. The details of the apparatus, paradigm and parameters are described in the following sections.

1.3.4.2 *Olfactometer (freely moving apparatus)*

Two of the modified eight-channel olfactometers^{10,140,141} were used to train mice on GNG operant conditioning task (Figure 1-6, A). The olfactometers were operated by the custom-

written program in Igor Pro (Wavemetrics, OR). Counterbalancing of the mice was done carefully between the two olfactometers. It consisted of a chamber made out of acrylic sheet (dimensions: 14.5 cm X 12 cm X 11.5 cm) with a metallic base, in which the mouse was put and allowed to freely move around and explore. One of the sides of the chamber had an opening into the sampling port. This circular opening is guarded by an IR beam and detector. When the mouse pokes its snout into the port, the beam is broken and the trial is initiated after a fixed delay. The sampling port allowed odor stimulus presentation to the mouse as well as the delivery of water reward via the lick tube. Usage of a single port enabled tight association between the stimulus and reward. Odor bottles carrying diluted odors in mineral oil were hung via the two sets of tubing (Cole-Parmer 6424-67) connected to the pinch solenoid valves. A total of 8 pinch valves were connected in the manifold of the apparatus which were controlled by two flowmeters. One flowmeter allowed entry of clean air stream while the other flowmeter controlled the delivery of odorized air. Two bottles of rewarded (S+) and non-rewarded (S-) odor each were connected randomly to any of the eight valves. During a trial, firstly, Diversion valve (DV) opened 500ms before the odor presentation that diverted the odorized airflow away from the mouse, towards the conduit for exhaust. After the DV is released, odor is presented for 2s. To restrict odorized air to the sampling port only was the operation of exhaust fan connected to one side of the chamber, opposite to the hole for the sampling port. The inward flow of air from the fan prevented the entry of odorized air into the chamber. The volume of water (3-4 μ L) as a reward was controlled by a solenoid valve which was tuned to open at the end of the presentation of a rewarded odor if the mouse met the criterion of a correct response. A manual console was connected and used to confirm if all the valves were functional or not. The digital I/O board allowed for the automation of the olfactometer by the software written in the Igor Pro.

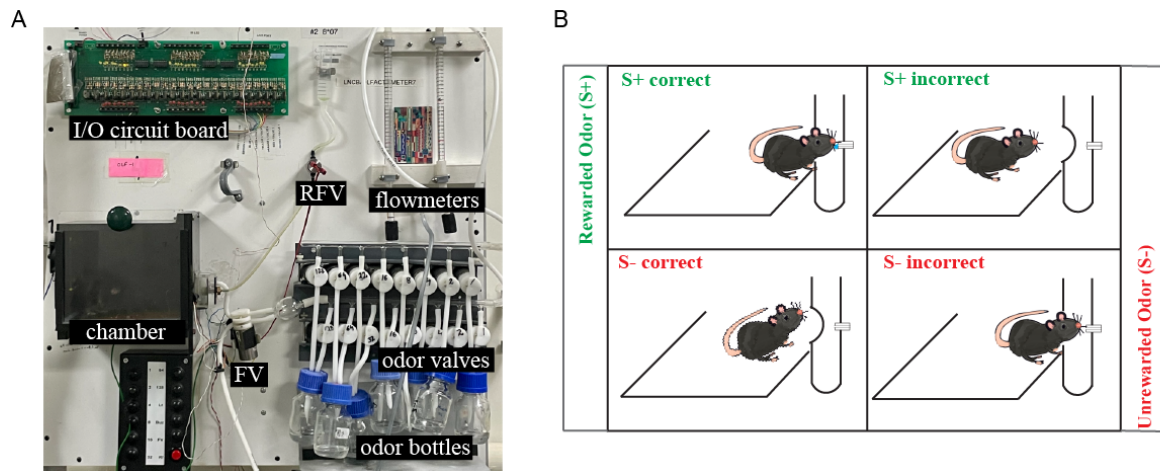


Figure 1-6: Go/No-go olfactory paradigm using a custom-made olfactometer

A. A picture of the custom-made 8 channel olfactometer employing the Go/No-go paradigm to quantify olfactory discrimination learning and memory. The components are labelled and the functioning of the system is explained in section 1.3.4.2 (RFV: Reinforcement Valve, FV: Final Valve).

B. A schematic diagram of the responses that an animal will generate towards the two types of odors, S+ and S-. By following the licking criterion correctly for S+ odor, animal gets the reward while failing to do so results in an incorrect trial. For S- odor, a learnt animal retracts its head while if it licks beyond the set criterion, the trial is considered incorrect.

1.3.4.3 *Task habituation training (Pre-training)*

Mice were water-restricted such that they got free water twice (10 minutes each time) in 24 hours. After 2-3 days of beginning with the restriction schedule, task habituation was done in which mice were put on the olfactometer to familiarize them with learning rules (procedural learning) of the conditioning task.. Initial step involved provision of water reward as and when the mouse poked into the sampling port. After 20 such trials of the first phase, second phase commenced. In this, mouse was then supposed to lick the lick tube (reward port) to get the water drop. In the third phase, an additional component of valve opening was imposed. From this phase onwards, an odor bottle containing 5mL of mineral oil (diluent/carrier) was connected to one of the pinch valves. The mouse had to sample the air coming from the sampling port and lick to get the reward. Over the subsequent phases, criterion of licking was progressively increased such that the mouse learnt to continuously lick during the odor (mineral oil) presentation so as to get the reward. This phase took 2-3 days for completion.

1.3.4.4 *Odors*

Odors used in this study were purchased from Sigma-Aldrich. The diluent of odors, mineral oil was bought from Oswal Pharmaceuticals, Pune, India. Following is the table of the details of the odors used in the study (Table 1-1). Odors were diluted to 1% (v/v) in mineral oil. Either simple or binary mixes of odors (60%-40%) were used. To determine odor discrimination threshold, odors were serially diluted to the concentrations (v/v) mentioned in the Figure 1-15 and the corresponding results section.

Sr No.	Name	Chemical Formula	Catalog	Physico-chemical parameters
1	Methyl Benzoate	C ₈ H ₈ O ₂	M29908	<1mmHg at 20°C
2	1-Nonanol	C ₉ H ₂₀ O	131210	0.02mmHg at 25°C
3	Acetophenone	C ₈ H ₈ O	00790	0.45mmHg at 25°C
4	Octanal	C ₈ H ₁₆ O	O5608	2mmHg at 20°C
5	Amyl (Pentyl) Acetate	C ₇ H ₁₄ O ₂	109584	4mmHg at 20°C
6	Ethyl Butyrate	C ₆ H ₁₂ O ₂	E15701	15.5mmHg at 25°C
7	1,4-Cineole	C ₁₀ H ₁₈ O	27395	1.93mmHg at 20°C
8	Eugenol	C ₁₀ H ₁₇ O ₂	E51791	0.02mmHg at 25°C
9	(+)-Carvone	C ₁₀ H ₁₄ O	22070	15.4mmHg at 20°C
10	R-(-)-Carvone	C ₁₀ H ₁₄ O	124931	0.4mmHg at 20°C

Table 1-1: Relevant information about the odors used in the study

1.3.4.5 *Olfactory discrimination learning training paradigm*

Trial begins when the mouse poked into the sampling port indicated by the IR beam break. After a 500ms delay (i.e when DV is released), odor is presented for 2s. Thus, a trial of the olfactory discrimination task included presentation of odor followed by a fixed time interval (called the inter-trial interval or ITI)^{10,142}. If it was a S+ trial, mouse needed to lick continuously during the trial so as to get water (3-4 mL) at the end of 2s. For a S- trial, mouse had to refrain from licking so as to generate a correct response. The 2s time window of odor delivery was also considered to be the reaction window where the mouse needed to take the action (or not) depending on the type of the stimulus (Figure 1-6, B). Reaction window of 2s was divided into 4 bins of 500ms. The licking criterion during these bins for the type of stimulus is as follows:

- For S+ stimulus, mouse needed to lick once in at least 3 out of 4 bins to get reward. Neither the punishment nor the reward was presented if it did not meet the criterion.
- For S- stimulus, mouse could lick in at most 2 out of 4 bins to make a correct response. Punishment was not imposed if it licked beyond the set criterion.

An ITI of 5s was applied at the end of each trial. This duration was sufficient for the animal to retract its head from the sampling/reward port after the trial was ended.

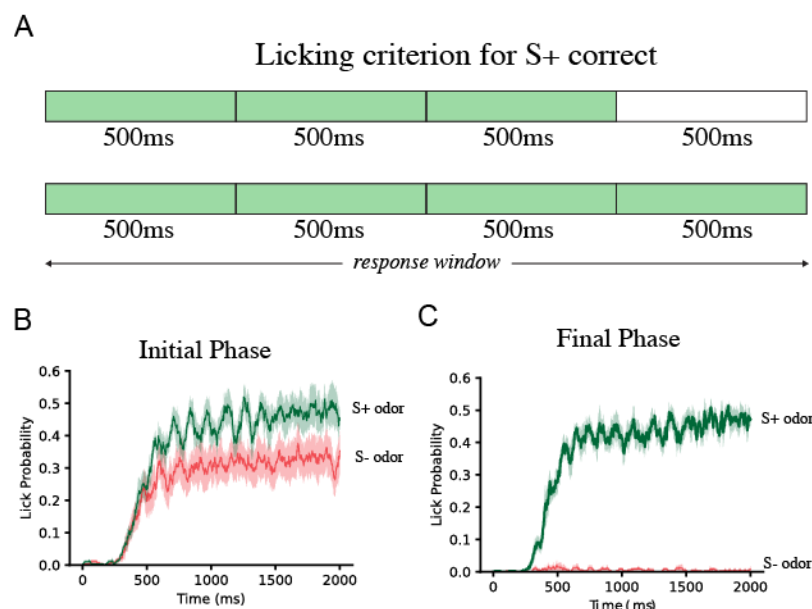


Figure 1-7: Licking criterion and evolution of licking probability with training in the Go/No-go olfactory paradigm

- A. Schematic diagram representing the licking criterion to carry out S+ trial correctly. The response window of 2s is divided into four bins. Two examples of correctly doing the S+ trial, i.e, licking for at least any of the three bins or all four bins fulfil the criterion.
- B. The licking probability, calculated for 50 S+ and 50 S- trials encompassing first 100 trials of Task 1, depicts higher licking for both type of odors during the initial phase of learning.
- C. Licking probability for S- reduces to 0 - 0.1 while stays higher for S+ trials when plotted for final 100 trials of Task 3, i.e, during the final phase of the learning.

Trials were put together in the form of blocks. Each block contained 20 trials, 10 S+ and 10 S-. These were arranged in a pseudo-randomized scheme such that not more than 2 consecutive trials were of the same stimulus type (S+/S-). A total of 900 trials (three tasks) for simple monomolecular odor pair and 1200 trials (four tasks) for binary mix of odors were carried out. Most often, optimally motivated mice carried out 100-160 trials in a single session of training.

1.3.4.6 Assessment of olfactory learning

Learning curves for odor pairs tested over increasing volumetric dilutions was carried out by averaging the accuracy of 100 trials (50 S+ and S-) for a total number of trials per animal. The mean \pm sem values were then plotted as the learning curve. For calculating d prime (d'), probability of both the hit trials (i.e correct S+) and False Alarm (FA) trials (i.e incorrect S-) were taken into account. Hit and FA probability were calculated as average of 100 trials per animal. The z value was calculated for both Hit and FA. d' was quantified as z(Hit)-z(FA) for each of the 100 trials. The progression of d' for the two groups of mice (normal and early weaned) was compared using Two-way ANOVA and post-hoc LSD Fisher test.

1.3.4.7 Assessment of olfactory memory

For the odor pairs for which the memory of association had to be assessed (i.e odor A paired with water v/s odor B unrewarded), a specific paradigm was followed. Once the mice had reached a learning performance of > 80% on an odor discrimination training, 'resistance to memory extinction' paradigm was carried out immediately after training is done. This task based on the 'Partial reinforcement theory' was done to stabilize the memory of the learned odors¹⁴³. 100 trials (50 S+ and S-) of the same odor pair was done, however, in this case, only half of the S+ trials were rewarded. This meant that the mouse could no longer reliably anticipate the reward. As the mouse was no longer able to predict the outcome of the trials

due to such a partial reinforcement, theoretically, it paid more attention to the stimulus itself. This strengthened the association of the stimulus type with the reward. We restricted the total number of trials to 100 as carrying it out for extended period could also bring about changes in the rule-learning of mice.

Memory was assessed 30 days after the task that allowed for ‘resistance to extinction’ was carried out for a particular odor pair (for example, A vs. B). Memory trials of A and B odors was assessed in the background of another odor pair (C vs. D). A total of 200 trials were done. First 60 trials were of the background odor pair (C vs. D), which the mouse had already learnt. In the subsequent 7 blocks (20 trials each) of background odor pair, four memory trials (2 of A and 2 of B) were inter-leaved in each block. This means the memory was checked for each odor for a total 28 trials (14 S+ and 14 S-). Memory was calculated as the average percent accuracy achieved for 28 trials per mouse.

1.3.5 Buried food pellet test

This test was done in the arena used for OFT. Mice were food-restricted on a 12 hour cycle. 2-3 days after beginning with the food deprivation, mice were allowed to find the food pellet buried 2cm below the bedding in the arena. This test was done for a total of 5 days with the food pellet buried at different positions in the arena (Figure 1-8, A). The bedding surrounding the food pellet was replenished after the task was carried out for each mouse. On day 6, surface pellet test was done as a control test wherein the food pellet was kept on the surface of the bedding. The behavior was recorded and the latency to find the food pellet per day for each mouse was calculated. This was confirmed and the tracks that mouse took were generated using the Noldus Ethovision 8.5 software.

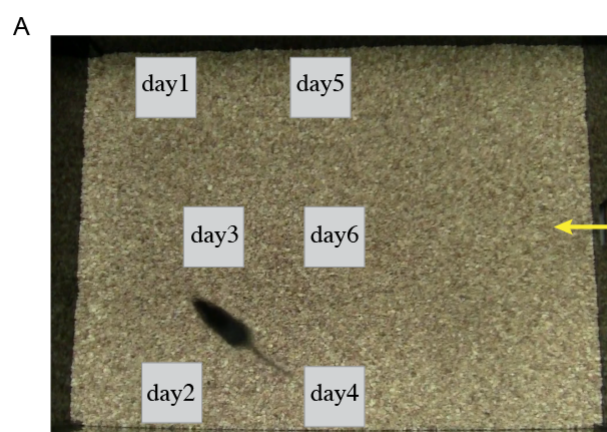


Figure 1-8: Buried food pellet test to assess olfactory detection of appetitive stimulus

A. Image of a mouse carrying out BFPT with laid-out areas marked as days 1 to 6. This defines the location in the arena where the pellet was buried from day 1 to 5. The pellet was kept on surface of the bedding on day 6, as a control test.

1.3.6 Environment Enrichment (EE) paradigm

A custom-built cage made out of acrylic sheet (90 cm X 60 cm X 45 cm) was used as the environmental enriched housing for mice (This work was carried out with Ms. Eleanor McGowan, Master's from University of Glasgow). It had supplies for sensory (smell and touch), motor and cognitive enhancement of the mice that are born and reared in this cage (Figure 1-19). The cage was connected to the existing IVC system using 3 inlets and 3 outlets for entry of clean air and removal of foul air from the cage. Bedding and nesting material were replaced weekly. A raised platform accessed via the stairs was also kept. 2-3 plastic running wheels, tunnels and wooden hut were placed. For olfactory enrichment, 2 cubical odor boxes (5 cm X 5 cm) with 2mm diameter holes on all but one side filled with natural odor sources (table 1-2) were kept. These were replaced every two days. For somatosensory enrichment, Lego (interlocking plastic pieces) as well as cubes with textured surfaces were provided. A maze made out of Lego was put on the raised platform for enhancing cognitive skills. The stairs to reach the maze was also created using Lego pieces. The maze track was changed every week. Food and water were provided *ad libitum*.

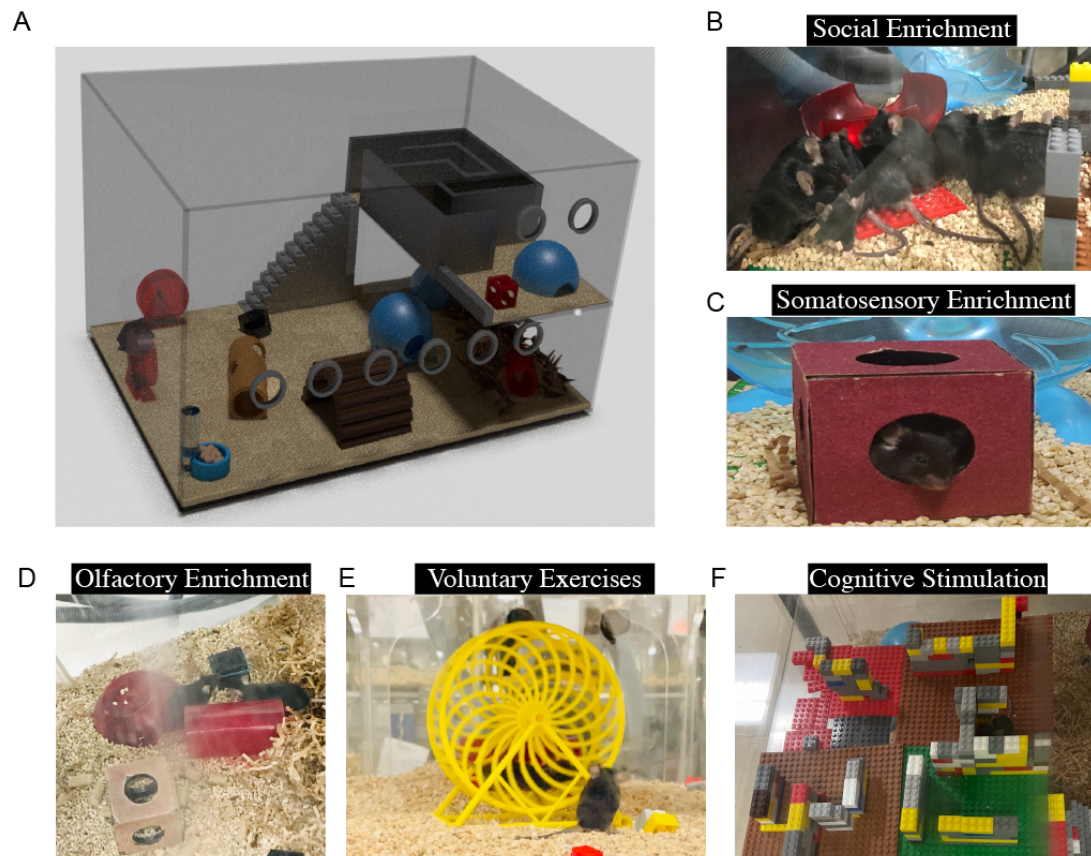


Figure 1-9: A novel Environmental Enrichment paradigm designed in our laboratory

A. Illustration depicting the housing cage used for environmental enrichment of mice (Courtesy: Ms. Eleanor McGowan).

B. Social enrichment as more mice were housed in the EE cage.

C. Tactile cues when mice brushed their whiskers past the sheets of differing textures could lead to somatosensory enrichment.

D. Natural odors present in cubical boxes were replaced every two days during the housing period allowed for olfactory enrichment conditions in the cage.

E. Running wheels, saucers and tunnels were kept for voluntary exercises.

F. Maze kept on the first floor was patterned differently every seven days during the housing period of the mice. Running through the maze could have allowed for cognitive stimulation of mice.

Sr No.	Type of enrichment	Items
1	Social Enrichment	More number of mice housed in a large cage
2	Olfactory Enrichment using Natural odors	Clove, Cardamom, Cinnamon, Almond, Bay leaf, Choco chip, Cumin, Coriander seed, raisin
3	Somatosensory Enrichment	Lego pieces, Cubical toys with textured sheets
4	Cognitive Stimulation	Maze made out of Lego
5	Aerobic Exercises	Running wheels and saucers, tunnels

Table 1-2: Types of enrichment & the required items provided for housing mice

1.3.7 Transcriptomic analysis of Control and EW mice

This part of work was done in collaboration with Ms. Ankita Sharma, SG Lab, IISER-Pune. Olfactory bulbs (pairs per animal) were dissected out and harvested in 500µl of Trizol reagent (Invitrogen, Catalog 15596018). It was lysed in 1mL of RNA iso-plus total RNA extraction reagent (DSS Takara, India). This was followed by carrying out standard extraction protocol. Tissue was homogenised using Pellet Pestle Motor Kontes very briefly. 200µl chloroform was added followed by centrifugation at 12,000 rpm at 4°C for 15 minutes.

Aqueous layer was collected in a fresh tube followed by another chloroform wash. Precipitation was performed by adding 10% of 3M sodium acetate solution and an equal volume of 100% isopropanol containing Glycoblue coprecipitant (Invitrogen, USA) and incubating at -20, °C overnight. RNA was pelleted at 12000g at 4 degrees, 1 hour followed by two washes of 75% ethanol at 12000g, room temperature, 5 minutes. Total RNA was resuspended in nuclease-free water (Ambion) followed by quantification using Qubit RNA HS system (Thermo Fisher Scientific) and RNA integrity (RIN) determination using RNA 6000 Nano Kit on Bioanalyser 2100 (Agilent). RNA samples with RIN value > 8 were used for library preparation. 500ng of total RNA was subjected to mRNA purification using NEBNext Poly(A) mRNA Magnetic Isolation Module (NEB, US) according to the manufacturer's instructions. The purified mRNA was utilized for library preparation using NEBNext Ultra II RNA Library Prep Kit for Illumina (NEB, US) using the protocol provided in the kit. The final libraries were purified using HighPrep PCR Clean-up System (MagBio Genomics, USA). The libraries were quantified using Qubit 1X HS DNA system (Thermo Fisher Scientific). These libraries were pooled in equimolar ratios and subjected to 75bp PE chemistry on Nextseq550, Illumina. The bcl files obtained from sequencing were demultiplexed and converted to fastq files for further analysis. The sequencing reads were aligned to mm10 genome assembly using HISAT2 alignment program. Gene feature counts were calculated using the FeatureCounts package from Rsubread. EdgeR was used to perform differential expression analysis for 3 replicates per group.

1.4 Results

1.4.1 Behavioral characterization of early weaned mice on the anxiety tests

ELS in mice and rats can be induced by using various protocols, from maternal separation during very early postnatal life to maternal deprivation for longer time period or by perturbing the maternal behavior by providing limited nesting and bedding material⁵⁸. The psychological and the emotional effects that a particular protocol of ELS generates, can vary depending on the species and the strain of the animals used¹⁴⁴. To ascertain the behavioral phenotype of the C57BL6/J mice upon early weaning at postnatal day 14, we conducted a battery of tests that are often used to study emotionality (i.e anxiety/depression). We carried out Open Field Test (OFT) to characterize the animals' behavior in an open, novel arena (Figure 1-10). Early Weaned (EW) mice exhibited anxious responses as they spent more time in the corners of the arena, less time in the center and made less number of entries into the central area (Figure 1-10, C1, C2, C4, $p < 0.05$, Unpaired t-test, two-tailed). As compared to control mice (Normal Weaned/NW), their average speed of movement was also significantly lesser and they spent most of the time being immobile in the arena (Figure 1-10, C3, C6, $p < 0.05$ Unpaired t-test, two-tailed). The quantification was done using Noldus Etho-vision software and the animals were tracked using their tip of the nose as the tracking point (Figure 1-5, Methods).

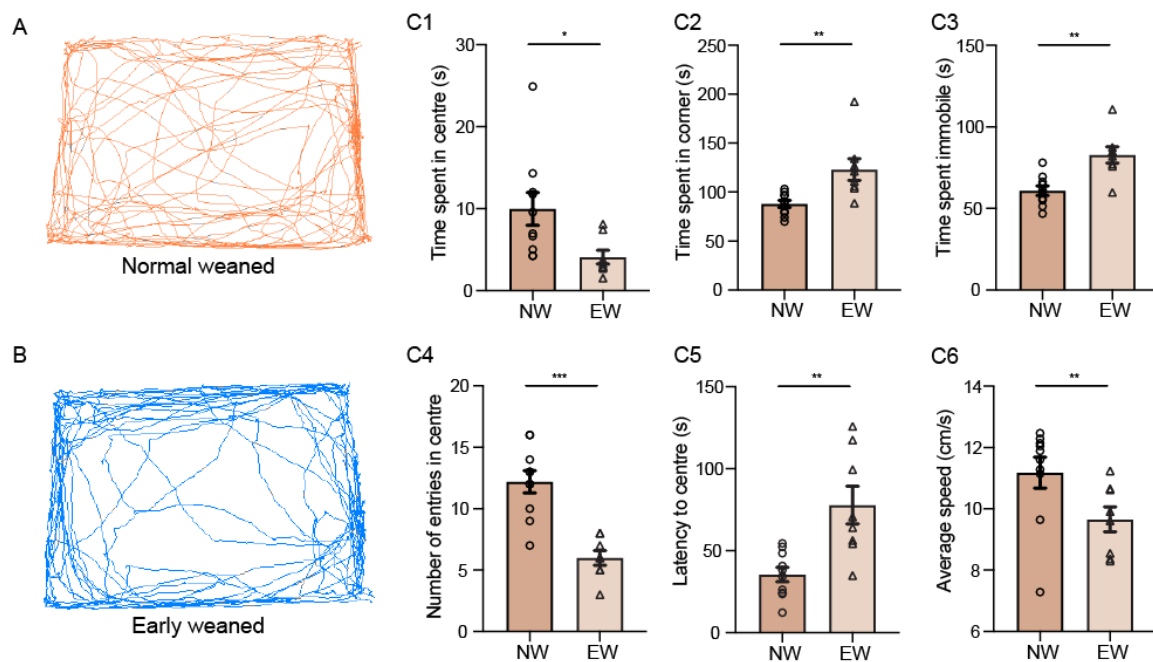


Figure 1-10: Anxiety-like responses of early weaned mice on open field test

A. Representative track traversed by a control, Normal weaned (NW) mouse in the novel arena of the Open Field Test (OFT). Video-tracking of the nose tip of the animals and the behavioral quantification are done using Noldus Etho-vision software.

B. Representative track traversed by an Early weaned (EW) mouse in the OFT indicating more time spent in corners and nearing the walls of the arena.

C1. Decreased time spent in the central area of the arena by EW mice as compared to the NW mice (N = 10 for NW group and N = 8 for EW group; $p = 0.024$ Unpaired t-test, two-tailed).

C2. Increased time spent by EW mice, in the corners of the arena in comparison to NW mice ($p = 0.004$, Unpaired t-test, two-tailed).

C3. The total time spent immobile was significantly more in EW mice ($p = 0.001$, Unpaired t-test, two-tailed).

C4. EW mice made less number of entries into the central, well-lit area of the arena as compared to NW mice ($p < 0.0001$, Unpaired t-test, two-tailed).

C5. The latency, i.e, the time taken to enter the central area for the first time during the session was significantly longer for EW mice ($p = 0.0018$, Unpaired t-test, two-tailed).

C6. The overall average speed recorded in cm/s was slower for EW mice as compared to NW mice ($p = 0.037$, Unpaired t-test, two-tailed).

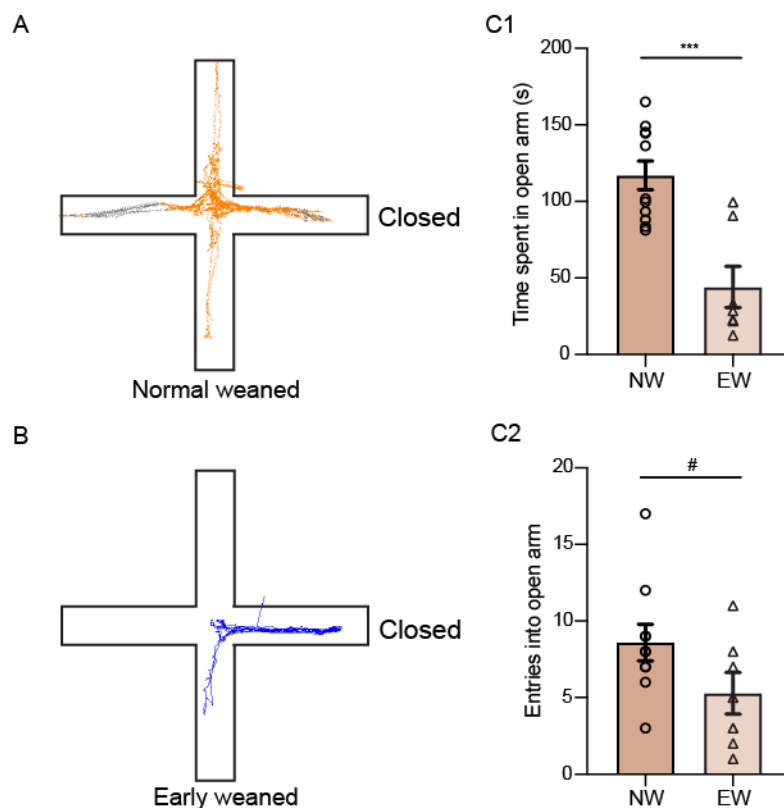


Figure 1-11: Anxiety-like responses of early weaned mice on elevated plus maze test

A. Representative track traversed by a control, Normal weaned (NW) mouse in the arms of the EPM. The mouse moves into both open as well as closed arms. Tracking of the nose tip of the animals and the analysis are recorded using Noldus Etho-vision software.

B. Representative track traversed by an Early weaned (EW) mouse in the EPM shows more time spent in the closed arms.

C1. Bar plot displaying significantly less amount of time spent by EW mice in the open arms of the EPM (N = 11 for NW and 7 for EW mice, $p = 0.0008$, Unpaired t-test with Welch's correction, two-tailed).

C2. EW mice display a trend towards making less number of entries into the open arms of the EPM ($p = 0.088$, Unpaired t-test with Welch's correction, two-tailed).

The anxiety like responses were further checked in another widely used test called the Elevated Plus Maze (EPM) test (Figure 1-5, Methods) (carried out along with Ms. Priya Srikanth). In this, the plus maze consists of two oppositely facing open arms and two closed arms (surrounded with walls) which are raised above the floor. EW mouse exhibited a trend of attempting fewer entries into the open arms and spent lesser time in the open arms (Figure 1-11, C1, $p = 0.0008$ and C2, $p = 0.08$, Unpaired t-test with Welch's correction, two-tailed). This test also, thus, indicated increased anxiety-like responses of EW mice.

These parameters, which are considered as the indices of anxiety measurement, indeed displayed that the EW mice were anxious during their young adulthood (2-3 months of age). We also carried out the OFT, in another cohort of mice, during their late adulthood (>1 year of age) and found that their responses were comparable to the NW mice suggesting that the ELS via EW induced maximal effect during the young age of the mice (Figure 1-12, C1 to C6, $p > 0.05$, Unpaired t-test with Welch's correction, two-tailed).

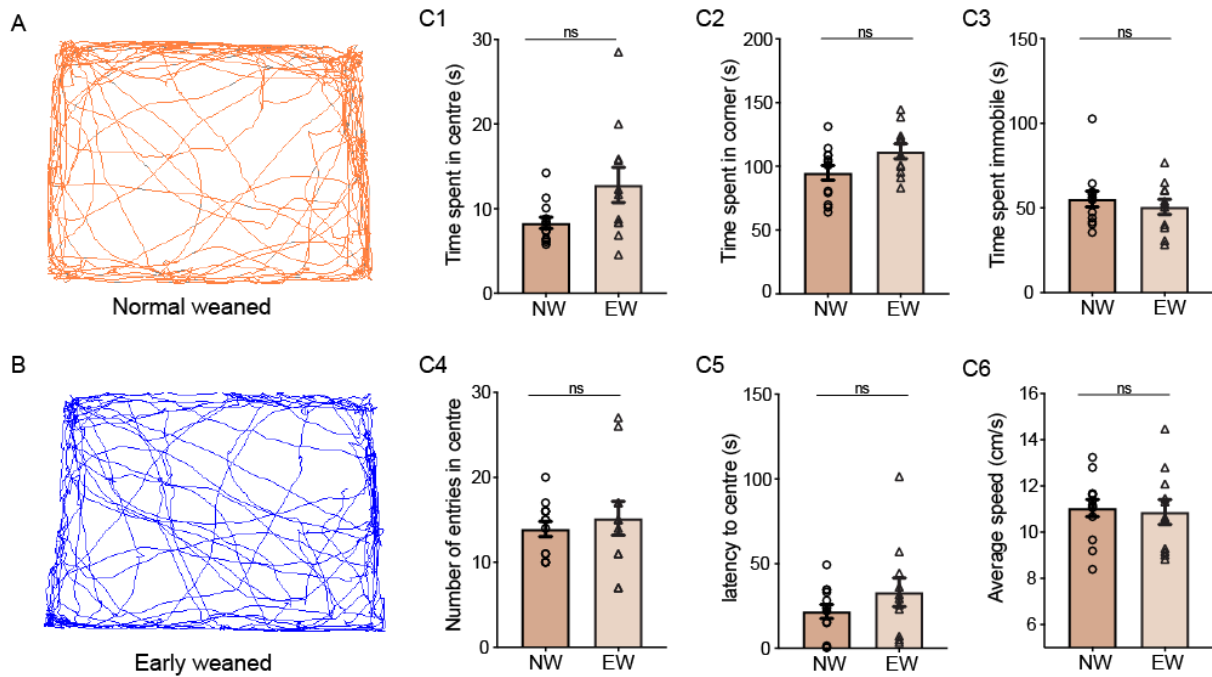


Figure 1-12: Anxiety-like responses were not observed in open field test in aged early weaned mice

A. Representative track traversed by a control, Normal weaned (NW) mouse in the novel arena of the Open Field Test (OFT). Tracking of the nose tip of the animals and the analysis are recorded using Noldus Etho-vision software.

B. Representative track traversed by an Early weaned (EW) mouse in the OFT.

C1. Similar time spent in the central area of the arena by both groups of mice (N = 13 for NW group and N = 11 for EW group; $p = 0.063$, Unpaired t-test with Welch's correction, two-tailed).

C2. Statistically similar time spent by EW mice, in the corners of the arena in comparison to NW mice ($p = 0.053$, Unpaired t-test with Welch's correction, two-tailed).

C3. The total time spent immobile was comparable between the two groups ($p = 0.47$, Unpaired t-test with Welch's correction, two-tailed).

C4. EW mice made number of entries into the central, well-lit area of the arena akin to NW mice ($p = 0.54$, Unpaired t-test with Welch's correction, two-tailed).

C5. The latency, i.e, the time taken to enter the central area for the first time during the recorded session was comparable between NW and EW mice ($p = 0.24$, Unpaired t-test with Welch's correction, two-tailed).

C6. The overall average speed recorded in cm/s was indistinguishable between NW and EW mice ($p = 0.79$, Unpaired t-test with Welch's correction, two-tailed).

EW mice were also tested on Forced swim test (FST) to confirm if they display any depressive symptoms. The time spent mobile vs. immobile in the water in FST by EW mice

were comparable to the NW mice (Figure 1-13, A, B1, $p > 0.05$, Unpaired t-test, two-tailed). Interestingly, in FST, the EW mice during their first minute of entry into the cylinder filled with water stopped their swimming bouts significantly more number of times as compared to NW mice (Figure 1-13, B2, $p > 0.05$, Unpaired t-test, two-tailed). However, over the total duration, the responses were comparable between the two groups. Overall, we found out that both during their young and old adulthood, EW mice exhibited similar responses as the NW mice suggesting that ELS did not induce behavioral despair (i.e depressive behavior) in these mice but primarily an increase in the anxiety (Figure 1-13, D1,D2, $p > 0.05$, Unpaired t-test, two-tailed).

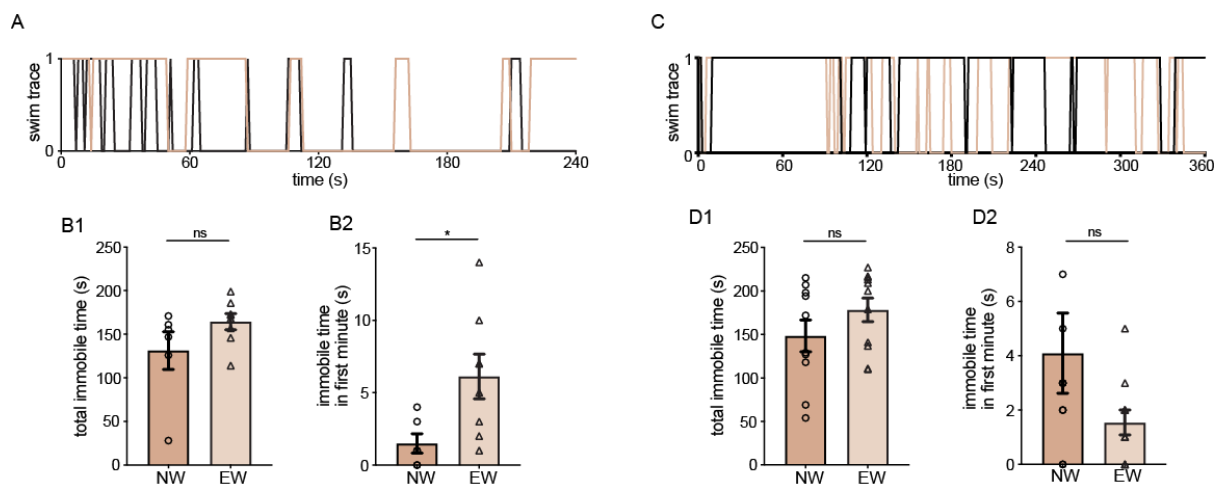


Figure 1-13: Early weaned mice do not exhibit behavioral despair in forced swim test

A. Representative swim trace over the total time of NW (brown) and EW (black) mouse exhibiting immobility during initial phase of swimming in an EW mouse.

B1. Total immobile time during the FST is comparable between the NW and EW groups during young adulthood (N = 6 for NW and 8 for EW mice, $p = 0.14$, Unpaired t-test, two-tailed).

B2. The initial one minute of swim trace indicates more immobility in EW mice as compared to NW mice ($p = 0.03$, Unpaired t-test, two-tailed).

C. Representative swim trace over the total time of NW (brown) and EW (blue) mouse from the aged group.

D1. Total immobile time during the FST is comparable between the NW and EW groups during late adulthood (N = 10 for NW and 11 for EW mice, $p = 0.19$, Unpaired t-test, two-tailed).

D2. No significant difference in immobility in the first minute of the FST between the two groups ($p = 0.107$, Unpaired t-test, two-tailed).

1.4.2 Olfactory food detection ability is not perturbed by early life stress

To begin with, we investigated the ability to detect food odor in EW vs. NW mice. Mice were food restricted at the beginning of the ‘buried food pellet test (BFPT)’. The food restriction allowed for minimal variance in the motivation of the animals to perform the assay. This test was carried out for a total of 5 days (Figure 1-6, Methods). The food pellet was buried 2cm below the bedding, at five different locations across the days of testing. The latency to find the buried food pellet was calculated using Noldus etho-vision software (Figure 1-14, A,B). On day 6, the food pellet was kept on the surface, which served as a control test to verify if the motivation of the mice is not depleted. Indeed, on day 6, all the mice could find the pellet in less than 20 s.

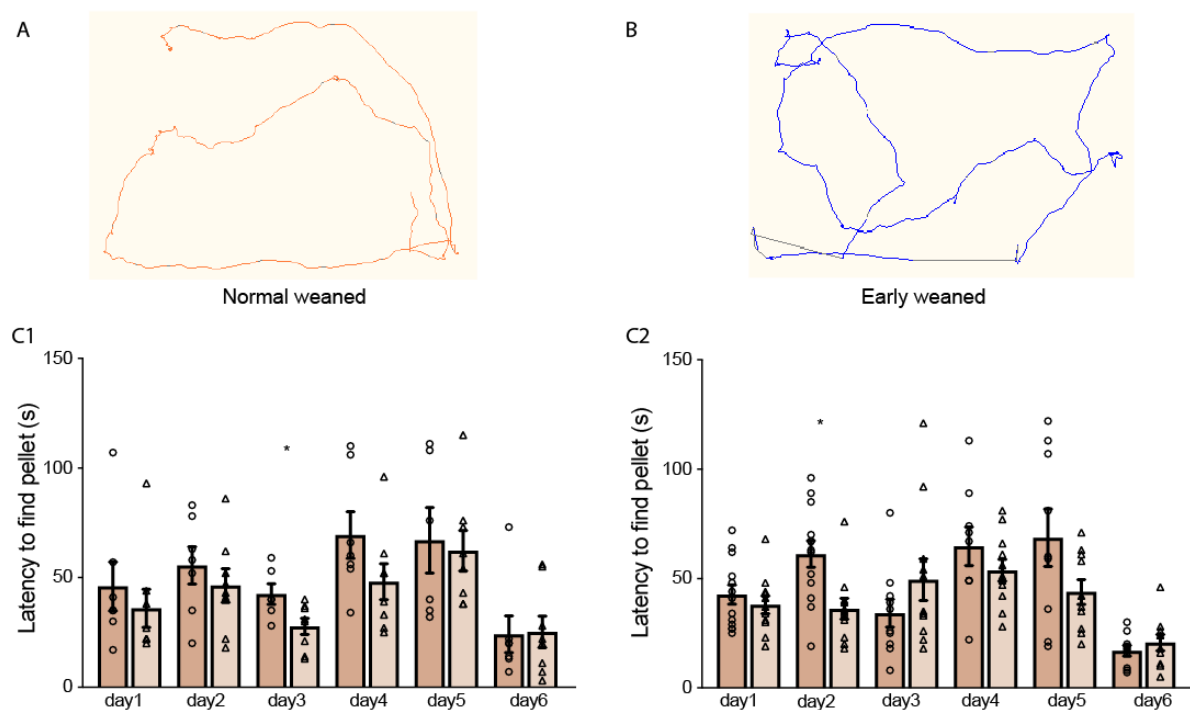


Figure 1-14: Food olfactory detection ability is normal in early weaned mice

A. Representative track of a NW mouse finding the food pellet in the test. Tracking is done using center-point feature of Noldus etho-vision.

B. Representative track of EW mouse finding the buried pellet in the test.

C1. Latency to find pellet from day 1 to day 5 of BFPT shows similar food detection ability in NW and EW groups of mice. Only on day 3, the EW mice had a significantly faster latency. However, on all other days, they take as much time to find the pellet as the NW mice (N = 7-8 for both groups, $p > 0.05$ for all days except day 3 for which $p = 0.03$, Unpaired t-test, two-tailed). On day 6, surface pellet test was done and the latency was much faster.

C2. Latency to find buried food pellet was also checked in the late adulthood of mice indicating similar food detection in both groups of mice on all except day 2 of BFPT (N = 11-13 for both groups, $p > 0.05$ for all days except day 2 for which $p = 0.004$, Unpaired t-test, two-tailed). On day 6, surface pellet test was done and the latency was much faster.

EW young mice found the buried pellet as quickly as the NW mice except on day 3 (Figure 1-14, C1, $p > 0.05$, Unpaired t-test, two-tailed). Across all other days, latency was comparable between the two groups. This was also checked in the old adulthood of mice and similar responses were found in the two groups of mice (Figure 1-14, C2, $p > 0.05$, Unpaired t-test, two-tailed). This test confirmed that the olfactory detection abilities are unaffected by ELS.

1.4.3 Early weaning causes changes in the learning ability but not the threshold of discriminating the odors

The next step was to find out if the olfactory discrimination learning can be altered under conditions of ELS. For this assessment, we used a well-known operant conditioning method, the Go/No-go (GNG) odor discrimination paradigm¹⁰ (Figure 1-6 in methods). Using this paradigm, we trained the mice on a scale of odor dilutions (v/v) starting from highly diluted odors ($10^{-10}\%$) to the perceivable dilution range (all the way up to 1%) (Figure 1-15, A1 to A3). This was carried out so as to figure if the threshold (dilution level) at which the odors can be discriminated are differing between the two groups of mice (Figure 1-15, B1,C1). In this paradigm, water restricted mice had to discriminate one odor which was paired with water reward from the other odor which was unrewarded. Counter-balancing of mice for the odor pairings was done to establish that there is no bias. No punishment was employed if the animal licked for the unrewarded odor.

We observed that the both NW and EW mice could start to discriminate a simple odor pair of acetophenone (AP) vs. Octanal (ON) at the same dilution level albeit with a lower accuracy in EW mice (Figure 1-15, B1, B2). This suggests that threshold to detect and thereby, to start to distinguish between the two odors was similar between the two groups. For AP vs. ON, the odor dilution level of $10^{-4}\%$ was when the learning started to occur (i.e above 60%) and reached to higher accuracy by the end of the task (at 1% odor dilution). However, during the learning period, EW mice learnt at a slower pace (Figure 1-15, B2, $p < 0.001$, $F = 438.8$, Two-way ANOVA, LSD Fisher test, *: $p < 0.05$ for data-points on learning curve). This was

followed by another complex odor pair (binary mix of 60%-40%) of Amyl acetate (AA) vs. Ethyl butyrate (EB) starting from 10⁻⁸% to 1% (Figure 1-15, C1, C2). Here also, we confirmed that the discrimination threshold was similar between the two groups (i.e 10⁻⁶%), however, EW mice learnt the task at a slower pace and thus, exhibit, a decrease in the olfactory learning ability (Figure 1-15, C2, $p < 0.001$, $F = 38.23$, Two-way ANOVA, LSD Fisher test, *: $p < 0.05$ for data-points on learning curve). We thus confirmed, that the discrimination threshold of the mice are unaffected by ELS, suggesting a specific learning deficit. In order to confirm that, we then carried out a series of simple and complex odor pairs with another cohort of mice at 1% dilution for which we assessed the learning as well as the memory. This part is discussed in the subsequent section.

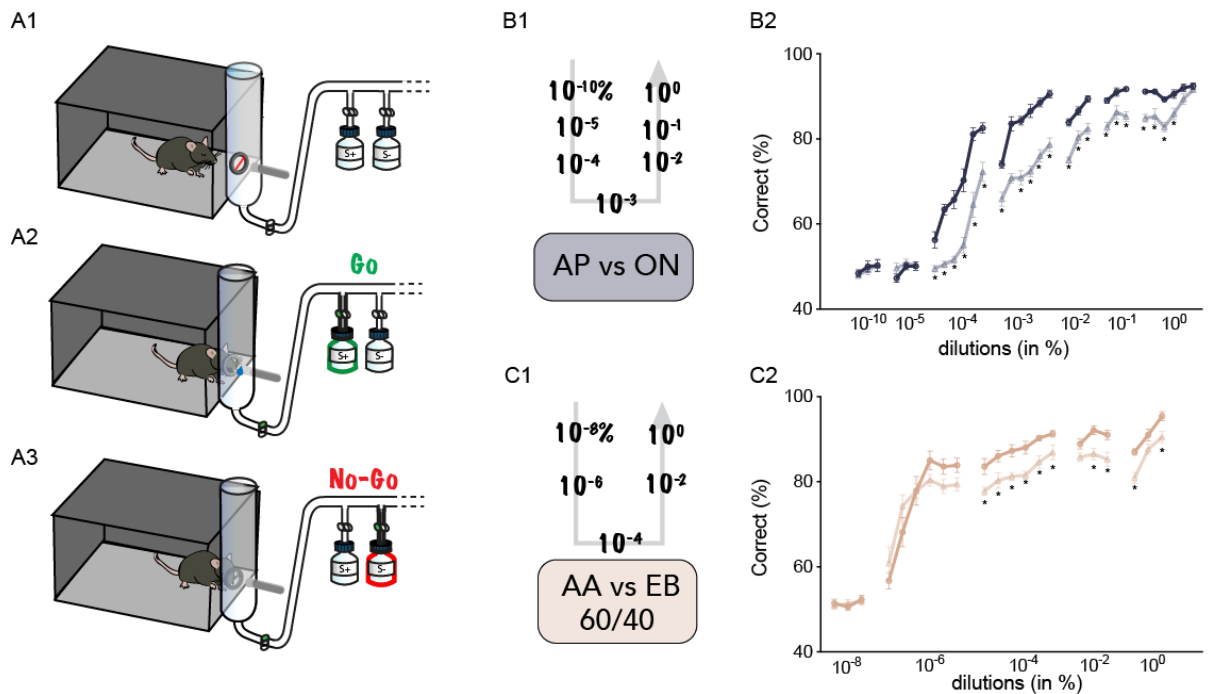


Figure 1-15: Odor discrimination threshold is not perturbed by early life stress

A1. Diagram displaying a water-restricted mouse in the chamber of the freely moving olfactometer used for carrying out Go/No-go odor discrimination paradigm. The sampling port is guarded by an IR beam which breaks when the mouse pokes its snout into the tube. Two types of odors, S+ (i.e rewarded) and S- (unrewarded) are provided (two bottles connected to the sampling tube), one at a time, for training the mice to be able to discriminate between the two.

A2. A 'Go' response is initiated by the mouse when S+ odor is presented. If the mouse does the trial correctly, it receives the water reward.

A3. A 'No-Go' response is initiated by a mouse who has learnt to discriminate. This response is towards S- odor, i.e, the animal retracts its head away from the port, after sampling the presented S-odor.

B1. Schematic of the dilution levels of odor pair AP vs. ON used for training the two groups of mice starting from 10⁻¹⁰% to 1% of odors diluted in mineral oil.

B2. Learning curve of NW (dark grey) vs. EW (light grey) mice on AP vs. ON discriminating learning over increasing levels of dilutions. Both groups started to distinguish odors from 10⁻⁴%, however, EW mice, showed a slower learning pace throughout the course of training (N = 7 for NW mice and 8 for EW mice, $p < 0.001$, $F = 438.8$, Two-way ANOVA, LSD Fisher test, *: $p < 0.05$ for data-points on learning curve).

C1. Schematic of the dilution levels of the binary mix (60% -40%) of odor pair AA vs. EB used for training the two groups of mice starting from 10⁻⁸% to 1% of odors diluted in mineral oil.

C2. Learning curve of NW (dark grey) vs. EW (light grey) mice on AA vs. EB 60-40 discrimination learning over increasing levels of dilutions. Both groups started to distinguish odors from 10⁻⁶%, however, EW mice, showed poorer learning pace throughout the course of training from 10⁻⁴ to 1% suggesting a specific sensory-cognitive learning deficit ($p < 0.001$, $F = 38.23$, Two-way ANOVA, LSD Fisher test, *: $p < 0.05$ for data-points on learning curve).

1.4.4 ELS induces olfactory learning and memory impairments in mice

We utilized an array of simple monomolecular and binary mixes of odor pairs across different chemical classes (Table 1-1, Methods) to test olfactory learning capabilities of EW mice on GNG odor discrimination paradigm (Figure 1-15, A1 to A3). To assess the learning, we used the measure of signal detection theory, called the d-prime (d') to quantify the responses of the animals¹⁴⁵. As the d-prime measurements takes into account both the hit trials (correctly doing a rewarded trial) and the false alarm trials (incorrectly licking for a unrewarded trial), we considered it to be useful in quantifying the discriminatory learning behavior of EW mice who made the errors in responding to both the rewarded and the unrewarded odors (Figure 1-16, A, B1, B2).

The training was generally done over a total of 900 (450 rewarded and 450 unrewarded) trials. Representative plots of the Hit and false alarm rates across different mice from NW group (circular data points) from the first 100 trials of learning to the last 100 trials of learning are shown in Figure 1-16, C1 to C9. During the initial phase of the discrimination learning, the probability of doing a hit was equally likely to doing a false alarm, and therefore, we observe all mice clustered towards the right top quadrant (Figure 1-16, C1 to

C5). The d' , in this, case ranges from 0 to 1.6. Over the learning, the hit rate increases and the false alarm decreases causing the cluster to shift towards top left corner (Figure 1-16, C6 to C9). At this point the d' value ranges between 2 to 3.

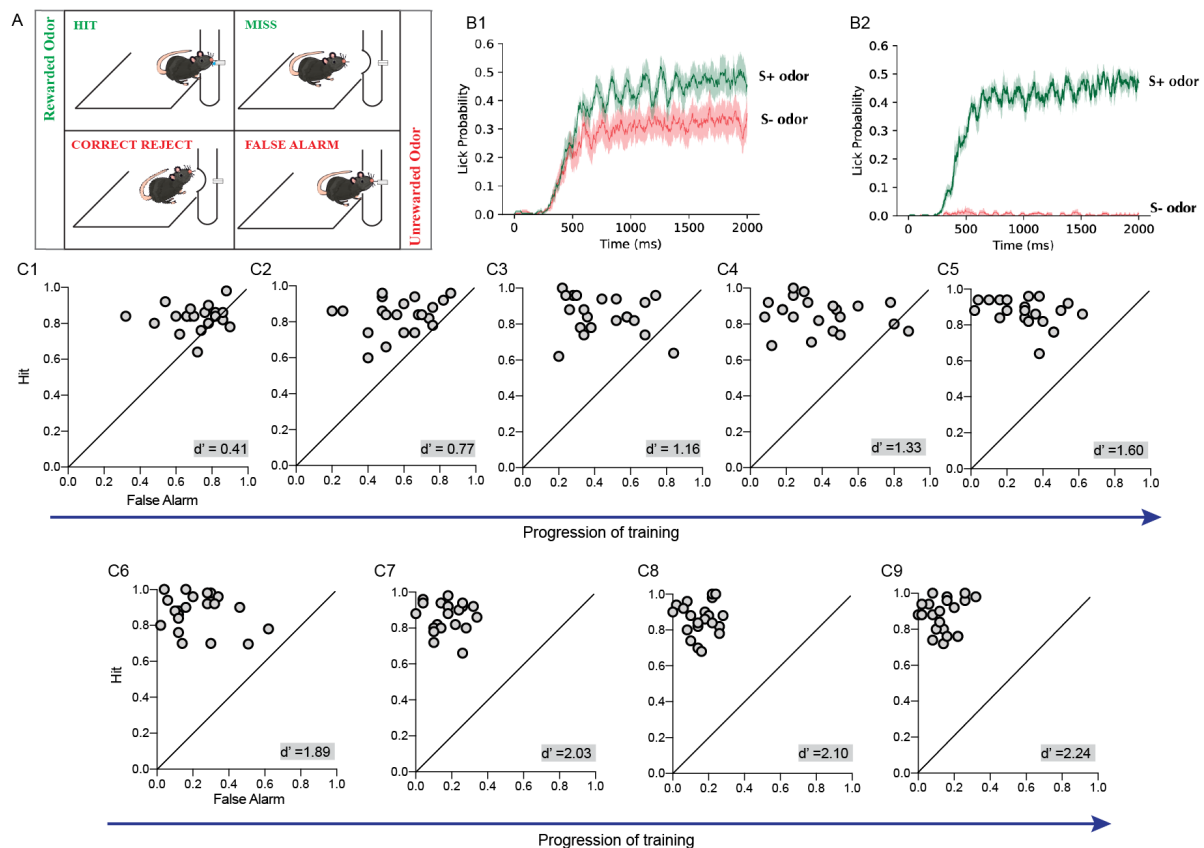


Figure 1-16: Assessment of olfactory learning capabilities

A. Schematic diagram showing four typical responses towards the two kinds of stimuli in a GNG paradigm. In case of rewarded odors presentation, mouse either performs a hit response when it licks for the S+ odor & receives the water reward or misses the reward by doing the trial incorrectly. In case of unrewarded odor, the mouse either correctly responds to S- trial by not licking onto the lick tube (or minimal licking) and thus, performs a correct reject or licks for the S- odor constituting a false alarm response.

B1. Lick probability for S+ and S- odors over the total stimulus duration during the initial phase of learning, averaged over a total of 100 trials. The difference in the lick probability is low when the animal is unable to distinguish between the two odors.

B2. Lick probability for S+ and S- odors over the total stimulus duration during the advanced phase of learning, averaged over a total of 100 trials. The licking for S- trials is very low and thus, the lick probability nears 0. The difference in the licking for the two odors indicates that animal can discriminate accurately

C1-C9. Plots representing the animal-wise distribution (each circular data-point) on the Hit-False alarm probability graph over the progression of training. Each plot has an average value of hit-false

alarm for 100 trials starting from 0-100 trials (C1) to the final phase of learning, 800-900 trials (C9). The d' values, written, on each plot is increasing as the distinction between the two odors are unravelling. Initially, the points are clustered towards top-right, however, with training, the probability of hit nears to 1 while that of false alarm to 0, causing the cluster to shift to top-left.

We began with a simple odor pair of Methylbenzoate (MB) vs. Nonanol (NN) for which we carried out a total of 1200 trials. We found significantly lowered d' for EW mice suggesting a deficit in the discriminating learning (Figure 1-17, B, $p = 0.04$, $F = 4.5$, Two-way ANOVA, LSD Fisher test, $p < 0.05$ for datapoints with asterisk). This learning deficits was also observed for the corresponding odor pairs on which the animals were trained, i.e, AP vs. ON, binary mix (60%-40%) of AP vs. ON, AA vs. EB and AA vs. EB (60%-40%) (Figure 1-17, C to F, $p < 0.05$ Two-way ANOVA, LSD Fisher test).

However, as the training progressed, EW mice were able to perform the task at a slightly faster pace (Figure 1-17, H, Cineole vs. Eugenol and I, it's binary mix) and acquired the pace of NW mice for the last complex odor pair of carvone enantiomers, (Figure 1-17, J, C+ vs. C-). This could happen as a result of extensive training such that the 'rule learning' of the task might have improved over the total 7 odor pairs and 2 memory tasks¹⁴⁶. On the other hand, it could also be a reflection of the negligible effect of ELS during the late adulthood of mice as was also reflected in the OFT test (Figure 1-12). However, to confirm if there is an age-dependence, we took a subset of mice from the existing cohort of mice and trained them for two odor pairs AP vs. ON and C+ vs. C- (60-40) during their late adulthood (> 1.5 years) (Figure 1-18, Work done along with Ms. Meher Kantroo, BSMS student at IISER Pune). These mice were not trained for a period of 6 months before the subsequent olfactory training in their old age. Thus, the aspect of rule learning should get abrogated over the non-training phase. We found out that even during late adulthood, the pace of the olfactory discrimination learning was slower in EW mice (Figure 1-18, A, B, $p < 0.05$, Two-way ANOVA, LSD Fisher test, $p < 0.05$ for all data points with asterisk), however, it was not as pronounced as in their young age. Although the involvement of rule learning in mediating faster learning over extensive training period needs to be closely studied, we concluded that the advancement in age had a minimal effect on the learning impairment that we observed.

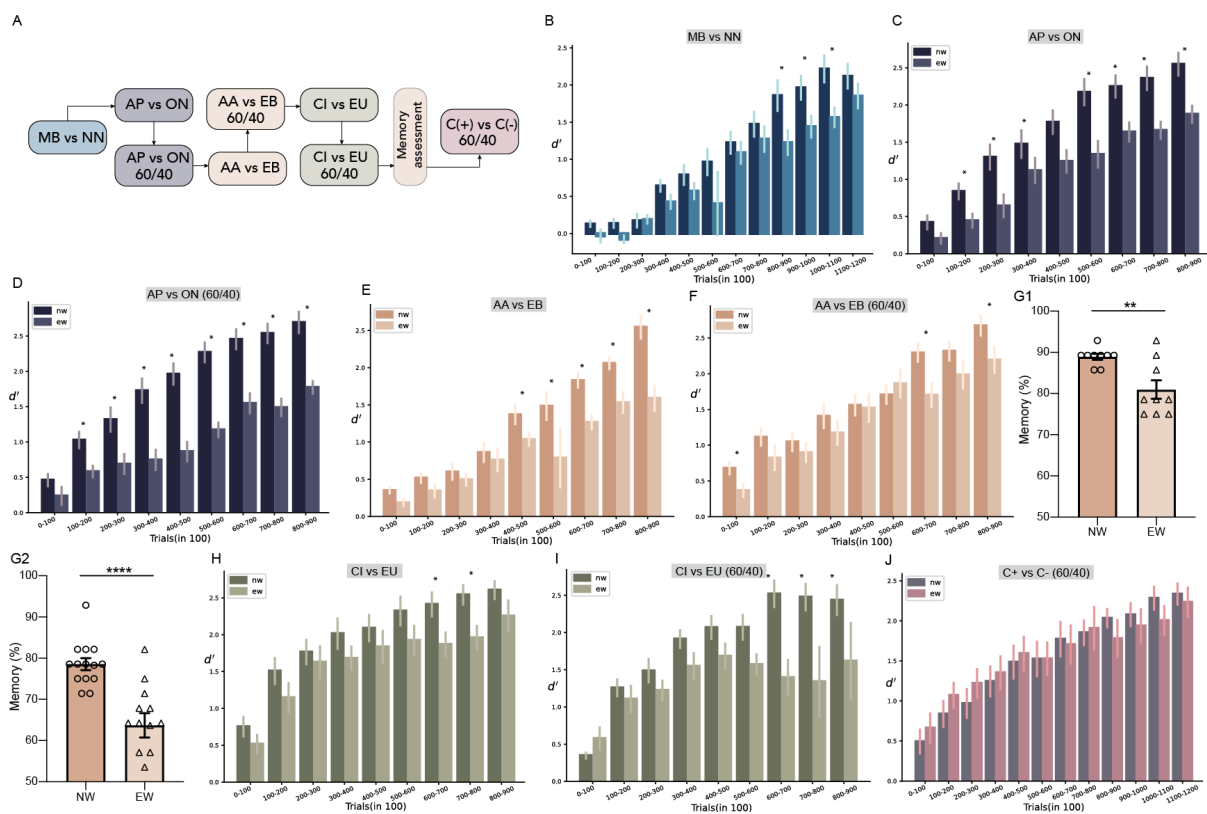


Figure 1-17: Early life stress induces poor olfactory learning and memory in mice

A. Schematic diagram showing the series of odor pairs (1% dilution) used in GNG paradigm to assess olfactory learning and memory capabilities of EW mice.

B. Bar plot showing increase in d' values over the trials, plotted in 100. Compared to NW group (dark blue), the EW mice (teal) learnt the MB vs. NN task at a slower rate (N = 15-19 for both groups, $p = 0.04$, $F = 4.5$, Two-way ANOVA, LSD Fisher test, $p < 0.05$ for datapoints with asterisk).

C. d' values plotted as bars for NW (dark gray) and EW (light gray) groups shows olfactory learning impairment in learning AP vs. ON odor discrimination ($p = 0.0013$, $F = 12.08$, Two-way ANOVA, LSD Fisher test, $p < 0.05$ for datapoints with asterisk).

D. Decreased olfactory learning in EW mice shown as slower increase in d' values over training period of the complex task of discriminating the binary mixes of AP vs. ON ($p < 0.0001$, $F = 30.2$, Two-way ANOVA, LSD Fisher test, $p < 0.05$ for datapoints with asterisk).

E. Slower olfactory learning rate for AA vs. EB odor discrimination in EW mice ($p = 0.003$, $F = 9.94$, Two-way ANOVA, LSD Fisher test, $p < 0.05$ for datapoints with asterisk).

F. As the training of odor pairs proceed, the learning impairment in EW mice tended towards improvement as seen in the discrimination task of AA vs. EB (60/40) ($p = 0.17$, $F = 1.9$, Two-way ANOVA, LSD Fisher test, $p < 0.05$ for datapoints with asterisk). This could possibly occur due to the strengthening of the ‘rule learning’ aspect as a result of extensive training.

G1. Olfactory memory of AA vs. EB plotted as the accuracy of remembering the association, one month after the training of the odor pair was carried. Significant reduction in olfactory memory is observed in EW group (N = 9 for both groups, $p = 0.0037$, Unpaired t-test, two-tailed).

G2. Olfactory memory impairment was also observed in the complex task of AA vs. EB (60/40) in EW mice (N = 14 for NW and 13 for EW group, $p = 0.023$, Unpaired t-test, two-tailed).

H, I, J. The olfactory learning impairment reduced in EW mice for the subsequent odor pairs used for training, CI vs. EU ($p = 0.11$, $F = 2.5$, Two-way ANOVA, LSD Fisher test, $p < 0.05$ for datapoints with asterisk), its binary mix CI vs. EU 60-40 ($p = 0.015$, $F = 6.5$, Two-way ANOVA, LSD Fisher test, $p < 0.05$ for datapoints with asterisk) and that of Carvones 60-40 ($p = 0.97$, $F = 0.0009$, Two-way ANOVA, LSD Fisher test).

We also tested for olfactory memory for AA vs. EB and its binary mix one month after the training of the respective odor pairs was carried out (Figure 1-17, G1, G2). The acquisition of memory was based on the theory of partial reinforcement¹⁴³. After the 900 trials of training for an odor pair was done, an additional 200 trials were carried out. In this additional phase, only half of the S+ trials were rewarded. The principle behind carrying this out was that the animals will pay more attention to the odor-value association which would strengthen their ability to remember and recall it at a later time point. During the memory recall task, animals were firstly trained on a yet another odor pair. Once they reached the criterion performance of $> 85\%$ on this odor pair, the memory trials (i.e. that of AA or EB) were interleaved in between the trials of the other odor pair. 28 memory trials (i.e. 14 S+ and 14 S-) for a total of 140 trials (i.e. 112 trials of the other odor pair) were tested. For the memory trials, the reward was not given to the mice as the recall of the reward-value association was indeed being checked. We restricted to a total of 28 trials per animal as we did not want the animals to unlearn and re-learn the associations. An average accuracy from these 28 trials was then calculated per mouse. We found out that for both the odor pairs, the NW mice achieved an average memory (%) values of 89% and 78.5% which were significantly higher than that of EW mice who could perform the memory task at 80.9% for AA vs. EB and 63.7% for the binary mix of AA vs. EB, respectively (Figure 1-17, G1, G2, $p < 0.05$, Unpaired t-test, two-tailed). Our experiments, thus, revealed that ELS due to early weaning affected the olfactory learning and memory capabilities of the mice.

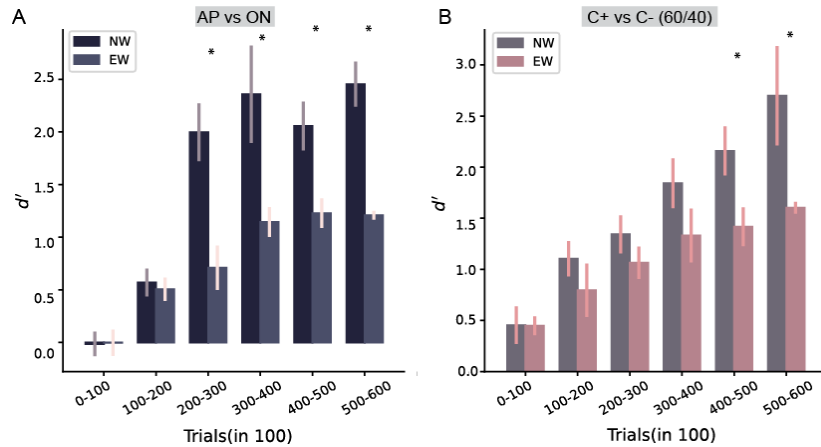


Figure 1-18: Effect of early life stress persists in the aged mice

A. Bar plot of d' values across AP vs. ON training for NW (dark gray) vs. EW (light gray) mice in their old adulthood (1.5 years of age) exhibit decreased learning pace for EW mice, even, in old adulthood ($N = 6$ for NW and 5 for EW groups, $p < 0.0001$, $F = 35.49$, Two-way ANOVA, LSD Fisher test, $p < 0.05$ for all data points with asterisk).

B. Slower learning pace was also shown for discriminating the binary mix (60/40) of Carvones odor pair by aged EW mice (mauve) as compared to old NW mice (dark mauve) ($p = 0.001$, $F = 12.01$, Two-way ANOVA, LSD Fisher test, $p < 0.05$ for all data points with asterisk).

Finally, as a control test, we also carried out the task of using Mineral oil (MO) as both the rewarded and the unrewarded odor for the subset of mice from the same groups. MO, which is the diluent used for preparing the odors for training, is minimally odorous on its own. For, MO vs. MO task, if the animals are not picking up any other cue apart from the olfactory ones, the learning should remain at chance level, i.e., at 50%. We did 600 trials of MO vs. MO on both NW and EW groups of mice to confirm that the olfactory learning impairment that was seen in EW mice was indeed due to their inability to discriminate odors. In other words, no other cue was affecting their performance. The d' values for the whole task remained near to 0 for both the groups suggesting the learning was reliably based on the odor cues (Figure 1-19, A).

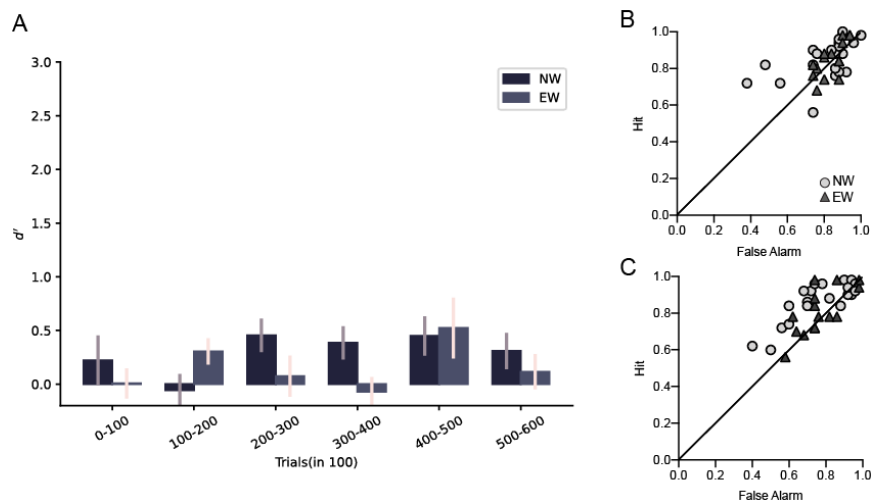


Figure 1-19: Odor discrimination learning is not dependent on other sensory cues originating from the olfactometer

A. Bar plot of d' values of NW and EW mice on a MO vs. MO task. The values range from -0.2 to 0.5 as an average of 100 trials over a total of 600 trials suggesting no other cue was affecting the learning (N=7 for NW and 5 for EW group).

B. Animal-wise distribution on a hit-false alarm probability plot for the first 300 trials of training on MO vs. MO. Each data point is for 100 trials per mouse.

C. Animal-wise distribution on a hit-false alarm probability plot for the last 600 trials of training on MO vs. MO. Each data point is for 100 trials per mouse.

1.4.5 Environment enrichment rescues the anxiety responses of early weaned mice

EE was employed as an extrinsic strategy to observe if ELS induced olfactory impairments could be rescued. EE housing is known to have a positive impact on the brain, improving, both the sensory as well as the cognitive skills of the animals¹³. This was carried out along with a MSc. student, Ms. Eleanor McGowan (University of Glasgow). In an EE housing arrangement (Figure 1-20, B), there are increased occurrences of social interactions as more mice are put together and the provision of stimulating sensory and motor activity materials (Figure 1-9, see Materials and methods, section 1.3.6). EE can exert its effects at several levels of the physiology of the animal, and, we began to measure its effect at the behavioural level. We had two parallel cohorts of NW and EW mice raised in separate EE cages (Figure 1-20, A,B). Pregnant dams were introduced in the EE cage and at PND14, dams as well as the female pups were removed in the case of EW mice. Dams and female pups of NW pups were removed at PND28 (Figure 1-20, C).

We carried out OFT and EPM to investigate if EE helped in reducing the anxiety-like responses of the EW mice. Indeed, the EE raised EW mice performed better at the anxiety tests. They spent more time in centre, lesser time in corners and made more number of entries in centre as compared to standard cage housed EW mice (Figure 1-20, D1 to D4, $p < 0.05$, Ordinary One-way ANOVA with LSD Fisher test). Even in EPM, the EE-EW mice made more number of entries and spent more time in the open arms of the maze as compared to the EW mice (Figure 1-20, E1, E2, $p < 0.05$, Ordinary One-way ANOVA with LSD Fisher test). Even the EE housed NW mice had better responses than the standard cage housed NW mice which was primarily observed in the OFT (Figure 1-20, D1, D4, $p < 0.05$, Ordinary One-way ANOVA with LSD Fisher test). This suggests that the EE housing allowed for an anxiolytic strategy for EW mice. We further wished to investigate the positive outcomes of EE, if any, on the olfactory behavior of the mice.

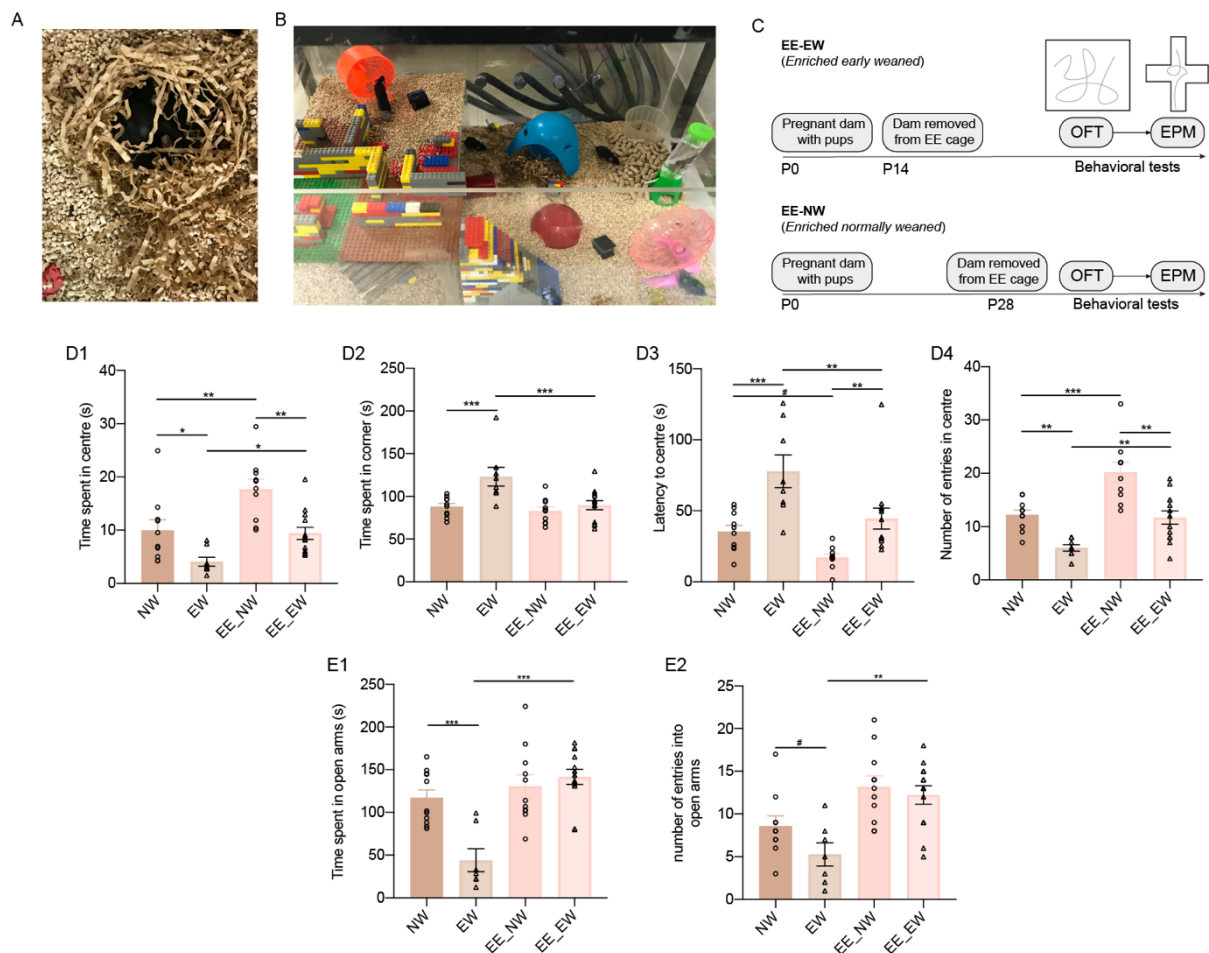


Figure 1-20: Environmental enriched housing rescues anxiety-like responses of early weaned mice

A. Pregnant dams were introduced into the EE cage. They formed a nest in the cage for nursing and caring of the pups. The pups stayed with dam till either postnatal day 14 (P14) or postnatal day 28 (P28) depending on the group to which they belonged.

B. Picture of EE cage with the air supplied from the IVC inlets. Picture depicts involvement of mice with the sensory stimuli (textured materials, natural odorous substances), doing voluntary exercises (running wheels and saucers) and engaging in cognitive tasks such as passing through the maze. Food and water were provided *ad libitum*.

C. Experimental timeline depicting the postnatal days dams were removed from the cage depending on whether it constituted the EE-EW (Enriched early weaned) or EE-NW (Enriched normally weaned) groups. This was followed by carrying anxiety tests, open field test and elevated plus maze test at 2 months of their age.

D1. EE-EW and EE-NW mice tended to spend significantly more time in the central area of OFT arena as compared to EW ($p = 0.02$, Ordinary One-way ANOVA with LSD Fisher test) and NW mice ($p = 0.001$, Ordinary One-way ANOVA with LSD Fisher test), respectively ($N = 8-13$ across all the four groups). The time spent in central area was significantly more for EE-NW as compared to EE-EW mice ($p = 0.0003$).

D2. EE-EW mice displayed decrease in the time spent in the corners of the arena, suggesting decreased anxiety and an increased motivation to explore the novel arena ($p = 0.0006$, Ordinary One-way ANOVA with LSD Fisher test).

D3. The latency to enter to the central area was significantly reduced for EE-EW mice as compared to standard cage reared EW mice ($p = 0.001$, Ordinary One-way ANOVA with LSD Fisher test). However, this was even faster for EE-NW mice as compared to the EE-EW mice ($p = 0.005$).

D4. Number of entries made into the central area also got improved in the EW mice reared in EE cage ($p = 0.004$, Ordinary One-way ANOVA with LSD Fisher test). However, this was still lesser than what was found in EE-NW mice ($p < 0.0001$). Overall, EE-EW mice exhibit clear decrease in anxiety, although, lesser than what was displayed by EE-NW mice.

E1. In case of EPM test as well, the EE-EW mice spent significantly more time in the open arms of the maze as compared to EW mice ($p = 0.0006$, Ordinary One-way ANOVA with LSD Fisher test). This was even comparable with the EE-NW mice ($p = 0.55$).

E2. EE-EW mice made more number of entries into the open arms as compared to EW mice ($p < 0.0001$, Ordinary One-way ANOVA with LSD Fisher test).

1.4.6 Environmental enriched housing ameliorates olfactory learning deficits in early weaned mice

The betterment in the anxiety responses of EE-EW mice led us to investigate if olfactory learning and memory can also be improved in the EE mice. To this end, we used both simple

and complex odor pairs namely, MB vs. NN, AP vs. ON, binary (60%-40%) of AP vs. ON and CI vs. EU . We trained both sets of EE-NW (control) as well as EE-EW (experimental) mice on the GNG odor discrimination paradigm. We also evaluated the olfactory memory for AP vs. ON odor pair one month after the respective trainings were finished. The memory data of these mice are compared with NW and EW mice trained on the head-restrained set-up.

We found out that the EE reared mice started to distinguish the odors from the first 100-200 trials of the discrimination training. A stark increase in the learning abilities of these mice were observed throughout the duration of the training period with the d' value reaching an average value of 3.24 for EE-EW group as compared to 1.59 for EW group for the last 100 trials of the MB vs. NN training (Figure 1-21, A, $p < 0.0001$, $F = 561.1$, Two-way ANOVA, LSD Fisher test, $p < 0.05$ for all data points with asterisk). Even for a complex AP vs. ON task, the d' for EE-EW reached to 3.64 in the final phase, while that of EW reached to 1.77 (Figure 1-21, C, $p < 0.0001$, $F = 522.5$, Two-way ANOVA, LSD Fisher test, $p < 0.05$ for all data points with asterisk).

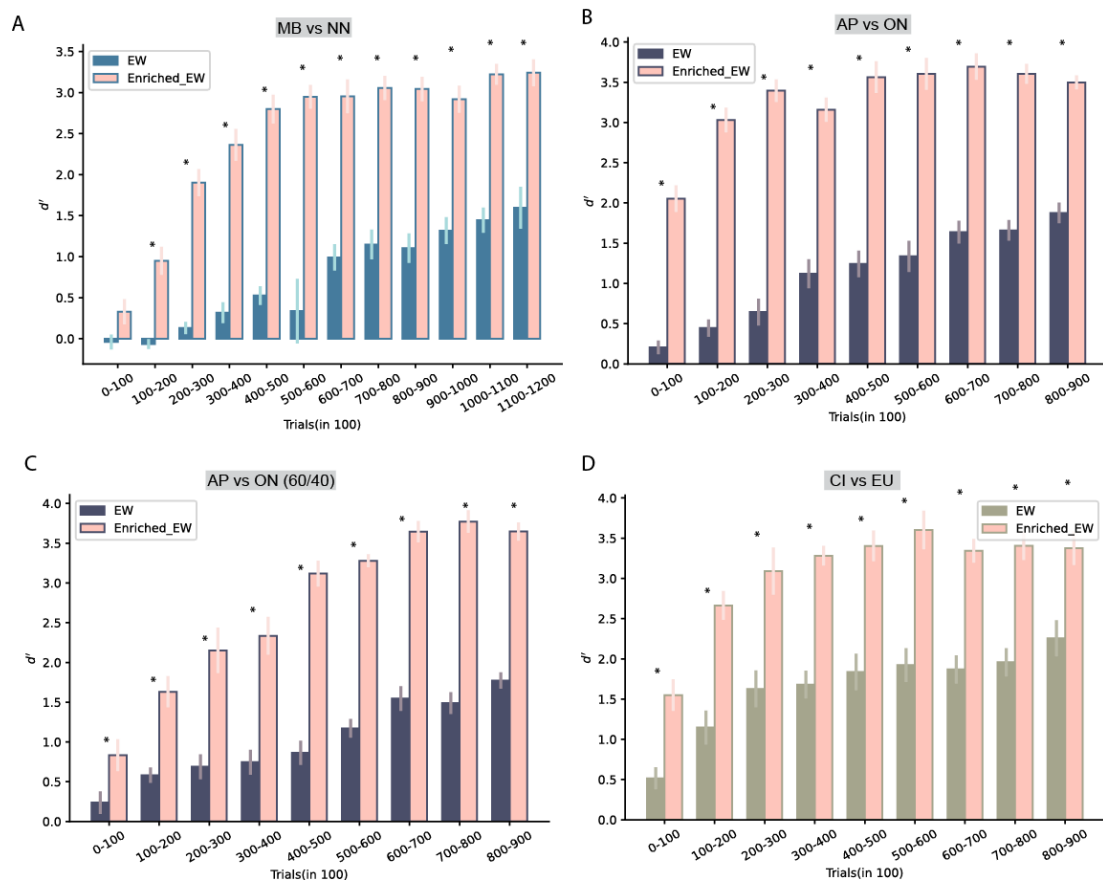


Figure 1-21: Environment enrichment ameliorates olfactory learning deficits in early weaned mice

A. A marked increase in the d' throughout the course of training of MB vs. NN was observed in EE-EW mice as compared to the EW mice ($N = 17$ for EW and 13 EE-EW mice, EW dataset is taken from the previous set of experiments shown in Figure 1-17, $p < 0.0001$, $F = 561.1$, Two-way ANOVA, LSD Fisher test, $p < 0.05$ for all datapoints with asterisk).

B. EE-EW continued to exhibit significantly improved performance on the olfactory GNG task ($p < 0.0001$, $F = 891.7$, Two-way ANOVA, LSD Fisher test, $p < 0.05$ for all datapoints with asterisk).

C. For complex task of distinguishing the binary mix of AP vs. ON (60/40), EE-EW learnt at a faster rate as seen by the higher d' values across the training ($p < 0.0001$, $F = 522.5$, Two-way ANOVA, LSD Fisher test, $p < 0.05$ for all datapoints with asterisk).

D. An increase in learning pace was also observed for CI vs. EU odor pair in EE-EW mice ($p < 0.0001$, $F = 225.9$, Two-way ANOVA, LSD Fisher test, $p < 0.05$ for all datapoints with asterisk).

To observe if we had the complete rescue of olfactory learning deficit, we also housed NW control mice in an EE setting, the same way as was done for EE-EW mice. The olfactory learning capabilities of NW mice raised in EE cage were improved for all the odor pairs that were used (Figure 1-22, A to D). For example, for MB vs. NN training, the d' value of EE-NW mice reached to 3.54 in the final 100 trials of the task as compared to 1.96 for the NW mice (Figure 1-22, A, $p < 0.0001$, $F = 523.3$, Two-way ANOVA, LSD Fisher test, $p < 0.05$ for all datapoints with asterisk). Even for a complex task of the binary mix of AP vs. ON, the d' value increased to 3.43 in the final phase of learning in the case of EE-NW mice while for NW mice, it increased to 2.69 (Figure 1-22, C, $p < 0.0001$, $F = 135.4$, Two-way ANOVA, LSD Fisher test, $p < 0.05$ for all datapoints with asterisk).

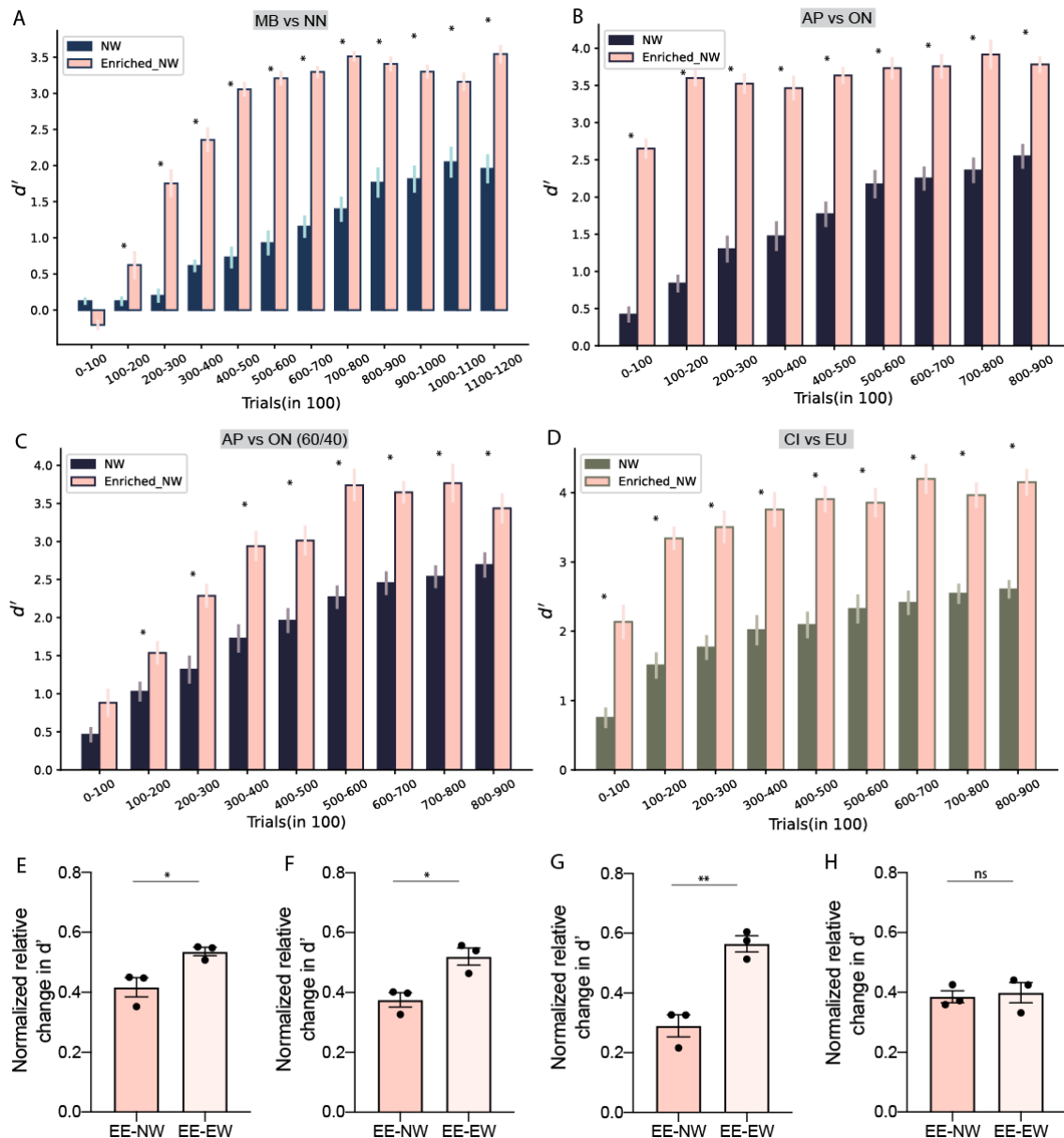


Figure 1-22: Environment enrichment improves olfactory discrimination learning abilities

A. An increase in the learning pace of discriminating MB vs. NN was observed in EE-NW mice as compared to NW mice as seen with a significant uptrend of d' values (N 21 = for NW and 12 EE-NW mice, NW dataset is taken from the previous set of experiments shown in Figure 1-17, $p < 0.0001$, $F = 523.3$, Two-way ANOVA, LSD Fisher test, $p < 0.05$ for all datapoints with asterisk).

B. An increase in the discrimination of AP vs. ON ensued in EE-NW mice ($p < 0.0001$, $F = 528.3$, Two-way ANOVA, LSD Fisher test, $p < 0.05$ for all datapoints with asterisk).

C. Even for complex mix of AP vs. ON discrimination task, EE-NW performed at a faster rate, although, the initial phase of learning was comparable to that of standard caged NW mice ($p < 0.0001$, $F = 135.4$, Two-way ANOVA, LSD Fisher test, $p < 0.05$ for all datapoints with asterisk).

D. Yet again, for the next odor pair in sequence, a simple CI vs. EU task displayed an improved learning in EE-NW mice ($p < 0.0001$, $F = 302.7$, Two-way ANOVA, LSD Fisher test, $p < 0.05$ for all datapoints with asterisk).

E, F, G, H. Relative change in the d' values between 'EE-NW and NW' versus 'EE-EW and EW' groups were compared for the final phase of learning, i.e, the last 300 trials. The values were normalized to the EE d' values for the respective groups. An overall increased relative difference in d' was seen for EE-EW mice for MB vs. NN (E, $p = 0.027$, Unpaired t-test, two-tailed), AP vs. ON (F, $p = 0.018$, Unpaired t-test, two-tailed) and the binary mix (60-40) of AP vs. ON (G, $p = 0.004$, Unpaired t-test, two-tailed). For CI vs. EU, as the EW mice had extensive training by then, the relative change in d' became comparable for both sets of mice (H, ns, $p = 0.74$, Unpaired t-test, two-tailed). This suggests that there was a complete rescue of olfactory learning impairment in EW mice by using the EE strategy as relative changes were either comparable or more for EE-EW mice as compared to EE-NW mice.

Upon comparing the difference in the discriminability of mice raised in EE to the ones raised in standard cages for other four odor pairs shows that there is a complete rescue of olfactory learning deficits induced by ELS (Figure 1-22, E to H).

Further, the olfactory memory was checked for simple monomolecular odor, AP vs. ON. For the controls and EW mice raised in standard cage, the animals were trained on the similar 'lick/no-lick' odor discrimination paradigm under head-restrained conditions. The details of the same is explained in Chapter 2. Although a slight yet significant improvement of the accuracy of performing the memory trials were observed in EE-NW mice, we found out that the EE-EW mice lacked the accuracy with which they could perform the memory trials. In other words, the EE-NW mice had significantly improved olfactory memory performance as compared to EE-EW mice (Figure 1-23, A, $p < 0.05$, Ordinary One-way ANOVA, LSD Fisher test). The positive impact of EE was clearly adequate in reversing the olfactory learning deficits, but, the olfactory memory remained poor in the EW mice (Figure 1-23, A, $p > 0.1$ for EW vs. EE-EW, Ordinary One-way ANOVA, LSD Fisher test).

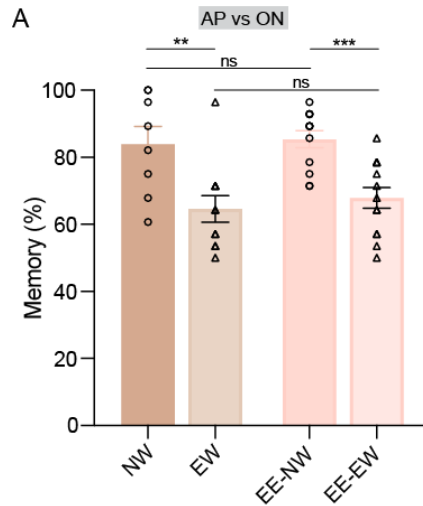


Figure 1-23: Environment enrichment does not improve olfactory memory

A. Olfactory memory % scores as an average of total 28 trials used for probing the odor value association memory per mouse. The bar graph is plotted for AP vs. ON where NW mice exhibited significantly higher memory than the EW mice ($p = 0.0012$, Ordinary One-way ANOVA, LSD Fisher test). The EE strategy did not facilitate improvement in the memory as is observed between EE- NW and NW ($p = 0.78$) as well as EE-EW and EW groups ($p = 0.51$).

1.5 Discussion

Our study investigated the effect of early rearing conditions on murine sensory perception. We began to assess the effect of ELS via early weaning on anxiety & behavioral despair-like conditions in C57BL6/J mice. After establishing increased anxiety-like responses in the OFT and EPM tests in EW mice, we then moved to assessing plausible sensory behavioral changes. As ELS can have maladaptive neuro-developmental and psychological consequences, we were interested to closely analyze its effect on the sensory brain regions that may be vulnerable to stress. Having confirmed that the olfactory detection capabilities were comparable to normally reared mice, we then tested EW mice on olfactory Go/No-go paradigm for learning to discriminate many odor pairs of varying physical and chemical properties. Our experiments revealed occurrence of olfactory perceptual learning and memory impairments in EW mice. The anxiety like behavior and perceptual learning impairment were rescued by providing environmental enriched housing to the EW mice. Olfactory memory, however, was not improved by using the EE strategy.

1.5.1 Early life stress can induce varied strain-specific responses

In neuroscience, different strains of mice are used to study the genotype to phenotype interactions¹⁴⁷. The changes in phenotype can occur as a result of the differential genetic make-up of the mice. Indeed, studies have pointed that the extent of ELS induced effects can vary depending on the genetic background and the environmental conditions of the pups^{144,148}. For example, similar anxiety levels were quantified using EPM in adult balb/c and C57Bl/6 strains which underwent Infant Maternal Separation (IMS) for 3 hours every-day from P2 to P15. However, balb/c mice additionally displayed depressive phenotype in FST, which was not exhibited by C57Bl/6 mice¹⁴⁹. On the other hand, a 3-hours separation done from P4-P22 in C57Bl/6 mice caused greater immobility in FST, specifically on the second day of carrying out the test¹⁵⁰. Even in case of 3-hours MS from P6-P10 or P1-P14 in both C57Bl/6 and balb/c strains did not induce anxiety¹⁵¹.

In fact, different models of ELS can alter the maternal behavior towards pups differently. The aftermath of this can be visualized in the varied responses of the pups of different strains^{152,153}. Generally, upon conducting MS for few hours per day and re-returning the pups to the dam ushers increased grooming and licking behavior and enhanced arched-back nursing by the mothers. This can inadvertently curtail the stress endured by the pups during

MS. It has also been observed that different routes of MS can even cause variations in the corticosterone levels, depending on the strain and sex of the mice. One study depicted increased adrenocorticotropin and corticosterone levels in CD1 strain male and female pups who suffered from 24 hour MS at P8^{154,155} while the other study showed no corticosterone variations in the CD1 male and female pups who underwent 3-hours MS per day from P2-P14¹⁵⁶. In case of C57Bl/6NCrIBR mice, 180 minute MS from P0-P9 caused increased corticosterone 60 minutes after the acoustic stress which was in contrast to decreased corticosterone levels 30 minutes after acoustic stress, in those pups which were handled for 10 minutes only between P0-P9¹⁵⁷.

In contrast to MS paradigms, behavioral changes are worse when pups are weaned during the late lactation period¹⁵⁸. As that period of postnatal life is attributed to be stress hyper-responsive, early separation of pups without returning has detrimental effects^{5,53}. Early or pre-weaning, in effect, can make pups more vulnerable while few hours of MS can facilitate developing resilience or limiting the vulnerability. Increased corticosterone for up to 48 hours after early weaning at P14 has been detected in both male and female ICR mice pups. Decreased BDNF and reduced DG neurogenesis has also been observed in male ICR mice during their young adulthood¹⁵⁹. Early weaning of C57Bl/6 mice at P16, however, led to impairment in fear extinction learning but no anxiety-like responses in another study¹⁶⁰. P16 is beyond the SHRP period of the pups' postnatal life and thus, may not lead to emotional vulnerability.

We decided to firstly assess these responses of the young and old cohorts of C57Bl/6/J male mice before probing for any sensory perceptual repercussions. Our ELS protocol involved weaning at P14 and raising the pups in a new cage with limited-to-zero nesting material. Pups were survived by provision of food slurry, intermittent cage heating and limited brush-stroking (only if absolutely needed). We showed that EW led to increased anxiety-like responses on day one of the OFT and EPM tasks in the young age (8-12 weeks) of male mice (Figure 1-10 and 1-11). Upon evaluating behavioral despair or the depressive symptoms using FST, we found no visible difference in the overall mobility of EW mice, calculated over 5 minutes, as compared to control mice (Figure 1-13). However, bouts of immobility were much higher in the first minute of starting the FST in case of young EW mice. This observation is similar to what was seen by Mehta 2012 where they predicted that the increased initial immobility of C57Bl/6 IMS mice may have attained a ceiling effect

already¹⁴⁹. However, standard assessment using FST generally takes into account immobility over the total duration or in the last four minutes. Hence, conclusive arguments cannot be made by just determining the behavioral display of immobility of EW mice in first minute of FST. Overall, we unarguably demonstrated that EW C57Bl/6J mice in their young-age displayed anxiety-like behavior which was not shown in the old cohorts of EW mice.

1.5.2 Early life stress alters sensory-cognitive perception

ELS predisposes individuals to problems associated with emotion and cognition. Understanding the underlying mechanism becomes a complicated task as multiple brain regions across different scales of complexity participate in generating behavioral dysfunctions¹⁶¹. Much of the surmounting literature in the field focuses on exploring behavioral consequences of ELS mediated by hypothalamus^{162,163}, hippocampus¹⁶⁴⁻¹⁶⁶ and amygdala^{167,168}. These regions constitute the limbic system and thus, serve as the main drivers in governing emotive as well as cognitive behaviors. We were intrigued at the existence of limited literature that paid attention to the sensory systems' functioning under the influence of ELS. Our interest stemmed from the knowledge of prevailing bi-directional connectivity of sensory system such as the olfactory system with the stress-sensitive brain regions^{71,74}. With the presence of glucocorticoid receptors, neurons that release stress-vulnerable neuropeptides, continual turn-over of inhibitory neurons of OB and the exposure of EW pups to olfactory depriving environment allowed us to hypothesize OB-dependent behavioral changes in mice upon enduring ELS. The behavioral manifestation, however, could possibly be either adaptive or degrading in nature. To test our hypothesis, we began to investigate the behaviors starting from olfactory dependent detection to higher-order learning and memory.

We carried out buried food pellet test on food-restricted mice for a period of 5 days wherein the food pellet was buried at 5 different locations in the arena (adapted from Alberts & Galef 1971)¹⁶⁹. Apart from measuring the motivation and hedonic preference towards the comfort food, i.e, the regular chow, it also tests olfactory detectability of rodents¹⁷⁰. We chose to use the regular food pellet as there is some data that argues preference of ELS induced rats towards comfort food over the other food items¹⁷¹. Over these 5 days, we found out that the EW mice managed to locate the pellet at a similar latency as the NW mice, except on day 3 (Figure 1-14). This suggests that the EW mice may behave normally in foraging and other olfactory driven detection behaviors. As LH-OB connections might govern food-seeking

behaviors in mice¹⁷², the Orexin-A neuropeptide release can be analyzed in two groups of mice under fed and food-restricted conditions to closely ascertain the neural correlates of this behavior & its possible modulation by ELS. BFPT, however, crudely assessed olfactory sensitivity as the temporal resolution of the test is poor and the odorant composition might differ from pellet-to-pellet¹⁷³. To assess the olfactory detection threshold in a controlled fashion with the precision in odor delivery, we used custom-built olfactometers¹⁰. We serially diluted the odors and created v/v dilutions from 10⁻¹⁰ to 1% in MO of AP and ON monomolecular odorants. To check the threshold at which they could start to discriminate these odorants and further the pace of learning the task, we started the GNG task at highest dilution level. EW mice began to sense the odor at same dilution level as the NW mice. However, the accuracy of discriminating the odors at this dilution and the further levels remained compromised in the EW mice (Figure 1-15). This phenotype was corroborated by using another task of discriminating across the varying dilutions of binary mix of AA vs EB odors in the same groups of EW and NW mice. We, thereby, confirmed that olfactory detection appeared unaffected by ELS and the slower learning pace in odor discrimination tasks hinted towards impaired cognitive abilities in EW mice. This was further verified by using multiple odor pairs for the discrimination learning and memory tasks.

The involvement of striatal and amygdalar regions in mediating behavioral deficits in ELS mice are already well-known¹⁷⁴. For example, in a modified version GNG paradigm, mice were trained to obtain sweetened milk as reward in their own home-cage (constituting the Go response) and subsequently tested to check their latency to reach for this reward in a new, bright-lit cage (No-Go response or delayed Go due to perceived threat in a novel, well-lit area). ELS mice displayed slower latency towards the reward on the day of testing which was correlated with heightened Amygdala activity using c-fos marker¹⁶⁸. In contrast to such GNG paradigms that test cognitive skills in the background of affective stimuli in ELS mice, our olfactory GNG paradigm particularly assessed sensory-cognitive skills. The GNG paradigm entailed mice to discriminate between two odor stimuli, one of which was paired with water¹⁰. Such an operant conditioning paradigm involved intact sensory and cognitive skills to carry out the task effectively. In fact, many studies have pointed that the performance of mice in this paradigm can be reliably connected to the neural representations in OB^{93,142,175}. Even, distinguishing a highly complex mixture of odors (a target odor in the background of fourteen odors) was directly linked to the difference in the OB glomerular activation profiles governed by the combinatorial coding principle¹⁷⁶.

These studies thus imply that the changes in behavioral performance on the olfactory GNG paradigm may be attributed to modulations happening in the OB circuitry. Our ELS mice were trained across different simple and complex odor pairs, namely, MB vs. NN, AP vs. ON and its mix, AA vs. EB and its mix, CI vs. EU and its mix as well as the mix of Carvones enantiomers, C+ vs. C- (Figure 1-17). We found out slower olfactory learning, measured using d' values over 100 trials for a total of 900/1200 trials. For certain odor pairs, AP vs. ON and its mix as well as AA vs. EB, EW mice performed at a poor pace even at the end of the training phase. The olfactory memory that was assessed for two of the odor pairs, AA vs. EB and its binary mix, was also significantly lower in EW mice. Such a specific learning and impairment in EW mice suggested changes in OB circuitry. The neural underpinning of this behaviors are explained in Chapter 2. Interestingly, we saw improvement in d' as the training progressed, i.e., in AA vs. EB mix, CI vs. EU mix and C+ vs. C- odor pairs where the extensive training improved their behavioral performance. We hypothesized that it could be due to the time-dependent improvement in ‘rule learning’ of mice. Learning of stimulus-reward association must have gotten improved due to extensive repetition of training across various odor pairs¹⁷⁷. To test if that was really the case, we stopped the training and housed mice with ad libitum water for a period of 6 months during which they were not trained. At the end of this period, we again trained them for two odor pairs, one for which learning was poor, AP vs. ON and the other for which learning improved, C+ vs. C- mix (Figure 1-18). We found that the olfactory learning impairment indeed persisted suggesting that the improvement that was seen earlier could be due to acquisition of the rules of the task over repetitive training. This also confirmed that EW had long-lasting olfactory learning deficits.

1.5.3 Environment enrichment is effective in ameliorating sensory deficits

Prolonged sensory experiences can bring about positive or negative changes in an individual’s cognitive capabilities. Depriving situations such as maternal separation or rearing in sub-optimal conditions can adversely affect cognitive behavior. Enriching environments, conversely, favor upliftment of cognitive skills of an animal. We already showed that an early depriving condition arising due to EW at P14 caused poor olfactory learning and memory phenotypes in male mice. To test if exposure to EE conditions can reverse such deficits, we reared the pups in an enriched housing (Figure 1-20). Pregnant dams were introduced to EE housing and pups were reared in such conditions from their birth. In case of EW mice, the dam and female pups were removed at P14. The male pups that

continued to stay in the EE cage were exposed to more social contact as well as were free to access the running wheels, tunnels, smell the natural odorants, brush their whiskers past the textured materials and navigate the Lego constructed maze. Rearing in such a holistic flourishing environment does lead to improvement in various behavioral tasks such as contextual conditioning, Morris water maze, avoidance and attention-shifting tasks^{13,14}. To uncover the effect of EE on the behavior of EW mice in their young adulthood, we carried out both the anxiety tests as well as the GNG paradigm. Significant improvement in anxious responses of EE raised EW mice were revealed on OFT and EPM tests (Figure 1-20). Our results corroborate to many studies where EE has shown to have positive influence in the emotive behaviors of rodents, improving both the anxiety and depressive phenotypes in mice model systems of neurobehavioral disorders^{178,179}.

Further, we evaluated their olfactory learning capabilities on GNG paradigm across multiple odor pairs, MB vs. NN, AP vs. ON and its mix and CI vs. EU. This was carried out for both EW and NW mice reared in the EE cages. A massive improvement in olfactory learning task in both groups of mice compared to the standard cage counterparts (Figure 1-21 and 1-22). This suggests that EE nullified the neuronal changes that governed poor learning in case of EW mice. Chronic models of stress have often been positively impacted by EE on neurobehavioral tasks via changes in BDNF protein levels in hippocampus^{180,181}, increased neurogenesis¹⁸² etc. Exposure to odor-enriched environment, for example, natural odor mixtures over 40 days cause increased neurogenesis and increased dendritic stability of Mitral/Tufted cells of OB¹⁸³⁻¹⁸⁵. An increased pace of learning in case of our EE mice could happen due to changes happening from the molecular, epigenetic to circuitual levels. One of the hypothesis could be due to the increased neurogenesis levels of OB as exposure to odor-rich environment as well as other materials are provided right from their early postnatal life. This is being checked in both GNG paradigm trained and untrained cohorts of mice. It could also be a modulatory effect which is to be investigated by assessing the role of neurotransmitters and neuropeptides in EE driven behavioral improvement. EE, in general, is known to have a more positive influence if applied in the early postnatal life of the animal which could be due to the malleability of the neural circuitry and the occurrence of critical periods, thereby, provision of a window of activity dependent plasticity. Hence, it is worthwhile to check whether the positive behavioral influence can be achieved if EE is applied in late postnatal life of EW mice or not.

Finally, EE applied to EW mice did not improve their olfactory memory scores when tested one month after they were trained for AP vs. ON (Figure 1-23). This showcases an existence of a conundrum and challenges the extent to which EE can bring about positive changes. EE mediated improvement in memory has often been observed in Hippocampal dependent tasks¹⁸⁶. However, at least one study suggests the aspect of ‘novelty’ in the EE cage in influencing short-term olfactory memory¹⁸⁷. Given that our EE cage had exposure to only a limited set of natural odors which were repeated and alternated after every few days and that the Lego based maze that we had put was not paired with reward (hence, no memory based training), which overall provided a rather ‘stable’ than ‘novel’ environment to mice. These reasons/hypothesizes, thereby, could underlie no significant improvement in olfactory memory in EE reared EW mice but are needed to be tested.

1.6 Future directions

1.6.1 Differential gene expression analysis in control, early weaned and enriched mice using Transcriptomics

To gain an integrated understanding of the environment induced transformations, an ongoing investigation of mapping transcriptomic changes to circuit-level dysfunctions is underway. To this end, we plan to carry out transcriptomic comparisons between the controls, early weaned and enriched mice. This work is being carried out along with Ms. Ankita Sharma, SG lab at IISER Pune. As the focus of our study is to dissect out pre-cortical OB mediated pathways, we primarily investigated the changes occurring in OB upon ELS (See Materials and methods, section 1.3.7).

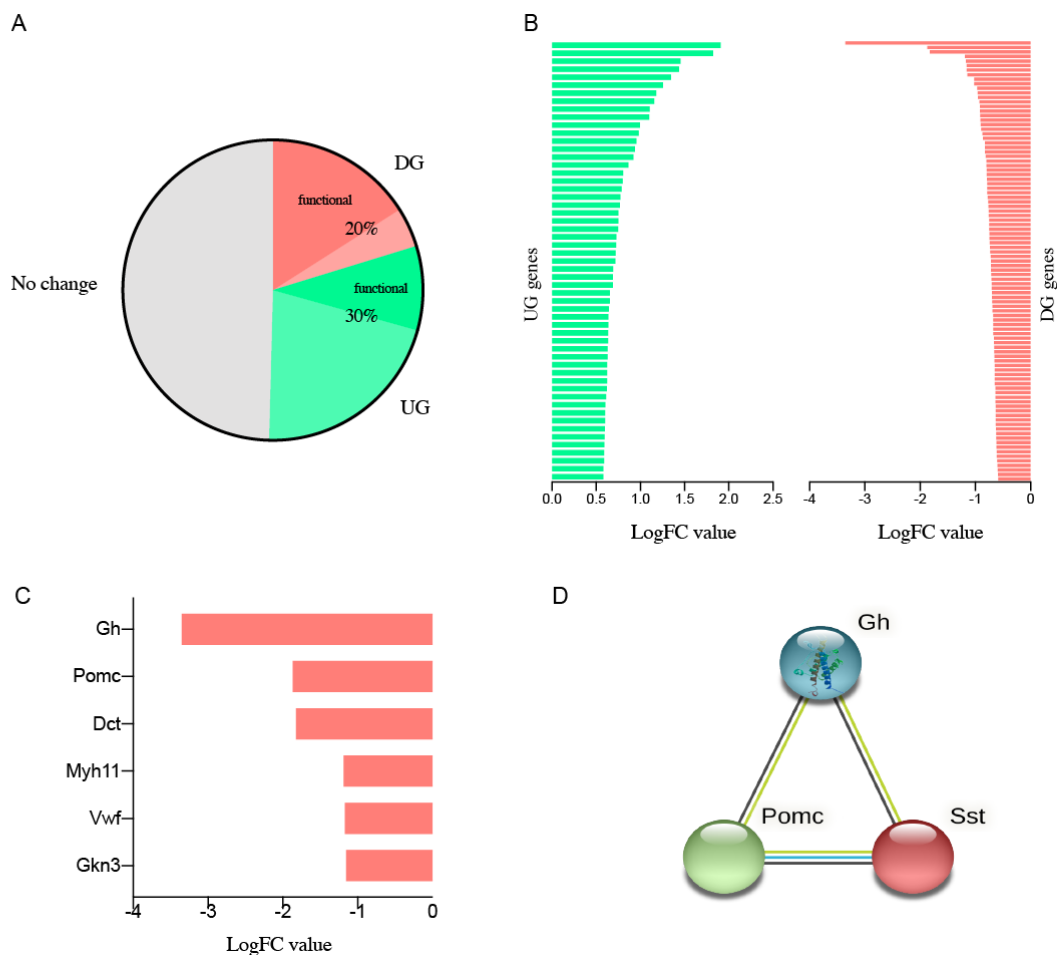


Figure 1-24: Differential gene expression in OB of early weaned mice

A. Pie chart depicting percent of functional genes which were found to be downregulated (DG) and upregulated (UG) in EW mice olfactory bulb tissue, upon mRNA sequencing. Sectors marked with ‘functional’ are those genes whose functional annotations are known, based on Gene Ontology searches.

B. Logarithmic fold change (Log FC) values of the genes in green (UG) and red (DG) in OB of EW mice, as compared to NW mice.

C. DG genes with highest fold-change values including Growth hormone (Gh) and Prepromineralocorticoid (Pomc) in EW mice.

D. Interactions of highly DG genes, i.e, Gh and Pomc with another protein, Sst shows that this system could de-regulated in OB of EW mice (STRING Database).

All the samples had RNA integrity values above 8. Around 50% of the total mRNAs expression were altered in case of ELS mice (Figure 1-24, $p < 0.05$, $N = 3 \times 3$ pairs of OBs per group). 123 genes were down-regulated in EW mice while 183 were up-regulated. Of the down-regulated genes, 97 already had functional annotations. Similarly, out of 183 up-regulated genes, 55 genes already were known to be functional in nature. This was checked using online gene ontology search tools. Interestingly, the genes with highest down-regulation in EW mice (i.e largest Fold-Change (FC)), Gh and Pomc (-3.35 and -1.85 logFC values respectively), are known to be close endocrine mediators of somatostatin neuropeptide. This was found out using STRING, a protein-protein interaction network, online database that form interactive maps of protein depending on how close the proteins function with each other is signalling pathways etc. (<https://string-db.org>). Future studies on their dysregulation upon ELS and thereby, changes in functional contribution leading to circuit-level deficits will be carried out in the laboratory.

1.6.2 Gender dependent effects of ELS on olfactory behavior of mice

Thus far, we have systematically investigated the effect of EW on the food detection, olfactory discrimination threshold, learning and memory on the male mice. As ELS is known to have gender-dependent effects, we are currently probing its effect on the odor discrimination learning and memory of female mice as well. Simultaneously, we are also looking at its effect on the anxiety and depressive behavior of the EW female mice. In chapter-3, the effect of ELS on social learning and memory based tasks has been investigated (See section 3.4.7).

Chapter 2

Involvement of Somatostatin releasing interneurons of Olfactory bulb in mediating ELS induced learning deficits

2.1 Abstract

Optical control of specific neuronal populations while animals are actively performing the behavioral tasks offer a robust strategy to study functional relevance and modulation under different contexts. We found out that ELS leads to olfactory discrimination learning and memory impairments in mice. Using *ex-vivo* olfactory bulb slices stimulation, we confirmed the release of the somatostatin neuropeptide on carrying out optogenetic activation of channelrhodopsin-2 (ChR2). Somatostatin has varying modulatory functions across different body organs and the areas of the central nervous system. This neuropeptide has been shown to have anxiolytic effects, however, the function of specific sub-population of GABAergic interneurons releasing somatostatin neuropeptide in pre-cortical brain region, olfactory bulb, remains unknown. To unravel the neural underpinnings of ELS dependent olfactory learning changes, we carried out bi-directional optogenetic modulation this sub-population. Upon photoactivating these interneurons *in vivo*, early weaned mice displayed improved complex odor discrimination learning. Photo-inhibiting these neurons using Archaeorhodopsin (Arch) in normally weaned mice resulted in the learning deficit observed in ELS mice. This optogenetic modulation, however, did not lead to improvement in the olfactory memory. We are currently investigating molecular and physiological correlates of the behavioral changes that we observed upon modulating this circuitry using optogenetics. To this end, we are carrying out calcium imaging using micro-endoscopy in anesthetized and behaving mice as well as the opto-electrophysiological recordings of the projection neurons of the OB upon optically modulating the bulbar SST releasing GABAergic neurons.

2.2 Introduction

2.2.1 Neuro-modulatory changes by Early Life Stress

Stress, as is known, is not a unitary event that would affect only specific mechanisms or particular brain regions. Rather, it is a multi-faceted phenomenon that exerts its effects on multiple levels. The levels at which stress affects, although can be discretely defined, are often inter-linked physiologically. Stress can lead to long-lasting behavioral and physiological impairments which have their roots lying in dysfunctions caused at molecular and circuit levels¹⁸⁸. In the Introduction of Chapter 1, I have summarized the diverse effects of ELS on brain and physiology of the animal with a detailed evaluation of its effects on sensory perception. In this section of Chapter 2, I will review the current literature on the effect of ELS on neuro-modulatory systems of the brain, specifically paying attention on its effect on neurotransmitters and neuropeptides. The sensory dysfunctions occurring due to changes in the transmitter & peptides dynamics will also be discussed to draw parallels between ELS mediated deficits and the impairments leading to sensory malfunctioning.

2.2.1.1 *Impact of early life environmental changes on neuropeptide and neurotransmitters*

One of the most evident target of ELS is the HPA axis²⁶. The prolonged exposure to stressors during early life averts the stress hypo-responsive period causing increased hypothalamic para-ventricular nucleus (PVN) activity and increasing the level of corticosteroids¹⁸⁹. The elevated levels of CRH and CRHR1 in PVN were found to be higher in ELS males as compared to females suggesting that the impact of ELS on neuropeptides is sex-selective in nature¹⁹⁰. Apart from its effects on the HPA axis, the responses are also potentiated in Amygdala & other stress selective regions. Tight functional reciprocal connectivity between the principal neurons and the GABAergic interneurons is important for normal postnatal development of Basolateral Amygdala (BLA)¹⁹¹. Indeed, the density of parvalbumin positive neurons in BLA was increased in the peri-weaning period of the ELS mice followed by inability to an auditory contextual dependent fear learning task. Optogenetic inhibition of parvalbumin (PV) positive neurons of BLA rescued the phenotype suggesting that the LBN paradigm of ELS delayed the maturation of specific classes of interneurons¹⁹².

Yet another pitfall that ELS endows the brain with is the shift in the excitation/inhibition (E/I) balance. A reduction in the number of GAD-67 positive interneurons as well as the inhibitory synapses in the mPFC followed by an impaired social recognition behavior was

observed in rats that underwent MS¹⁹³. In a recent study, mPFC of MS suffered rats exhibited increased E/I balance during their adolescence as was measured by assessing charge transfer ratio of spontaneous excitatory post-synaptic (sEPSCs) to spontaneous inhibitory post-synaptic currents (sIPSCs) in the layer 5 pyramidal neurons of the prelimbic area of mPFC. Further, using micro dialysis, enhanced extracellular glutamate levels were found which resulted in lowered evoked-EPSC paired pulse ratio of pyramidal neurons¹⁹⁴. This could occur as a result of impaired pre-synaptic glutamate release leading to abnormal glutamatergic levels. Receptor level expression changes, such as, increase in Excitatory Amino acid transporter 1 (EAAT1) and a decreased expression of vesicular glutamate transporter 1 & 2 (VGlut1, 2) along with decreased GABA transporter (VGAT) was found in the hippocampus of Aged MS rats¹⁹⁵. EAAC1 (carrier protein for excitatory amino acids) however, was, specifically decreased in PV-positive GABAergic interneurons in the hippocampus of neonatal maternally separated rats in another study.

Neuropeptide functioning too, can be plastic in nature depending on the early life environmental conditions¹⁹⁶. One of the ways by which hippocampal behavioral deficits upon ELS are caused is due to the loss of Neuropeptide Y (NPY) releasing GABAergic hilar interneurons that provide inhibition to the DG-CA3 circuitry. This results in changes in the E/I balance resulting in the development of altered functional changes¹⁹⁷. Oxytocin neuropeptide has also been studied in the context of stress reactivity. In case of humans, intranasal application of oxytocin causes reduction in behavioral response to stressors as well as decreases the rise in cortisol levels¹⁹⁸. In ELS exposed individuals, oxytocin has been shown to confer resilience by attenuating the limbic regions' deactivation & curtailing the responsivity of HPA axis when faced with psychosocial stressors in adulthood, suggesting, that it alters the optimal stress responsivity in ELS subjects¹⁹⁹. Additionally, ELS has been shown to cause kainate receptor dependent changes in the inhibitory control in the lateral amygdala by causing loss of PV neuronal inhibition and increase in the firing rate of somatostatin (SST) releasing neuronal population. The molecular underpinning of the same was found out to be downregulation of *Grik1* gene encoding kainite receptors, locally in the amygdala²⁰⁰. PV and SST inter-neuronal densities were also found to be lowered in the Dentate Gyrus region of the mice that underwent MSEW paradigm, which caused accumulated stress. Although the cell loss was not seen, the expression of PV and SST were reduced in this region²⁰¹.

2.2.1.2 *Somatostatinergic pathways are modulated by stress & enrichment*

SST neuropeptide has multiple effects across the different body organs, ranging from maintenance of growth hormone, insulin, cholecystokinin, glucagon and thyroid stimulating hormone levels to regulating immune responses to its role as both a transmitter and a modulator within the CNS²⁰². SST neurons of stress-sensitive brain areas, in general, are known to exhibit vulnerability to stress and depression^{203,204}.

Low levels of SST have been found in the cerebrospinal fluid of the MDD patients²⁰⁵. SST expression was also reduced in anterior cingulate cortex, dorsolateral prefrontal cortex and amygdala of individuals who suffered from MDD²⁰⁶. On the other hand, intravenous injection of SST produced anti-depressant like effects in rats, as seen by their improved responses in EPM and FST¹⁵. Specific transcriptomic alterations have been detected in cortical SST releasing interneurons upon subjecting the rodents to unpredictable chronic stress paradigm. Such molecular deregulations were mostly affected in the pathways that involved protein translation through EIF2 α signaling²⁰⁷. The EIF2 α mediated susceptibility of these neurons to stress follow the similar phenotype as is seen in pathological neurodegenerative disorders. Indeed, treatment with the inhibitor of the kinase (PERK inhibitor) for activating the EIF2 α pathways caused anxiolytic effects which has also been seen in the models of neurodegenerative disorders²⁰⁸. Brain derived neurotrophic factor (BDNF), another protein known for its modulation by ELS, controls the SST expression in brain. BDNF-SST expression changes along with downregulation of enzyme synthesizing GABA in SST-positive neurons of the stress exposed rodents indicate the vulnerability of these neurons to stress²⁰⁷. In addition to providing dendritic inhibition to the principal/projection neurons of multiple cortical and sensory brain regions, SST-GABAergic interneurons might also be involved in mediating a local inhibitory tone in a circuit by inhibiting other interneurons²⁰². The frontal cortical SST-GABAergic neurons display differential effects on the behavioral emotionality in mice. While the acute inhibition of these interneurons increased anxiety responses, chronic pharmacogenetic mediated inhibition of the same neurons reversed the effects²⁰⁹. This points to the notion that homeostatic mechanisms might be playing a role in case of chronic loss of function of SST neurons of the frontal cortex. SST also induces its anxiolytic effects by blocking the release of ACTH by Pituitary. In vitro studies have shown that both the isoforms of SST, sst-14 and sst-28 as well as selective agonists for sst-receptors, sst-2 and sst-5 block corticotrophin releasing factor induced ACTH release by the specific

cell lines derived from the pituitary gland²¹⁰. In this way, SST can also be hypothesized to exert its control on the HPA axis as the sst receptor sub-types are widespread across the different stress-sensitive brain regions. Although all these studies suggest that the neuropeptide-transmitter dynamics of these neurons are vulnerable to stress, their modulation due to ELS is not yet deciphered.

Apart from their altered functioning in anxiety and depression, SST neurons are also emerging to play a role in learning and memory. Simultaneous two-photon calcium imaging of SST cells of visual cortex of mice while performing a visual discrimination task allowed to detect the activity of SST cells during learning. SST neurons tended to decorrelate from the local neuronal activity during learning. This was hypothesized to act as a mechanism to enhance V1 circuit plasticity once the stimuli become relevant to the animal's behavior¹⁶. In another study, optogenetic inhibition of SST interneurons of mPFC during training on spatial memory task disrupted working memory. Further, it also disturbed the mPFC to hippocampus synchrony suggesting that the controlled activity of SST neurons was important for learning and performing the working memory task optimally¹⁷.

SST neurons are also located in OB and the other connecting regions of the olfactory cortex²¹¹. In case of OB, they line the inner part of the external plexiform layer and are also found in the GCL, mainly resembling the morphology of deep short axon cells¹⁸. They are also present in AON sub-regions. Cell bodies also reside in layer II and III of the piriform cortex while the target dendrites are located in the layer III. These neurons are also located in the 'olfactory' (lateral) entorhinal cortex as well as in the deep layers of the olfactory cortical regions of Amygdala²¹². The receptor sub-types occupy all the layers of the OB and using trans-synaptic viral tracing, are shown to be present in piriform cortex, anterior cortical & posteromedial cortical nuclei of Amygdala and within the entorhinal cortex as well²¹³. The functional contribution of the SST neurons and their receptors in olfactory regions are rather limited in the field. Using local field potential recordings, SST neurons of OB were shown to modulate the gamma power oscillations generated by the mitral cells. This was done by using the sst2 receptor antagonist in wild-type and receptor knock-out mice and was proposed to be changing due to changes in the dendro-dendritic inhibitory tone on the mitral cells. This consequently affected the fine odor discrimination capabilities of the mice²¹⁴. Finally as SST levels are known to be affected under conditions that result in cognitive impairments¹⁹, we

decided to investigate their role in interceding the olfactory discrimination learning deficits observed in early weaned male mice by using state of the art techniques used in neuroscience research.

2.2.2 Optogenetics: A tool to study neural circuitry dynamics and functioning

Behavior of an animal is generated by the brain. In case of mice, brain consists of ~70 million neurons. Such high density of neurons connect to form circuits that function together to control specific behaviors. The scientific community is continually growing and innovating tools and techniques to investigate how circuits operate optimally to execute behaviors. Such tools also allow to assess adaptive or maladaptive changes that occur in circuits which lead to either betterment of behavior or causes dysfunctions²¹⁵ .

Cell genomics based studies using cell sorting and sequencing have facilitated the cell-types identification across different brain regions. Further, the recombinant viral tracing methods determine the connectivity between cell-types²¹⁶. Indeed, pseudo-typing certain viruses with different glycoprotein can cause it to either become anterograde or retrograde viruses that can cross the synapses. Such studies set the groundwork for functional assessment of neural circuits which allows for manipulating specific cell-types from macroscopic to microscopic resolution scale²¹⁷. Cre-dependent transgenic mice provide a powerful strategy of promoter driven manipulation of neuronal sub-populations by using optogenetics under physiologically relevant conditions, while the animal is actively performing the behavior. Optogenetic strategies comprise of recombinant protein channels that change their conformation upon exposure to light of specified wavelengths. These can be driven in cells using Cre-lox strategy which upon photo-stimulation can either cause the neurons to fire an action potential or hyper-polarize them. Wide variety of microbial opsins, such as blue light responsive opsins Channelrhodopsin-2 (ChR2), ChR2 variant E123T i.e, ChETA; red-shifted opsins and step-function opsins are used to modulate the functions of neurons. ChR2, for example, does so by selectively allowing cations into the cell^{218,219}. Other proteins such as Archaeorhodopsin (Arch) causes neuronal silencing upon amber colored light stimulation by allowing the protons to be pumped out of the cell²²⁰. These variants of microbial opsins utilized for optogenetics are ever-evolving in the field, by engineering them so as to suit specific characteristics such as decay kinetics, conductance etc. to certain experimental needs.

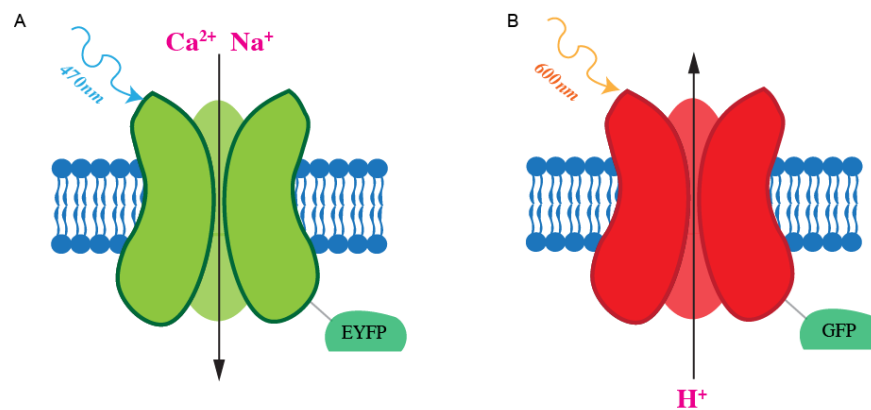


Figure 2-1: Light-activated channels for optogenetic control of cells

A. Channel rhodopsin-2 (ChR2) channel opens upon blue light stimulation. Upon opening, cations enter the channel which leads to depolarization of the cell leading to neuronal activation.

B. Archaeorhodopsin (Arch) channel opens up upon amber colored light stimulation. Upon opening, it allows H^+ ions to move outside the cells which leads to cell hyperpolarization. This, in effect, causes neuronal inhibition.

Studies pertaining to murine models of stress and disease are often involving optogenetics to specifically probe for neural populations that govern behavioral changes. Optogenetic activation of neurons projecting from Ventral Tegmental Area to medial PFC decreases social avoidance behavior in mice that suffered from social defeat stress. Stimulation of mPFC neurons projecting to basolateral amygdala prevented stress-induced sociality deficits. Such studies indicate the role of mPFC in social avoidance behavior upon stress²²¹. Even in case of sensory brain areas, optogenetic manipulations are being used to identify the functionality of specific cell types. For example, selective M72 sensory neuronal optogenetic stimulation allowed for investigating glomerulus responses⁴¹. Transgenic lines such as *Lbhd2-CreERT2*, *Pcdh21-Cre* and *Tbx21* can be used to manipulate activity of the projection neurons, M/T cells, thus, providing a valuable tool to probe olfactory circuitry function^{222–224}. For revealing dynamics of inhibitory circuits as well, sub-types of granule cells, can be independently modulated using optogenetics²²⁵. Viral delivery of optogenetic constructs under *Synapsin-1*, *Syn1* promoter injected in lateral ventricle are utilized for understanding the role of adult-born neurons in olfactory guided behaviors²²⁶. Optogenetic activation and silencing of granule cells has been shown to cause changes in OB output and olfactory discrimination behavior, thus, indicating the role of OB as a pattern separator⁹³. Finally, OB micro-circuitry such as those neurons releasing the peptides such as CRH²²⁷ as well as

inhibitory transmitters⁹³, are also being optogenetically targeted to study their function in controlling OB output²²⁸.

2.3 Materials and Methods

2.3.1 Subjects

A total of 62 male transgenic were utilized for the experiments covered in Chapter 2. For optogenetic modulation behavioral experiments under head-restrained conditions, following genotypes (obtained from The Jackson laboratory) were crossed to obtain the desired transgenic mice:

- B6.Cg-Sst^{tm2.1(cre)Zjh}/J (*SST-IRES-Cre*, 013044) with B6.Cg-Gt(ROSA)26Sor^{tm1(EYFP)Cos}/J (*R26R-EYFP*, 006148) to express reporter protein Enhanced Yellow Fluorescent Protein (EYFP) in SST-positive cells.
- B6.Cg-Sst^{tm2.1(cre)Zjh}/J (*SST-IRES-Cre*, 013044) with B6.CgGt(ROSA)26Sor^{tm32(CAG-COP4*H134R/EYFP)Hze}/J (*Ai32*, 024109) to express Channelrhodopsin-2 (ChR2)/EYFP construct in the SST positive cells.
- B6.Cg-Sst^{tm2.1(cre)Zjh}/J (*SST-IRES-Cre*, 013044) with B6.CgGt(ROSA)26Sor^{tm35.1(CAG-aop3/GFP)Hze}/J (*Ai35D*, 012735) to express Archaeorhodopsin (Arch)/GFP construct in the SST positive cells.

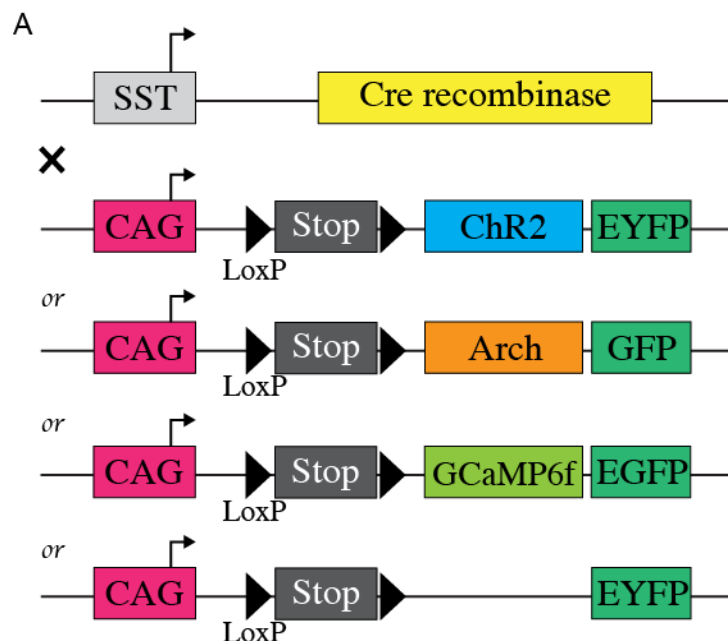


Figure 2-2: Cre-Lox strategy for obtaining desired transgenic mice

A. Homozygous SST-Cre mice were mated with homozygous LoxP-flanked mouse lines to obtain desired protein expression, i.e, ChR2-EYFP or Arch-GFP or GCaMP6f-EGFP or EYFP alone in SST-positive cells.

For both the experimental groups of Normal weaned (NW) and Early Weaned (EW) mice, all three optogenetic conditions were carried out for the olfactory learning and memory behavioral tasks. NW groups consisted of 8 SST-EYFP, 8 SST-ChR2 and 7 SST-Arch mice (hereafter named as NW(EYFP), NW(ChR2) and NW(Arch), respectively). EW groups consisted of 7 SST-EYFP, 8 SST-ChR2 and 6 SST-Arch mice (hereafter named as EW(EYFP), EW(ChR2) and EW(Arch), respectively).

For morphological quantification of the SST-positive cells found in the Olfactory bulb of the NW and EW groups, 1 NW and 1 EW mice were utilized. To quantify the release of SST neuropeptide in an *ex vivo* OB slice preparation under EYFP and ChR2 conditions, 8 EYFP (NW+EW) and 8 ChR2 (NW+EW) mice were utilized. For micro-endoscopic *in vivo* calcium imaging experiments, B6.Cg-Sst^{tm2.1(cre)Zjh}/J (*SST-IRES-Cre*, 013044) were crossed with B6;129S-Gt(ROSA)26Sor^{tm95.1(CAG-GCaMP6f)Hze}/J (*Ai95D*, 024105) to obtain the desired phenotype. 6 SST-GCaMP6f NW mice were used for the experiment.

2.3.2. Genotype and Phenotype details

Homozygous mice (SST-Cre and other lox lines) were genotyped and maintained for rounds of breeding. The genotyping was carried out along with the staff members of National Facility for Gene Function in Health & Disease, IISER Pune. A 2-3mm long tip of the mouse's tail was clipped and collected in a 1mL eppendorf tube. DNA was isolated using the KAPA express extract kit (KAPA biosystems). Further, KAPA2G fast genotyping mix (KAPA biosystems) was then used for carrying out the Polymerase Chain Reaction (PCR). Suitable primers were bought from the Jackson's laboratories for PCR process. 2% agarose gel made in TAE buffer (Tris base, acetic acid & EDTA) to run the PCR products. 14ml of PCR product was mixed with 1ml of loading dye (6x) and loaded into the well. 4ml of 100 base pair ladder was added in one of the wells. Gel was run at 100V for 30 to 45 minutes for separating the bands. The band sizes for each of the transgenic constructs were confirmed from the datasheets provided by the Jackson's laboratories.

One of the F1 generation obtained by crossing the SST-Cre with any of the loxP flanked lines (Figure 2-2) are phenotyped. Trans-cardial perfusion was carried (30-40mL of 1X PBS to flush the blood out followed by 30-40mL of 4% paraformaldehyde for fixing the tissue), following which, the brain was dissected out. The brain was fixed overnight, after which, it was transferred to 30% sucrose and stored in cold for 1-2 days. Cryotome sectioning at 50µm

thickness was done to obtain freely floating sections in PBS. DAPI staining (1:500, Sigma) was done and sections were mounted on the clean glass slides using Vectashield anti-fade mounting medium (Vector Labs, H-1000). Sections were visualised and imaged under Leica sp8 confocal microscope to confirm the reporter protein expression. The expression was further confirmed by using antibody against SST (Figure 2-3, D). SST positive neurons are densely found in the inner EPL and also in the GCL as was observed by Lepousez et al. 2010¹⁸. For antibody staining, the sections were first blocked using 5% Normal Goat Serum (NGS) +1% triton-X solution (prepared in PBS) for 2 hours at room temperature. They were then incubated with Rabbit anti-somatostatin antibody (1:1250) (Invitrogen, PA5-82678) at 4°C for 16-18 hours. PBS washes (thrice, 15 minutes each) were given to remove excessive antibody. Sections were then incubated with secondary antibody (1:1000) Anti-rabbit Alexa Fluor 594 (Jackson's Immunoresearch) for 2 hours at room temperature (prepared in 1% normal goat serum). PBS washes (thrice, 15 minutes each) were given and then the sections were mounted on the glass slides.

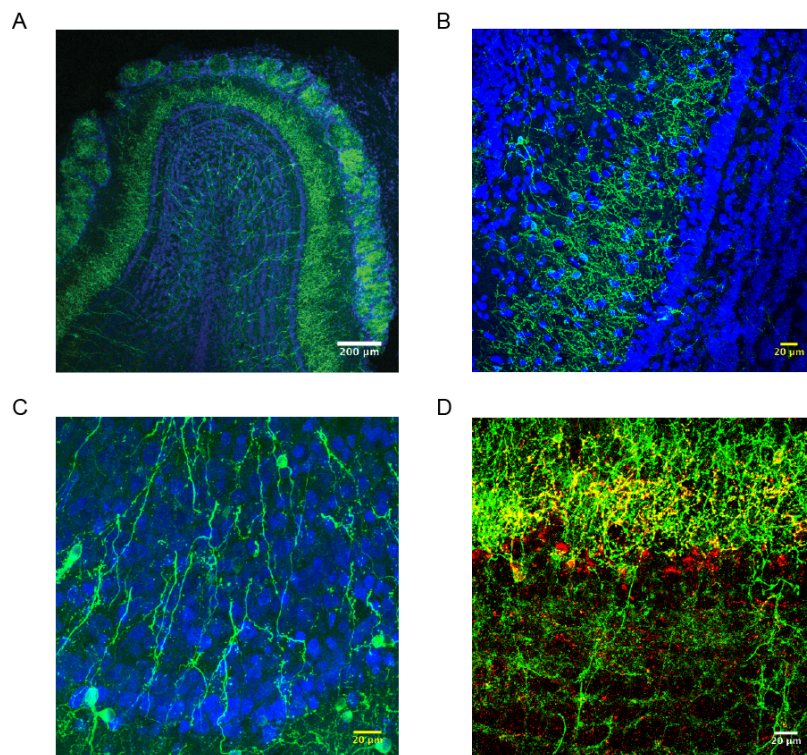


Figure 2-3: Specific expression of transgenes in SST-positive neurons of Olfactory Bulb

A. SST-EYFP expression in a coronal section of OB exhibiting localized expression to EPL and sparsely in GCL. Blue: DAPI, Green: EYFP. Scale bar: 200 μ m (Image Courtesy: Dr. Anindya Bhattacharjee, LNCB, IISER Pune).

B. Immunofluorescence image depicting SST-Arch GFP expression in EPL of MOB. Blue: DAPI, Green: GFP. Scale bar: 20 μ m.

C. Immunofluorescence image depicting SST-GCaMP6f EGFP labelled neurons in the GCL of the MOB. Blue: DAPI, Green: EGFP. Scale bar: 20 μ m.

D. Co-localisation of inherent transgene expression with the SST antibody labelled cells in the inner EPL and GCL of MOB. Green: EYFP, Red: SST antibody. Scale bar: 20 μ m.

2.3.3. Ex-vivo Olfactory bulb slice preparation to quantify neuropeptide release

In order to investigate if the neuropeptide SST is released upon neuronal activation by optogenetics, we carried out ex vivo slice preparation of OB. SST-ChR2 mice were used for quantifying release upon photo-stimulation while the SST-EYFP mice were used as control. Essentially, the mouse was anesthetized and decapitated. The brain was removed within 1-2 minutes of sacrificing the animal and placed in high-sucrose modified artificial Cerebrospinal fluid (ACSF) (Table 2-1). Two-third of the cortex was removed by doing a slant cut using a blade during the dissection. 150 μ m thick coronal slices were cut on the vibratome (Leica VT 1200S) in high-sucrose ACSF. Slices were transferred to a holding chamber containing normal ACSF (Table 2-1) maintained at 31°C in an incubator and constantly bubbled with carbogen gas (5% CO₂, 95% O₂). Slices were shielded from light until photo-stimulation.

Chemicals	High-Sucrose ACSF (pH 7.4) (in mM)	Normal ACSF (pH 7.4) (in mM)
Sucrose	194	-
Sodium Chloride	20	124
Potassium Chloride	4.4	4.4
Calcium Chloride	2	2
Magnesium Chloride	1	-
Sodium Phosphate monobasic	1.2	1
Magnesium sulphate	-	1
Glucose	10	10
Sodium hydrogen carbonate	26	26

Table 2-1: Chemicals used in ACSF preparation for maintaining acute OB slices

2.3.3.1 *Fabrication of multi-LED assembly*

Multi-LED assembly was custom-built to allow for photo-stimulation of OB coronal slices in a 12-well plate (set-up fabrication done by Mr. Surya Deopa, Physics Department, IISER Pune). It consisted of two modules with 6 LEDs each, connected in series. The two modules were then connected in parallel to each other. Voltage drop across a single LED was measured so as to quantify the total voltage required to power the whole assembly. Due to the high operational voltage of these LEDs, a MOSFET controlled by an Arduino Nano board was necessary to be used. They were powered to operate at 40Hz frequency, switching on for 2s and shutting off for 13.2s. These settings were the same as what were used in the in vivo optogenetic modulation of the circuit. Assembly was switched on and off by a push button switch.

2.3.3.2 *Photo-stimulation paradigm and ELISA*

For each mouse, at least 4 pairs of OB slices were obtained by vibratome sectioning. The procedure that we followed was inspired by Dao et al. 2019²²⁹. 2 pairs of acute OB slices were transferred to wells containing 500 μ l of ACSF (oxygenated) such that two wells were assigned to one animal. Once the slices were placed, the 12-well plate was transferred to a dark box with the lid of the plate fixed with the multi-LED assembly. Photo-stimulation was carried out for 20 minutes. 3 X 50 μ l of the ACSF from each of the wells were collected in Eppendorf tubes on ice and no peptidase inhibitors were added to the samples. Once all samples were ready, they were pipetted into a 96well Somatostatin-14 ELISA plate (S-1179, BMA Biomedicals, Switzerland). ELISA was carried out as per manufacturer's instruction. Fresh standard samples were prepared in a standard diluent (ACSF) each time before conducting ELISA. 50 μ L of standard or sample was added to the well along with 25 μ L of antiserum. Antiserum were freshly prepared in the Enzyme Immunoassay (EIA) buffer. For the blank well, 50 μ L of diluent was added instead of the sample or standard. This incubation was done at room temperature for 1 hour. Following this, 25 μ L of rehydrated Biotin-tracer was added to each well followed by incubation at room temperature for 2 hours. Immunoplate was then washed for five times using 300 μ L of the EIA buffer. After thorough washing, 100 μ L of streptavidin-HRP was added to each well and incubated for 1 hour. Again after washing for five times, TMB solution (100 μ L per well) was added. Just after terminating the reaction upon adding 100 μ L of 2N HCl to each well, absorbance was read at

450nm in Perkin Elmer EnSight, Multimode Plate Reader. SST was quantified in ng/mL by obtaining values from the standard curves.

2.3.4 Surgical procedures for optogenetic modulation

Different groups of mice were utilized to carry out headpost implantations for carrying out head-restrained olfactory learning behavior. After few days (2-3) of recovery and starting the water restriction schedule (12-14 hours), they were pre-trained on the apparatus. After pre-training, they were no longer water restricted and the cranial window + LED implantation was carried out. Training was resumed within 1-2 days of recovery from the surgery.

2.3.4.1 *Headpost implantation for carrying out olfactory behavior under mouse head restrained (MHR) condition*

Mouse was intraperitoneally injected with a mix of Ketamine (50mg/g) and Xylazine (10mg/g) for anesthetizing for the surgical procedure. Absence of a pedal reflex indicated deep anesthesia has reached. Anesthetized mouse was mounted on the stereotactic instrument by moving the ear-bars to hold its zygomatic arches, inserting the incisors in the tooth bar and positioning the nose clamp to secure the snout. Eyes were hydrated with 1% (w/v) carboxymethylcellulose (Refresh liquigel, Allergen India) sterile eye lubricant to prevent dryness. The skin overlaying the skull was removed by first making a straight horizontal cut using scalpel blade (skin overlaying the anterior-posterior suture) and extending it posteriorly using scissors (to just before bregma) so as to form a circular hole. Connective tissue layer (periosteum) over the skull was gently removed by peeling and cutting by simultaneously using fine forceps and a scalpel blade. After gentle cleaning with ACSF, a minute amount of etching agent (Ivoclar Vivadent EcoEtch[®]) was applied for 5-6 seconds. The etching agent, phosphoric acid, facilitated roughening by forming porosities in the dorsal side of the skull. This promotes adherence of the cement in the subsequent steps. Excessive agent was removed by using cotton buds dipped in ACSF and the surface was then air-dried. Dental primer (Ivoclar Vivadent Te-Econom Bond) was applied on the etched area and was polymerized using UV light flashes for 30-40s. Finally, dental cement (Ivoclar Vivadent Tetric N-Ceram) was quickly applied and spread to periphery of the exposed skull, in a textured fashion. It was UV polymerized (3 cycles of 20s) for hardening. A stainless steel headpost was taken and its legs were covered in the same dental cement from all sides. This was then fused with the cement on the skull and once it was settled in the desired position,

UV polymerization was done (3-4 cycles of 20s). The surrounding exposed area of the skull not covered with the headpost was shielded using the dental acrylic cement (DPI RR Cold cure, acrylic repair material).

2.3.4.2 Cranial window and LED implantation

Headpost implanted anesthetized mouse was mounted on the stereotactic instrument. The skin overlaying the OB was removed using blade and scissors. The cut was extended to 1mm anterior to the OB. Connective tissue layer was peeled out using fine forceps. The dense musculature surrounding the eye was gently cut without damaging the blood vessels as much as possible. Cleaning using ACSF was carried out. A biopsy punch (2.5mm) was placed on the skull surface above the center of OB barring the anterior-posterior suture area. It was rotated in either direction to create a shallow groove in the skull. A hand-held drill was then used to deepen the groove. This drilling was only done in short burst to avoid heating the brain area beneath the skull surface. ACSF was applied time and again during this process. Once the bone in the groove was visibly thinned, the central skull island was tapped using forceps to test if it flexes upon tapping. Using a small needle to enter the thinned bone groove and one tip of forceps to enter the opposite side, the central bone island was lifted upwards without damaging the dura. ACSF was applied to the dura. Small pieces of Gelfoam (AbGel, SGK labs, Mumbai) pre-soaked in ACSF were used to coagulate the bleeding. Once the bleeding subsided, a drop of Dexamethasone was put on the dura to prevent inflammation. A clean coverslip was held from its edge using a forceps and placed carefully on the exposed circular area. The dura beneath contained ACSF to fill the window when the coverslip was placed. The surrounding bony area, however, was dried using cotton swab. Once the coverslip settled, it was held in its location using a Hamilton syringe placed perpendicular to the lens (Figure 2-4, B). Dental acrylic cement was used to seal the window from all sides. Surrounding exposed skull area was also covered with the cement. Once it was dried, a drop of hot-melt glue was placed on top of the coverslip to prevent the animal from scratching the window. If the cranial window remained visibly clear for up to 4-6 days after surgery, a 2mm LED (either blue: NFSB036BT or orange: NJSA172, Nichia Corporation) connected to a header-socket arrangement (ED11100-ND, ED8250-ND, Digikey) was held right above the coverslip and fixed using the dental acrylic cement. Once it dried, the animal was removed from the stereotactic instrument and allowed to recover. Optimal intermittent heating and ad libitum water and food were provided as a part of the post-operative care.

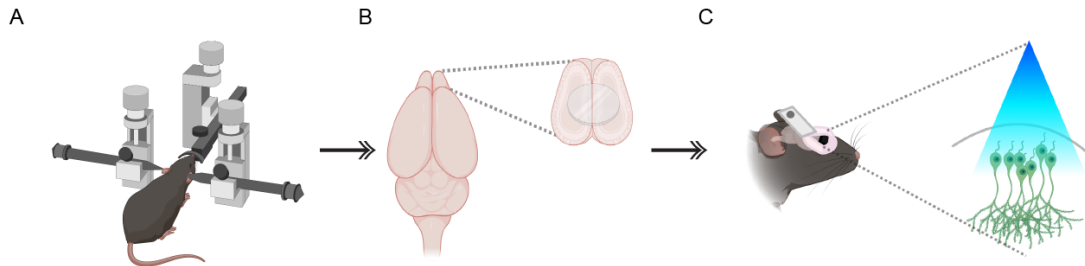


Figure 2-4: Surgical procedure for optogenetic modification of OB micro-circuitry

A. Anesthetized mouse placed in a stereotaxic instrument for carrying out cranial window and LED implantation.

B. Image representing a 3mm glass cover-slip placed in the center of the olfactory bulbs of the mouse after removing a circular piece of skull using a 2.5mm biopsy punch.

C. Headpost, cranial window and LED implanted on the OB of the mouse. The blue LED will allow photoactivation of SST+ interneurons of the OB upon stimulation (Created in BioRender.com).

2.3.5 Olfactory learning and memory behaviors under MHR conditions

2.3.5.1 *Olfactometer*

A custom-built olfactometer in conjunction with a lickometer was utilized for this study. 10-channel olfactometer controlled by 10 mini Mass Flow Controllers (MFCs), 1 Main MFC (Pnucleus technologies, NH) and electromagnetic solenoid valves (PMC pneumatic, Switzerland) allowed for an optimal and temporally precise odor delivery to the mouse. Manifold inside the olfactometer allowed for diverting the clean air-stream (room air pumped into the system using an aquarium pump) into the MFCs. Air that passed via mini-MFCs entered the saturated odor containing glass bottles. Air via the main-MFC served as an air-dilution stream. The odorized air and dilution streams met at the T-junction of the multi-channel glass nozzle (Figure 2-5, A) where they are mixed before getting delivered to the nose. This way the odor was diluted to 1% in mineral oil and further to 1:20. An exhaust outlet of the nozzle allowed for odorized air to be passed to the exhaust during the pre-loading time of 3.2s before odor presentation (Figure 2-5, B). This allowed for the odor plume stream to reach a steady state before it is delivered to the nose during the odor presentation time window of 2s. The lickometer allowed for recording and digitizing the licks that the mouse performed on the licking tube. Breathing was monitored using an air-pressure based sensor (AWM2300V, Honeywell) which is digitized by the lickometer circuit.

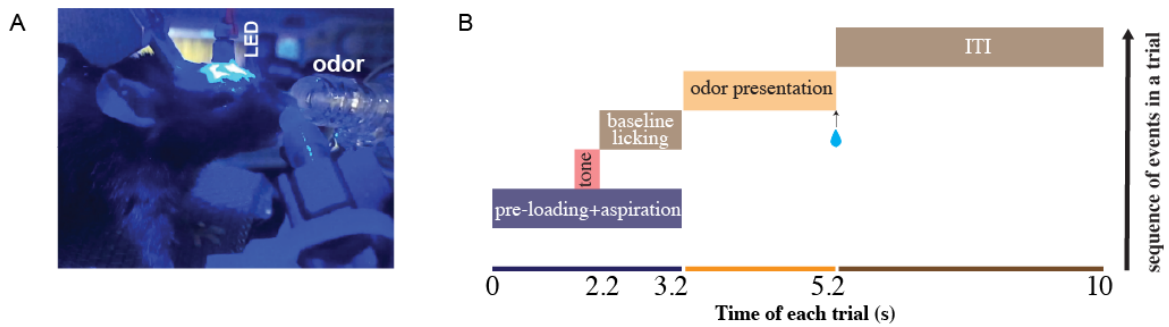


Figure 2-5: Olfactory training paradigm under MHR condition

A. A headpost implanted mouse restrained on the set-up for performing the odor discrimination task under photo-stimulation ‘on’ conditions. The mouse rests its paws on the metallic mesh covered on a plexiglass platform which is inserted in the PVC tube. Odor is delivered via a multi-channel nozzle placed laterally to one of the nostrils. The breathing is recorded via an air-pressure sensor placed near to the other nostril. The LED placed on the OB is switched on at 40Hz frequency during the odor presentation window. The background LED is turned on even before stimulus delivery to mask the light produced by blue LED alone during odor presentation.

B. The schematic displaying sequence of events that happens in a single trial of odor presentation in a olfactometer under MHR condition. Upon fulfilling the optimal licking criterion for a S+ trial, water is provided at the end of odor presentation duration (indicated by a blue drop in schema).

2.3.5.2 *Olfactory learning and memory paradigm*

2-3 days after beginning of water-restriction schedule, mice were trained to acquire the procedural aspects of the paradigm. To this end, task habituation or pre-training was carried out. Mouse was placed inside the PVC tube and given free water drops from the licking tube. First stage of pre-training (Pt 2.1) was started the next day. It consisted of 40 trials when just after the tone of 200ms, a water drop (~3 μ l) was presented to provoke licking by the water-restricted mouse. This delay period between tone and water delivery was gradually increased in Pt 2.1. In the next phase, Pt 2.2, Mineral Oil was presented for 2s in each trial. The baseline licking was taken into account which facilitated the mouse to learn to wait for odor presentation to get the reward. During odor presentation, the total lick time needed during the odor presentation was increased step-by-step from 40ms to 240ms²³⁰. If animal licks during baseline, a lick penalty in the form of increased licking duration during stimulus period needed to get the reward, was imposed. In Pt2.3, Mineral Oil was replaced by 1% (v/v) Methyl benzoate. Minimum 40 trials were done using the same licking criterion as during the odor discrimination learning paradigm. This was followed by Cranial window and LED

implantation. Post recovery from the surgery, animal was trained for photo-stimulation ‘on’ conditions for 1% MB detection (40 trials) and 1% 2-Pentanone (40 trials with and without light each) in Pt 2.3 stage. During this stage, LED power utilized for each animal was standardised. The temperature was kept ambient (near to body temperature of the animal) and was measured using Luxometer (Power & Energy meter, Lab-max TOP, Coherent). For SST-EYFP group, least LED power was used (0.6-1.1 mW/mm²). For both ChR2 and Arch groups, the least LED power which resulted in similar licking as under no-light conditions, per animal, were chosen to be used for further experiment.

During odor discrimination learning training, after the pre-loading time of 3.2s, odor was presented for 2s (Figure 2-6). For Carvones (+) and (-) binary mixture experiment, SST neurons were photo-stimulated (Figure 2-6, A). The background LED switched on before the odor presentation to ensure that the light from LED on cranial window is masked. This way the animal did not associate the light emitted from the LED placed on the cranial window with the reward. The fixed inter-trial interval was that of 13.2s (10s + 3.2s of pre-loading time). For rewarded (S+) trials, if animal had not licked during the baseline period, the criterion to get the water reward was to lick for a total time of 80ms in three out of four bins of 500ms each, during the stimulus duration. For S- or unrewarded trial, a maximum total time of 80ms in one out of the four time bins was accepted. Only when they licked during baseline period of an unrewarded trial, the trial was counted correct if their licking during stimulus presentation did not exceed 25% of their licking during baseline. Tone signal was only restricted to pre-training period and was kept off during odor discrimination learning.

2.3.5.3 *Odors*

All odors were bought from Sigma-Aldrich and the diluent, mineral oil was bought from Oswal Pharmaceuticals, Pune, India. Methyl benzoate (MB) and 2-Pentanone (PN) were used for odor detection task. For odor discrimination, Acetophenone (AP), Octanal (ON), Amyl acetate (AA), Ethyl butyrate (EB), Carvone-(+) and Carvone-(-) were used for odor discrimination tasks. Odors are diluted to 1% in mineral oil. Either simple or binary mixes of odors (60%-40%) were used. Physico-chemical properties details are given in Table 1-1.

2.3.5.4 *Data analysis*

For quantifying odor learning in a discrimination task, d-prime (d') calculation was done as explained in section 1.3.4.6. For assessing their lick probability, custom-written Python

scripts were made to calculate the licking achieved during S+ and S- trials for every 100 trials, for a total of 900 trials. The lick probability was calculated throughout the 2s odor duration. The Area under the Curve (AUC) was calculated for both S+ and S- curves and the values were statistically compared across the normal and early weaned groups under photo-stimulation off and on conditions. Following formula was used: $AUC = (AUC_{S+} - AUC_{S-}) / AUC_{S+}$.

2.3.6 Morphological quantification of SST positive neurons

We utilized P16 mice to quantify the immediate effect of ELS on the morphology of SST interneurons using the transgene (EYFP/GFP) expression. To this end, P16 mice (control: P16 mice weaned and sacrificed immediately, experimental: early weaned at P14 and then sacrificed on P16). Trans-cardial perfusion was done as explained before (section 2.3.2) and the brains were dissected out. After sectioning, sections were incubated in a blocking solution for 2 hours at room temperature. Sections were DAPI stained at 1:500 dilution and imaged under confocal microscope. Sections were then incubated in a primary antibody, Chicken anti-NeuN (1:1000) (ABN91, Merck) for 16-18 hours in a blocking solution (1% NGS + 0.1% Triton-X) at 4°C. Post the PBS washes, sections were further incubated in secondary antibody (Anti-Chicken Alexa flour 647, 1:1000, Jackson's immunoresearch) for 2 hours at room temperature. Finally, sections were incubated in DAPI for 5 minutes before mounting them on the slides. Confocal microscopy (Leica sp8) was done at higher magnification (63x) to capture a single neuron in one frame. For analysing the morphology of the SST-positive neurons, Imaris software was used. Dendritic lengths were measured using the 'filaments' tool and the number of contact made by each neuron with the NeuN-positive nuclei were calculated. For each sample, ~ 15 cells per section were imaged.

2.3.7 Micro-endoscopic calcium imaging

For Calcium imaging, we utilized NW SST-GCaMP6f mice (N = 6) under anesthetized and awake states for recording from these neurons of OB during odor detection and olfactory learning. Craniotomy (~1mm) using hand-held drill was carried out in center of the right bulb. As a first step towards carrying out micro-endoscopic microscope implantation, a Protrusion Adjustment Ring (PAR) was screwed onto the lens assembly. The implanted GRIN canula lens (1mm length) attached to the dummy microscope was moved slowly into the hole created upon craniotomy. Dura was carefully removed from the reference point. A

clean dura without any bleeding would allow for optimal image quality while the lens was lowered. The PAR was glued such that ~0.6-0.7mm depth (into the EPL of the OB) was achieved while implanting the lens. Cyanoacrylate gum mixed with dental cement was applied between the skull surface the PAR system. This was done to secure the cannula in place. Once this surgery was done, dummy microscope was carefully removed by loosening the barrel and unclipping the canula clamps. Upon removing it from the imaging canula, a protective cap was placed on the canula so as to protect the lens. Mouse was singly caged post-surgery until the end of the experiment to prevent any disturbances to the surgical preparation.

The CE:YAG fluorescence source (Doric Lenses Inc.) was tuned to ~350mA. The miniscope was clamped on the imaging canula after removing the protective cap. To record in anesthetized condition, IP injection of a mix of ketamine-xylazine was done, just before the session. Odor detection under passive conditions was done at 1% as well as at 50% for Hexanal. For other mono-molecular odors, 1% concentration was tried. For each odor, 20 trials with an inter-trial interval of 13.2s were done which were pseudo-randomized. For each trial, imaging was carried out for 10s with an initial 1.2s counted as baseline and the subsequent 2s as the stimulus duration. Under awake conditions, both odor detection and discrimination learning were done. AP vs. ON, Carvones 60-40 and AA vs. EB 60-40 odor pairs for discrimination learning were carried out. 40 trials from each phase of learning (task 1 to task 4) were carried out, i.e, a total of 200 trials were imaged per mouse. The data analysis was done using custom-written Python scripts using cv2 library. Relative change in fluorescence, $\Delta F/F$ was calculated per trial by subtracting fluorescence from the baseline time bins to all the bins during the stimulus duration.

2.4 Results

In this section of Chapter 2, I will be summarizing results obtained upon bidirectional optogenetic modulation of OB circuitry by focusing on the SST-releasing interneuron sub-population.

2.4.1 Ex vivo optogenetic characterization of somatostatin peptide release by OB neurons

SST neuropeptide releasing sub-population of bulbar interneurons have been characterized in a previously published study by Lepousez et al. 2010^{18,214}. Since then, although their receptor types and possible connectivity have been investigated²¹³, the plausible modulation under different physiologically relevant conditions have not been examined. Here, we were interested to probe the activity of SST-releasing GABAergic interneuron population of MOB to investigate their role in ELS mediated olfactory deficits. To this end, we first needed to confirm if the peptidergic release occurs upon induction of photo-stimulation at specific settings of light frequency and time. These settings were then kept the same for *in vivo* optogenetic experiments as explained in the subsequent sections.

For this, we followed a similar protocol used in a recent study by Dao et al. 2019²²⁹. Our Custom-built Multi-LED array assembly (section 2.3.3, Materials and Methods) allowed for optogenetic stimulation by 473nm LEDs (Nichia corporation) placed close (0.5mm) to the OB slices of 150 μ m thickness in a 12-well plate (Figure 2-6, A). The LEDs were activated at 40Hz frequency for 2s with a gap of 13.2s. This paradigm matched with that of odor training wherein the odor pulse was presented for 2s followed by a fixed inter-trial interval of 13.2s, except for the plausible additional effect of the additional stimulation caused by the odor stimuli (Figure 2-6, B). Arduino controlled LED stimulation was done for 20 minutes on the OB slices freely floating in 500 μ L of ACSF (Recipe in Table 2-1). ELISA based quantification of neuropeptide release was carried out on ACSF samples collected after photo-stimulation paradigm was completed. We observed increased concentration of SST in SST-ChR2 OB slices as compared to SST-EYFP OB slices when calculated in ng/mL by estimating from the ELISA standard curve (Figure 2-6, B, $p < 0.0001$, Unpaired t-test, two-tailed, $N = 8$ SST-EYFP and 8 SST-ChR2 mice combining both normal and early weaned groups). The concentrations plotted are duplicates from each well of the 12-well plated containing two pairs of OB slices. From each brain, 4-6 slices were utilized. Similar strategy

will also be used to quantify the release of GABA neurotransmitter upon optogenetic activation.

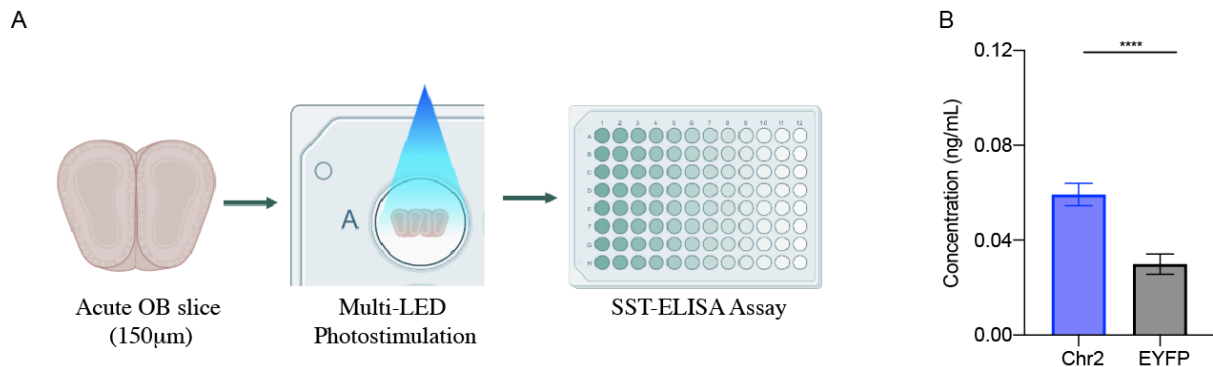


Figure 2-6: Somatostatin peptidergic release upon optogenetic modulation of OB interneurons

A. Schematic diagram of the procedure of *ex vivo* optogenetic activation of SST neurons of OB (created in BioRender.com).

B. Significantly higher release of SST in SST-ChR2 group as compared to SST-EYFP group, measured in ng/mL using ELISA ($p < 0.0001$, Unpaired t-test, two-tailed, $N = 8$ SST-EYFP and 8 SST-ChR2).

2.4.2 Olfactory discrimination learning of simple odor pair under MHR condition

Before probing the effect of optogenetic modulation of SST releasing GABAergic interneurons of OB, we trained the different cohorts of transgenic mice on a simple odor pair Acetophenone (AP) vs. Octanal (ON) using olfactometer under MHR condition. Essentially, we utilized 6 cohorts of mice:

- SST-EYFP normal weaned (**EYFP-NW**) and early weaned (**EYFP-EW**) acting as controls for light stimulation. These cohorts were implanted with Blue LED (473nm).
- SST-ChR2 normal weaned (**ChR2-NW**) and early weaned (**ChR2-EW**) for optogenetically activating the neuronal population.
- SST-Arch normal weaned (**Arch-NW**) and early weaned (**Arch-EW**) for optogenetically inhibiting the neuronal population.

Under no photo-stimulation conditions for this odor pair, we compared the learning pace of NW cohorts with that of EW cohorts. To this end, we compared the pooled data from EYFP+ChR2 and EYFP+Arch groups under NW and EW conditions. Here, as was found out under freely moving conditions, we found that EW groups had a slower learning pace (Figure 2-7, B, C: $p < 0.05$, Two-way ANOVA, LSD Fisher test) for AP vs. ON odor pair, which was also the first odor pair that was used to train them in head-restrained

conditions. We also calculated their lick probability over the training for S+ and S- trials. In case of NW mice, as was expected, the licking probability for S+ trials increased and while that for S- trials decreased to nearly 0 as learning progressed. We then quantified the normalized Area Under the Curve (AUC) values per 100 trials for a total of 900 trials. These values are plotted in Figure 2-7, D4 show slower ability to discriminate between S+ and S- trials in EW (beige) mice as compared to NW (dark brown) mice. By carrying out olfactory training under ‘photo-stimulation off’ condition on a simple odor pair, we confirmed the inability of transgenic EW mice to learn the task as efficiently as the transgenic NW mice under MHR condition.

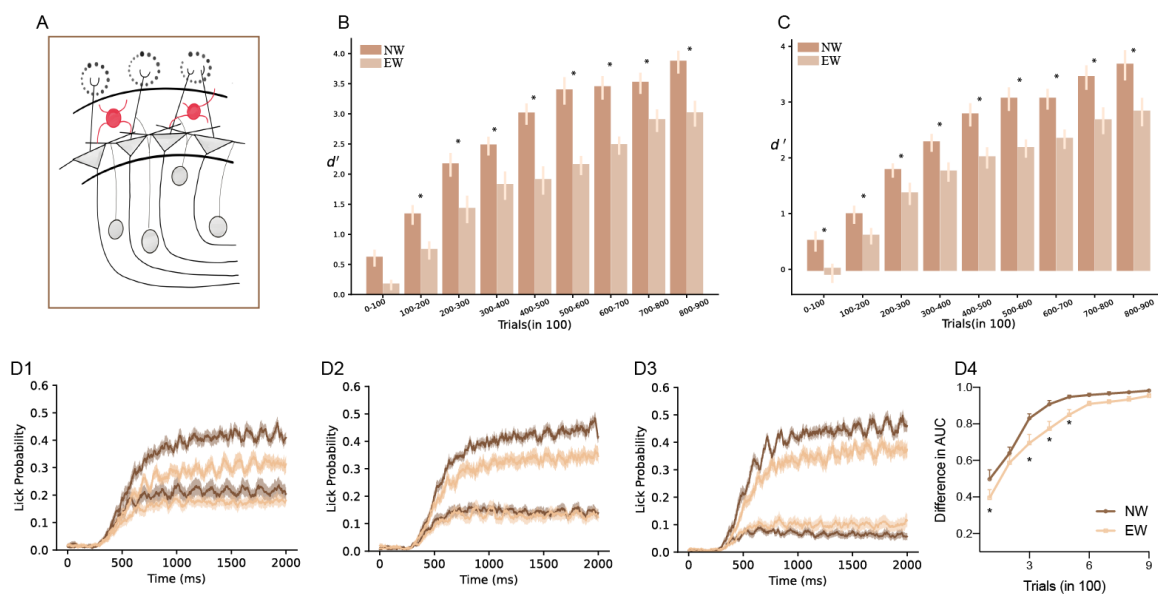


Figure 2-7: Slower olfactory discrimination learning in EW mice under MHR conditions

A. Schematic diagram of OB circuitry exhibiting glomeruli projecting to M/T cells (Triangular gray cells). Red neurons indicate SST inhibitory interneurons in internal EPL layer of OB.

B. Significantly slower olfactory learning in case of EW mice (EYFP+ChR2, light brown) upon comparing d' values for AP vs. ON odor pair learning task done under photo-stimulation off conditions ($p < 0.0001$, $F = 84.41$, Two-way ANOVA, LSD Fisher test, *: $p < 0.05$ for all data points, $N = 15-17$ per group).

C. Slower olfactory learning in case of EW mice (EYFP+Arch, light brown) upon comparing d' values for AP vs. ON odor pair learning task done under photo-stimulation off conditions ($p < 0.0001$, $F = 102.8$, Two-way ANOVA, LSD Fisher test, *: $p < 0.05$ for all data points, $N = 17$ per group).

D1 to D3. Lick probability curves for first 300 trials of training. Each plot consisted for 50S+ and 50S- trials. Dark brown: NW and Beige: EW. These plots indicate that the NW mice are able to distinguish S+ from S- faster than EW mice ($p = 0.0005$, $F = 14.17$, Two-way ANOVA, LSD Fisher test).

D4. Difference in AUC of S+ and S- lick probability curves plotted for the complete training period ($p < 0.0001$, Two-way ANOVA, LSD Fisher test).

2.4.3 Optogenetic activation of OB SST-interneurons improved perceptual learning of EW mice

We utilized Chr2 NW and EW cohorts of mice to photo-stimulate the OB circuitry by activating the SST-interneurons while they were being trained for Carvones enantiomers binary mix of 60%-40% (v/v dilution in mineral oil). An external background LED was also placed perpendicular to the PVC tube onto which the animal was restrained via headpost. This was raised 10-12 cm above the PVC tube and switched on before the delivery of odor. This masked the light emitted from the LED implanted on the animal's head (Figure 2-5, A). The implanted LED which was controlled by a driver (LEDD1B, T-cube LED Driver, Thor Labs) was functional (at 40Hz frequency) only during the stimulus duration window of 2s. The optogenetic manipulation using this strategy was done for both S+ and S- trials throughout the course of training them on Carvones complex mixture task. We found out that in case of NW mice, optogenetic activation of GABAergic and SSTergic circuitry of OB did not lead to improvement in the overall learning of the mice on a complex mix task. Only a marginal increase was observed during the early phase of learning the task (Figure 2-8, B, $p < 0.05$ only for one data point on d' plot, Two-way ANOVA, LSD Fisher test). This observation was in contrast with a previous study where addition of SST agonist result in increased discrimination performance²¹⁴. Difference between the two studies could arise as a result of variation in the techniques utilized. Also, it remains elusive whether optogenetic activation could cause changes in learning highly complex discrimination tasks, i.e, a multi-component task. Contrasting to this, when we photo-activated these neurons in Chr2-EW mice, we found a betterment in the learning pace when compared to the EYFP-EW mice (Figure 2-8, C, $p < 0.05$, Two-way ANOVA, LSD Fisher test). Even upon comparing the lick probabilities and the corresponding AUC, the EW-ChR2 mice outperformed the EYFP-EW mice. This was especially observed during initial phases of learning as observed in the lick probability curves in Figure 2-8 E1 to E3 that constitutes the licking for first 300 S+ & S- trials ($p < 0.0001$, $F = 17.2$, Two-way ANOVA, LSD Fisher test, *: $p < 0.05$). However, such an increase was not seen in case of NW mice, which is concomitant to d' measurements as well (Figure 2-8, D1 to D4, $p = 0.8$, $F = 0.03$, Two-way ANOVA).

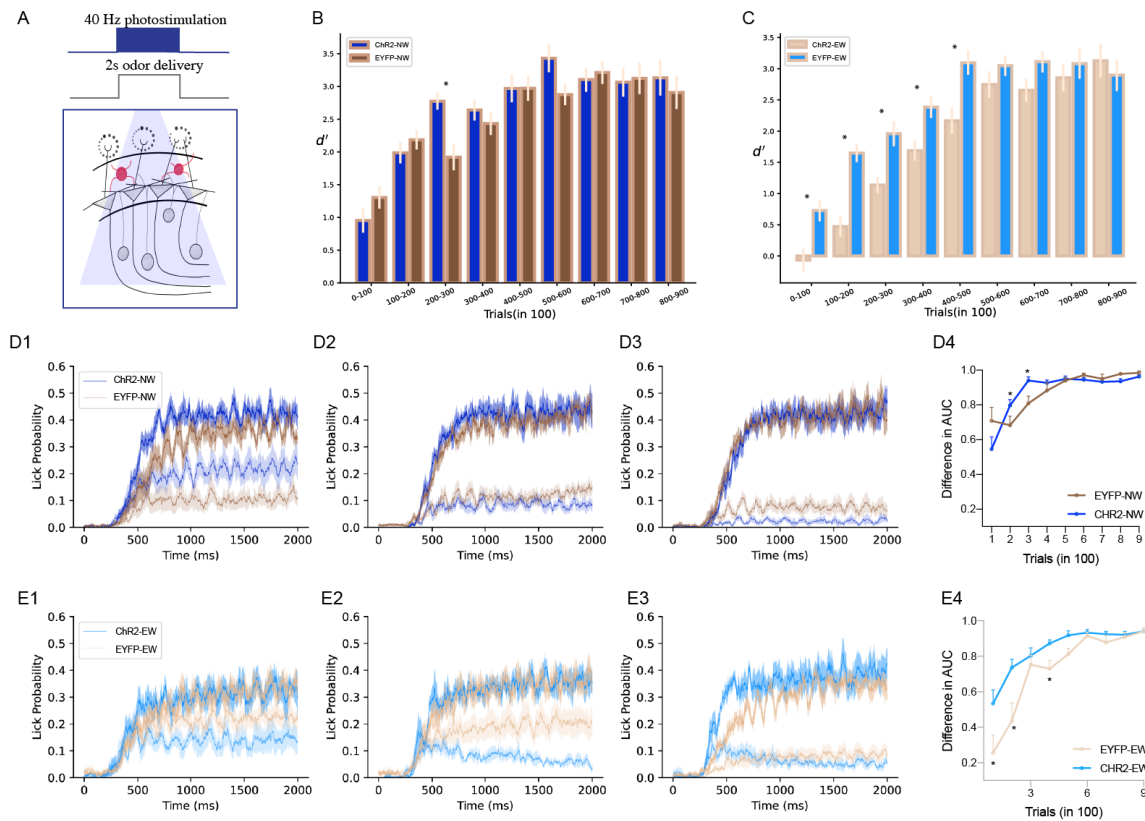


Figure 2-8: Optogenetic activation of SST-releasing bulbar interneurons leads to faster olfactory discrimination learning in EW mice

A. Schematic diagram of OB circuitry exhibiting glomeruli projecting to M/T cells (Triangular gray cells). Red neurons indicate SST inhibitory interneurons in internal EPL layer of OB. Blue light indicates ChR2 photo-stimulation.

B. Negligent increase in learning of ChR2-NW mice on Carvones complex learning task as compared to EYFP-NW mice ($p = 0.37$, $F = 0.79$, Two-way ANOVA, LSD Fisher test, *: $p < 0.05$ for one data point, $N = 7$ per group).

C. Faster learning on a complex carvones task was observed upon photo-stimulating these neurons in EW mice, i.e., upon comparing ChR2-EW mice vs. EYFP-EW mice ($p = 0.0001$, $F = 25.27$, Two-way ANOVA, LSD Fisher test, *: $p < 0.05$, $N = 5-8$ per group).

D1 to D3. Lick probability curves for first 300 trials of training. Each plot consisted for 50S+ and 50S- trials. Blue: ChR2-NW and brown: EYFP-NW.

D4. Difference in AUC plotted for NW mice shows a marginal increase in the value during initial phase of learning to discriminate, in case of ChR2-NW mice ($p = 0.8$, $F = 0.03$, Two-way ANOVA, LSD Fisher test, *: $p < 0.05$).

E1 to E3. . Lick probability curves for first 300 trials of training. Each plot consisted for 50 S+ and 50 S- trials. Light blue: ChR2-EW and light brown: EYFP-EW.

E4. Difference in AUC plotted for EW mice shows an increase in the value in case of ChR2-EW mice ($p < 0.0001$, $F = 17.2$, Two-way ANOVA, LSD Fisher test, *: $p < 0.05$).

2.4.4 Opposing behavioral manifestations upon optogenetic inhibition of OB SST-interneurons

We showed enhancement in odor discrimination learning upon optogenetic activation. We were also interested in assessing how do animals behave if we carry out the optogenetic modulation in an opposite direction. To this end, we assessed the effect of photo-inhibition of SST-releasing GABAergic bulbar interneurons on their decision-making behavior (Figure 2-9, A).

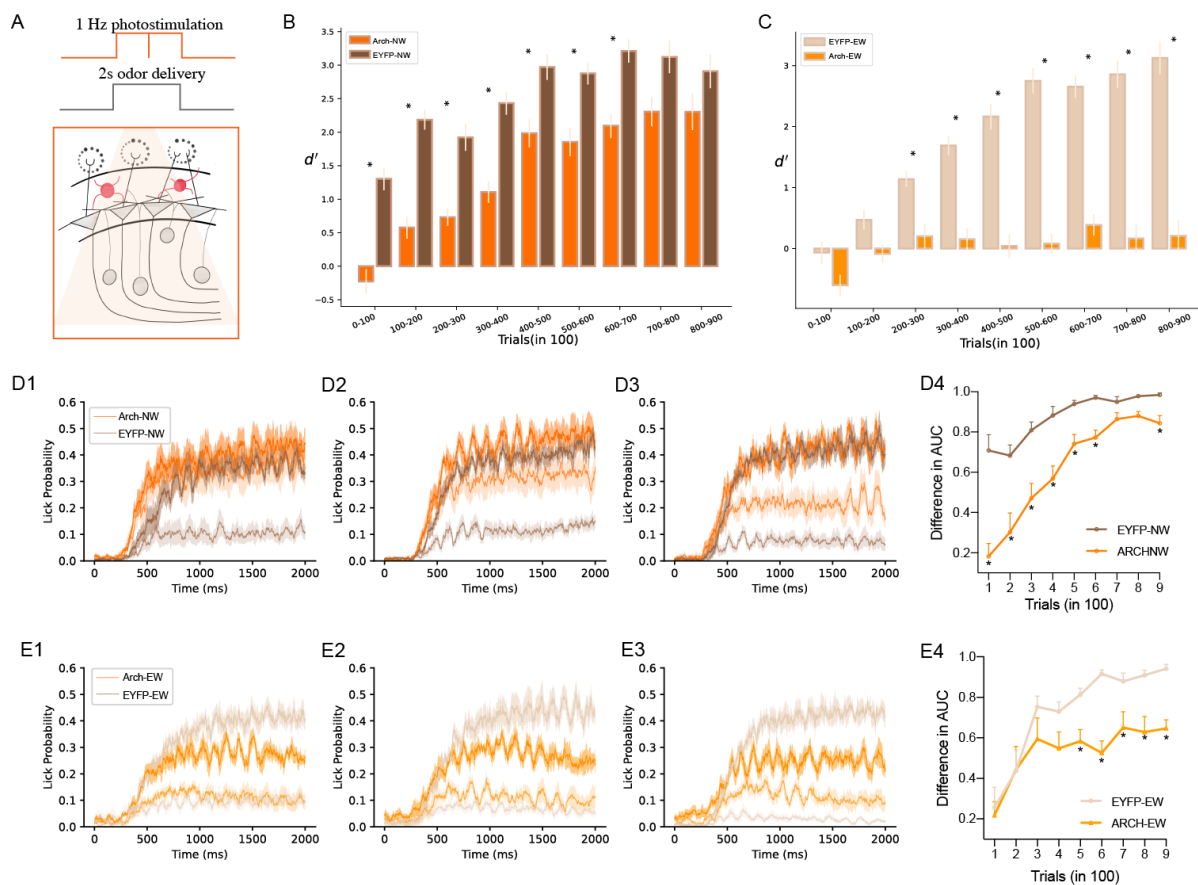


Figure 2-9: Optogenetic inhibition of Somatostatinergic pathway of OB circuitry results in behavioral impairments

A. Schematic diagram of OB circuitry exhibiting glomeruli projecting to M/T cells (Triangular gray cells). Red neurons indicate SST inhibitory interneurons in internal EPL layer of OB. Orange light indicates Arch photo-stimulation.

B. A significant decrease in d' is observed throughout the progression of training for ARCH-NW mice as compared to EYFP-NW indicating that inhibiting the bulbar SST releasing interneurons disrupt normal olfactory learning ($p < 0.0001$, $F = 68.06$, Two-way ANOVA, LSD Fisher test, *: $p < 0.05$ for all data points, $N = 6-7$ per group).

C. Inhibiting the neurons in Arch-EW mice leads to chance level performance as visible by significantly decreased d' values. This suggests that animals are unable to discriminate, when compared to EYFP-NW mice ($p < 0.0001$, $F = 296.7$, Two-way ANOVA, LSD Fisher test, *: $p < 0.05$ for all data points, $N = 6-8$ per group).

D1 to D3. . Lick probability curves for first 300 trials of training. Each plot consisted for 50 S+ and 50 S- trials. Dark Orange: Arch-NW and Dark Brown: EYFP-NW.

D4. Difference in AUC plotted for NW mice shows a decrease in the value in case of Arch-NW mice as compared to EYFP-NW mice ($p < 0.0001$, $F = 127$, Two-way ANOVA, LSD Fisher test, *: $p < 0.05$ for all data points).

E1 to E3. Lick probability curves for 300 trials (50 S+ vs. 50 S- trials per plot) of final training phase where clear difference in discriminatory power of mice is displayed. Light orange: Arch-EW and light beige: EYFP-EW.

E4. Difference in AUC plotted for EW mice shows a decrease in the value in case of Arch-EW mice as compared to EYFP-EW mice ($p < 0.0001$, $F = 39.90$, Two-way ANOVA, LSD Fisher test, *: $p < 0.05$ for all data points).

We found out that upon optogenetically inhibiting these neurons, Arch-NW mice performed the odor (Carvones complex) discrimination learning task poorly when compared to EYFP-NW mice (Figure 2-9, B, $p < 0.05$, Two-way ANOVA, LSD Fisher test). Moreover, while comparing their lick probability AUCs, we saw declined performance of discriminating the S+ and S- odors (Figure 2-9, D1 to D4, $p < 0.05$, Two-way ANOVA, LSD Fisher test). Arch-EW mice displayed a stronger behavioral phenotype upon photo-inhibiting the somatostatinergic circuitry, i.e, they could not learn the discrimination learning task as was visible in their d' values hovering between -1 to 1 throughout the course of training (Figure 2-9, C, $p < 0.05$, Two-way ANOVA, LSD Fisher test). This was also visible in their lick probability curves where the sharp differences in the S+ and S- curves were never observed during the whole training paradigm (Figure 2-9, E1 to E4, $p < 0.05$, Two-way ANOVA, LSD Fisher test). Finally, upon comparing EYFP-EW mice with Arch-NW mice, we observed minute significant changes in d' values between these two cohorts and negligent changes in their lick probability curves (Figure 2-10, A, $p < 0.05$ for two data points, Two-way ANOVA, LSD Fisher test). This indicated that the photoactivating this circuitry in NW mice worsened their learning performance which was coarsely equivalent to the EYFP-EW mice. This suggests a possible causal role of these interneurons in mediating the learning deficit observed in EW mice.

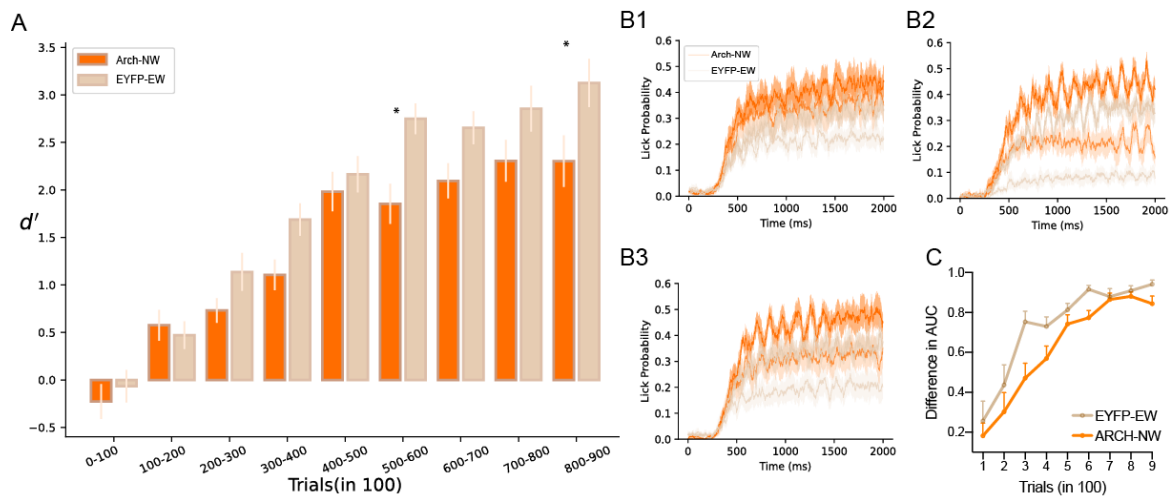


Figure 2-10: Optogenetic inhibition of bulbar SST-releasing interneurons in NW mice mimics ELS induced learning deficit

A. Negligible changes in d' values throughout training on carvones complex task in ARCH-NW mice vs. EYFP-EW mice suggesting onset of learning deficit in NW mice upon optogenetic inhibition which mimics the pace of EW mice ($p < 0.0001$, $F = 20.08$, Two-way ANOVA, LSD Fisher test, $p < 0.05$ for 2 data points only, $N = 6-8$ per group).

B1 to B3. Lick probability curves for first 300 trials (50 S+ vs. 50 S- trials per plot) indicating similar discriminatory power of both cohorts of mice. Orange: Arch-NW and light beige: EYFP-EW.

C. Difference in AUC plots depicts a slight overall difference between the two graphs, however, no difference was found in the post-hoc test ($p = 0.0049$, $F = 11.49$, Two-way ANOVA, LSD Fisher test, $p > 0.05$ for all data points).

We continued to train these cohorts of mice on another complex odor task, AA vs. EB 60-40 binary mix, under, photo-stimulation or inhibition off conditions. This was to confirm that after optogenetic modulations for an odor pair, how do animals perform again on a complex task when the photo-stimulation is off. We observed that the NW mice performed normally on a complex task and reaching to d' value of ~ 3 at the end of olfactory training. This was comparable between both EYFP-NW and Arch-NW cohorts, as this odor pair was done under light off conditions (Figure 2-11, A).

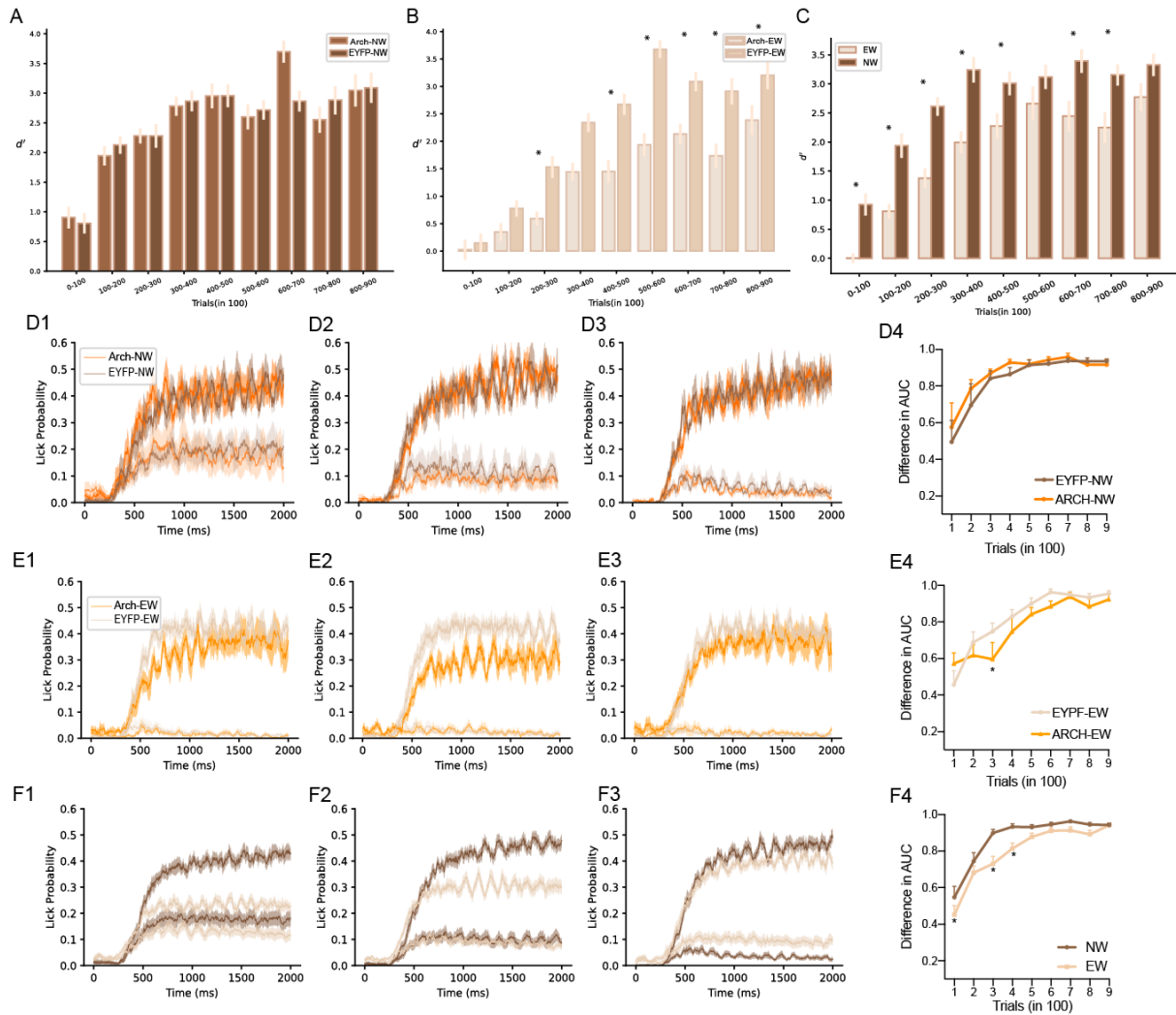


Figure 2-11: Learning on a complex odor without optogenetic manipulation of bulbar circuitry

A. Similar d' values between ARCH-NW and EYFP-NW mice (Intra-NW groups) for AA vs. EB 60-40 complex task, third odor pair in sequence of training. This task is done under photo-stimulation off condition ($p = 0.9$, $F = 0.01$, Two-way ANOVA, LSD Fisher test, $p > 0.05$ for all data points, $N = 6-9$ per group).

B. Chance-level learning for previous odor pair (done under photo-inhibition) led to intra-EW group changes for the next odor pair, AA vs. EB 60-40 complex as observed lower d' values achieved by Arch-EW mice as compared to EYFP-EW mice ($p < 0.0001$, $F = 39.89$, Two-way ANOVA, LSD Fisher test, $p > 0.05$ for all data points, $N = 6-10$ per group).

C. Overall learning pace for NW vs. EW mice differs as observed by reduced d' values for this task, done under light off condition ($p < 0.0001$, $F = 83.59$, Two-way ANOVA, LSD Fisher test, $p < 0.05$ for data points, $N = 18-22$ per group). This comparison contains mice from all three groups in NW and EW cohorts.

D1 to D3. Lick probability curves for first 300 trials indicating similar discriminatory power of both cohorts of mice. Dark orange: Arch-NW and Dark brown: EYFP-NW.

D4. Difference in AUC over the training period shows no difference in discrimination between EYFP-NW and ARCH-NW mice ($p = 0.24$, $F = 1.36$, Two-way ANOVA, LSD Fisher test, $p > 0.05$ for all data points).

E1 to E3. Lick probability curves for first 300 trials indicating marginally different discriminatory power of both cohorts of mice. Light orange: Arch-EW and Light beige: EYFP-EW.

E4. Difference in AUC over the training period shows minute overall difference in discrimination between EYFP-EW and ARCH-EW mice ($p = 0.04$, $F = 4.2$, Two-way ANOVA, LSD Fisher test, $p < 0.05$ for one data point).

F1 to F3. Lick probability curves for first 300 trials indicating slower discrimination of EW mice again when photo-stimulation is kept off for a complex AA vs EB task. Light brown: EW and Dark brown: NW.

F4. Difference in AUC over the training period shows overall difference in discrimination between NW and EW mice ($p < 0.0001$, $F = 26.44$, Two-way ANOVA, LSD Fisher test, $p < 0.05$ for data points).

For 900 trials of training of Arch-EW mice while inhibiting these neurons led to chance level accuracy of performing the discrimination task. This may have influenced the rule learning of the mice and thus, can affect subsequent learning in case of stressed mice, especially. We, indeed, observed a reduction in the learning of Arch-EW mice as compared to EYFP-EW on AA vs. EB complex task. This task, as mentioned before, was carried out under no light conditions hence we did observe learning even in Arch-EW mice, but, at a slower rate (Figure 2-11, B). Finally, when pooled groups of NW and EW cohorts were compared on this task, we saw a reduced performance again on this task (Figure 2-11, C). The corresponding AUC differences in the S+ and S- lick probability curves also displayed slower performance in discriminating the odors (Figure 2-11, F1 to F4). Thus, we showed that upon bi-directional modulation of the somatostatinergic circuitry existing in OB, olfactory learning capabilities can be altered which suggests direct role of these neurons in governing olfactory perception. Activation via ChR2 photo-stimulation of these neurons can rescue the ELS behavioral phenotype while inhibiting them using Arch in NW mice mimics the learning pace of EW mice.

2.4.5 Olfactory memory remained unaffected by the optogenetic manipulation of bulbar circuitry

We also observed olfactory memory deficits in case of EW mice (Figure 1-17, Chapter 1). As we observed improvement in learning deficits of mice that suffered from ELS by optogenetic

activation of SST releasing GABAergic bulbar interneurons, we also quantified their olfactory memory. For this, training was carried out under photo-stimulation for Carvones 60-40 and the mice also continued with resistance to memory extinction task. Memory for the odor pair was tested one month later in the background of another odor pair, geraniol vs. nonanol. Photo-stimulation was only done during training and RME task and not while testing memory. We found that across all three odor pairs, AP vs. ON, Carvones 60-40 and AA vs. EB 60-40, olfactory memory remained impaired in case of EW mice (Figure 2-12, A,C: $p < 0.05$, Unpaired t-test or one-way ANOVA for B). Encoding of olfactory memory consolidation and recall would need optimal circuit functioning which probably constitutes the cortical regions such as AON. The neural underpinning of impaired olfactory memory thus remains elusive. Our data suggests that the SST-neuronal sub-population of OB constitutes a micro-circuitry that may not play a major role in governing olfactory memory.

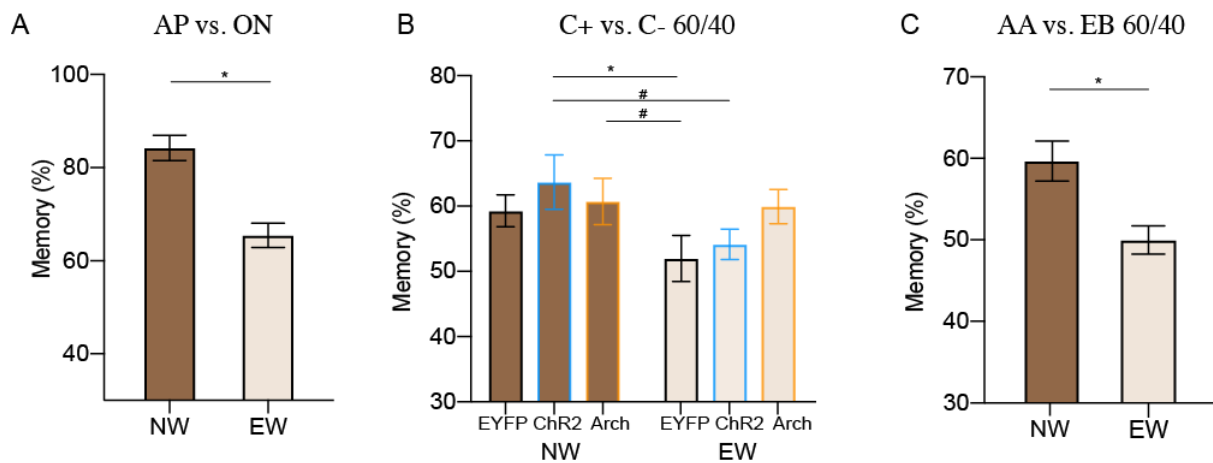


Figure 2-12: Olfactory memory remains poor in EW mice irrespective of any optogenetic modulations

A. Lower olfactory memory % in EW mice as compared to NW mice for a simple AP vs. ON odor pair under no condition of optogenetic manipulations ($p < 0.0001$, Unpaired t-test, two-tailed, $N = 22-24$ per group as all three transgenic cohorts are combined per NW and EW group).

B. All 6 groups in NW and EW cohorts are shown. Blue outline shows photo-activation while orange show photo-inhibition while carrying out learning of Carvones 60-40 task. No optogenetic modulation was done during the memory recall task. We observed that the memory % ranges between 50-78% in NW mice while it ranges from 39-64.2% in EW mice. Overall, memory impairments are observed upon comparing EW mice groups to NW (*: $p = 0.01$ for ChR2-NW vs. EYFP-EW, #: $p = 0.057$ for ChR2-NW vs. ChR2-EW and #: $p = 0.07$ for Arch-NW vs. EYFP-EW, One-way ANOVA, LSD Fisher test, $N = 5-9$ per group).

C. Lower olfactory memory % in EW mice as compared to NW mice for a complex AA vs. EB 60-40 odor pair under no condition of optogenetic modifications ($p = 0.0032$, Unpaired t-test, two-tailed, $N = 16-17$ per group).

2.5 Discussion

2.5.1 Optogenetic activation of inter-neuron population of Olfactory bulb

Numerous transgenic mouse lines labelling the neurons of OB circuitry have been utilized to specifically characterize their functional connectivity and relevance in behaviors. Interneurons residing in the EPL of OB which are positive for parvalbumin (PV) and SST are known to form dendro-dendritic synapses with the projection neurons, thereby, modulating the OB output^{95,214}. We have found out that the OB micro-circuitry consisting of SST-releasing GABAergic play a crucial role in reducing learning deficits induced by ELS. Using Arch channel based photo-inhibition of this circuitry in NW mice led to deterioration of olfactory learning for the same odor pair, Carvones complex 60-40 task. Our data suggests that in NW mice, even after photo-activation of these neurons, not much improvement in the learning was observed. Thus, it could be hypothesised that the circuit may be working optimally and could not be more fine-tuned by further photo-activation, at least in case of NW mice. It could also be that the activation of this circuit may be required for much more complex odor discrimination learning tasks. However, interestingly, inhibiting this circuitry did cause a decrease in learning on the same task in Arch-NW mice. This explained the importance of a fully functional circuit, disrupting which, led to behavioral impairments. However, we need to take an integrated approach to understand how the modulation of these interneurons change the output of the OB. Such approaches are well-known in the field. For example, a combined approach of optogenetically activating the Vasoactive intestinal peptide (VIP) positive interneurons of OB and extracellularly recording from M/T cells displayed direct inhibitory connections of the interneurons to the projection neurons²³¹. Yet another study that did optogenetic activation of glutamatergic neurons releasing the preproglucagon found in GCL, recorded both IPSCs and EPSCs in M/T cells. This is yet another unique microcircuit of OB that controls its output in a multi-phasic fashion via both mono-synaptic and di-synaptic connections to the M/T cells²²⁸. We are currently employing optogenetic targeting of the SST+ population and simultaneously recording from the projection neurons of the OB slices to selectively dissect the role of this node in the OB circuitry.

Pharmacogenetic inactivation of PV+ neurons of OB showed that these cells can linearly control the output of OB without altering their tuning properties^{95,120}. While GCs can cause changes in odor selectivity and thereby, odor tuning, PV cells of EPL are proposed to control

the gain of OB without disrupting odor selectivity. In comparison to GCs which receive ~6% of excitatory contacts from M/T cells, PV cells receive 60% contacts in 200µm area and more than 80% of these contacts are reciprocal⁹⁵. Neurons of EPL are then plausibly poised to contact many projection neurons receiving inputs from multiple glomeruli and can thus, facilitate inter-glomerular inhibition. Another population of EPL neurons that co-localise CRH with PV are also shown to control the gain output of the OB⁹⁶. These neurons, too, make mono-synaptic contacts with M/T cells and inhibit them. Although they just constitute 30% of the total EPL population, it remains unknown whether they themselves perform specialized functions. However, local CRH signalling has been shown to promote adult born neuronal integration by stabilizing its synapses, suggesting, a neuro-modulatory role of these neurons in OB²²⁷. Given that a proportion of these neurons also co-localize for SST, it would be worth probing how the dynamics of the release of these peptides and transmitters would change under stress.

2.5.2 Neuropeptides are released upon optogenetic modulation

Optical control of cells has gained popularity since 2005 when millisecond level neuronal activation was displayed in mammalian neuronal cells²³². Since then, most of the optogenetic based studies are based upon release of GABA and Glutamate neurotransmitters which facilitate the understanding of synaptic connectivity²³³. It thus becomes an important tool to deconstruct precise circuits that can modulate specific behaviors. Usage of optogenetics is recently being done to also evoke release of biogenic amines and peptides²³³. Neuropeptides are often known to be co-released along with the transmitters yet their role is generally studied by creating knock-outs or by adding agonists or antagonists. Most often, low frequency light stimulation is used for release of transmitters and higher frequency stimulation parameters with longer durations could be used for orexin peptide release²³⁴. Using an *ex-vivo* approach of applying photo-stimulation at 40Hz to the viable OB slices, which were continuously bubbled with carbogen at ambient temperature, we found out that in Chr2 mice, SST neuropeptide was released as quantified using ELISA approach. Similar experiment is to be done to investigate the release of transmitter as well.

2.6 Future directions

2.6.1 Morphological quantification of SST-releasing inhibitory interneurons of OB

To observe if the SST-releasing GABAergic interneurons are altered in case of EW mice, we started to investigate the morphological features of these neurons. We began with quantifying and re-constructing neurons from OB slices (50 μ m) of the SST-Arch mice belonging to NW and EW groups (N = 1 per group, currently). We started to probe the morphology starting from the very early time-points of their postnatal life. Here, we utilized P16 mice so as to begin to understand the plausible age-dependent and ELS modulatory changes in the structure of these neurons. The sparse neurons found in the GCL were imaged using a confocal microscope (Figure 2-13, A). Preliminary data analysis involving primary dendrite length, branches and spine quantification was carried out using the semi-automatic ‘filament’ tool of Imaris software. We found out that the number of spines varied between the two mice belonging to NW and EW groups. Our preliminary analysis show lowered spine number, suggesting of ELS modulated effects on the activity-dependent structural changes in the neurons. We are currently trying to quantify cell body numbers in the EPL and increase the sample size . Due to dense branch cross-overs observed in SST labelled neurons (see Figure 2-3, B), the branching pattern per neuron could not be re-constructed.

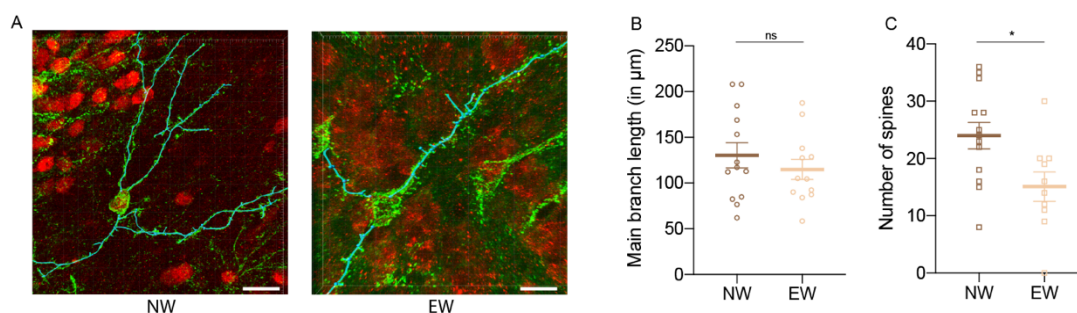


Figure 2-13: Morphological analysis of SST-releasing inhibitory interneurons of OB

A. Immunofluorescence images of re-constructed (in cyan) SST-releasing GABAergic interneuron of a NW (left, scale bar: 10 μ m) and EW (right, scale bar: 7 μ m) mice. Transgene GFP expression was imaged using Leica sp8 as SST-Arch mice were utilized for this experiment. The branching pattern and spines were reconstructed using the semi-automatic ‘Filament’ tool of Imarisx64 (Bitplane, Oxford Instruments) software. These neurons are located in the GCL of the OB. Green: GFP, Red: NeuN.

B. The preliminary analysis of the main branch (primary dendrite) length quantification revealed similar length (in μ m) between a NW (Average length: 130.3 μ m) and EW (Average length: 114.9 μ m)

of mouse OB ($p = 0.3$, Unpaired t-test, two-tailed, $n = 11-12$ neurons per mouse, $N = 1$ mouse per group).

C. The preliminary analysis of number of spines per neuron reveals significantly lower number of dendritic spines of these neurons in EW mouse OB ($p = 0.017$, Unpaired t-test, two-tailed, $n = 11-12$ neurons per mouse, $N = 1$ mouse per group).

2.6.2 Imaging of SST-interneurons and recording of Olfactory bulb projection neurons in early weaned and control mice

To probe the system-level understanding of bulbar SST-releasing interneurons in NW vs. EW conditions, first step is to probe their functionality. We firstly used the approach of calcium imaging during anesthetized and awake states of the mice (Carried out along with Mr. Sarang Mahajan). To this end, we implanted lens canula in 6 NW mice at $0.6-0.7\mu\text{m}$ depth so as to record changes in Ca^{2+} signals from the EPL neurons (See methods, section 2.3.7). In anesthetic conditions, odor detection recordings were carried at 1% (v/v). However, we observed varied relative fluorescence changes across different mice. A representative relative fluorescence change is plotted in Figure 2-14, B across four different odors, averaged for 20 trials per odor for a mouse (HX: Hexanal, PN: 2-Pentanone, O(-): Octanal(-) and O(+): Octanal(+)).

The inter-mouse variations and a minute relative change in fluorescence could occur as a result of sparse localization of SST-neuronal cell bodies in the EPL. The signal was captured using the Doric Inc. lenses with a field of view of $350\mu\text{m} \times 350\mu\text{m}$ at 10Hz frame rate and the images are further cropped to $300\mu\text{m} \times 300\mu\text{m}$ to get rid of the vignettes at the edges of the frames. In this frame dimensions, the number of cell bodies that would be chronically imaged would indeed be very few to nil. Although the craniotomy was carried out at similar location and the lens on each animal has been placed at similar depth, slight changes are expected. We continued to carry out calcium imaging during odor discrimination tasks, as well (Figure 2-14, C) where we observed an overall decrease in the amplitude as the training progressed. For each task of 300 trials, calcium responses were only recorded for 40 trials per animal. Such a decrease could be indicative of activity-dependent refinement of the neuronal responses during learning.

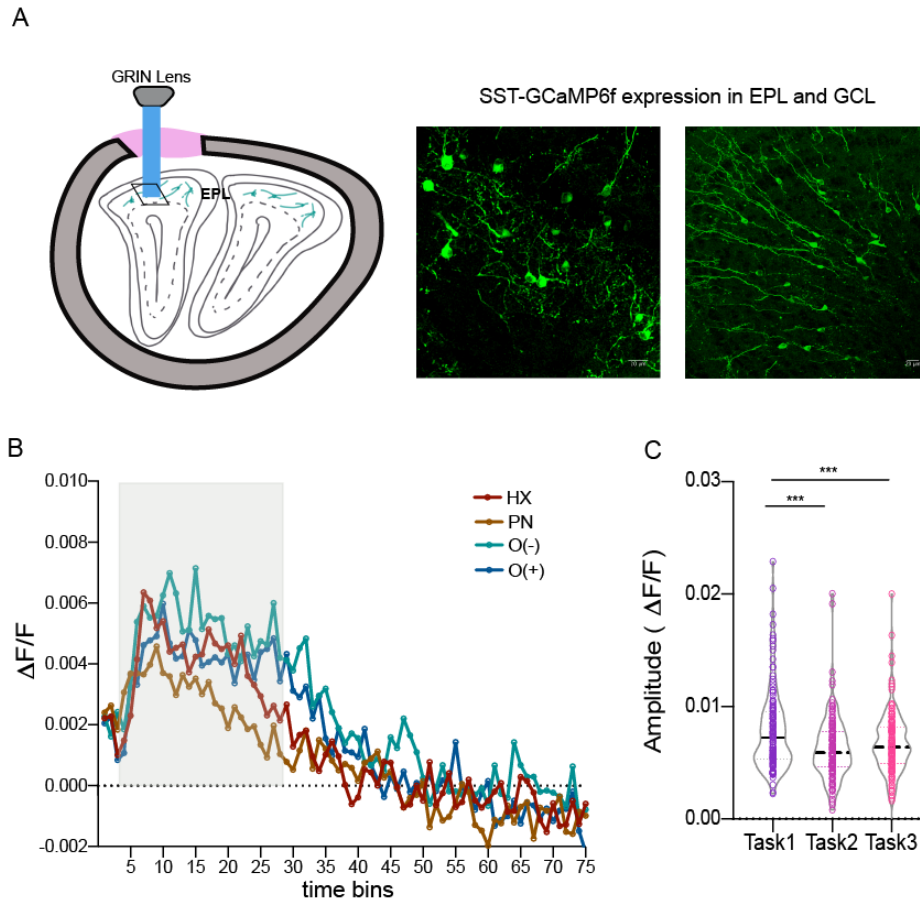


Figure 2-14: Response of SST releasing GABAergic interneurons under anesthetized and awake conditions

A. Schematic depicting GRIN lens implanted in the EPL of OB. Cranial window was drilled at the top of one of the OB to allow for implantation of lens canula. The exposed area was covered using acrylic cement. A protective cap over the miniscope was put when imaging was not being done. SST-GCaMP6f expression was observed in OB EPL and GCL. Dulbecco PBS (modified solution was used when the animal was perfused. OB slices sectioning was also carried out in this solution that allowed for enriching the GFP signal for imaging using confocal microscope (Scale bar: 20 μ m).

B. Relative fluorescence changes (averaged over trials) for an animal for four different odors under anesthetized condition over time (each time bin = 10ms) (HX: Hexanal, PN: 2-Pentanone, O(-): Octanal(-) and O(+): Octanal(+)). The gray box indicates the duration for which the stimulus was presented. This suggests that SST-releasing GABAergic interneurons respond during the delivery of odor after which the responses goes to baseline level.

C. A significant decrease in the amplitude of the relative fluorescence changes (during stimulus duration) was observed as the training progressed from task 1 to 2 and from task 1 to 3 ($p < 0.0001$, $F = 11.64$, One-way ANOVA, $N = 5$ mice). Such a decrease over training progression could be indicative of activity-dependent refinement of neuronal responses during learning.

Finally, to dissect out the ELS mediated deficits in the responses of these neurons and the subsequent effect on the output of the OB, we are carrying out opto-electrophysiological recordings of the projection neurons of the OB upon optically modulating the bulbar SST releasing GABAergic neurons.

Chapter 3

Involvement of multiple sensory systems in learning of pheromonal locations

Adapted from: *Pardasani, Meenakshi, Shruti D. Marathe, Maitreyee Mandar Purnapatre, Urvashi Dalvi, and Nixon M. Abraham. "Multimodal learning of pheromone locations." The FASEB Journal 35, no. 9 (2021): e21836²².*

3.1 Abstract

Learning to find pheromonal locations is a quintessential task for rodents to find mates and avoid the competitors. This sensory information is processed by both the main and accessory olfactory systems. In nature, mice might find the scent marks sprayed upon textured entities of varying shapes and sizes which can cause activation of whisker subsystems. Role of somatosensation in memorizing the pheromone locations remain largely unexplored. We investigated the role of multiple sensory systems by training female mice by building a novel socio-sexual task to locate pheromones. This task enabled sampling of volatiles emanating from male urine through holes of varying dimensions or shapes that are sensed by their whiskers and vibrissae. Establishing this paradigm also facilitated investigating the olfactory based social learning behavior of ELS mice.

Using this assay, we found out the preference of female mice' toward male urine scent decayed over time when they were permitted to explore pheromones vs neutral stimuli, water during the initial phase of testing. On actively training them for the associations involving olfactory and whisker systems, they were able to memorize the location of opposite sex pheromones, when tested 15 days later. This memory was not formed either when the somatosensory inputs through whisker pad were blocked or when the opposite sex pheromonal cues were replaced with that of same sex. We, also confirmed the involvement of these sensory systems by the enhanced expression of the activity-regulated cytoskeleton protein. Furthermore, in case of early weaned female mice, multimodal memory was not established and the Arc expression indicated significantly lesser activity in olfactory bulb, somatosensory cortex and dentate gyrus regions.

3.2 Introduction

3.2.1 Social odors in rodent world

Rodents navigate through olfactory landscapes where they encounter odors emanating from food, mates and predators²³⁵. This entails occurrence of progressive events, i.e, active sniffing of odors followed by odor localization and finally, generation of appropriate physiological and behavioral responses. Memory of such highly relevant olfactory instances can also be formed and recalled later on. One of the physiologically relevant examples is that of exposure to social odors or pheromones^{236,237}. Pheromones (*Pherein*: to carry and *omones*: to excite) are semio-chemicals which when released by the members of the same species, can generate attraction in the opposite sex or defensiveness and aggression in the same sex^{238,239}. The underlying neural processes for encoding pheromonal information have been worked out in rodents^{240,241}. In this section of chapter 3, I will summarize the existing literature on pheromonal processing, plausible usage of more than one sensory system in mediating the social interactions and changes in such behaviors under special contexts (stress) and situations (internal states).

3.2.1.1 Scent marking in rodents

Rodents tend to mark their surroundings using their urine and other bodily fluids (saliva, feces) which serve as communication signals²⁴²⁻²⁴⁴. Many animals such as voles, hamsters, ungulates and even primates line their scent marks to be sensed and perceived by the members of their species²⁰. They mark and even over-mark the scent marks which can be distinctly sensed by the receivers. For example, a dominant male mouse countermarks the scent marks of other males but not of their own^{245,246}. The scent marks may provide unique information about the sender to which the receiver can choose to respond or avoid depending upon the context (such as territoriality) and the sex of the depositor^{247,248}. Scent-marking is usually done by males of the species (in mice) as it is an androgen-dependent process²⁴⁹. Indeed, it has been shown that female mice who were neonatally androgenized, exhibited more marking behavior as compared to normal female mice or the ovariectomized mice suggesting the role of sex steroids in mediating this behavior²⁵⁰. However, this is not applicable to all other species, as animals like female Meadow voles also use scent marks to attract the males²⁵¹.

Male urinary marks do influence the female physiology and such effects are rather well-known in the field. Repeated exposure to male urine can induce and synchronize the estrous cycle in female mice, referred to as the Whitten effect^{252–254}. The urine of dominant males can accelerate the onset of puberty in female mice. This effect is called as Vandenberg effect²⁵⁵. Apart from these endocrine influences, an unfamiliar male mouse scent can block the pregnancy in a female mouse. It happens via blocking the release of prolactin and failure of the embryo to get implanted and is called as the Bruce effect^{256,257}. All these effects are obviously mediated by the chemical constituents of the urine marks. It has been shown that the unfamiliar male, who is genetically different from the stud male at Major histocompatibility complex (MHC) locus can cause the pregnancy block effectively²⁵⁸. Urine constituents consists of both MHC dependent volatiles, non-volatiles as well as Major Urinary Proteins (MUP)²⁵⁹. Male mice display different MUPs in their marks so as to be distinguished from another male's deposits^{260,261}. MUPs can also bind small volatile chemicals and release it into the air in a testosterone dependent fashion, thus, advertising the presence of a sexually receptive male in vicinity^{262–264}. The scent marking in mice is thus, the job of males primarily to signal the receptive female mice for mating²⁶⁵. In the next subsection, the neural processing of pheromonal volatiles and non-volatiles by the olfactory system is discussed in detail.

3.2.1.2 *Pheromone guided information processing*

Olfactory system consists of the Main Olfactory Epithelium (MOE) and the Vomeronasal Organ (VNO) as the peripheral recipients of odors which then pass on the information to MOB and Accessory Olfactory bulb (AOB), respectively^{240,266}. The VNO is a vasomotor pump like organ present at the rostral end of the nasal cavity, and can collect the non-volatile odors present in the fluids^{267,268}. Arousal or exposure to novel situations can cause blood flow changes in the vessel near to the VNO which can facilitate widening of VNO lumen leading to gathering of the stimuli by the peripheral organ²⁶⁹. The VNO consists of three types of Vomeronasal receptors²⁷⁰. These, like, the receptors present in OSNs, belong to the G-protein coupled receptor (GPCR) family²⁷¹. V1Rs and V3Rs are present in the apical domain while V2Rs are located in the basal domain of the VNO^{272–275}. Another type of receptors bind to formyl peptides^{276,277}. All these types are present in different vomeronasal sensory neurons (VSNs).

A

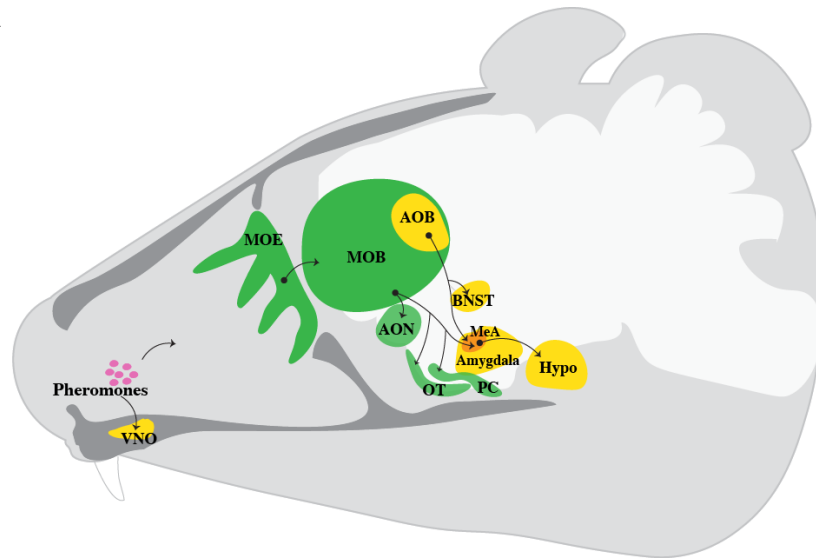


Figure 3-1: Processing of pheromones by olfactory subsystems

A. Illustration depicting the murine neural circuitry involved in pheromone processing. Pheromones that are non-volatile are sensed by the sensory neurons of the VNO while the volatile pheromones are sensed by MOE olfactory sensory neurons. These project to AOB and MOB, respectively. The olfactory cortical regions that form the underlying cortical processing involves the AON which send projections to OT and PC. The AOB send projections to BNST, Amygdala and finally hypothalamic regions. Finally, hypothalamic projections to periaqueductal gray. This region underlies the lordosis movements of the female mouse. VNO: Vomerolnasal Organ, MOE: Main Olfactory Epithelium, MOB: Main Olfactory Bulb, AOB: Accessory Olfactory Bulb, AON: Anterior Olfactory Nucleus, BNST: Bed Nucleus of Stria Terminalis, MeA: Medial Amygdala, OT: Olfactory Tubercle, PC: Piriform Cortex, Hypo: Hypothalamus (adapted from Asaba et al. 2014)²⁷⁸.

In contrast to the promiscuous nature of OSNs, VSNs are highly specific in binding to pheromonal molecules. Further, the projection patterns of the VSNs remains segregated until their termination in the glomeruli of AOB²⁷⁹. The binding of different types of vomeronasal receptors to various intra and inter-specific stimuli reveals that V1Rs have generalized activation profiles and that they bind to steroids. V2Rs, on the other hand, are more specifically activated by compounds released, for example, by a particular sex in a particular ethological context²⁸⁰. The information is relayed to AOB which further projects to Medial Amygdala (MeA) and Postero-medial cortical amygdala (PMcO) and bed nucleus of stria terminalis (BNST) which further impinge on the hypothalamic neurons²⁸¹. The Ventrolateral hypothalamus (VMHvl), both in male and female mice, controls for the sexual behaviors^{282–284}. Using activity dependent labelling methods, Ishii & colleagues delineated the neural

circuitry from VSR via VMHvl neurons to dorsal Periaqueductal gray (PAG) that regulated the lordosis behavior of female mice upon exposure to the major component of male mouse lacrimal gland secretion, an exocrine gland secreting peptide-1^{285,286}.

MOB is also known to be involved in the pheromone information processing. Indeed, the notion of the dichotomous functionality of the main and the accessory olfactory sub-systems has been questioned by several experimentalists²⁸⁷. It is no longer believed that the VNO alone encodes the pheromonal stimuli while the MOE encodes other non-pheromonal volatiles²⁷⁰. Urine activated immediate early genes (IEG) were found out to be present in the ventro-lateral glomeruli of MOB²⁸⁸. In an elegant study that combined the extracellular electrophysiology with the simultaneous solid phase micro-extraction gas chromatographic separation of pheromonal volatiles in mice revealed presence of urine volatile specific Mitral/Tufted cells in both female and male mice²⁸⁹. Neural tracing methods that showed direct connections of the dedicated OSNs found in medial olfactory mucosa to the Luteinizing hormone releasing hormone (LHRH) secreting population of hypothalamic neurons indicated role of main olfactory system in reproductive behaviors²⁹⁰. Although the connectivity of MOB neurons to olfactory cortex and the anterior and posterolateral cortical amygdala is known, a report that retrogradely traced the MeA projecting M/T cells of MOB exists too. This population of projection neurons were shown to be active by the urinary volatiles of male mouse by c-fos labelling²⁹¹, thereby, providing the evidence of a direct pathway from MOB to MeA in pheromonal processing. A fairly recent study dissected the specific role of dorsal OSNs in mediating social behavior. A conditional *cng2a* (cyclic nucleic acid gate channel-2) knock-out in specifically the dorsal zone OSNs led to VNO-independent display of aberrant social and defensive behaviors in both male & female mice. Further, they found out that the functional inactivation of dorsal MOB by creating this knock-out led to reduction of c-fos positive cells in Anterior olfactory nucleus (AON) suggesting the possible role of AON in pheromone dependent behaviors. Using the lesion based disruption of AON, they further found out that they project to the down-stream amygdaloid & hypothalamic nuclei to which the VNS converge and generate the socio-sexual behaviors²⁹². Thus, both MOB and AOB are quintessential in mediating pheromonal dependent behaviors in rodents.

3.2.1.3 *Modulation of social communication strategies by internal & external factors*

Social communication and cognition are important for carrying out mate choice^{293–295}. It involves various sensory & cognitive steps to be undertaken by an individual to have a successful mating experience. This entails sequence of events, starting with, reliably receiving the direct and indirect cues of the opposite sex which can be either proximally or distally present^{21,296}. The sensation and processing of cues can require more than one sensory system's activity. Olfaction, audition, somatosensation and vision can all play a role in successfully detecting the pheromonal cues^{296–298}. Thus, depending on where the depositions are made, the differential role of the sensory systems can come into play. This can lead to generation of varying social communication strategies, for example, ultrasonic vocalizations coupled with smelling scent marks^{299,300}.

Detection and further attraction towards the scent marks can also vary depending on the status of individual's health and the quality of the immediate environment. For example, olfaction can facilitate detection of infectious or unfamiliar mating partners which are then not favored by the female mice^{301,302}. Infection thus becomes one of the internal factors that causes avoidance by the opposite sex³⁰³. Indeed, changes in the MHC class-II genes upon infection can cause changes in the volatile compounds released which are then avoided by the opposite sex²¹. Apart from the effect of health status, the environmental conditions in which animals are reared can have a lasting impact on the social behaviors. Solitary housing, for example, in case of social rodents, can have a massive negative effect on female mice³⁰⁴. It causes hyperactivity of adrenal glands, impairments in mating behavior as well as poor learning and aggressive behavior³⁰⁵. Female mice models of social instability which includes both isolation & social crowding of males and females disrupts the Hypothalamic-Pituitary-Gonadal (HPG) axis causing alterations in the levels of prolactin, luteinizing hormones and changes in estrous cycle. A chronic model of such social instability can lead to anhedonia and development of depressive disorders^{306,307}.

'Mate-choice copying' is yet another phenomenon that can change how a female mouse perceives an opposite sex's scent mark³⁰⁸. Dependence of sexually naïve females on the preference of other in-estrous female mouse for a particular mating partner indicates that they learn from peers to choose a high-quality male over others. Females sniff those male scent marks more which are counter-marked by another estrous female than the other scent marks which are either not counter-marked or are associated with marks of a non-estrous female³⁰⁹. Such a cognitive strategy of a female mouse can change depending on the environmental

conditions she is presented with. It can also be affected by events that can cause changes in the level of neuropeptides such as Oxytocin which mediate such complex social interactions³¹⁰.

Factors leading to disruption or augmentation of neurobiological mechanisms governing social interactions, learning and memory can thus directly or indirectly affect the mating preference. Oxytocin which is released by the Supraoptic and Paraventricular nuclei of hypothalamus exert its influence on social behaviors by binding to its cognate receptors present in various brain regions including OB, olfactory cortex, insular cortex, thalamus, hippocampus & amygdala³¹¹. Females with deleted oxytocin gene or with injected oxytocin antagonists cannot distinguish infected male and also fail to carry out mate-choice copying²¹. Thus, modulation of oxytocin and their receptors under conditions of stress and enrichment can influence social detection and learning in female mice. Yet another neuro-hormonal mechanism that influences the female reproductive behavior involves estrogens. A study proposes a four gene 'micronet' system acting in the forebrain in modulating social recognition. Ovarian estrogens act on ER- β receptors to regulate oxytocin secretion in paraventricular nucleus of hypothalamus. It can also bind to ER- α receptors present in amygdala that can modulate the density of oxytocin receptors in amygdala³¹². All these studies thereby indicate that social behaviors are under a great deal of modulation by the animal's internal states and the environmental conditions that it is exposed to.

3.2.2 Whisking the odors

When rodents are involved in exploratory behaviors, smelling and whisking work in concert. This implies the existence of a phase-locked rhythm controlling the sniffing and whisker movement, first reported by Welker in 1964³¹³. Sniffing is a vital rhythmic motor process that allows for odor sensation. Indeed, while exposed to odors in operant tasks or while encountering novel odors, sniffing frequency reaches up to 8-12 Hz from the basal level of 2-4 Hz³¹⁴. In a study using rats, a thermocouple was implanted in the nasal cavity to record sniffing frequencies. It was shown that while tracking the odor trails, the sniffing rate fluctuated which mimicked what an optimal Shannon-Nyquist sampling criterion would display. This meant that the rat was sniffing close to 2-3 times every time the nose was crossing the trail to near-optimally sample the signal (odor)³¹⁵. What is also important to note is that the sequence of whiskers' movements starting from protraction to retraction are coupled to the sweep of a single sniff in rodents^{313,316}. In this part of Introduction, I will focus

on the multisensory strategies, including the sniffing-whisking strategies that rodents display to optimally make decisions and how that is dynamically modulated by specific neural circuits.

3.2.2.1 *Multisensory strategies for learning and memory*

Multisensory actions leading to improvement in learning and memory were initially easily studied in large mammals such as humans and macaques. To uncover neural circuits governing the enhanced responses that multisensory actions can generate, requires the usage of rodents and the transgenic strategies that it offers^{317,318}. Multisensory enhancement often requires temporal synchrony, i.e, the stimuli activating the different modalities are presented in a paired fashion, or in other words, are provided to the animal simultaneously^{319,320}.

Associative conditioning tasks, thus, becomes, a route of introducing multisensory decision-making tasks to the individual³²¹. Such tasks allow us to record the changes in the accuracy and the time-scales of making perceptual decisions under uni-sensory and multisensory conditions. For example, an operant chamber was used to train mice to visual and auditory stimuli alone and they were later, checked for multisensory responses to paired audiovisual stimuli. In the uni-sensory training task, mice were first trained to flash of light when it poked its snout to either of the left or right hole. It needed to associate the hole paired with light and enter that again to get the reward. This task was followed by an auditory task where tone was paired to the left hole and a white noise to the right hole. Upon the completion of training, testing the responses for single and combined stimuli for different stimulus durations revealed higher performance accuracy and larger multisensory gain for audiovisual combined stimuli³²². Thus, such a temporal synchrony during the presentation of multisensory stimuli can actually help the animals to locate objects if both the sensory cues, for example, are related to the same object. However, in nature, one or both of the cues may be continuously being received, and may not be tightly presented in a precise time window. This could be true, for example, when a continuous stream of auditory stimuli reaches the ear or the plume of scent marks exists in the immediate environment of an animal. Such stochastic time-varying stimuli, thus, characterize what animals face in the natural world. Hence, the strictly associative tasks depending on the mechanisms governing only synchronous stimuli are indeed being adapted and modified to more ethological tasks so as to assess the multisensory behavior as a function of time^{323,324}. Nevertheless, multisensory research has uncovered

several neural mechanisms that are modified during training with either congruous or incongruous stimuli. These circuit adaptations support multisensory learning and memory.

A

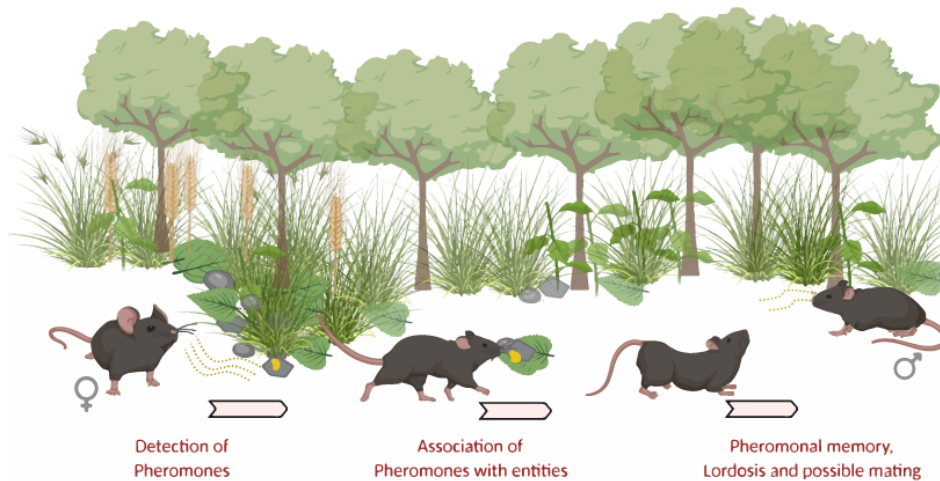


Figure 3-2: Simultaneously occurring multi-sensory cues in natural surroundings

A. Illustration depicting a hypothetical female mouse smelling the volatiles emanating from the urinary scent mark deposited in the natural surroundings by the opposite sex. The volatiles may help to locate the source, which could be marked on the pebbles, stones and leaves of different textures and sizes. The simultaneous brushing of whiskers and sniffing the pheromonal cues may help in associating the cues and thereby, may facilitate retention of multimodal memory. Finally, female mouse would then lordosis-like behavior that could lead to mating (Image created in BioRender.com).

Initial view suggested that the sensory systems need to be activated and converge onto ‘multisensory neurons’ of the cerebral cortex that integrates the inputs to form a multisensory percept³²⁵. In fact, by using single and multi-unit recordings of different regions, one can distinguish unimodal from bimodal/trimodal neurons and also can characterize those neurons which can be ‘sub-threshold’ multisensory neurons, i.e, activated primarily by one sensory stimulus but whose activity can also modulated by other sensory stimulus³²⁶. In one study, authors employed neuronal tracing combined with electrophysiology and two-photon calcium imaging (*in vivo*) to dissect out areas responsible for encoding and retrieving associative signals in a cross-modal reflex task. Pairing of odor and whisker signals led to generation of odor-induced whisker motion in mice. Repeated association caused afferent pathways for whisker movement, i.e, input from thalamus and that for processing odor, i.e, from the piriform cortex integrating their information at the level of barrel cortical neurons. They found out that the barrel cortical neurons primarily served as the associative memory cells

that governed the generation of reflex as they started to encode both whisker as well as odor related information. The barrel cortical neurons differed in their strength of encoding odor or whisker motion and together mediated the cross-modal behavioral effects³²⁷. The molecular underpinnings for the formation of associative engrams was found out to be lying in generation of new synaptic connections. An mi-RNA-324 mediated signaling cascade led to dephosphorylation of Tau protein causing stabilization of microtubules leading to axonal growth and synaptic recruitment from piriform cortex to barrel cortical neurons³²⁸. In case of natural surroundings, rodents recruit both the nose and the whiskers, i.e, their muzzle to find objects of ethological relevance and to interact with the other members of the same or different species. Using a head-fixed whisker based object localization paradigm, mice were trained to gauge the distance of the pole from the whiskers. The pole that made contact with whiskers were divided into go and no-go trials depending on their position relative to the whiskers. Upon learning, by using calcium recording, it was found out that the excitatory neurons of Layer 2/3 of barrel cortex could discriminate between the trial types with high accuracy³²⁹. This suggested the involvement of barrel cortical neurons in localization of object. How the information pertaining to odorous object localization is encoded still remains an open issue. It is feasible to predict that apart from the sensory systems coordinating to form multi-sensory decisions, other areas such as Hippocampus and the connected cortical areas can further be involved in forming multisensory memory and retrieving it when the need arises³³⁰. For example, a new recombination behavioral paradigm combining the learning of both olfactory and tactile stimuli with a food reward revealed the utilization of lateral entorhinal cortical neurons in a cross-modal task learning. Blockade of NMDA receptors of LEC neurons resulted in impairment in acquiring a cross-modal task but not individual unimodal tasks suggesting it be yet another important area in mediating multisensory responses³³¹. In our study, we wished to examine the behavioral and neural correlates of a multimodal task combining both odor and whiskers in generating the memory of pheromonal locations. Before we delve into our hypothesis, the final section of introduction reviews the existing literature on using Immediate Early Genes (IEG) expression pattern and modulation under conditions of uni and multisensory behaviors.

3.2.3 Immediate early genes as a tool to assess brain region specific activation profiles

To observe the activity dependent changes in neuronal cells, the mRNA levels of the Immediate Early Genes (IEGs) and their translated protein products are usually quantified. IEGs are an important and powerful tool to map the neuronal assemblies that can get

activated at a short latency after the stimulus presentation and are not affected even in the presence of protein synthesis inhibitors³³²⁻³³⁴. Thus, these genes do not require *de novo* protein synthesis. Their induction can be transient in nature, i.e, they have faster decay times and the enhancement in their expression can be dependent on the extent of training or learning a task³³⁵. IEGs, indeed, can be activated by several stimulating factors and this has been assessed in several vertebrates, for example, in response to avoidance learning in rats and chicks, upon LTP induction in specific brain regions, after carrying out sensory discriminative tasks, in response to exposure to social and reproductive stimuli among others^{336,337}.

The IEGs belong to different classes of genes including inducible transcription factors, growth factors, cell-surface receptors and protein kinases. *c-fos* and *c-jun* are extensively studied IEGs that serve to activate the downstream processes upon neuronal activation. These genes act as transcription factors that activate late-effector genes which constitute the ones that synthesize neurotransmitters, the cytoskeletal proteins for growth of spines etc³³⁸⁻³⁴⁰. IEGs allow for determining how sensory information can be stored in brain regions, thereby, providing a first-line of investigating specific neural circuits and assemblies upon experiencing a specific sensory stimulus or repertoire of stimuli. Multiphoton *in vivo* imaging of a type of IEG, *Egr-1* tagged with EGFP reporter protein in cortical layers, unveiled sparse coding of memory traces and their activation are dependent on the context and complexity of the learning task³⁴¹. In a similar study, by tracking the temporal profile of IEG *cfos-eGFP* in retrospleinal cortex using two-photon microscopy, varied neuronal populations getting activated following dual context exposure³⁴². Another study that combined photo-acoustic imaging with *Fos-LacZ* expressing rats allowed for large field of view and high spatial resolution based ex vivo imaging of mPFC following cocaine induction³⁴³.

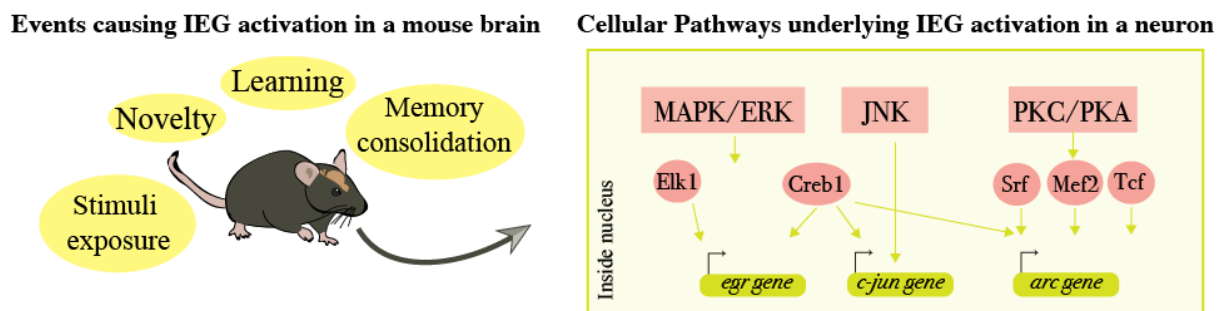


Figure 3-3: Activation of Immediate Early Genes (IEGs)

Illustration depicting events that activate the IEGs in the neurons by using specific signaling pathways. As an example, cellular pathways for activating three IEGs are shown. The factors of the MAP kinase, Jun Kinase and Protein Kinase A and Protein Kinase C pathways cause transcriptional activation of IEGs such as Egr, c-Jun and Arc genes. MAPK: Mitogen-activated protein kinase, ERK: Extracellular signal-regulated kinase, JNK: c-jun N-terminal kinase, PKC: Protein kinase C, PKA: Protein kinase A, Elk1: ETS-like 1, Creb1: CAMP responsive element binding protein 1, Srf: Serum response factor, Mef2: Myocyte-enhancer factor 2, Tcf: T-cell factor.

With the prevalence of multiple IEGs, it is important to understand their mesoscale organization, i.e, how do the different IEG- defined neuronal assemblies correlate with each other, how they differ from one brain region to the other and the extent to which they get activated upon induction of a particular stimulus or training program or a memory task. One study specifically checked the sub-region specific distribution of three IEGs, Arc, Egr2 and Nr4a1 in the striatum upon acute cocaine exposure by multiplexing the single molecule fluorescent in-situ hybridization and single cell-RNA sequencing. They found that within striatum, expression of these IEGs appeared to be graded and is largely correlated at the level of a single neuron. They also found occurrence of neuronal ‘superensembles’ which are the clusters of cells that have robust expression of the three studied IEGs³⁴⁴. However, the extent of IEG activation, i.e, the spatio-temporal dynamics can differ depending on their differential engagement within the circuit. Comparison of Arc, c-fos and zif268 IEGs after spatial learning task in rats exhibited that although all three IEGs showed similar activation levels, the Arc RNA expression was higher in those rats that were most proficient in doing the task and those who learned a new unfamiliar trial³⁴⁵. In another study that involved studying IEGs’ expression upon exposing female mice to clean bedding vs. the soiled bedding of male mice demonstrated that at the level of VNO, the pheromone-induced activation was highest for Egr-1 gene as compared to c-fos, c-jun, Arc, Fos-B and Nr4a1²⁸⁰. These studies suggest that the variation in activation profiles of IEGs depends primarily on the context of the task or the identity of the stimulus.

Indeed, effector IEGs such as Activity-regulated Cytoskeleton (Arc) may be more efficient in tasks involving experience-dependent synaptic plasticity that needs to remain stabilized over time. Arc gene transcribed mRNA is found to be much more specifically located in the synapses that are activated³⁴⁶. Arc/Arg3.1 protein itself is a reliable marker for learning and memory as it can be maintained at steady-state levels in specific neuronal networks. Its

expression can be consistently found during the repeated exploration of the same spatial locations. It is also known to play a role in memory consolidation. Arc expression can be sustained for longer times as compared to other IEGs as was observed 24 hours after contextual fear conditioning tasks in mice³⁴⁷. Arc/Arg3.1 knock-out mice, despite the intact short-term, are not able to form long-lasting memory of implicit hippocampal-independent and explicit hippocampal-dependent learning tasks. This was in coexistence with a failure to consolidate the potentiation at CA1 region and a reduction in long-term depression as well³⁴⁸. Hence, one could argue that Arc plays a major role in homeostatic plasticity by being involved in both Long-term potentiation and depression mechanisms. It does so by regulating actin and cytoskeletal dynamics which underlies LTP the and receptor endocytosis mechanisms which mediate LTD³⁴⁹. This was also elegantly demonstrated in the neuronal culture experiments where heightened activity leading to increased Arc expression caused endocytosis of AMPA receptors and subsequent downregulation of synaptic AMPA receptors, thereby, allowing for optimal synaptic scaling by controlling the trafficking of these receptors³⁵⁰. Thus, IEGs offer a rather straight-forward technique to locate specifically activated neuronal assemblies, however, their appropriate selection should be based on the type of experimental paradigm used.

3.3 Materials and Methods

3.3.1 Subjects

115 C57BL/6J female (10-14 weeks, Jackson Laboratories) and 20 C57BL/6J male mice (~2-3 months age) were used for experiments pertaining to the Multimodal Pheromonal Learning paradigm. Out of the total number of male mice, 12 mice were used for urine collection for different groups of mice as explained. Remaining 8 mice were used for the test of multimodal pheromonal memory.

In total, eight cohorts of female mice trained and tested on ‘multimodal pheromonal learning’ paradigm were used. Cohort 1 comprised of eight whisker intact female mice trained to associate the Male soiled Bedding and Urine volatiles (MBU) with that of a specific diameter on the plate that guarding chamber 1, where the stimulus was introduced. This training, thus, involved, association of Opposite Sex Pheromones (OSP) vs. water, a Neutral Stimuli (NS). Cohort 2 consisted of eight female mice. Their whiskers were trimmed and further, the anesthetic gel was applied on their muzzle each day during the training phase. They were also trained with MBU. With the same group, however, whiskers were kept intact during initial testing and memory testing phases. Cohort 3 comprised of eight whisker intact female mice, but they were trained with Female soiled Bedding and Urine (FBU) instead of MBU. This training, thus, involved, association of Same Sex Pheromones (SSP) vs. water, a Neutral Stimuli (NS). Cohort 4 had eight whisker intact female mice trained for MBU vs. the neutral stimulus associated with the different shapes, i.e, a circle vs. triangle (Perimeter/Circumference of 31.4mm) of the plate guarding the chamber. Cohort 5 comprised of six whisker intact female mice trained for OSP (i.e, MBU) but their memory was investigated in a new but identical set-up devoid of pheromonal residual cues. The apparatus and the plates were identical to the ones utilized during the training phase. Cohorts 6 and 7 had whisker-trimmed female mice trained for OSP for size (circles of 10mm/5mm) based association and the ones trained for OSP in a shape based association (circle of 10mm vs. a triangle of an equivalent perimeter), respectively. In these mice, anesthetic gel was not applied during the training phase. This was done so that any obstruction that the gel might cause in smelling ability will be taken care, hence, only four and five mice were used respectively. Cohort 8 consisted of five whisker deprived (trimming plus anesthetic gel) mice trained for shape based association in OSP multimodal pheromonal learning task. Cohort 9 comprised of seven early weaned female mice trained for the OSP vs. NS task and their

memory was checked on 15th day post training. Protocol of early weaning was followed the same as explained in Chapter 1, section 1.3.2. Female mice were early weaned at Postnatal day 14. The male mice used for the training and testing of memory of female pheromones (FBU) were whisker intact. No change in paradigm was done for male mice, however, a new dedicated apparatus was used.

For the experiments involving training and memory testing phases of the ‘multimodal pheromonal learning’ paradigm, fresh voided male urine, uncontaminated from the feces, was collected from either one male mouse or two mice housed together. Female urine was also collected in a similar manner, from one or two female mice. Soiled bedding was collected from the respective cages, just before the commencement of the experiment.

We took four mice each from cohorts 1, 2 and 3 for studying their sniffing behavior towards pheromonal volatiles under mouse head restrained (MHR) conditions, using an air-pressure based sensor. For Arc immunohistochemical studies, 2-6 mice across the specific experimental conditions were used to quantify Arc-positive cells upon activation due to training and memory recall. These conditions were as follow: whisker intact mice trained for OSP, sacrificed on Training Day 15th (N = 3), whisker deprived mice trained for OSP, sacrificed on Training Day 15th (N = 2), whisker intact mice trained for OSP, sacrificed on Memory Day 15th (N = 6), whisker free mice trained for OSP, sacrificed on Memory Day 15th (N = 6), whisker intact female mice trained for SSP, sacrificed on Memory Day 15th (N = 3), whisker intact mice trained for OSP, sacrificed on Memory Day 30th (N = 3), early weaned whisker intact mice trained for OSP, sacrificed on Memory Day 15th (N = 3), whisker intact mice trained for OSP in a shape based task (circle vs. triangle), sacrificed on Memory Day 15th (N = 2) and singly housed naïve mice (N=2) for calculating the basal number of Arc activated cells. Unless specified, all groups were trained and tested for the size based multimodal pheromonal learning task.

To carry out non-pheromonal volatiles discrimination training¹⁰, 30 female mice (~8-14 weeks) were taken. One cohort (experimental) were exposed to MBU volatiles along with soiled bedding every-day while their discrimination training period was underway. Control cohort, on the other hand, were not exposed. Animal care as well as the procedures were in agreement with Institutional Animal Ethics Committee (IAEC) at IISER Pune and the

Committee for the Purpose of Control and Supervision of Experiments on Animals (CPCSEA), Government of India.

3.3.2 Multimodal Pheromonal Learning Apparatus

Set-up for conducting MPL paradigm was an arena of dimensions: 60cm (l) x 30cm (b) x 15cm (h), which was partitioned into 3 equal spaced zones (Figure 3-4, B). The chambers of dimensions: 10cm x 10cm x 15cm, were oppositely faced in Zone 1 and Zone 2. They were guarded by removable plates. Equidistant 10mm of diameter holes were perforated on one of the removable guarding plate. The plate guarding the opposite chamber had 5mm holes perforated equidistantly. The three other sides of both the chambers were completely closed and could not be removed. The mouse could then sniff the volatiles emanating from the stimulus (OSP/SSP vs. NS) present inside these chambers through only the front side (i.e the guarding plate). For each animal, the plates guarding the associated chambers were kept constant throughout the all phases of the MPL paradigm. A total of 4 plates, were used for a single set-up and the plates guarding urine chamber were never mixed with the NS plates.

Set-up was custom-built using black acrylic sheet material. Each chamber housed a 55mm petri-dish. 100 μ L of urine was pipetted to one petri-dish (i.e, the attractive opposite sex pheromonal stimulus in chamber 1) or OSP, while water (Neutral stimulus or NS) was pipetted in another petri-dish kept in chamber 2 (Figure 1B). Four different apparatuses were used for carrying out the MPL paradigm across different experimental conditions. Fourth set-up was not used for training but only for memory testing in Cohort 5. For Cohorts 4,7 and 8, one of the plates of one chamber instead was perforated with triangle shaped orifice. In these experiments that involved shape based multimodal associations, the other plate was perforated with the 10mm diameter holes. It was taken care that the circular holes circumference on one plate, are equivalent to the perimeter of triangle-shaped orifices of the other plate.

3.3.3 Multimodal Pheromonal Learning paradigm

Paradigm divided into three phases, was as follows: Initial phase of testing their preference (4 days), active Training phase (15 days) Memory testing phase 15th and 30th day after last day of training as shown in Figure 3-4, A. The initial testing phase involved checking if sensory intact female mice exhibited any innate preference towards MBU zone presented with

attractive volatile and non-volatile pheromones from male mice over the one containing NS. Set-up was moved by 180° everyday during testing as well as training phases. This was done to prevent associations occurring as a result of stimulus present in one spatial location throughout training. Our task was thus, a whisker based task and did not depend on directional/spatial cues.

Counter-balancing of animals for the pairing of particular diameter for circular holes and the volatile cue associations (i.e, Size cohort, Urine-5mm vs. Water-10mm and Urine-10mm vs. Water-5mm, Cohorts 1, 2, 3, 5, 6 & 9) and for triangular or circular with volatile cues (Shape cohort, Urine-triangular orifices vs. Water-circular holes as well as Urine-circular shaped orifices v/s Water/triangular shaped orifices, Cohorts 4, 7 and 8). This counterbalancing was done to eradicate any predisposition of mice towards particular shapes or diameters. This meant that once the chamber was assigned to either OSP or NS, it remained the same throughout the experiments for different cohorts of mice.

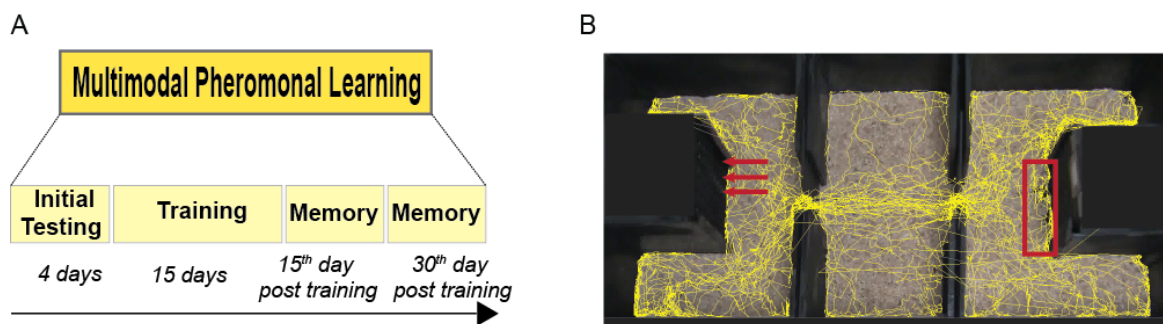


Figure 3-4: Multimodal Pheromonal Learning paradigm and apparatus

A. Sequence of events in the MPL paradigm which involves four days of initial testing followed by 15 days of training for OSP vs. NS chambers. Memory for the pheromonal location is checked on 15th and 30th day after the end of training.

B. The apparatus for MPL paradigm consisting of two chambers containing OSP and NS stimuli. The red arrows pointed towards the holes of the guarding plate indicate the parameter, ‘number of active attempts’, i.e the nose pokes by the animal. The red rectangle demarcating the region in front of the opposite chamber depicts another parameter, ‘time spent’ in an area in front of chamber. Track is quantified using the nose point feature of the animal on memory day, using Noldus Ethovision.

Training phase spanned for 15 days. During this phase, the mouse was constrained in both the zones for a period of 15 minutes each (interspersing between zone 1 and 2 every 5 minutes) per day. The pheromonal stimuli (volatile and non-volatile) as well as water stimulus were discarded and set-up was thoroughly cleaned after the last training day and also the day

before the testing of memory. However, as a confirmatory test, we also tested cohort 5 in a new set-up too. This was basically done to ensure that the set-up along with the removable plates were lacking residual pheromonal traces that might act as a confounding factor.

To investigate if somatosensation played a role in mediating pheromone location learning and memory, an anesthetic cream (Lignocaine Hydrochloride gel- Lox-2% jelly, Neon laboratories) was applied on the snout of the mice during the training phase (Cohorts 4 and 8). Just after the application of gel, the animal was kept in an empty cage (same dimension as the home cage) for 5 minutes until it was visibly normal and no longer anxious due to handling and gel application. Only after this was ensured, it was put in the set-up for training. Trimming of whiskers was carried out every five days from the commencement of the training phase (Figure 3-7). Whiskers were allowed to grow post the training phase. On Memory Day 15th, animals had re-growing whiskers. This strategy allowed for investigating the function of somatosensation in mediating the learning of the multimodal association. To ensure that is no effect of the application of anesthetic gel (during training phase) on the sensation of olfactory stimuli, Cohorts 6 and 7 (only whisker-free and no anesthetic applied) were utilized for size and shape based association tasks, respectively. In these groups, whisker trimming was carried out the same way as in the deprived groups.

3.3.4 Behavior quantification

EthoVision software (Noldus Information Technology) was used for mouse tracking and quantification of behavioral parameters. One of the parameters, ‘time spent’ in front of the two chambers were quantified using the software’s ‘nose point’ feature (Figure 3-4, B). Active attempts, another parameter that allowed for quantifying the nose pokes the animal made on the two chambers was measured manually. One poke corresponded to one attempt.

3.3.5 Sniffing behavior towards pheromones

We recorded sniffing behavior of mice upon precise delivery of urinary volatiles (male/female) to mice belonging to whisker-intact and free cohorts. This was done by using a head-restraining technique, putting an air-pressure sensor (AWM2300V, Honeywell) near to one nostril and delivering the volatiles from a nozzle for a period of 2s³⁵¹. To this end, we utilized four mice each from Cohorts 1, 2 and 3. These mice were tested on Memory day 30th and were kept in cage for two months. Head post implantation was carried out on these mice using the strategy mentioned in methods section of Chapter 2 (explained in detail in section

2.3.4, Materials and Methods, Chapter 2). After recovery (2 days) from the surgical procedure, they were placed in the PVC tube, fitted on the set-up by screwing the headpost such that the mouse sits comfortably, resting its paws on the mesh floor of the tube (see in Figure 3-9). Urine volatiles and air delivery was carried out in pseudorandom manner. 100 μ L of undiluted, fresh urine was used everyday. Stimulus presentation was done for 2s per trial. This was recurred for ten such presentations of the same stimulus (total twenty presentations), totaling to a 20s time of exposure to pheromonal volatiles on a single day³⁵¹. This paradigm was followed for four days (the same time period as that chosen for Initial Testing Phase) across the three groups of mice belonging to different groups.

3.3.6 Arc protein immunohistochemistry

Transcardial perfusion of the animal was done using 50mL of 1X Phosphate buffered saline (PBS) that flushed the blood out. Then, 50mL of 4% (w/v) Paraformaldehyde (PFA) was injected through the heart to cause fixation of the tissues. Upon dissection of intact brain tissue, it was kept in 4% PFA at 4⁰C. Before carrying out cryotome sectioning, brain was cryo-preserved by immersing it in freshly prepared 30% sucrose. Cryo-preserved brain was embedded in optimal cutting temperature (OCT) medium (Leica, 14020108926) and then placed on the cryotome chuck so as to obtain sections from anterior to posterior, i.e, 50 μ m thick coronal sections. Sections were selected after every 300 μ m and these were then utilized for immunohistochemistry. Briefly, they were washed using PBS to get rid of the OCT medium. 300 μ L of the blocking solution (5% Bovine Serum Albumin (BSA) + 1% Triton-X in TBS) was pipetted to the plate wells and incubated for 1.5 hours. Arc Primary antibody (Rabbit anti-Arc, Arc-156003, Synaptic Systems) (1:1250) was diluted in blocking solution (1% BSA, 0.1% Triton-X in TBS) and pipetted to the wells and kept for for 14 hours at 4⁰C. Upon giving three washes of TBS (15 minutes per wash) to the primary antibody labelled sections, secondary antibody was added (Anti-Rabbit AF 594, Jackson's Immunoresearch) diluted 1:500 in 1% BSA in TBS and the plate was kept undisturbed for 2 hours. Finally, after three washes, sections were stained with DAPI (4',6-diamidino-2-phenylindole) (Sigma, 1:500). Vectashield anti-fade mounting medium was used to mount these sections on the glass slide (Vector labs, H-1000).

Confocal Imaging and cell count quantification: Arc labeled nuclei across different brain regions were imaged on a Lecia SP8 confocal microscope (3-8 sections imaged per brain

area, per mouse). Arc-positive cells quantification was carried out using the Imarisx64 software (Bitplane, Oxford Instruments). For each image quantification, a z-stack (imaged at 1µm optical step size) was loaded in the software. Gaussian filter (constant value) was applied to each stack so as to reduce the background noise. A constant value XY diameter was then applied to the Arc antibody stained cells. Threshold of counting the positive cells throughout the whole thickness of the z-stack was automatically set by Imaris. False-positive counts were manually removed. For each brain region, total cells were equivalent to the sum of the cell counts per stack. The total volume was obtained by multiplying thickness of the stack with the X-Y dimensions of the image acquired (Σ of sampled area in mm² * stack thickness in mm). Cell count was denoted as the total number of Arc-positive cells in 1 mm³.

3.3.7 Adult neurogenesis quantification

Bromodeoxyuridine (BrdU) injection protocol: BrdU chemical (obtained from TCI chemicals, and further dissolved in freshly prepared, filtered 0.9% NaCl), a marker of DNA synthesis in newly born cells³⁵² was injected intraperitoneally in mice four times, at two hours gap, in a day (100mg/kg of mouse body weight dose). After giving four injections, animals were housed for 28 days. During the 28 days, exposure to urine was carried out via the MPL paradigm. At the end of four weeks, brain was dissected after transcardial perfusion. Such a protocol allowed for visualization of BrdU labelled neurons in OB rather than at the site of the cell birth³⁵³.

Immunohistochemistry: Tissue processing was done in the same way as carried out for Arc staining (See methods section 3.3.6). 9/10 sections per OB were taken. Blocking solution (BS) was prepared using 5% Normal goat serum (NGS) (Abcam, ab 7481) and 1% Triton-X-100 (Sigma) in 1X PBS. Sections in the well were incubated with BS for two hours at room temperature. Sections were further incubated with 1:1000 diluted primary antibodies- Rat anti-BrdU (Biorad, MCA2060) and Chicken anti- NeuN (Millipore, ABN91). For BrdU staining, pre-treatment with 1N HCl was done at 37°C for 45 minutes to cause slight DNA denaturation. Incubation was carried out for 22 hours at 4°C. After three washes with PBS, secondary antibodies diluted in 1% NGS blocking solution were pipetted to the wells. These were Donkey anti-rat AF 488 (1:500 dilution) and donkey anti-chicken AF 647 (1:500 dilution) (712-544-150 and 703-605-155, Jackson ImmunoResearch, USA). Sections were incubated with these secondary antibodies for two hours at room temperature. After washes with PBS (three washes of fifteen minutes each), sections were incubated with the DAPI stain

(Sigma, 1:500). Mounting was carried out in the same way as previously written (See methods section 3.3.6).

Confocal Imaging and analysis: BrdU labelled nuclei in the MOB and AOB were imaged using Leica SP8 confocal microscope. Images were analyzed using Fiji ImageJ³⁵⁴ using the ‘analyze particles’ plugin. This number was further inspected using Fiji’s ‘count cell’ feature. The number of BrdU-positive cells was quantified for 18 MOB and 10-12 AOB coronal sections from a single animal (N = 3 per group). Imaging was done using 10x lens (0.75 zoom). Image frame XY is of 1.55mm x 1.55mm dimensions. z-stacks were obtained at optical length of 1µm. Total number of BrdU-positive cells was measured in perm³ [= (total number of cells)/(number of sections x 1.55 x 1.55 x 0.05)].

3.3.8 Go/No-go odor discrimination

3.3.8.1 **Odors:** 1,4-Cineol (CI), Eugenol (EU), Amyl acetate (AA), Ethyl butyrate (EB), Benzaldehyde (BZ), Nonanol (NN), Hexanal (HX) and 2-Pentanone (PN) were used in the study pertaining to non-pheromonal volatiles discrimination learning task (Table 3-1). Dilution and purchase details are same as mentioned before (See methods, section 1.3.4.4).

Sr No.	Name	Chemical Formula	Catalog	Physico-chemical Parameters
1	1,4-Cineole	C ₁₀ H ₁₈ O	27395	1.93mmHg at 20°C
2	Eugenol	C ₁₀ H ₁₇ O ₂	E51791	0.02mmHg at 25°C
3	Amyl (Pentyl) Acetate	C ₇ H ₁₄ O ₂	109584	4mmHg at 20°C
4	Ethyl Butyrate	C ₆ H ₁₂ O ₂	E15701	15.5mmHg at 25°C
5	Benzaldehyde	C ₇ H ₆ O	12010	4mmHg at 45°C
6	Nonanol	C ₉ H ₂₀ O	131210	0.02mmHg at

				25°C
9	Hexanal	C ₆ H ₁₂ O	115606	10mmHg at 20°C
10	2-Pentanone	C ₅ H ₁₀ O	448516	27mmHg at 20°C

Table 3-1: Relevant information about the odors used in the study

3.3.8.2. **Apparatus:** The experiments were carried out in two custom designed eight channel olfactometers controlled by software compiled in Igor Pro (Wavemetrics, OR). The olfactometer functioning and the paradigm details (task habituation, learning and memory task) are followed the same as in Chapter 1 (Section 1.3.4, Materials and Methods).

3.3.9 Vaginal Smear collection & visualization

The vaginal smear was collected by using a fresh cotton bud dipped in distilled water. The cotton bud was rolled at the vagina 2-3 times by gently lifting the hind limbs of the female mouse. The bud was then rolled on a clean glass slide for the cells to be deposited onto the slide. For staining using crystal violet (0.1%), the slide was dipped in the solution in a coplin jar for 1 minute. This was followed by washing the excess stain for 30s in a coplin jar containing distilled water. To evaluate the phase of the estrous cycle, they were imaged using a bright field microscope.

3.3.10 Statistical analyses

Data which is represented as Mean ± Standard Error of Mean were analyzed in Graphpad Prism 8.0 (Graphpad Software Inc, USA). Shapiro-Wilk test was applied for data normality assessment (for all data with N = 3 and above). Data which followed normal and/or lognormal distribution, parametric test., i.e, Unpaired two-tailed t-test, Paired two-tailed t-test, One-way Analysis of Variance (ANOVA) and two-way ANOVA with *post hoc* Bonferroni's multiple comparison testing were done. For data that was not normal, Mann-Whitney and Wilcoxon matched pairs signed rank tests were done. * represent $p < 0.05$, ** $p < 0.01$, *** $p < 0.001$ and **** $p < 0.0001$.

3.4 Results

In this chapter, I have explained our findings on developing a learning and memory task that utilizes murine olfactory and whisker systems to work in concert to form decisions of socio-sexual importance. This work has been published in The FASEB Journal (DOI: [10.1096/fj.202100167R](https://doi.org/10.1096/fj.202100167R)). Upon establishing this paradigm, we tested early weaned female mice and assessed their memory in a multimodal pheromonal learning task.

3.4.1 Paradigm of multimodal learning results in memory for pheromone location in female mice

The custom-built instrument for ‘Multimodal Pheromonal Learning ’ (MPL) paradigm allowed the mice to associate the hole diameter of the plate guarding the chamber containing opposite sex pheromones (OSP), i.e, urine and that of the plate guarding neutral stimulus (NS) i.e water. Male soiled bedding was also kept near the OSP chamber as the non-volatile pheromones present in soiled bedding serve as primers to generate attraction in the opposite sex³⁵⁵. Female mice display preference towards OSP, but, can they learn and remember where it was located? We had hypothesized that in natural settings (Figure 3-2, in Introduction) female mice will encounter multiple entities such as pebbles, stones and leaves of different shapes, sizes and textures, in the field, on which scent markings of the opposite sex, in the form of urine could be streaked upon. While sensing these pheromones, they would sniff and move their muzzle across these entities, several times. The multiple encounters might strengthen their association of the OSP with the entity on the ground. This would cause activation of somatosensory system, in addition to the nose, in case of female mice. To test if the additional whisker system activation would facilitate the memory of the location, we developed the MPL paradigm (Figure 3-5, A). In a laboratory setting, we first let the whisker intact, sexually mature, female mice astray in the MPL apparatus, one at a time. This constituted the ‘Initial Testing Phase’ (Figure 3-5, B) where for a four consecutive days, a female mouse was put in the central zone (zone 2) and the doors to both the oppositely located zones were released and the mouse was permitted to explore the arena for a total of ten minutes. Each day, apparatus was rotated by 180 such that the positions of OSP and NS chambers were opposite to the previous day. The plates with specific diameters (10mm and 5mm) were counterbalanced such that for half of mice, 10mm plate was paired with urine while for the rest, 5mm plate was paired.

The initial testing phase was done to first check the innate preference of the animals towards the urinary stimulus by letting them in the apparatus for a brief period. We used two parameters, time spent near the chamber and active attempts' number (nose pokes in the holes of guarding plates to sense the stimulus present inside). The set-up rotation was done to avoid directional bias of the animal, i.e, learning to favor OSP chamber over time due to its fixed position in the space. We found out that mice, initially, on day 1 and 2, displayed increased time and more active attempts towards the OSP chamber (Figure 3-5, C2, C3: $p = 0.059$ & $p = 0.078$ respectively for Day 1, D2, D3: $p = 0.05$ & $p = 0.0094$ respectively for Day2, Paired t-test, two-tailed). However, over time, the preference was decayed as seen on day 3 and 4 where they tended to spend similar time and made almost equal nose pokes into both the chambers (Figure 3-5, E2, E3, F2, F3: $p > 0.05$, Paired t-test, two-tailed). Initial preference happening just due to exploration, thus, may not be enough to keep it sustained over time.

Figure 3-5: Decayed preference towards opposite sex pheromones location when exposed to a choice of urine and water

A. MPL paradigm was utilized to test the multimodal learning and memory of female mice towards OSP. In this, the chamber 1 and 2 were guarded with plates containing holes of two different diameters.

B. Initial testing phase of the MPL paradigm consisting of four days, over which the animal's innate preference towards one chamber over the other was tested. The set-up was rotated 180 after every day for a total of four days.

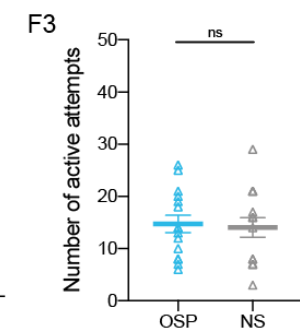
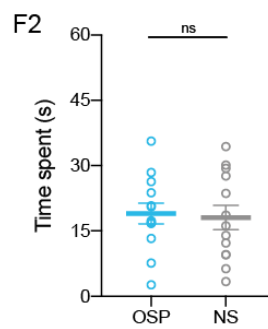
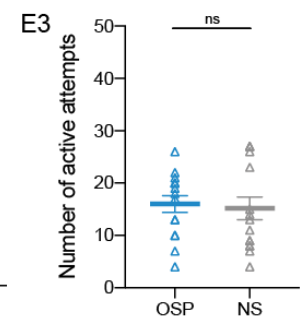
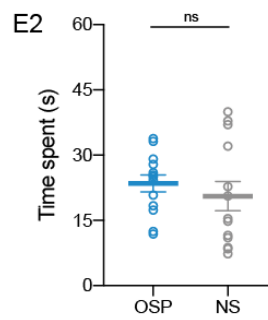
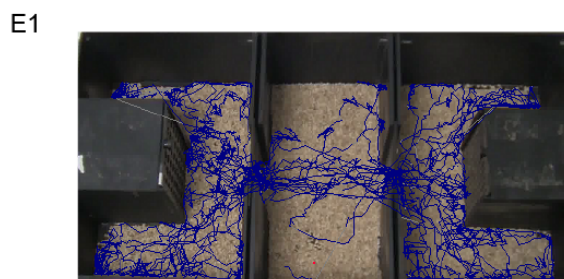
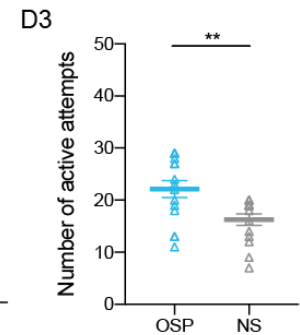
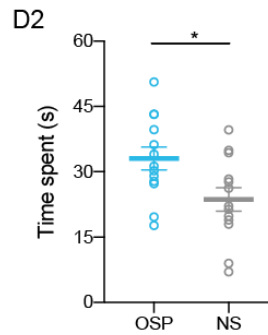
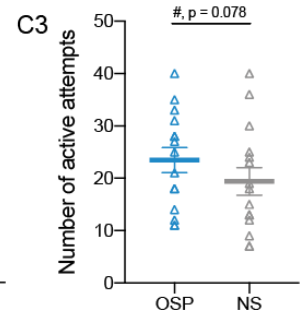
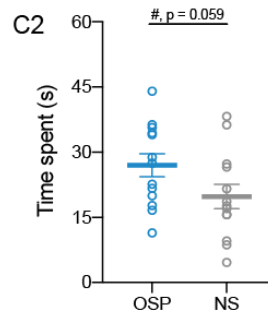
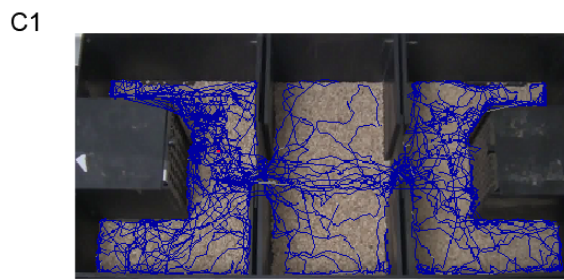
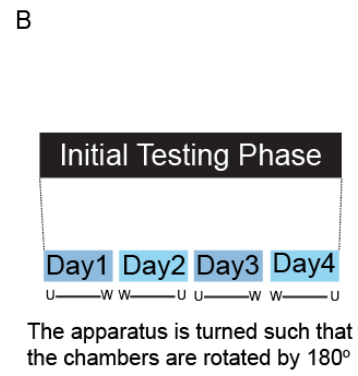
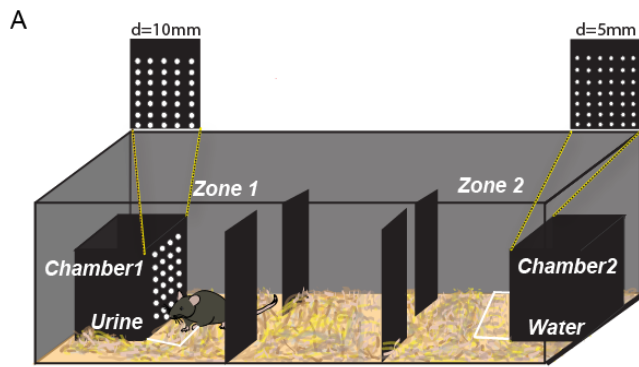
C1, D1, E1, F1. Tracks taken by a female mouse over the four days of Initial testing phase (day 1: C1 to day4: F1). The nose point feature was used to find the path traversed by the mouse using Noldus Ethovision software.

C2, C3. Trend for increasing time spent as well as number of active attempts towards OSP chamber when the mice were put into the set-up for the first time, on Day 1 (N = 13-15 whisker intact female mice, C2: $p = 0.059$ and C3: $p = 0.078$, Paired t-test, two-tailed).

D2, D3. A significant preference by augmentation of the values of time spent and active attempts was found on Day 2 too (D2: $p = 0.05$ and D3: $p = 0.0094$, Paired t-test, two-tailed).

E2, E3. Decay in innate preference was observed upon continuous exploration of the zones and chambers of the arena as seen by similar time spent and active attempts (E2: $p = 0.47$ and E3: $p = 0.65$, Paired t-test, two-tailed).

F2, F3. This pattern of decayed preference remained even on day 4 of testing phase (F2: $p = 0.75$ and F3: $p = 0.62$, Paired t-test, two-tailed). This showed that just exploration of the stimuli during the initial testing phase did not result in a sustained preference for the OSP chamber.



To challenge the mice to form an association between the stimulus and the hole diameter of the plate, we continued with the same cohort of whisker intact female mice to carry out extensive training for 15 days. This way, we also wanted to confirm that they actively come in contact with the plates and sense the stimuli more often by restricting them in the zones for fixed amount of time. Training, thus, entailed a mouse to remain restricted to either zone 1 or 3 for a period of 5 minutes, and then moving to the opposite zone. This alternation was done to train them for a total of 30 minutes, 15 minutes (5 minutes X 3 times) in zone containing OSP chamber and 15 minutes in the zone containing NS chamber. Each day in the training phase also, the set-up was rotated by 180 to ensure there is no directional bias. Upon culmination of training phase, mice were not exposed to the apparatus until the day of testing of memory. This period went on for 15 days where the mice were just housed in the home-cage and not exposed to opposite sex pheromones. Memory was then tested, 15th day after the end of training period, during which the OSP and NS stimuli were not kept but the plates guarded the empty chambers. We hypothesized that if the mice had memory of the association formed, they would spend more time and make more active attempts towards the plate which guarded the urine chamber. Indeed, we found significant preference memory when checked for these whisker-intact female mice (Figure 3-6, A2, A3, $p < 0.05$, Paired t-test, two-tailed) on Memory day 15th (MD 15). To really ascertain that on MD 15, no pheromone residual cues were present, we carried out memory testing of another cohort of female mice in a new set-up devoid of pheromonal residues. In this case too, mice displayed the pheromonal location memory confirming that it was indeed being formed as a result of robust associations formed between olfactory and whisker subsystems and are independent of pheromonal residues causing the preference (Figure 3-6, B2, B3, $p < 0.05$, Paired t-test, two-tailed). We further substantiated our paradigm, by also checking for association on a shape-based MPL paradigm for another cohort of female mice. Here, animals had to associate the shape, instead of sizes of the holes on the plate (triangle versus circle of 10mm size) during the training phase. This was done to establish that our MPL paradigm is pervasive for varying shapes and sizes. Indeed, on MD 15, the mice could retain the association and thus, displayed more nose pokes and longer times towards the chamber which had the plate that guarded the OSP chamber during the training phase (Figure 3-6, C2, C3 $p < 0.05$, Paired t-test, two-tailed).

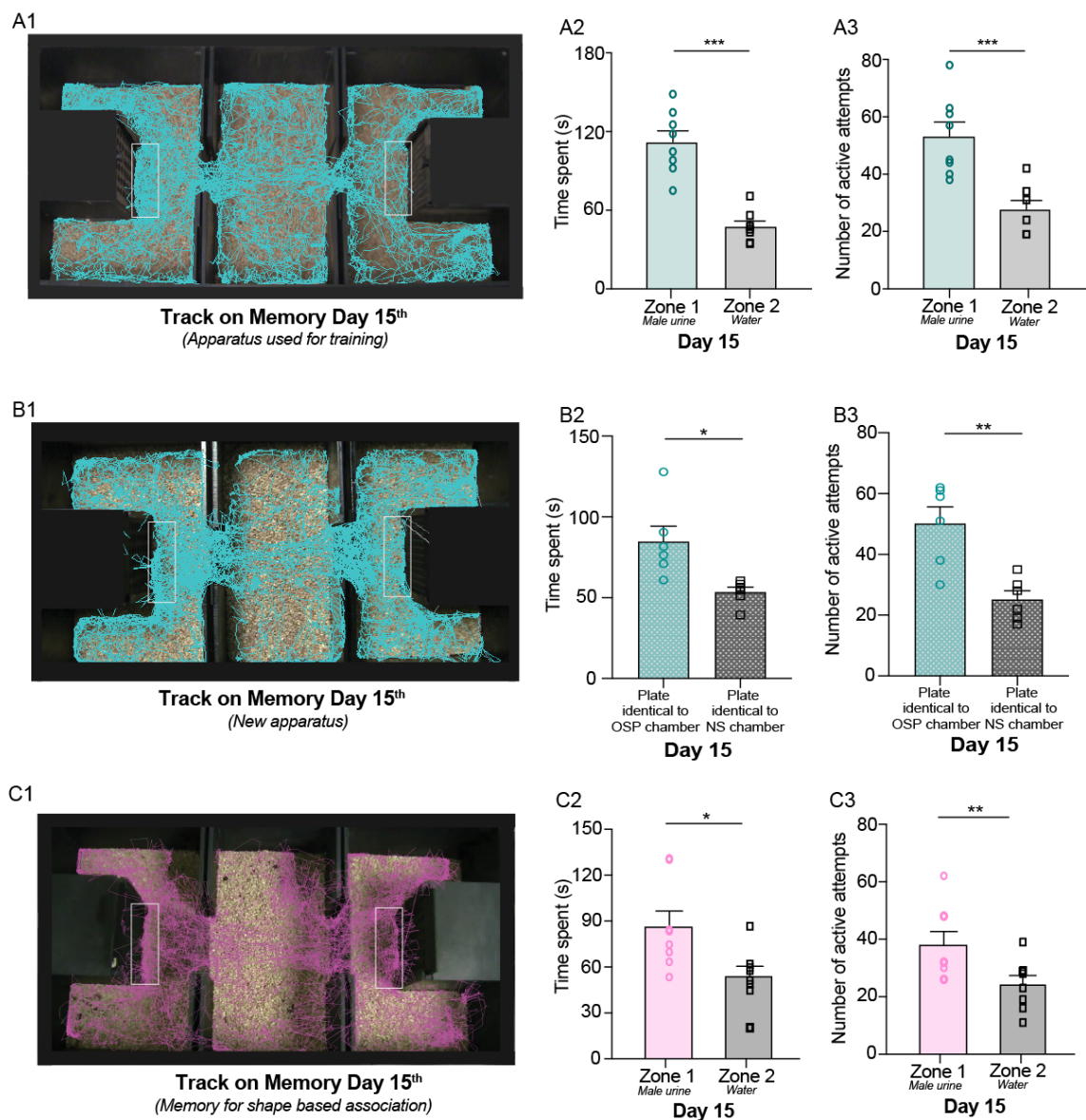


Figure 3-6: Multimodal learning causes formation of pheromone location memory in female mice

A1. Track traversed by nose point of the female mouse on MD 15. The memory was tested in absence of olfactory stimuli but the plates were retained. The white area demarcates the region used for quantifying time spent in front of the two chambers of the set-up.

A2. Significantly longer time is spent near to the OSP chamber on MD 15 by whisker intact female mice (N = 8, $p = 0.0002$, Paired t-test, two-tailed).

A3. Significantly higher frequency of active attempts were made by whisker intact mice on the plate which was guarded on the OSP chamber during training phase by the mice on the day of MD 15 testing ($p = 0.0004$, Paired t-test, two-tailed).

B1. Track of a female mouse on MD 15 in a new, pheromone residuals free apparatus. In this scenario also, the mouse squandered near the plate that was identical to one used in training period for guarding the OSP chamber, as seen by the track.

B2, B3. Increased time spent and more number of active attempts parameters that confirmed the intact multimodal memory in case of female mice tested on MD 15 in a new but identical apparatus (N = 6, B2: $p = 0.01$ & B3: $p = 0.003$, Paired t-test, two-tailed).

C1. Track traversed by a female mouse in an apparatus for shape based multimodal association (triangle vs. circular holes of 10mm sizes).

C2, C3. In a task to memorize the association of shape rather than size of the holes with the stimulus present inside, whisker intact female mice could display the multimodal memory on MD 15 as indicated by increased time spent (N = 8, $p = 0.011$, Paired t-test, two-tailed) & more active attempts ($p = 0.004$, Paired t-test, two-tailed).

3.4.2 Olfactory and whisker systems are involved in the formation of multimodal pheromonal location memory

We next probed the involvement of whisker system to study the multimodality involved in the memory formation. To do that, we took cohorts of female mice and deprived them of whiskers during the training phase. The whiskers were deprived by trimming them on Training Day 1, before commencing the behavior. Since they were re-growing within 4-5 days, they were trimmed after every 5 days during the training period. Whiskers were re-growing post the completion of training phase and they were never trimmed afterwards. Thus, all the mice had grown whiskers on MD 15. This way, we could specifically assess if the absence of whiskers during the training phase brought about disruptive changes in learning the association and thus, causing an ill effect on the memory recall. In whisker deprived cohort, we applied anesthetic gel on the whisker pads each day, 15 minutes before beginning the training. This ensured that the micro-vibrissae and the nerve endings of the whiskers were also not responsive³⁵⁶. Whisker deprived mice did not display pheromonal location memory on MD 15 suggesting the importance of responding to tactile cues during the training phase. On MD 15, these mice spent equal time in front of both the chambers and made nearly similar nose pokes into the OSP & NS chambers (Figure 3-7, C1, C2: $p > 0.1$, for both parameters, Paired t-test, two-tailed). This was even confirmed for a shape based multimodal task as well (Figure 3-7, E1, E2: $p > 0.1$, Paired t-test, two-tailed). To ensure that the anesthetic gel is not interfering with the olfactory detection capacity of mice, we took two more cohorts of female mice and did whisker trimming alone. In these whisker trimmed mice as well, the multimodal memory was not found to be present on MD 15 both in size and

shape based MPL tasks (Figure 3-7, B1, B2, E1, E2: $p > 0.1$, Wilcoxon matched pairs signed rank test or Paired t-test depending on the normality of the data).

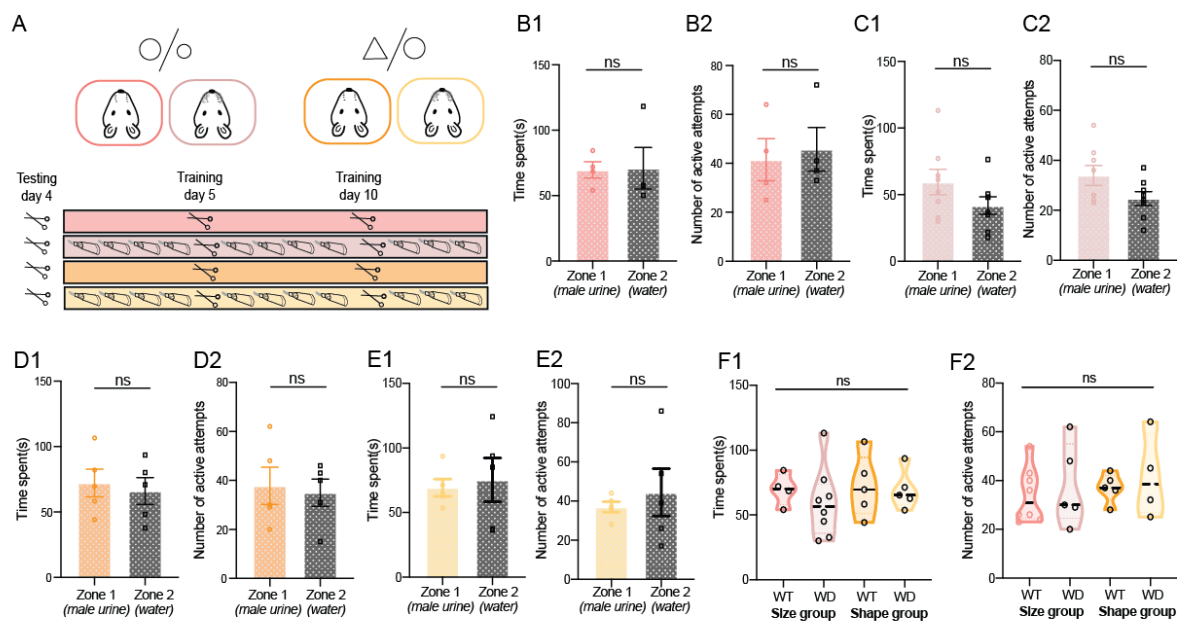


Figure 3-7: Whisker deprivation during training period hampers multimodal pheromonal location memory

A. Illustration depicting procedure of sensory deprivation by either whisker trimming alone or both trimming followed by applying of anesthetic gel on the muzzle every day before starting the training on the apparatus. The trimming was done on testing day 4, training day 5 and 10. The whiskers were left to regrow after the training period was done.

B1, B2. Whisker trimmed group (not followed by gel anesthetic) trained for size based multimodal association displayed similar time spent and active attempts for both the zones on MD 15 suggesting whisker deprivation led to impaired multimodal memory (N =4, B1: $p > 0.9$, Wilcoxon matched pairs signed rank test , B2: $p = 0.71$, Paired t-test, two-tailed).

C1, C2. Whisker trimming and further anesthetic gel application on the whisker pad during training also hampered the multimodal memory recall on MD 15 for the size based group (N = 8, C1, C2: $p > 0.1$ for both parameters, Paired t-test, two-tailed).

D1, D2. Whisker trimmed group trained for shape based multimodal association displayed similar time spent and active attempts for both the zones on MD 15 suggesting whisker deprivation led to impaired multimodal memory (N = 5, D1: $p = 0.7$, D2: $p = 0.68$, Paired t-test, two-tailed).

E1, E2. Whisker trimming and further anesthetic gel application during training also hampered the multimodal memory recall on MD 15 for the shape based group (N = 5, D1: $p = 0.76$, D2: $p = 0.53$, Paired t-test, two-tailed).

F1, F2. Comparison of all groups for the two parameter (time spent, active attempts) near the OSP chamber depicts indistinguishable values for all mice, whether, whisker trimmed or deprived

suggesting absence of memory in MPL paradigm when checked on MD 15 (F1: $p = 0.73$, $F = 0.43$ and F2: $p = 0.81$, $F = 0.31$, Ordinary one-way ANOVA).

We compared and contrasted the whisker deprived group data with that of the whisker intact mice on MD 15. Along with this, we also performed the task for another control cohort of female mice who were trained against female urine (same sex pheromones or SSP) and bedding vs. water. These mice were whisker intact. Even they exhibited significantly lower memory as compared to whisker intact group trained with OSP (Figure 3-8, B, D: $p < 0.0001$ for the two parameters, Ordinary One-way ANOVA, Bonferroni's multiple comparison test). Thus, on MD 15, significantly lesser time and lower number of active attempts were shown by both whisker deprived mice trained with OSP and those female mice trained with SSP when compared to whisker intact OSP trained mice. This confirmed that olfactory and whisker subsystems robustly and specifically mediates attractive pheromonal location learning & memory in our MPL paradigm under sensory-intact conditions.

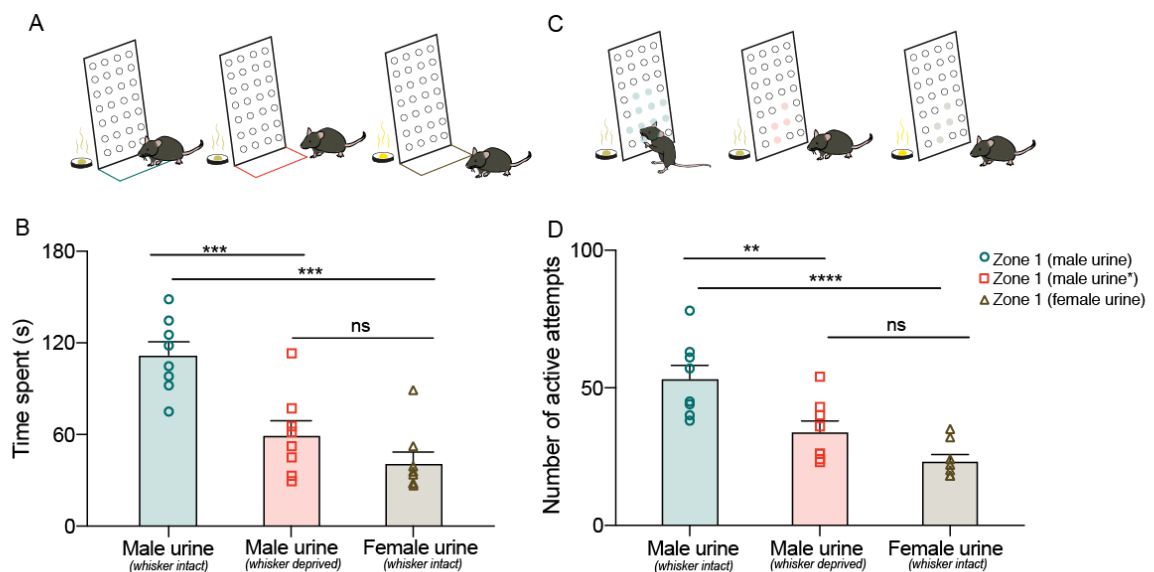


Figure 3-8: Olfactory and whisker systems govern the formation of pheromonal location memory

A. Illustrations depicting a female mouse spending time near the chamber containing urine. The other side of the plate depicts a petri-dish containing male urine for the teal group (whisker intact female mice) and red group (whisker deprived female mice) and the third petri-dish contains female urine (brown color: whisker intact female mice trained for SSP). On MD 15, the urinary & water stimuli are not present. The line demarcating the region represents the zone used for calculating time spent values.

B. Both the whisker deprived and the mice trained for SSP spend significantly lesser time on MD 15 suggesting the importance of sexually attractive OSPs and the intact whiskers in mediating pheromonal location memory ($p < 0.0001$, $F = 18.69$, Ordinary One-way ANOVA, Bonferroni's multiple comparison test; Male urine (teal) vs. Male urine* (red): $p = 0.0008$, Male urine (teal) vs. Female Urine (brown): $p < 0.0001$ and Male urine* (red) vs. Female urine (brown): $p > 0.1$, $N = 8$ mice for all groups) (* represents whisker deprived).

C. Illustrations depicting female mouse making nose pokes/active attempts in the holes of the plate guarding the male urine. This helps them sniff the volatiles emanating from the urine. The following two illustrations are that of whisker deprived mouse being trained for OSP and whisker intact mouse trained for SSP.

D. Both the whisker deprived and the mice trained for SSP made significantly lower active attempts on MD 15 ($p < 0.0001$, $F = 15.27$, Ordinary One-way ANOVA, Bonferroni's multiple comparison test; Male urine (teal) vs. Male urine* (red): $p < 0.01$, Male urine (teal) vs. Female Urine (brown): $p < 0.0001$ and Male urine* (red) vs. Female urine (brown): $p > 0.1$, $N = 8$ mice for all groups) (* represents whisker deprived).

3.4.3 Sampling strategies of mice are similar under whisker intact and deprived conditions

One of the factors leading to the absence of memory in whisker deprived and SSP groups could be reduction in sniffing of the odors emanating from urine. This reduction in sampling might occur due to whisker deprivation or due to the non-attractiveness of the SSP containing female urine to female mice. To quantify the sniffing strategies of mice under different conditions of sensory deprivation, we recorded the sniff frequency of these three groups of mice under head-restrained conditions. This was done 3 months after the MD 15 of the respective groups. The breathing frequencies during presentation of olfactory stimuli were found comparable for these groups of mice and remained similar over the four days (Figure 3-9, $p > 0.1$, Ordinary One-way ANOVA). This suggests that the sampling strategies of the mice belonging to different groups did not influence the memory. It, thus, corroborates to the point that multisensory associations are indeed leading to generation of memory.

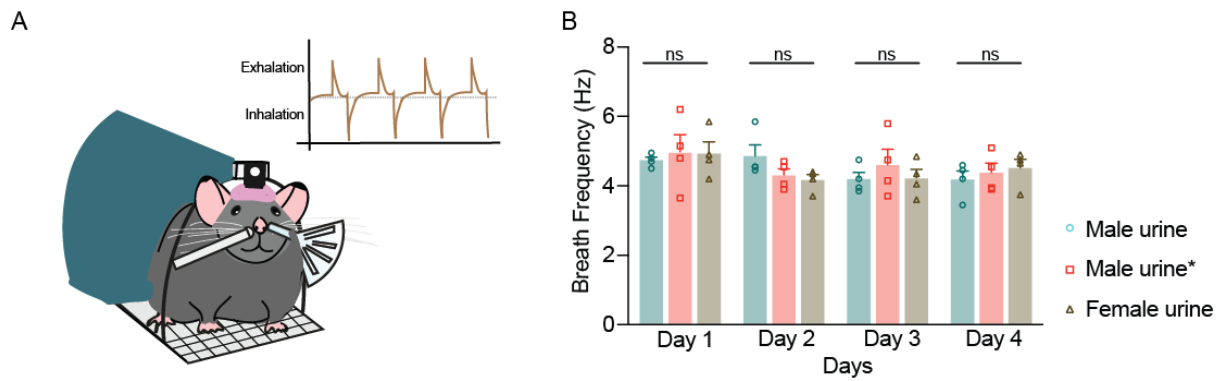


Figure 3-9: Sniffing frequency remains unchanged in whisker deprived condition

A. Illustration depicting a female mouse restrained on the apparatus that allowed measurement of breath frequency (using a pressure-based sensor) as shown near left nostril. The odor volatiles (either male or female urine) is delivered to the mouse via the nozzle (near right nostril) for fixed amount of time. The trace in the inset shows an illustration of inhalation-exhalation cycle of the mouse while sniffing the presented odor.

B. Breath or sniffing frequencies towards urinary volatiles were recorded for a subset of mice from all three cohorts, done under head restrained condition. Similar frequencies when recorded over days, reveals that all mice had similar sampling strategies under whisker deprived conditions or sampling the SSP. This confirms that all groups could sense the volatiles normally during the training phase (day 1, $p = 0.9$, $F = 0.1$; day 2, $p > 0.1$, $F = 2.2$; day 3, $p = 0.6$, $F = 0.50$; day 4, $p = 0.67$, $F = 0.40$; Ordinary One-way ANOVA, Bonferroni's multiple comparison test, $p > 0.1$, $N = 4$ animals per group) (Male urine* denotes the whisker deprived cohort).

3.4.4 Arc activation in olfactory bulb, somatosensory cortex and hippocampus is enhanced in whisker intact mice displaying multimodal memory

In the previous sections, we established that the pheromonal location memory in our paradigm required a fully functional muzzle, i.e., both nose and whiskers to learn the association of hole size/shape with the olfactory stimulus. In order to confirm their involvement, our first step of action was to figure the brain areas which were activated while the animals were being tested for memory recall on MD 15. We assessed Immediate Early Gene (IEG) protein marker activation, Arc or Activity-regulated cytoskeleton on MD 15. Arc protein is known to reliably encode the memory traces³⁵⁷. We utilized immunohistochemistry to specifically observe Arc activation patterns in different brain regions.

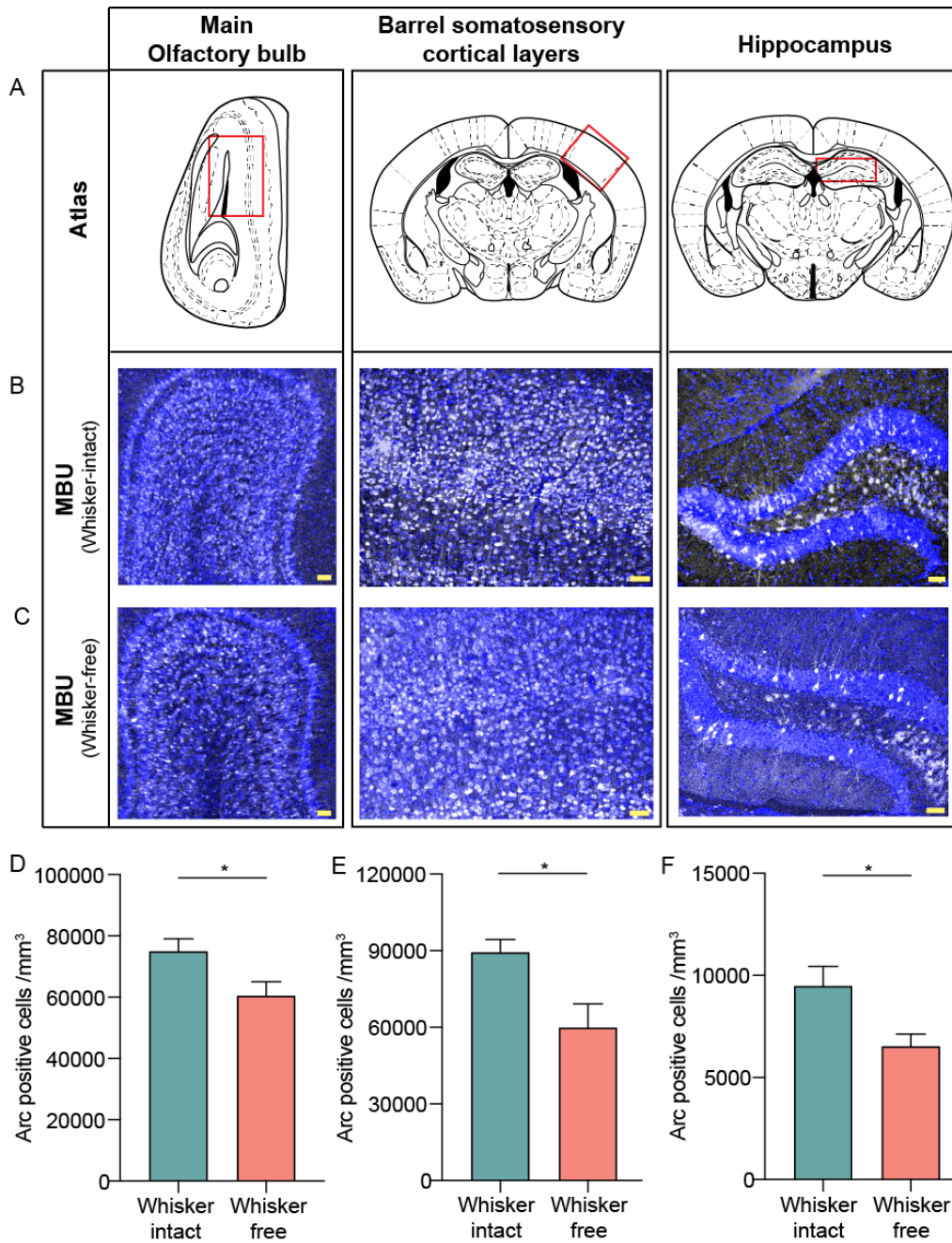


Figure 3-10: Immediate early gene product activation as a correlate of pheromonal location memory in the Multimodal pheromonal learning paradigm

A. Atlas map drawings (adapted from The mouse brain in Stereotaxic Coordinates by Paxinos) depicting regions of interest, Main olfactory bulb, barrel cortical layers of Somatosensory cortex and Hippocampus. The red line shows demarcated areas on the coronal sections used for the quantification Arc protein, an IEG product.

B. Immunofluorescence images of coronal sections of MOB, SSC and DG of hippocampus obtained from whisker intact mouse, on MD 15. MBU stands for whisker intact cohort trained for associating MBU with the specific hole size. Blue: DAPI, Yellow: Arc. Scale bar = 50 μ m.

C. Immunofluorescence images of coronal sections of MOB, SSC and DG of hippocampus obtained from whisker free mouse, on MD 15. Quantification includes both whisker trimmed and deprived animals trained with MBU (or OSP). Blue: DAPI, Yellow: Arc, Scale bar = 50 μ m.

D, E, F. Bar plots showing number of Arc positive cells per mm³ in MOB (D), SSC (E) and DG (F) areas for whisker intact (teal) and whisker free groups (orange). A significant higher number of Arc positive cells were found in whisker intact mice in all three brain regions (N = 6 mice per group for all regions, D: $p = 0.03$, E: $p = 0.019$, F: $p = 0.02$, Unpaired t-test, two-tailed).

We found maximum Arc immunoreactivity in Main olfactory bulb, barrel cortical layers of Somatosensory cortex (SSC) and the Dentate gyrus (DG) of Hippocampus (Figure 3-10, B,C). To evaluate the changes in Arc expression upon sensory deprivation conditions, we compared to Arc positive cells in whisker intact and deprived mice. Lower number of Arc positive cells were present in the whisker-free (trimmed/deprived) mice who did not exhibit memory on MD 15 (Figure 3-10, D, E, F: $p < 0.05$ for all brain regions).

We also quantified the extent of Arc activation from the last day of training, i.e, Training day 15th (TrD 15) to MD 15 under both whisker intact and deprived conditions, in the three mentioned regions (Figure 3-11, A, B). On TrD 15, both the whisker intact and deprived groups received comparable olfactory inputs during training period as just the somatosensory inputs were perturbed under whisker deprived condition. As an effect, comparable Arc activation was found to be happening in the MOB of both the groups of mice (Figure 3-11, C, $p = 0.5$, Unpaired t-test, two-tailed). However, the increase in MOB Arc activation from TrD 15 to MD 15 happened specifically in whisker intact group trained with OSPs (Figure 3-11, C: WI TrD 15 to WI MD 15, $p = 0.003$, Unpaired t-test, two-tailed). This increased activation correlated with the existence of memory recall in whisker intact mice on MD 15. In case of SSC brain region, a massive increase in Arc-positive cells was seen from TrD 15 to MD 15, specifically in whisker-intact cohort (Figure 3-11, D: WI TrD 15 to WI MD 15, $p = 0.02$, Unpaired t-test, two-tailed). Mice that were whisker deprived during the training period did not exhibit an increase in Arc-positive cells on MD 15, although they had re-grown whiskers on MD 15 (Figure 3-11, WD TrD 15 to WD MD 15, $p = 0.48$, Unpaired t-test, two-tailed). This suggests that the extent of activation of Arc in these regions may be necessary for the memory recall. Lastly, in DG, the trend in the increase of Arc positive cells occurred for both whisker intact and deprived groups (Figure 3-11, E: $p = 0.07$ for WI and $p = 0.01$ for WD groups from TrD 15 to MD 15, Unpaired t-test, two-tailed), leaving the involvement of

hippocampus in processing multimodal memory recall an open question to be closely investigated. Importantly though, the average number of Arc-positive cells was higher for WI mice as compared to WD mice, on TrD 15 (Figure 3-11, E: $p = 0.031$, Unpaired t-test, two-tailed) suggesting its role in encoding the memory during training days, specifically, for WI group. Thus, with the current set of experiments, we could reliably correlate the increased Arc activation in MOB and SSC with the occurrence of multimodal memory specifically in whisker intact mice.

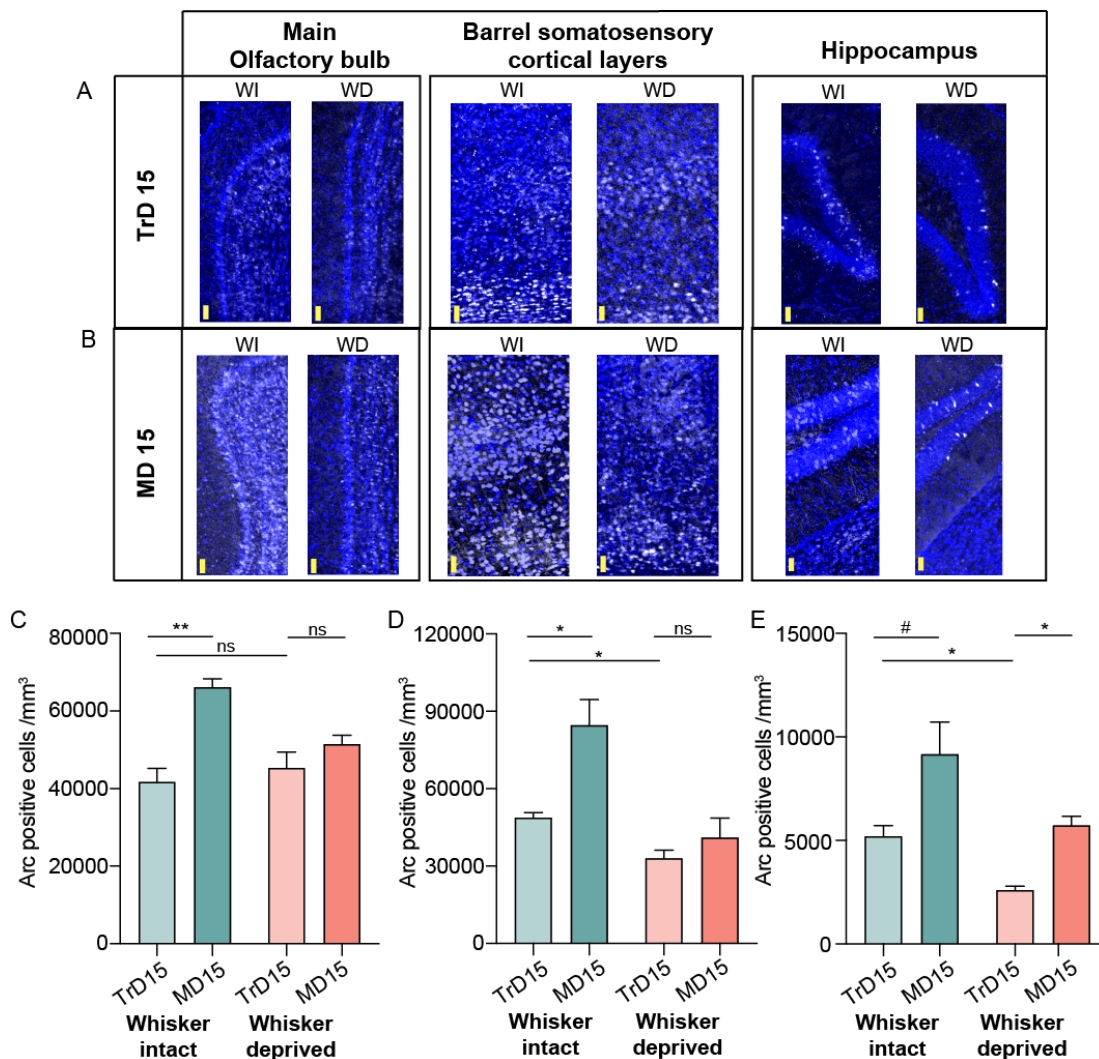


Figure 3-11: Arc activation changes from training to memory phase of multimodal pheromonal learning paradigm

A. Immunofluorescence images of MOB, SSC and Hippocampus under Whisker intact (WI) and deprived (WD) conditions when checked on TrD 15. Blue: DAPI, Yellow: Arc. Scale bar = 50 μ m.

B. Immunofluorescence images of MOB, SSC and Hippocampus under Whisker intact (WI) and deprived (WD) conditions when checked on MD 15. Blue: DAPI, Yellow: Arc. Scale bar = 50 μ m.

C. Increase in MOB Arc positive cells from TrD 15 to MD 15 in whisker intact mice (N = 3 per group, $p = 0.003$, Unpaired t-test, two-tailed) was observed which was in contrast to similar Arc activation from training to memory period in case of whisker deprived mice (N = 2-3 mice per group, $p = 0.24$, Unpaired t-test, two-tailed).

D. Whisker deprived mice displayed lower Arc activation in SSC too, both on TrD 15 (N = 2-3 mice per group, $p = 0.02$, Unpaired t-test, two-tailed) and MD 15 ($p = 0.024$, Unpaired t-test, two-tailed) as compared to the whisker intact mice. A significant increase in Arc immunoreactivity was seen in whisker intact mice from TrD 15 to MD 15 suggesting the involvement of SSC neurons in pheromonal location memory recall (N = 3 WI mice, $p = 0.031$, Unpaired t-test, two-tailed). This increase from training to memory recall phase was not observed in WD mice (N = 2-3, $p = 0.48$, Unpaired t-test, two-tailed).

E. A trend of increase in Arc activation in Hippocampus was seen in both whisker intact (N=3, $p = 0.07$, Unpaired t-test, two-tailed) and deprived group (N = 2-3, $p = 0.01$, Unpaired t-test, two-tailed), although, it is higher in whisker intact mice as compared to deprived mice on TrD 15 (N = 2-3 mice per group, $p = 0.031$ Unpaired t-test, two-tailed).

3.4.5 Naïve female mice and female mice trained for same sex pheromones display significantly lower Arc activation than the ones trained for opposite sex pheromones

We saw clear differences in the extent of Arc activation between the whisker intact and deprived groups (Figure 3-10). We used two groups to verify that the confirmed activation was specific to the MBU based multimodal learning and memory in the paradigm.

In one control group, we took naïve mice who were just singly housed in the home cage and were not exposed to experimental set-up or training. Since, they were singly housed, the exposure to pheromones was also negligible (Figure 3-12, A, B). As was expected, negligible Arc activation in MOB, SSC and DG areas when compared to whisker intact trained mice was found in the naïve mice (Figure 3-12, C, D, E: $p < 0.05$ for all brain regions, Unpaired t-test, two-tailed). To confirm if the activation was specific to MBU, another control group consisting of whisker intact cohort trained for SSP (female bedding and urine) was utilized. Upon comparing, we found lowered Arc activation in MOB and SSC of FBU group (Figure 3-13, C, D: $p < 0.05$, Unpaired t-test, two-tailed). This correlates with decreased time spent and active attempts in the FBU group on MD 15

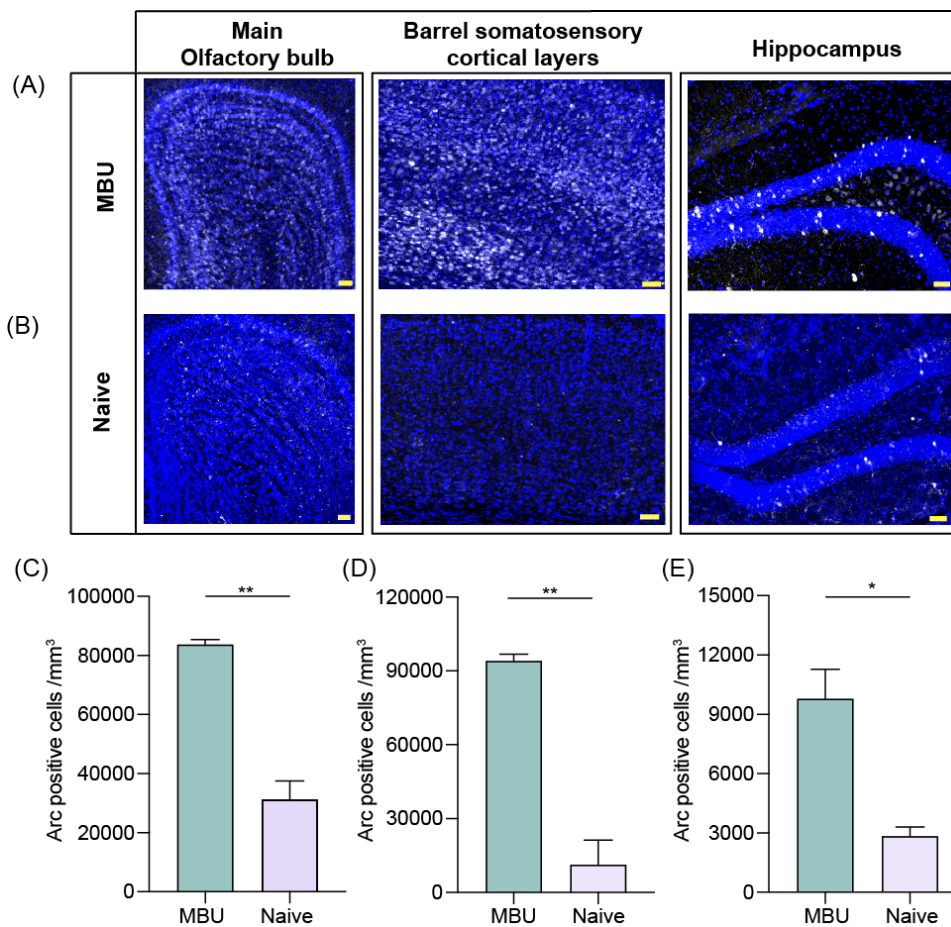


Figure 3-12: Lowered Arc expression in naïve female mice

A. Immunofluorescence images of MOB, SSC and Hippocampus of MBU trained whisker intact mouse. Blue: DAPI, Yellow: Arc. Scale bar = 50 μ m.

B. Immunofluorescence images of MOB, SSC and Hippocampus of naïve whisker intact mouse. Blue: DAPI, Yellow: Arc. Scale bar = 50 μ m.

C, D, E. Naïve control group have significantly lower number of Arc positive cells in MOB, SSC and DG areas (N = 2 naïve and 3 whisker intact mice, C: p = 0.02, D: p = 0.02, E: p = 0.03, Unpaired t-test, two-tailed).

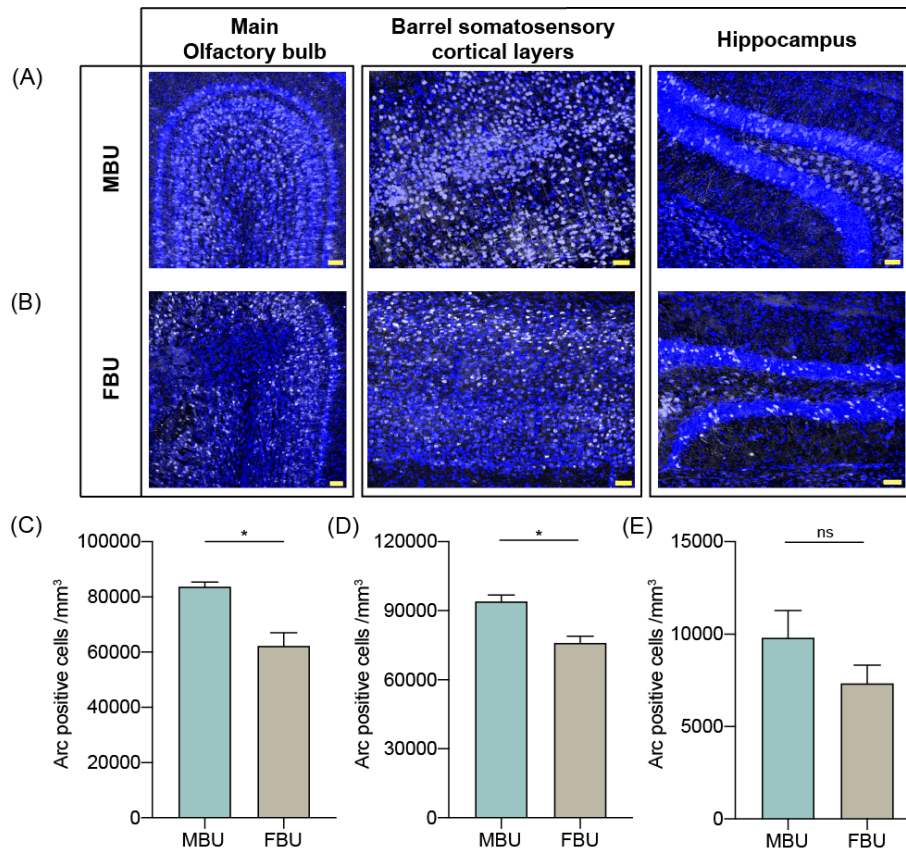


Figure 3-13: Lowered Arc expression in FBU trained female mice on Memory Day 15th

A. Immunofluorescence images of MOB,SSC and Hippocampus in MBU trained whisker intact mouse. Blue: DAPI, Yellow: Arc. Scale bar = 50 μ m.

B. Immunofluorescence images of MOB, SSC and Hippocampus in FBU trained whisker intact mouse. Blue: DAPI, Yellow: Arc. Scale bar = 50 μ m.

C, D, E. FBU trained female mice show significantly lower number of Arc positive cells (N = 3 mice per group) in MOB ($p = 0.013$, Unpaired t-test, two-tailed) and SSC ($p = 0.012$, Unpaired t-test, two-tailed) but similar activation in DG areas ($p = 0.23$, Unpaired t-test, two-tailed) on MD 15. Similar exploratory behavior of both groups (similar pathlength covered in the arena by both groups of mice, $p = 0.23$, Unpaired t-test, two-tailed) of mice on the MD15 might be leading to similar Arc activation in DG.

3.4.6 Female mice are unable to recall multimodal memory on Day 30th post training

Further on, we evaluated if such a multimodal neural activation in case of whisker-intact group can cause prolonged persistence of memory. Conditioned place preference for pheromone location was earlier shown to retained till days 14 after exposure to Darcin in a particular spatial location³⁵⁸. However, in that case, associative learning was due to presence of spatial cues. Here, we hypothesized that since both olfactory and whisker subsystems are

getting activated, the multimodal memory for pheromonal location might persist for longer time. Hence, we continued to check for memory on 30th day post training (MD 30) in a subset of whisker-intact mice trained for size based multimodal pheromonal learning task. The same set of mice were also used to assess memory on MD 15 where they displayed intact multimodal memory. On MD 30, however, we found that these mice spent similar time and made similar number of attempts for both the OSP and the NS chambers. This suggested that indeed the multimodal memory was not prolonged. This, as has been previously speculated, could be due to quick extinction of pheromonal memory in prolonged absence of cues. Corroborating to the behavioral results, we also found significantly reduced activation of Arc in MOB, SSC and the DG of hippocampal regions on MD 30 (Figure 3-14, E,F,G, $p < 0.05$, Unpaired t-test, two-tailed). Our paradigm that employed usage of multisensory pathways could not prolong the memory consolidation. The plausible reasons and short-comings are further discussed in the Discussion section 3.5.

Figure 3-14: Absence of multimodal memory on Day 30th post training phase in whisker intact female mice

A. Track traversed by female mouse on MD 30. The memory was tested in absence of olfactory stimuli but the plates were retained. The white area demarcates the region used for quantifying the time spent in front of the chamber.

B1. Similar time spent near to both OSP and NS chambers on MD30 by whisker-intact female mice ($p = 0.109$, Wilcoxon matched pairs signed rank test, $N = 7$).

B2. Similar number of active attempts were made by the whisker intact mice on MD 30 suggesting that they no longer remembered the pheromonal location ($p = 0.125$, Wilcoxon matched pairs signed rank test, $N = 8$).

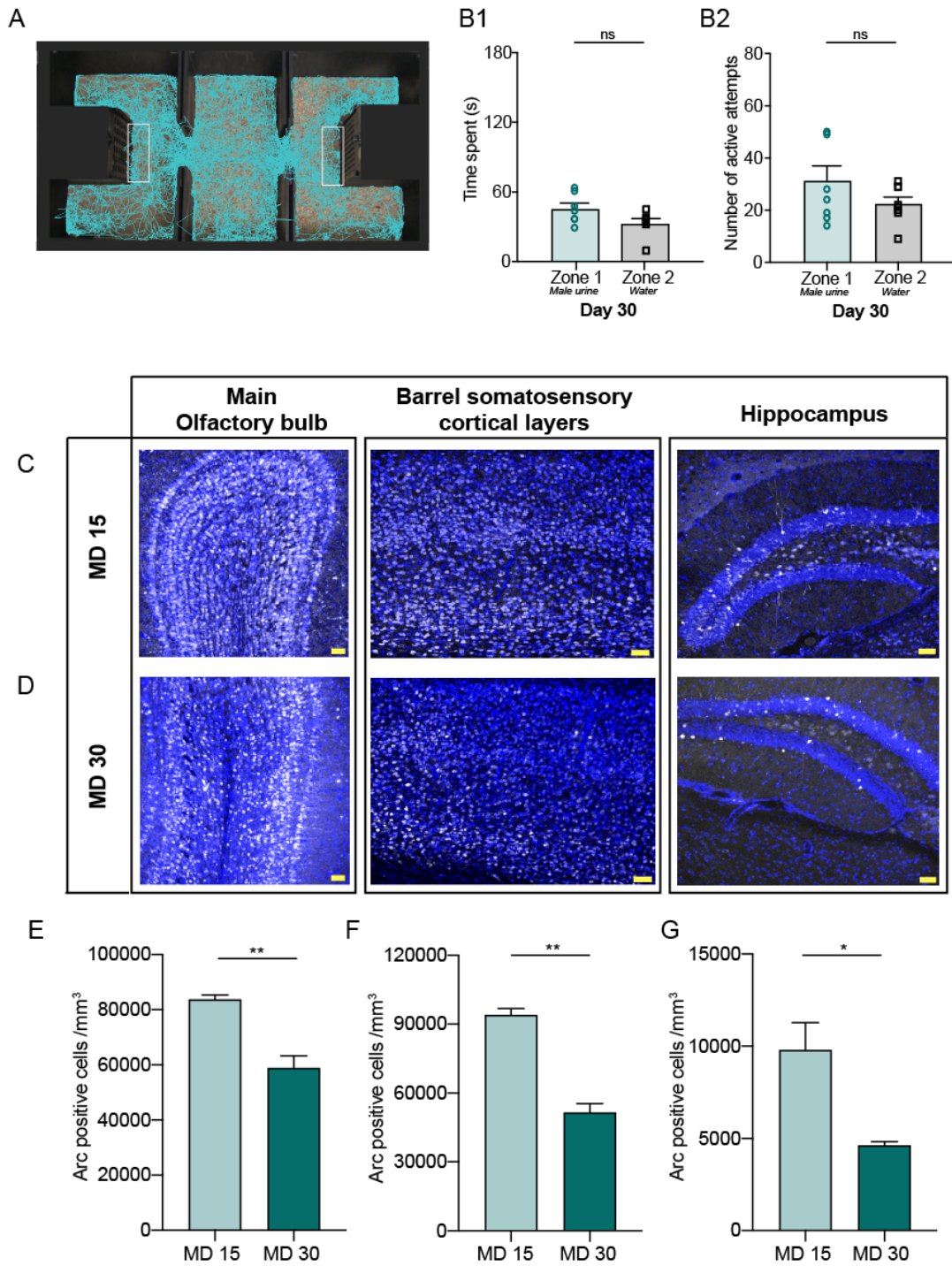
C. Immunofluorescence images of MOB, SSC and Hippocampus in MBU trained whisker intact mouse on MD 15. Blue: DAPI, Yellow: Arc. Scale bar = 50 μ m.

D. Immunofluorescence images of MOB, SSC and Hippocampus in MBU trained whisker intact mouse on MD 30. Blue: DAPI, Yellow: Arc. Scale bar = 50 μ m.

E. Significant reduction in Arc positivity was observed in MOB of whisker intact mice on MD 30 ($p = 0.006$, Unpaired t-test, two-tailed, $N = 3$ mice each for MD 15 and 30)

F. Arc positive cells were also found to be lower in SSC on MD 30 ($p = 0.0009$, Unpaired t-test, two-tailed, $N = 3$ mice each for MD 15 and 30).

G. As memory on MD 30 was not intact, Arc positive cells density also exhibited reduction on MD 30 ($p = 0.025$, Unpaired t-test, $N = 3$ mice each for MD 15 and 30).



3.4.7 Early weaned female mice exhibit poor multimodal pheromonal memory but their sensory detection is intact

Finally, as we observed that early weaned mice performed poorly in odor discrimination learning and memory tasks (Chapter 1, Results section 1.4.4), we were also interested in assessing their performance in this multimodal task. This task not only assesses the sensory capabilities of mice towards attractive pheromonal cues (i.e during testing phase) but also

involves cognitive skills to form the association (i.e during training phase) and recall it during MD 15. We used female mice who were early weaned at postnatal day 14 and tested them at 2 months of their age in the MPL paradigm (This work was done along with a BS student, Ms. Saanchi Thawani).

Consistent with similar sensory capabilities shown by both control and EW mice in Buried Food Pellet test (Figure 1-14, Chapter 1 results section 1.4.2), we found out that the early weaned female mice also had similar pheromonal sensing as compared to whisker intact control mice. They indeed exhibited an initial increase in preference towards the OSP chamber on Day 2, which rapidly decayed as the days progress. The extensive training however did not result in intact multimodal memory when checked on MD 15 (Figure 3-15, B1 and B2). It could be due to poor learning attained during the training phase. Although we know that they displayed poor memory on MD 15, it remains an open question that the cause is either poor associative learning or inability to recall. This could be tested by reducing the training phase and then assessing memory at different time points. We also quantified Arc on MD 15, just after they performed the task. We found out lowered Arc activation in all three brain regions suggesting a deficit in the extent of neuronal activation in MOB, SSC and DG areas (Figure 3-15, C1, C2 and C3, $p < 0.05$ for all comparisons, Unpaired t-test, two-tailed).

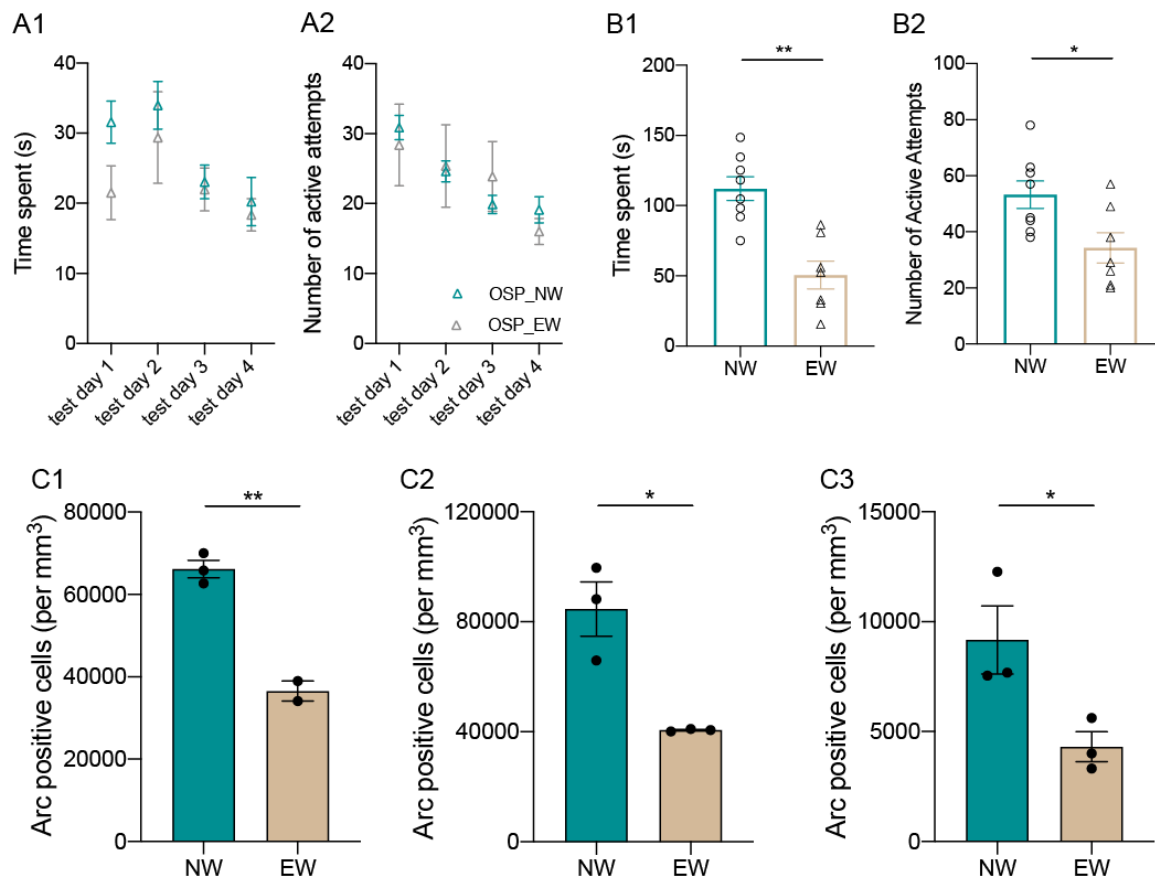


Figure 3-15: EW female mice show poor multimodal memory and lower Arc immunoreactivity

A1, A2. Comparison of initial testing phase (four days of testing) urinary pheromonal detection (using time spent and active attempts) based attraction suggests that EW mice have normal detection abilities (A1: $p = 0.23$, $F = 1.72$, A2: $p = 0.95$, $F = 0.0038$, RM Two-way ANOVA, Bonferroni's test).

B1, B2. The EW female mice showed significantly lower time spent and made lesser number of active attempts towards OSP chamber as compared to the whisker-intact NW mice (B1: $p = 0.0004$, B2: $p = 0.021$, Unpaired t-test, two-tailed, $N = 7-8$ mice per group).

C1, C2, C3: Significantly lower Arc immunoreactivity in MOB (C1), SSC (C2) and DG of Hippocampus (C3) of EW mice on MD 15 ($p < 0.05$ for all, Unpaired t-test, two-tailed, $N = 3$ mice per group).

3.5 Discussion

3.5.1 Olfactory and whisker systems facilitate memory of socio-sexual encounters in murine world

Socio-sexual interactions in rodents entail communication via chemicals and ultrasonic vocalizations^{278,359}. Pheromonal cues in nature are deposited via urinary scent marks. The chemical signals in form of these marks can co-occur with other relevant sensory stimuli. We asked the following question: ‘To what extent do the memory of the pheromones depend on the associations occurring across sensory modalities?’ As male mice mark their surrounding surfaces by depositing urinary marks³⁶⁰, are olfactory cues alone sufficient for localizing and memorizing the pheromonal scent markings? In this study, we focused on the olfactory as well as whisker system modalities of the female mice working in concert to detect, ascertain and memorize the location of pheromone depositions (Figure 3-2). We investigated this in a laboratory setting by creating a training arena in which mice needed to exploit their whiskers for sensing volatile pheromonal cues through holes of specific diameters and shapes (Figure 3-6 and Figure 3-7). We have shown the role of whisker and olfactory systems in enabling the means of gathering enough information about pheromone locations to form a memory.

The interesting question to discuss is that why would rodents bank on more than one modality to respond to and remember the location of pheromonal cues? We know that the environmental setting of the rodent habitats are bursting with a milieu of volatile and non-volatile odors³⁶¹. Non-volatile proteinaceous compounds such as major urinary protein can be the natural reinforcers for attracting the opposite gender³⁶². However, it contains a cocktail of volatile pheromonal compounds that can mediate attraction of the opposite gender. Production of volatile urinary cues is dependent on the testosterone levels of the male mouse that puts the male’s reproductive capabilities at display²⁶³. A female mouse, thus, should be proficient enough to remember the male-specific pheromonal signals in the ever-evolving turbulent olfactory space. Studies pertaining to scent tracking strategies suggest that the scent trails are a rather complex amalgamation of odors which are distributed in a non-continuous manner and are challenged by various constraints such as turbulence etc.^{363,364}. Reddy et al. 2022 propose a search strategy and presents a normative theory of trail tracking by an agent (a reinforcement learning agent)^{365,366}. According to this study, the inter-detection intervals that the agent faces as well as the angle of heading towards the trail determine whether it

would be able to successfully detect the trail or not³⁶⁵. In a follow-up observation, they also found out that the agent tries to do extensive alternation (i.e resting on its hind limbs with nose in the air to detect air-borne cues) during the cast-and-surge behavior so as to minimize the search time³⁶⁷. In case of detecting pheromones as well, such alternation and casting behaviors must be occurring for successful detection of pheromonal locations. In addition to this, the repeated movement of whiskers while simultaneously trying to smell deposited pheromones might actually facilitate the search strategy. There exists a large milieu of pheromones that a female mouse is exposed to. This raises the question as to whether the olfactory system alone is capable of remembering such deposited cues? This, we hypothesized that the response to co-occurring non-olfactory information might be necessitated in such a scenario. Simultaneous whisking strategies of the mice might facilitate the process of remembering and memorizing the locations³⁶⁸. We base this on this assumption: the potential connection of volatile and non-volatile pheromonal marks with size, shape and textures of the materials on which they are deposited might mediate memory of the locations of the deposited marks in a dynamic environment of the rodent habitat.

In our MPL paradigm, volatiles are being sensed with simultaneous movement of whiskers and micro-vibrissae along the curves of the holes punched on the guarding plate of the OSP chamber. These behavioral events could be central to forming association between the olfactory and somatosensory systems. This is because, in mice which were whisker-free, either via trimming only or trimming + applying lidocaine on vibrissae³⁵⁶, we found out that the mice could not form the memory of location (Figure 3-7 and Figure 3-8). Mice indeed had regrown whiskers on MD 15 which suggested that the MPL training without whiskers played a role in the inability to recall the task, 15 days post that period. Sampling frequency for volatile urinary pheromones was comparable to the control mice (Figure 3-9). This ensures that the lack of memory in sensory deprived conditions was primarily caused by the altered association between the two quintessential sensory systems, and not due to changes in sampling frequency. We also think that the extent of learning happening in the MPL paradigm and thereby the memory formation is decided by dynamically weighing different sensory cues during decision-making process. Changing pheromonal cues from OSP to SSP changed their preference which was reflected in the parameters that we assessed in the MPL paradigm on Memory Day 15th (Figure 3-8). In such associative tasks, different sensory systems can contribute to the final behavioral response variedly, rather than, additively³²⁴. For example, Garcia's rats, gustatory stimulus was particularly avoided in case of pairing

tasty water with a noxious drug. However, it was not affected when a bright-noisy water (an audio-visual stimulus) was conditioned with the noxious stimulus³⁶⁹. Details of such associations are written in detail in the subsequent section.

3.5.2 Multi-sensory associations can be differently weighted by different cues

Another observation to ponder upon is that of shape based associations in our MPL paradigm (a triangle vs. a circle with OSP and NS). In this case, two differing shapes were paired with OSP and NS, in contrast to the associations based on differences in the diameter of the circular holes. It is known that whiskers mediated encoding information of textures, shapes, and even surface angles at a resolution of 15 degree³⁷⁰. Animal memorized pheromone location even when they were associated with varying shapes in MPL paradigm. We hypothesised that attractive pheromonal volatiles could be more contingent to the animals when associated to varying somatosensory stimuli. It is known that rhythmic movement of whiskers permit close inspection of the surfaces which encodes evidences relating to shape, texture, angle amongst other features³⁷¹. The motion of the nose is highly coordinated with whisking motions, as seen under restrained and freely moving conditions in rats. Such a highly controlled multi-sensory action is predicted to be of importance to mice for locating odor sources³⁷². Biased lateral movement of the nose along with an increased activity of *deflector nasi* muscles are observed to happen ipsilaterally when the odor of home cage soiled bedding are presented on one lateral side of the animal's snout. Although the fact that nose is required for odor localisation is obvious, it was also shown that the vibrissae too banked towards the direction of odor³⁷³. Further, it has been characterised that mice can learn to accurately distinguish object angles at as high resolution as 15 degrees. Perceptual training to discriminate object angles led to angle-tuning of certain subsets of neurons in barrel cortical layers of S1 area, which were stably maintained during the course of training³⁷⁰. This displays the ability to reliably maintain stimulus dependent selectivity during a perceptual whisker-mediated learning task. It could be that the size differences made a comparatively dramatic effect and induced more robust learning as the circles of varying diameters were perceived more differently by mice. It could also be that distinct columns of barrel cortical layers were activated as different sets of whisker pad columns may be utilized in carrying out the size discrimination. The training dependent differences in the perception of the curvature of holes between triangles and circles versus circles of different diameters can affect selectivity of neurons. Thus, it remains open to find out how sampling behaviour, in terms of

rapid movements of whiskers, vibrissae and nose can be affected while making pokes into circle of different diameters versus triangles of comparable dimensions. Simultaneous behavioural monitoring and *in vivo* recording in barrel cortical layers will allow us to probe for such phenomena.

3.5.3 Immediate early gene Arc reliably encodes activation of multiple sensory systems during recall of pheromonal location memory

The behavioural results that we obtained shows the importance of intact sensory systems functioning together to memorize pheromone location. To probe activation of specific circuits along with their modulation under varying conditions of sensory functioning, we investigated the expression of an IEG, Arc protein. We found maximal Arc activation in MOB, SSC layers and DG of Hippocampus (Figure 3-10). Arc gene expression is dependent on the neural plasticity based mechanisms. It's increased activation has been observed under certain behavioral and physiological conditions³⁷⁴. For example, Arc is activated by tasks requiring exposure to novel sensory stimuli as well as active learning³⁷⁵. Significantly lowered expression of Arc in mice trained with FBU as compared to those trained with OSP in the MOB, when checked on MD 15. This result correlated with the absence of memory for SSP on MD 15. One of the ways that can lead to higher Arc activation in MOB could be due to higher cell density being activated. It could occur as a result of preferential recruitment of bulbar adult-born granule cells during location learning and memory tasks such as our MPL paradigm.

MOB processes the information relating to urinary volatile cues. The extensive training and the intact memory could thus, aided by increased MOB neurogenesis and increased activation of the newly born neurons. Learning in odor discrimination tasks has shown to lead to increased MOB neurogenesis^{376,377}. Indeed, in MPL paradigm, mice are carrying out active learning involving associations of pheromones with size of holes rather than 'exposure alone' studies¹⁴⁵. The aspect of involvement of adult neurogenesis in the MPL paradigm is discussed in the future directions (Section 3.6.1). This will be assessed by quantifying Arc expression in adult born granule cells present in the olfactory subsystems to evaluate their role in pheromonal memory retrieval.

Further, Arc⁺ cells were lesser in the barrel cortical layers in mice that were whisker free during training. This correlated with decreased number of active attempts on MD 15 (Figure

3-10 and Figure 3-11). Whisker stimulation leads to increased Arc expression in the somatosensory areas³⁷⁹. In a previously published behavioral task that involved olfactory-whisker paired stimulations to the animal caused augmented functional connectivity between the cortices receiving information from both the sensory areas³²⁷. Decrease in the Arc positivity from MD 15 to MD 30 in MOB and SSC exhibits the dependence of the multimodal memory on the activation of both these regions (Figure 3-14). Finally, Hippocampus is a region highly known for activity dependent plasticity. It receives inputs from multiple sensory areas, including olfactory and somatosensory regions^{7,380,381}. DG is involved in context-dependent discrimination learning as well as storing long-term memory³⁸². The decrease in the Arc immunoreactivity on MD 30 displays its plausible role in recall in MPL paradigm (Figure 3-14). Further experiments combining circuit specific calcium imaging while recording behavior will reveal how circuit functioning evolve as learning progresses. Indeed, freely moving calcium imaging is becoming a popular technique to quantify brain activity while animals are engaged in natural behaviors³⁸³.

3.5.4 Social cognitive behavior is compromised in early weaned female mice

Social olfactory-based recognition and generation of memory are modulated by neuropeptides such as oxytocin and vasopressin. It is rather important to assess their functionality governing the MPL learning behavior and its modulation under ELS. We also found absence of multimodal memory and decreased Arc expression in early weaned female mice when trained on the MPL paradigm. The circuit dysfunctions at the level of neuropeptide and receptor-level changes could be one line of investigation that can reveal the behavioral deficits. Oxytocin receptors are primarily present GCL of OB³⁸⁴, AON and PC³⁸⁵. The signaling through these receptors encode for stimulus specificity and facilitates enhancement of signal-to-noise ratio for odorants³⁸⁶. Oxytocin is rather indispensable for associative social learning but not non-social learning paradigms through its functionality in PC³⁸⁷. As PC pyramidal neurons undergo activity-dependent changes under whisker deprivation conditions³⁸⁸, we would further look into the modulation of this processing through oxytocin in PC in whisker intact and free cohorts as well as in early weaned mice trained on the MPL paradigm.

3.6 Future directions

3.6.1 Multimodal pheromonal learning and Adult neurogenesis

Modulation in adult neurogenesis of MOB and AOB after MPL learning could be an important read-out determining the involvement of the new-born neurons in a multimodal behavior. To this end, BrdU staining can be done and assessed on MD 15. Higher number of BrdU positive cells were observed in the MOB of female mice trained with OSP as compared to the SSP, in our preliminary analysis. (Figure 3-16, A1-A4: $p < 0.05$, Unpaired t-test, two-tailed) As was observed, animals were indeed sensing pheromonal volatiles through the holes during the extensive training phase. On MD 15, upon quantifying the parameter of active attempts, we found that they remembered the pairing of volatile cues with the plate holes. As MOB processes incoming information via the urinary volatiles, it is possible that the intact memory for volatiles emanating from opposite sex urine could be aided by increased MOB neurogenesis.

However, we did not find a significant increase in BrdU positive cell numbers upon quantifying AOB neurogenesis (Figure 3-16, B1 to B4, $p > 0.05$, Mann-Whitney test). It could be that prolonged gap after the final exposure to pheromonal cues would have re-tuned the AOB neurogenesis to its basal level. In our case, we had assessed BrdU positive cells 15 days after the training phase, i.e., 15 days of no exposure to MBU. Overall, we observed similar AOB neurogenesis levels in mice exposed to male urine and female urine. The Arc positive quantification can also be done in AOB and co-localization with BrdU can depict functional involvement of adult-born neurons in learning and memory. This needs to be assessed in case of EW female mice that could show compromised neurogenic mechanisms which could lead to poor learning and memory dysfunctions.

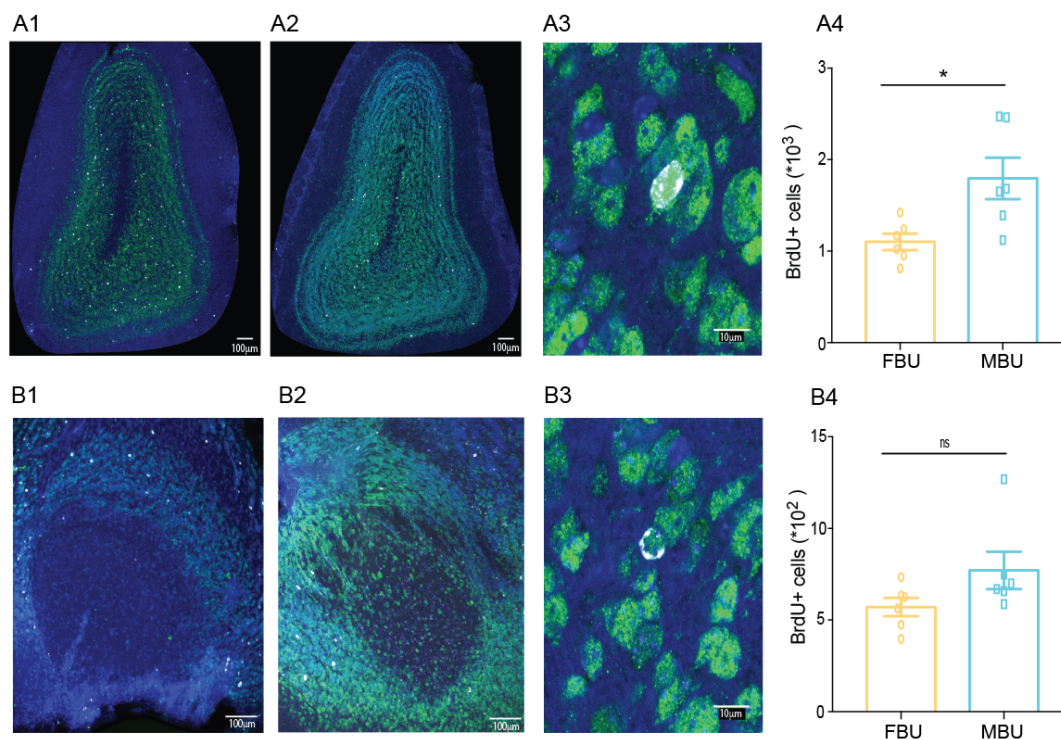


Figure 3-16: Effect of the multimodal training on the OB neurogenesis of female mice

A1. Immunofluorescence image of coronal MOB section of an animal trained with MBU in MPL paradigm. Blue: DAPI, Green: NeuN, Gray: BrdU, Scale bar = 100 μ m.

A2. Immunofluorescence image of coronal MOB section of an animal trained with FBU in MPL paradigm. Blue: DAPI, Green: NeuN, Gray: BrdU, Scale bar = 100 μ m.

A3. A higher magnification (100X) of co-localized NeuN+ -BrdU+ cell in MOB. Scale bar = 10 μ m.

A4. Significantly higher BrdU+ cells were found in MBU trained mice as compared to FBU trained mice ($p < 0.05$, unpaired t-test, two-tailed $N = 3$ per group, $n = 6$ MOBs).

B1. Immunofluorescence image of coronal AOB section of an animal trained with MBU in MPL paradigm. Scale bar = 100 μ m.

B2. Immunofluorescence image of coronal AOB section of an animal trained with FBU in MPL paradigm. Scale bar = 100 μ m.

B3. A higher magnification (100x) of co-localized NeuN+ -BrdU+ cell in AOB. Scale bar = 10 μ m.

B4. AOB neurogenesis was comparable between MBU and FBU trained mice as quantified after performing MD 15 ($p > 0.05$, Mann-Whitney test, $N = 3$ per group, $n = 6$ AOBs).

3.6.2 Estrous cyclicity does not influence odor discrimination learning and memory in female mice

Our MPL task brought about activation of MOB circuitry in whisker intact female mice. We observed that the male urine and bedding based training caused increased MOB circuitry activation via carrying out Arc immunohistochemistry. This was found in both TrD 15 and MD 15 days of the MPL (Figure 3-11, C). We further decided to evaluate the attractive pheromonal cues dependent activation of OB circuit in modulating other olfactory guided behaviors. For this, we induced estrous cyclicity by Whitten effect and checked for changes in non-pheromonal but olfactory based learning and memory changes. We first carried out CI vs EU pair for discrimination learning training for two cohorts of mice. For one cohort, no exposure to MBU was done. The experimental cohort also did not undergo Whitten effect for this odor pair. This was served as a test to assess if any inter-group variability is seen even before introducing estrous cyclicity was induced (Figure 3-17, A: CI vs. EU Ordinary Two-way ANOVA, Bonferroni's multiple comparison test, $p > 0.05$). Whitten effect was induced by exposing them directly to MBU every day before and during the training. Once the estrous induction and synchronization was accomplished, these mice were trained on subsequent odor pairs. No difference arising due to MOB activation upon estrous induction was observed in the experimental cohort when compared to the control ones (Figure 3-17, A: AA vs EB: $p > 0.1$, $F = 0.12$; BZ vs NN: $p > 0.1$, $F = 1.43$; HX vs PN: $p > 0.1$, $F = 0.19$; Two-way ANOVA). Motivation, as observed by their inter-trial intervals while training for these odor pairs remained comparable between the two cohorts (Figure 3-17, C). Individual day accuracies were plotted for AA vs EB odor pair in order to have an accuracy output values per mouse to be mapped to its estrous on that day (as the estrous cycle was of 4 days length in synchronized group) during the discrimination training days (Figure 3-17, B, $p > 0.1$, $F = 0.49$, Two-way ANOVA). These values were indeed independent of the estrous stages mice were in, regardless of whether the cycle was induced or not. We also checked for long-term memory for AA vs EB odor pair one month later post training. Overall, we concluded that the OSP based exposure which caused induction of Whitten effect did not show any modification in their non-pheromonal volatile discrimination behavior (Figure 3-17, D, $p > 0.1$, Mann-Whitney test). These results indicate estrous stages are least influencing the behavior that we assessed using the Go/No-go paradigm. We would like to investigate if ELS dependent effects are observed in this kind of non-pheromonal odor discrimination learning paradigm.

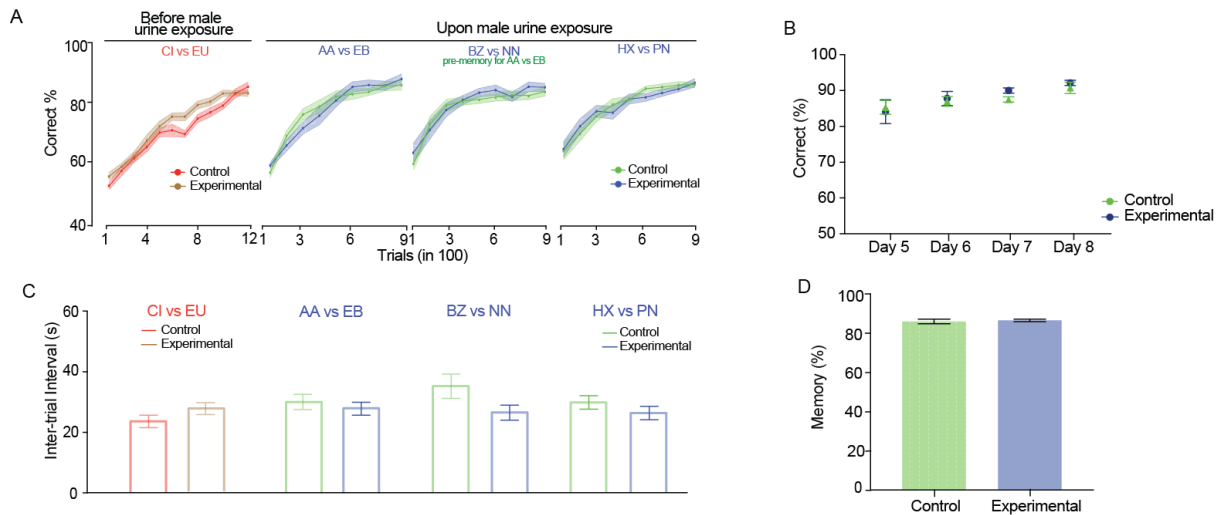


Figure 3-17: Estrous cycle induction and synchronization does not alter in non-pheromonal volatiles discrimination learning and memory performance

A. Learning curves before and after estrous cycle induction as well as synchronization are plotted that showed similar learning accuracy achieved across different odor pairs in experimental mice (AA vs. EB: $p > 0.1$, $F = 0.12$; BZ vs. NN: $p > 0.1$, $F = 1.43$; HX vs. PN: $p > 0.1$, $F = 0.19$; Two-way ANOVA).

B. Accuracy levels, tracked over four days of AA vs. EB training, remained unaffected by the stage of the estrous cycle in both control and experimental cohorts ($p > 0.1$, $F = 0.49$, Two-way ANOVA).

C. Motivation, as observed by their inter-trial intervals while training for these odor pairs remained comparable between the two cohorts ($p > 0.05$, Unpaired t-test/Man-Whitney test).

D. Memory % values remained similar when checked one month after the training for AA vs. EB task between the control and experimental cohorts ($p > 0.1$, Mann-Whitney test).

Publications

1. **Pardasani Meenakshi**, Shruti D. Marathe, Maitreyee Mandar Purnapatre, Urvashi Dalvi, and Nixon M. Abraham. "Multimodal learning of pheromone locations." *The FASEB Journal* 35, no. 9 (2021): e21836.

Manuscripts under review:

1. Mehak Malhotra, **Meenakshi Pardasani**, Nixon M. Abraham, and Manickam Jayakannan. Star Block Unimolecular micelles to breach blood-brain barrier.
2. Rajdeep Bhowmik, **Meenakshi Pardasani**, Sarang Mahajan, Rahul Magar, Samir V. Joshi, Anindya S. Bhattacharjee, and Nixon M. Abraham. Persistent olfactory learning deficits during and post-COVID-19 infection.

Manuscripts under preparation:

1. **Meenakshi Pardasani**, Priya Srikanth, Meher Kantroo, Sarang Mahajan, Eleanor McGowan, Nixon M. Abraham. Effect of Early life stress on olfactory perceptual learning deficits.
2. Sarang Mahajan, **Meenakshi Pardasani**, Anindya S. Bhattacharjee, Nixon M. Abraham. Breathing patterns of humans in an olfactory decision-making task.

Appendix

Copyright form



Multimodal learning of pheromone locations

Author: Meenakshi Pardasani, Shruti D. Marathe, Maitreyee Mandar Purnapatre, et al

Publication: THE FASEB JOURNAL

Publisher: John Wiley and Sons

Date: Aug 18, 2021

© 2021 The Authors. The FASEB Journal published by Wiley Periodicals LLC on behalf of Federation of American Societies for Experimental Biology

Open Access Article

This is an open access article distributed under the terms of the [Creative Commons CC BY](#) license, which permits unrestricted use, distribution, and reproduction in any medium, provided the original work is properly cited.

You are not required to obtain permission to reuse this article.

For an understanding of what is meant by the terms of the Creative Commons License, please refer to [Wiley's Open Access Terms and Conditions](#).

Permission is not required for this type of reuse.

Wiley offers a professional reprint service for high quality reproduction of articles from over 1400 scientific and medical journals. Wiley's reprint service offers:

- Peer reviewed research or reviews
- Tailored collections of articles
- A professional high quality finish
- Glossy journal style color covers
- Company or brand customisation
- Language translations
- Prompt turnaround times and delivery directly to your office, warehouse or congress.

Please contact our Reprints department for a quotation. Email corporatesaleseurope@wiley.com or corporatesalesusa@wiley.com or corporatesalesDE@wiley.com.

References

1. LeDoux, J. E. Emotion circuits in the brain. *Annu Rev Neurosci* **23**, 155–184 (2000).
2. Kohli, P., Soler, Z. M., Nguyen, S. A., Muus, J. S. & Schlosser, R. J. The association between olfaction and depression: a systematic review. *Chem Senses* **41**, 479–486 (2016).
3. Deisseroth, K. Circuit dynamics of adaptive and maladaptive behaviour. *Nature* **505**, 309–317 (2014).
4. Kikusui, T., Nakamura, K., Kakuma, Y. & Mori, Y. Early weaning augments neuroendocrine stress responses in mice. *Behavioural brain research* **175**, 96–103 (2006).
5. Schmidt, M. *et al.* The postnatal development of the hypothalamic--pituitary--adrenal axis in the mouse. *International journal of developmental neuroscience* **21**, 125–132 (2003).
6. Chaudhury, D., Escanilla, O. & Linster, C. Bulbar acetylcholine enhances neural and perceptual odor discrimination. *Journal of Neuroscience* **29**, 52–60 (2009).
7. la Rosa-Prieto, D. *et al.* Olfactory and cortical projections to bulbar and hippocampal adult-born neurons. *Front Neuroanat* **9**, 4 (2015).
8. McLean, J. H. & Shipley, M. T. Serotonergic afferents to the rat olfactory bulb: I. Origins and laminar specificity of serotonergic inputs in the adult rat. *Journal of Neuroscience* **7**, 3016–3028 (1987).
9. Shipley, M. T. & Adamek, G. D. The connections of the mouse olfactory bulb: a study using orthograde and retrograde transport of wheat germ agglutinin conjugated to horseradish peroxidase. *Brain Res Bull* **12**, 669–688 (1984).
10. Abraham, N. M. *et al.* Maintaining accuracy at the expense of speed: stimulus similarity defines odor discrimination time in mice. *neuron* **44**, 865–876 (2004).
11. Nithianantharajah, J. & Hannan, A. J. Enriched environments, experience-dependent plasticity and disorders of the nervous system. *Nature Reviews Neuroscience* **7**, 697–709 (2006).
12. Kempermann, G. Environmental enrichment, new neurons and the neurobiology of individuality. *Nature Reviews Neuroscience* **20**, 235–245 (2019).
13. van Praag, H., Kempermann, G. & Gage, F. H. Neural consequences of environmental enrichment. *Nature Reviews Neuroscience* **1**, 191–198 (2000).
14. Pang, T. Y. C. & Hannan, A. J. Enhancement of cognitive function in models of brain disease through environmental enrichment and physical activity. *Neuropharmacology* **64**, 515–528 (2013).
15. Engin, E., Stellbrink, J., Treit, D. & Dickson, C. T. Anxiolytic and antidepressant effects of intracerebroventricularly administered somatostatin: behavioral and neurophysiological evidence. *Neuroscience* **157**, 666–676 (2008).
16. Khan, A. G. *et al.* Distinct learning-induced changes in stimulus selectivity and interactions of GABAergic interneuron classes in visual cortex. *Nat Neurosci* **21**, 851–859 (2018).
17. Abbas, A. I. *et al.* Somatostatin interneurons facilitate hippocampal-prefrontal synchrony and prefrontal spatial encoding. *Neuron* **100**, 926–939 (2018).
18. Lepousez, G. *et al.* Somatostatin interneurons delineate the inner part of the external plexiform layer in the mouse main olfactory bulb. *Journal of Comparative Neurology* **518**, 1976–1994 (2010).

19. Epelbaum, J. *et al.* Somatostatin, Alzheimer's disease and cognition: an old story coming of age? *Prog Neurobiol* **89**, 153–161 (2009).
20. Johnston, R. E. Chemical communication in rodents: from pheromones to individual recognition. *J Mammal* **84**, 1141–1162 (2003).
21. Kavaliers, M. & Choleris, E. Social cognition and the neurobiology of rodent mate choice. *Integrative and Comparative Biology* **57**, 846–856 (2017).
22. Pardasani, M., Marathe, S. D., Purnapatre, M. M., Dalvi, U. & Abraham, N. M. Multimodal learning of pheromone locations. *The FASEB Journal* **35**, e21836 (2021).
23. Teicher, M. H. & Samson, J. A. Annual research review: enduring neurobiological effects of childhood abuse and neglect. *Journal of child psychology and psychiatry* **57**, 241–266 (2016).
24. Kim, J. & Cicchetti, D. Longitudinal trajectories of self-system processes and depressive symptoms among maltreated and nonmaltreated children. *Child Dev* **77**, 624–639 (2006).
25. Jumper, S. A. A meta-analysis of the relationship of child sexual abuse to adult psychological adjustment. *Child abuse & neglect* **19**, 715–728 (1995).
26. Chen, Y. & Baram, T. Z. Toward understanding how early-life stress reprograms cognitive and emotional brain networks. *Neuropsychopharmacology* **41**, 197–206 (2016).
27. Worlein, J. M. Nonhuman Primate Models of Depression: Effects of Early Experience and Stress. *ILAR Journal* **55**, 259–273 (2014).
28. Murthy, S. & Gould, E. Early life stress in rodents: animal models of illness or resilience? *Front Behav Neurosci* **12**, 157 (2018).
29. Schmidt, M. v, Wang, X.-D. & Meijer, O. C. Early life stress paradigms in rodents: potential animal models of depression? *Psychopharmacology (Berl)* **214**, 131–140 (2011).
30. Agorastos, A., Pervanidou, P., Chrousos, G. P. & Baker, D. G. Developmental trajectories of early life stress and trauma: a narrative review on neurobiological aspects beyond stress system dysregulation. *Front Psychiatry* **10**, 118 (2019).
31. Juruena, M. F., Bourne, M., Young, A. H. & Cleare, A. J. Hypothalamic-Pituitary-Adrenal Axis Dysfunction by Early Life Stress. *Neuroscience Letters* 136037 (2021).
32. Weber, K. *et al.* Stress load during childhood affects psychopathology in psychiatric patients. *BMC Psychiatry* **8**, 1–10 (2008).
33. Kessler, R. C. *et al.* Childhood adversities and adult psychopathology in the WHO World Mental Health Surveys. *The British journal of psychiatry* **197**, 378–385 (2010).
34. Hughes, K. *et al.* The effect of multiple adverse childhood experiences on health: a systematic review and meta-analysis. *The Lancet Public Health* **2**, e356–e366 (2017).
35. Meyer, A. *et al.* Self-reported and observed punitive parenting prospectively predicts increased error-related brain activity in six-year-old children. *J Abnorm Child Psychol* **43**, 821–829 (2015).
36. Dich, N. *et al.* Early life adversity potentiates the effects of later life stress on cumulative physiological dysregulation. *Anxiety, Stress, & Coping* **28**, 372–390 (2015).
37. Widom, C. S., Horan, J. & Brzustowicz, L. Childhood maltreatment predicts allostatic load in adulthood. *Child abuse & neglect* **47**, 59–69 (2015).

38. Sol\`is, C. B. *et al.* Adverse childhood experiences and physiological wear-and-tear in midlife: Findings from the 1958 British birth cohort. *Proceedings of the National Academy of Sciences* **112**, E738--E746 (2015).
39. Bick, J. & Nelson, C. A. Early adverse experiences and the developing brain. *Neuropsychopharmacology* **41**, 177–196 (2016).
40. Tottenham, N. *et al.* Prolonged institutional rearing is associated with atypically large amygdala volume and difficulties in emotion regulation. *Dev Sci* **13**, 46–61 (2010).
41. Schaan, V. K. *et al.* Childhood trauma affects stress-related interoceptive accuracy. *Front Psychiatry* **10**, 750 (2019).
42. Rahal, D. *et al.* Early life stress, subjective social status, and health during late adolescence. *Psychology & health* **35**, 1531–1549 (2020).
43. Danese, A., Pariante, C. M., Caspi, A., Taylor, A. & Poulton, R. Childhood maltreatment predicts adult inflammation in a life-course study. *Proceedings of the National Academy of Sciences* **104**, 1319–1324 (2007).
44. Danese, A. & Lewis, S. J. Psychoneuroimmunology of early-life stress: the hidden wounds of childhood trauma? *Neuropsychopharmacology* **42**, 99–114 (2017).
45. Higley, J. D., Suomi, S. J. & Linnoila, M. A longitudinal assessment of CSF monoamine metabolite and plasma cortisol concentrations in young rhesus monkeys. *Biol Psychiatry* **32**, 127–145 (1992).
46. Spinelli, S. *et al.* Early-life stress induces long-term morphologic changes in primate brain. *Arch Gen Psychiatry* **66**, 658–665 (2009).
47. Lyons, D. M., Parker, K. J. & Schatzberg, A. F. Animal models of early life stress: implications for understanding resilience. *Dev Psychobiol* **52**, 402–410 (2010).
48. Liu, D. *et al.* Maternal care, hippocampal glucocorticoid receptors, and hypothalamic-pituitary-adrenal responses to stress. *Science (1979)* **277**, 1659–1662 (1997).
49. WALKER, C.-D., SCRIBNER, K. A., CASCIO, C. S. & DALLMAN, M. F. The pituitary-adrenocortical system of neonatal rats is responsive to stress throughout development in a time-dependent and stressor-specific fashion. *Endocrinology* **128**, 1385–1395 (1991).
50. van Oers, H. J. J., de Kloet, E. R., Whelan, T. & Levine, S. Maternal deprivation effect on the infant's neural stress markers is reversed by tactile stimulation and feeding but not by suppressing corticosterone. *Journal of Neuroscience* **18**, 10171–10179 (1998).
51. Wiedenmayer, C. P., Magarinos, A. M., McEwen, B. S. & Barr, G. A. Mother lowers glucocorticoid levels of preweaning rats after acute threat. *Ann N Y Acad Sci* **1008**, 304–307 (2003).
52. Levine, S. The Ontogeny of the Hypothalamic-Pituitary-Adrenal Axis. The Influence of Maternal Factors a. *Ann N Y Acad Sci* **746**, 275–288 (1994).
53. Eiland, L. & McEwen, B. S. Early life stress followed by subsequent adult chronic stress potentiates anxiety and blunts hippocampal structural remodeling. *Hippocampus* **22**, 82–91 (2012).
54. Lehmann, J. & Feldon, J. Long-term biobehavioral effects of maternal separation in the rat: consistent or confusing? *Reviews in the Neurosciences* **11**, 383–408 (2000).
55. Lundberg, S., Abelson, K. S. P., Nylander, I. & Roman, E. Few long-term consequences after prolonged maternal separation in female Wistar rats. *PLoS One* **12**, e0190042 (2017).

56. Llorente, R. *et al.* Early maternal deprivation and neonatal single administration with a cannabinoid agonist induce long-term sex-dependent psychoimmunoendocrine effects in adolescent rats. *Psychoneuroendocrinology* **32**, 636–650 (2007).
57. Carlyle, B. C. *et al.* Maternal separation with early weaning: a rodent model providing novel insights into neglect associated developmental deficits. *Dev Psychopathol* **24**, 1401–1416 (2012).
58. Rice, C. J., Sandman, C. A., Lenjavi, M. R. & Baram, T. Z. A novel mouse model for acute and long-lasting consequences of early life stress. *Endocrinology* **149**, 4892–4900 (2008).
59. Wang, X.-D. *et al.* Early-life stress-induced anxiety-related behavior in adult mice partially requires forebrain corticotropin-releasing hormone receptor 1. *European Journal of Neuroscience* **36**, 2360–2367 (2012).
60. Uchida, S. *et al.* Early life stress enhances behavioral vulnerability to stress through the activation of REST4-mediated gene transcription in the medial prefrontal cortex of rodents. *Journal of Neuroscience* **30**, 15007–15018 (2010).
61. Benekareddy, M., Vadodaria, K. C., Nair, A. R. & Vaidya, V. A. Postnatal serotonin type 2 receptor blockade prevents the emergence of anxiety behavior, dysregulated stress-induced immediate early gene responses, and specific transcriptional changes that arise following early life stress. *Biol Psychiatry* **70**, 1024–1032 (2011).
62. Wu, Y., Patchev, A. v, Daniel, G., Almeida, O. F. X. & Spengler, D. Early-life stress reduces DNA methylation of the Pomc gene in male mice. *Endocrinology* **155**, 1751–1762 (2014).
63. Husum, H. & Mathé, A. A. Early life stress changes concentrations of neuropeptide Y and corticotropin-releasing hormone in adult rat brain. Lithium treatment modifies these changes. *Neuropsychopharmacology* **27**, 756–764 (2002).
64. Champagne, D. L. *et al.* Maternal care and hippocampal plasticity: evidence for experience-dependent structural plasticity, altered synaptic functioning, and differential responsiveness to glucocorticoids and stress. *Journal of Neuroscience* **28**, 6037–6045 (2008).
65. Reshetnikov, V. v, Ryabushkina, Y. A. & Bondar, N. P. Impact of mothers' experience and early-life stress on aggression and cognition in adult male mice. *Dev Psychobiol* **62**, 36–49 (2020).
66. Bubl, E., Kern, E., Ebert, D., Bach, M. & van Elst, L. T. Seeing gray when feeling blue? Depression can be measured in the eye of the diseased. *Biol Psychiatry* **68**, 205–208 (2010).
67. Takatsuru, Y., Yoshitomo, M., Nemoto, T., Eto, K. & Nabekura, J. Maternal separation decreases the stability of mushroom spines in adult mice somatosensory cortex. *Brain Res* **1294**, 45–51 (2009).
68. Takatsuru, Y., Nabekura, J., Ishikawa, T., Kohsaka, S. & Koibuchi, N. Early-life stress increases the motility of microglia in adulthood. *The Journal of Physiological Sciences* **65**, 187–194 (2015).
69. Pause, B. M., Miranda, A., Göder, R., Aldenhoff, J. B. & Ferstl, R. Reduced olfactory performance in patients with major depression. *J Psychiatr Res* **35**, 271–277 (2001).
70. Pause, B. M. *et al.* Convergent and divergent effects of odors and emotions in depression. *Psychophysiology* **40**, 209–225 (2003).
71. Negoias, S. *et al.* Reduced olfactory bulb volume and olfactory sensitivity in patients with acute major depression. *Neuroscience* **169**, 415–421 (2010).

72. Krusemark, E. A., Novak, L. R., Gitelman, D. R. & Li, W. When the sense of smell meets emotion: anxiety-state-dependent olfactory processing and neural circuitry adaptation. *Journal of Neuroscience* **33**, 15324–15332 (2013).
73. Kelly, J. P., Wrynn, A. S. & Leonard, B. E. The olfactory bulbectomized rat as a model of depression: an update. *Pharmacology & therapeutics* **74**, 299–316 (1997).
74. Morales-Medina, J. C., Iannitti, T., Freeman, A. & Caldwell, H. K. The olfactory bulbectomized rat as a model of depression: the hippocampal pathway. *Behavioural Brain Research* **317**, 562–575 (2017).
75. Glinka, M. E. *et al.* Olfactory deficits cause anxiety-like behaviors in mice. *Journal of Neuroscience* **32**, 6718–6725 (2012).
76. Kondoh, K. *et al.* A specific area of olfactory cortex involved in stress hormone responses to predator odours. *Nature* **532**, 103–106 (2016).
77. Manella, L. C., Alperin, S. & Linster, C. Stressors impair odor recognition memory via an olfactory bulb-dependent noradrenergic mechanism. *Front Integr Neurosci* **7**, 97 (2013).
78. Croy, I. *et al.* Reduced olfactory bulb volume in adults with a history of childhood maltreatment. *Chem Senses* **38**, 679–684 (2013).
79. Siopi, E. *et al.* Anxiety-and depression-like states lead to pronounced olfactory deficits and impaired adult neurogenesis in mice. *Journal of Neuroscience* **36**, 518–531 (2016).
80. Czarnabay, D. *et al.* Repeated three-hour maternal deprivation as a model of early-life stress alters maternal behavior, olfactory learning and neural development. *Neurobiol Learn Mem* **163**, 107040 (2019).
81. Mirescu, C., Peters, J. D. & Gould, E. Early life experience alters response of adult neurogenesis to stress. *Nat Neurosci* **7**, 841–846 (2004).
82. Mirescu, C. & Gould, E. Stress and adult neurogenesis. *Hippocampus* **16**, 233–238 (2006).
83. Moriceau, S., Shionoya, K., Jakubs, K. & Sullivan, R. M. Early-life stress disrupts attachment learning: the role of amygdala corticosterone, locus ceruleus corticotropin releasing hormone, and olfactory bulb norepinephrine. *Journal of Neuroscience* **29**, 15745–15755 (2009).
84. Mori, K., Nagao, H. & Yoshihara, Y. The olfactory bulb: coding and processing of odor molecule information. *Science* (1979) **286**, 711–715 (1999).
85. Yokoi, M., Mori, K. & Nakanishi, S. Refinement of odor molecule tuning by dendrodendritic synaptic inhibition in the olfactory bulb. *Proceedings of the National Academy of Sciences* **92**, 3371–3375 (1995).
86. Buck, L. & Axel, R. A novel multigene family may encode odorant receptors: a molecular basis for odor recognition. *Cell* **65**, 175–187 (1991).
87. Greer, P. L. *et al.* A family of non-GPCR chemosensors defines an alternative logic for mammalian olfaction. *Cell* **165**, 1734–1748 (2016).
88. Nara, K., Saraiva, L. R., Ye, X. & Buck, L. B. A large-scale analysis of odor coding in the olfactory epithelium. *Journal of Neuroscience* **31**, 9179–9191 (2011).
89. Mombaerts, P. *et al.* Visualizing an olfactory sensory map. *Cell* **87**, 675–686 (1996).
90. Murphy, G. J., Darcy, D. P. & Isaacson, J. S. Intraglomerular inhibition: signaling mechanisms of an olfactory microcircuit. *Nat Neurosci* **8**, 354–364 (2005).
91. Parsa, P. V., D'Souza, R. D. & Vijayaraghavan, S. Signaling between periglomerular cells reveals a bimodal role for GABA in modulating glomerular microcircuitry in the

- olfactory bulb. *Proceedings of the National Academy of Sciences* **112**, 9478–9483 (2015).
92. Isaacson, J. S. & Strowbridge, B. W. Olfactory reciprocal synapses: dendritic signaling in the CNS. *Neuron* **20**, 749–761 (1998).
 93. Gschwend, O. *et al.* Neuronal pattern separation in the olfactory bulb improves odor discrimination learning. *Nat Neurosci* **18**, 1474–1482 (2015).
 94. Hamilton, K. A. *et al.* Properties of external plexiform layer interneurons in mouse olfactory bulb slices. *Neuroscience* **133**, 819–829 (2005).
 95. Kato, H. K., Gillet, S. N., Peters, A. J., Isaacson, J. S. & Komiyama, T. Parvalbumin-expressing interneurons linearly control olfactory bulb output. *Neuron* **80**, 1218–1231 (2013).
 96. Huang, L., Garcia, I., Jen, H.-I. & Arenkiel, B. R. Reciprocal connectivity between mitral cells and external plexiform layer interneurons in the mouse olfactory bulb. *Front Neural Circuits* **7**, 32 (2013).
 97. Garcia, I. *et al.* Local corticotropin releasing hormone (CRH) signals to its receptor CRHR1 during postnatal development of the mouse olfactory bulb. *Brain Structure and Function* **221**, 1–20 (2016).
 98. Lois, C. & Alvarez-Buylla, A. Proliferating subventricular zone cells in the adult mammalian forebrain can differentiate into neurons and glia. *Proceedings of the National Academy of Sciences* **90**, 2074–2077 (1993).
 99. Lledo, P.-M. & Saghatelian, A. Integrating new neurons into the adult olfactory bulb: joining the network, life--death decisions, and the effects of sensory experience. *Trends Neurosci* **28**, 248–254 (2005).
 100. Garcia-González, D. *et al.* Serotonergic projections govern postnatal neuroblast migration. *Neuron* **94**, 534–549 (2017).
 101. Lenington, J. B. *et al.* Midbrain dopamine neurons associated with reward processing innervate the neurogenic subventricular zone. *Journal of Neuroscience* **31**, 13078–13087 (2011).
 102. Arruda-Carvalho, M. *et al.* Posttraining ablation of adult-generated olfactory granule cells degrades odor--reward memories. *Journal of Neuroscience* **34**, 15793–15803 (2014).
 103. Breton-Provencher, V., Lemasson, M., Peralta, M. R. & Saghatelian, A. Interneurons produced in adulthood are required for the normal functioning of the olfactory bulb network and for the execution of selected olfactory behaviors. *Journal of Neuroscience* **29**, 15245–15257 (2009).
 104. Ming, G. & Song, H. Adult neurogenesis in the mammalian brain: significant answers and significant questions. *Neuron* **70**, 687–702 (2011).
 105. Fletcher, M. L. & Chen, W. R. Neural correlates of olfactory learning: critical role of centrifugal neuromodulation. *Learning & memory* **17**, 561–570 (2010).
 106. Kunze, W. A. A., Shafton, A. D., Kemm, R. E. & McKenzie, J. S. Effect of stimulating the nucleus of the horizontal limb of the diagonal band on single unit activity in the olfactory bulb. *Neuroscience* **40**, 21–27 (1991).
 107. Castillo, P. E., Carleton, A., Vincent, J.-D. & Lledo, P.-M. Multiple and opposing roles of cholinergic transmission in the main olfactory bulb. *Journal of Neuroscience* **19**, 9180–9191 (1999).

108. Mandairon, N. *et al.* Cholinergic modulation in the olfactory bulb influences spontaneous olfactory discrimination in adult rats. *European Journal of Neuroscience* **24**, 3234–3244 (2006).
109. Miranda, M. I., Ortiz-Godina, F. & Garcia, D. Differential involvement of cholinergic and beta-adrenergic systems during acquisition, consolidation, and retrieval of long-term memory of social and neutral odors. *Behavioural brain research* **202**, 19–25 (2009).
110. Nickell, W. T. & Shipley, M. T. Neurophysiology of magnocellular forebrain inputs to the olfactory bulb in the rat: frequency potentiation of field potentials and inhibition of output neurons. *Journal of Neuroscience* **8**, 4492–4502 (1988).
111. Kaufer, D., Friedman, A., Seidman, S. & Soreq, H. Acute stress facilitates long-lasting changes in cholinergic gene expression. *Nature* **393**, 373–377 (1998).
112. Nai, Q., Dong, H.-W., Linster, C. & Ennis, M. Activation of α_1 and α_2 noradrenergic receptors exert opposing effects on excitability of main olfactory bulb granule cells. *Neuroscience* **169**, 882–892 (2010).
113. Bouret, S. & Sara, S. J. Locus coeruleus activation modulates firing rate and temporal organization of odour-induced single-cell responses in rat piriform cortex. *European Journal of Neuroscience* **16**, 2371–2382 (2002).
114. Nai, Q., Dong, H.-W., Hayar, A., Linster, C. & Ennis, M. Noradrenergic regulation of GABAergic inhibition of main olfactory bulb mitral cells varies as a function of concentration and receptor subtype. *J Neurophysiol* **101**, 2472–2484 (2009).
115. McLean, J. H., Shipley, M. T., Nickell, W. T., Aston-Jones, G. & Reyher, C. K. H. Chemoanatomical organization of the noradrenergic input from locus coeruleus to the olfactory bulb of the adult rat. *Journal of Comparative Neurology* **285**, 339–349 (1989).
116. Petzold, G. C., Hagiwara, A. & Murthy, V. N. Serotonergic modulation of odor input to the mammalian olfactory bulb. *Nat Neurosci* **12**, 784–791 (2009).
117. Kapoor, V., Provost, A. C., Agarwal, P. & Murthy, V. N. Activation of raphe nuclei triggers rapid and distinct effects on parallel olfactory bulb output channels. *Nat Neurosci* **19**, 271–282 (2016).
118. Lowry, C. A., Johnson, P. L., Hay-Schmidt, A., Mikkelsen, J. & Shekhar, A. Modulation of anxiety circuits by serotonergic systems. *Stress* **8**, 233–246 (2005).
119. Houwing, D. J., Buwalda, B., van der Zee, E. A., de Boer, S. F. & Olivier, J. D. A. The serotonin transporter and early life stress: translational perspectives. *Front Cell Neurosci* **11**, 117 (2017).
120. Miyamichi, K. *et al.* Cortical representations of olfactory input by trans-synaptic tracing. *Nature* **472**, 191–196 (2011).
121. Igarashi, K. M. *et al.* Parallel mitral and tufted cell pathways route distinct odor information to different targets in the olfactory cortex. *Journal of Neuroscience* **32**, 7970–7985 (2012).
122. Cádiz-Moretti, B., Abellán-Álvaro, M., Pardo-Bellver, C., Martínez-García, F. & Lanuza, E. Afferent and efferent connections of the cortex-amygdala transition zone in mice. *Front Neuroanat* **10**, 125 (2016).
123. Sevelinges, Y. *et al.* Adult depression-like behavior, amygdala and olfactory cortex functions are restored by odor previously paired with shock during infant's sensitive period attachment learning. *Developmental Cognitive Neuroscience* **1**, 77–87 (2011).

124. Scott, J. W. & Leonard, C. M. The olfactory connections of the lateral hypothalamus in the rat, mouse and hamster. *Journal of Comparative Neurology* **141**, 331–344 (1971).
125. Barnett, W. S. Long-term effects of early childhood programs on cognitive and school outcomes. *The future of children* 25–50 (1995).
126. Zigler, E. & Styfco, S. J. *The hidden history of Head Start*. (Oxford University Press, 2010).
127. Dickinson, D. K. & Caswell, L. Building support for language and early literacy in preschool classrooms through in-service professional development: Effects of the Literacy Environment Enrichment Program (LEEP). *Early Childhood Research Quarterly* **22**, 243–260 (2007).
128. Smyke, A. T., Zeanah, C. H., Fox, N. A. & Nelson, C. A. A new model of foster care for young children: the Bucharest early intervention project. *Child and Adolescent Psychiatric Clinics* **18**, 721–734 (2009).
129. McLaughlin, K. A. *et al.* Delayed maturation in brain electrical activity partially explains the association between early environmental deprivation and symptoms of attention-deficit/hyperactivity disorder. *Biol Psychiatry* **68**, 329–336 (2010).
130. Fox, N. A., Almas, A. N., Degnan, K. A., Nelson, C. A. & Zeanah, C. H. The effects of severe psychosocial deprivation and foster care intervention on cognitive development at 8 years of age: findings from the Bucharest Early Intervention Project. *Journal of Child Psychology and Psychiatry* **52**, 919–928 (2011).
131. Humphreys, K. L. *et al.* Foster care promotes adaptive functioning in early adolescence among children who experienced severe, early deprivation. *Journal of Child Psychology and Psychiatry* **59**, 811–821 (2018).
132. Wade, M., Fox, N. A., Zeanah, C. H. & Nelson, C. A. Effect of foster care intervention on trajectories of general and specific psychopathology among children with histories of institutional rearing: a randomized clinical trial. *JAMA Psychiatry* **75**, 1137–1145 (2018).
133. Oddi, D. *et al.* Early social enrichment rescues adult behavioral and brain abnormalities in a mouse model of fragile X syndrome. *Neuropsychopharmacology* **40**, 1113–1122 (2015).
134. Bechar, A. R., Cacodcar, N., King, M. A. & Lewis, M. H. How does environmental enrichment reduce repetitive motor behaviors? Neuronal activation and dendritic morphology in the indirect basal ganglia pathway of a mouse model. *Behavioural brain research* **299**, 122–131 (2016).
135. Mazarakis, N. K. *et al.* ‘Super-enrichment’ reveals dose-dependent therapeutic effects of environmental stimulation in a transgenic mouse model of Huntington’s disease. *J Huntingtons Dis* **3**, 299–309 (2014).
136. Passineau, M. J., Green, E. J. & Dietrich, W. D. Therapeutic effects of environmental enrichment on cognitive function and tissue integrity following severe traumatic brain injury in rats. *Exp Neurol* **168**, 373–384 (2001).
137. Lima, M. G. P. *et al.* Environmental enrichment and exercise are better than social enrichment to reduce memory deficits in amyloid beta neurotoxicity. *Proceedings of the National Academy of Sciences* **115**, E2403–E2409 (2018).
138. Kikusui, T., Takeuchi, Y. & Mori, Y. Early weaning induces anxiety and aggression in adult mice. *Physiology & behavior* **81**, 37–42 (2004).
139. Nakamura, K., Kikusui, T., Takeuchi, Y. & Mori, Y. Changes in social instigation-and food restriction-induced aggressive behaviors and hippocampal 5HT1B mRNA

- receptor expression in male mice from early weaning. *Behavioural brain research* **187**, 442–448 (2008).
140. Bodyak, N. & Slotnick, B. Performance of mice in an automated olfactometer: odor detection, discrimination and odor memory. *Chem Senses* **24**, 637–645 (1999).
 141. Slotnick, B. & Restrepo, D. Olfactometry with mice. *Curr Protoc Neurosci* **33**, 8–20 (2005).
 142. Abraham, N. M. *et al.* Synaptic inhibition in the olfactory bulb accelerates odor discrimination in mice. *Neuron* **65**, 399–411 (2010).
 143. Bouton, M. E. & Sunsay, C. Contextual control of appetitive conditioning: Influence of a contextual stimulus generated by a partial reinforcement procedure. *The Quarterly Journal of Experimental Psychology Section B* **54**, 109–125 (2001).
 144. Holmes, A. *et al.* Early life genetic, epigenetic and environmental factors shaping emotionality in rodents. *Neuroscience & Biobehavioral Reviews* **29**, 1335–1346 (2005).
 145. Steckler, T. Using signal detection methods for analysis of operant performance in mice. *Behavioural brain research* **125**, 237–248 (2001).
 146. Cohen, Y., Reuveni, I., Barkai, E. & Maroun, M. Olfactory learning-induced long-lasting enhancement of descending and ascending synaptic transmission to the piriform cortex. *Journal of Neuroscience* **28**, 6664–6669 (2008).
 147. Kendler, K. S. “A gene for...”: the nature of gene action in psychiatric disorders. *American Journal of Psychiatry* **162**, 1243–1252 (2005).
 148. Kendler, K. S. & Baker, J. H. Genetic influences on measures of the environment: a systematic review. *Psychol Med* **37**, 615–626 (2007).
 149. Mehta, M. & Schmauss, C. Strain-specific cognitive deficits in adult mice exposed to early life stress. *Behavioral neuroscience* **125**, 29 (2011).
 150. MacQueen, G. M., Ramakrishnan, K., Ratnasingan, R., Chen, B. & Young, L. T. Desipramine treatment reduces the long-term behavioural and neurochemical sequelae of early-life maternal separation. *International Journal of Neuropsychopharmacology* **6**, 391–396 (2003).
 151. Savignac, H. M., Dinan, T. G. & Cryan, J. F. Resistance to early-life stress in mice: effects of genetic background and stress duration. *Front Behav Neurosci* **5**, 13 (2011).
 152. Priebe, K. *et al.* Maternal influences on adult stress and anxiety-like behavior in C57BL/6J and BALB/cJ mice: A cross-fostering study. *Dev Psychobiol* **47**, 398–407 (2005).
 153. Millstein, R. A. & Holmes, A. Effects of repeated maternal separation on anxiety- and depression-related phenotypes in different mouse strains. *Neuroscience & Biobehavioral Reviews* **31**, 3–17 (2007).
 154. Schmidt, M. v *et al.* Glucocorticoid receptor blockade disinhibits pituitary-adrenal activity during the stress hyporesponsive period of the mouse. *Endocrinology* **146**, 1458–1464 (2005).
 155. Schmidt, M. v, Oitzl, M. S., Levine, S. & de Kloet, E. R. The HPA system during the postnatal development of CD1 mice and the effects of maternal deprivation. *Brain Res Dev Brain Res* **139**, 39–49 (2002).
 156. Venerosi, A., Cirulli, F., Capone, F. & Alleva, E. Prolonged perinatal AZT administration and early maternal separation: effects on social and emotional behaviour of periadolescent mice. *Pharmacol Biochem Behav* **74**, 671–681 (2003).

157. Parfitt, D. B. *et al.* Differential early rearing environments can accentuate or attenuate the responses to stress in male C57BL/6 mice. *Brain Res* **1016**, 111–118 (2004).
158. Kikusui, T. & Mori, Y. Behavioural and neurochemical consequences of early weaning in rodents. *J Neuroendocrinol* **21**, 427–431 (2009).
159. Kikusui, T., Ichikawa, S. & Mori, Y. Maternal deprivation by early weaning increases corticosterone and decreases hippocampal BDNF and neurogenesis in mice. *Psychoneuroendocrinology* **34**, 762–772 (2009).
160. Mogi, K., Ishida, Y., Nagasawa, M. & Kikusui, T. Early weaning impairs fear extinction and decreases brain-derived neurotrophic factor expression in the prefrontal cortex of adult male C57BL/6 mice. *Dev Psychobiol* **58**, 1034–1042 (2016).
161. Bolton, J. L., Molet, J., Ivy, A. & Baram, T. Z. New insights into early-life stress and behavioral outcomes. *Current Opinion in Behavioral Sciences* **14**, 133–139 (2017).
162. Eghbal-Ahmadi, M., Avishai-Eliner, S., Hatalski, C. G. & Baram, T. Z. Differential regulation of the expression of corticotropin-releasing factor receptor type 2 (CRF2) in hypothalamus and amygdala of the immature rat by sensory input and food intake. *Journal of Neuroscience* **19**, 3982–3991 (1999).
163. Gunn, B. G. *et al.* Dysfunctional astrocytic and synaptic regulation of hypothalamic glutamatergic transmission in a mouse model of early-life adversity: relevance to neurosteroids and programming of the stress response. *Journal of Neuroscience* **33**, 19534–19554 (2013).
164. Ivy, A. S. *et al.* Hippocampal dysfunction and cognitive impairments provoked by chronic early-life stress involve excessive activation of CRH receptors. *Journal of Neuroscience* **30**, 13005–13015 (2010).
165. Naninck, E. F. G. *et al.* Chronic early life stress alters developmental and adult neurogenesis and impairs cognitive function in mice. *Hippocampus* **25**, 309–328 (2015).
166. Molet, J. *et al.* MRI uncovers disrupted hippocampal microstructure that underlies memory impairments after early-life adversity. *Hippocampus* **26**, 1618–1632 (2016).
167. Rainecki, C., Cortés, M. R., Belnoue, L. & Sullivan, R. M. Effects of early-life abuse differ across development: infant social behavior deficits are followed by adolescent depressive-like behaviors mediated by the amygdala. *Journal of Neuroscience* **32**, 7758–7765 (2012).
168. Cohen, M. M. *et al.* Early-life stress has persistent effects on amygdala function and development in mice and humans. *Proceedings of the National Academy of Sciences* **110**, 18274–18278 (2013).
169. Alberts, J. R. & Galef Jr, B. G. Acute anosmia in the rat: a behavioral test of a peripherally-induced olfactory deficit. *Physiology & behavior* **6**, 619–621 (1971).
170. Yang, M. & Crawley, J. N. Simple behavioral assessment of mouse olfaction. *Curr Protoc Neurosci* **48**, 8–24 (2009).
171. Machado, T. D. *et al.* Early life stress is associated with anxiety, increased stress responsivity and preference for “comfort foods” in adult female rats. *Stress* **16**, 549–556 (2013).
172. Gascuel, J. *et al.* Hypothalamus-olfactory system crosstalk: orexin a immunostaining in mice. *Front Neuroanat* **6**, 44 (2012).

173. Johnson, M. E. *et al.* Deficits in olfactory sensitivity in a mouse model of Parkinson's disease revealed by plethysmography of odor-evoked sniffing. *Sci Rep* **10**, 1–13 (2020).
174. Fareri, D. S. & Tottenham, N. Effects of early life stress on amygdala and striatal development. *Dev Cogn Neurosci* **19**, 233–247 (2016).
175. Erskine, A., Bus, T., Herb, J. T. & Schaefer, A. T. Autonomouse: High throughput operant conditioning reveals progressive impairment with graded olfactory bulb lesions. *PLoS One* **14**, e0211571 (2019).
176. Rokni, D., Hemmelder, V., Kapoor, V. & Murthy, V. N. An olfactory cocktail party: figure-ground segregation of odorants in rodents. *Nat Neurosci* **17**, 1225–1232 (2014).
177. Millman, D. J. & Murthy, V. N. Rapid learning of odor–value association in the olfactory striatum. *Journal of Neuroscience* **40**, 4335–4347 (2020).
178. Jha, S. *et al.* Antidepressive and BDNF effects of enriched environment treatment across ages in mice lacking BDNF expression through promoter IV. *Transl Psychiatry* **6**, e896–e896 (2016).
179. Huang, H. *et al.* Effects of enriched environment on depression and anxiety-like behavior induced by early life stress: A comparison between different periods. *Behavioural Brain Research* 113389 (2021).
180. Sun, H. *et al.* Environmental enrichment influences BDNF and NR1 levels in the hippocampus and restores cognitive impairment in chronic cerebral hypoperfused rats. *Curr Neurovasc Res* **7**, 268–280 (2010).
181. Bekinschtein, P., Oomen, C. A., Saksida, L. M. & Bussey, T. J. Effects of environmental enrichment and voluntary exercise on neurogenesis, learning and memory, and pattern separation: BDNF as a critical variable? in *Seminars in cell & developmental biology* vol. 22 536–542 (2011).
182. Kempermann, G., Kuhn, H. G. & Gage, F. H. More hippocampal neurons in adult mice living in an enriched environment. *Nature* **386**, 493–495 (1997).
183. Rochefort, C., Gheusi, G., Vincent, J.-D. & Lledo, P.-M. Enriched odor exposure increases the number of newborn neurons in the adult olfactory bulb and improves odor memory. *Journal of Neuroscience* **22**, 2679–2689 (2002).
184. Mizrahi, A. & Katz, L. C. Dendritic stability in the adult olfactory bulb. *Nat Neurosci* **6**, 1201–1207 (2003).
185. Ma, D. K., Kim, W. R., Ming, G. & Song, H. Activity-dependent extrinsic regulation of adult olfactory bulb and hippocampal neurogenesis. *Ann N Y Acad Sci* **1170**, 664 (2009).
186. Hüttenrauch, M., Salinas, G. & Wirths, O. Effects of long-term environmental enrichment on anxiety, memory, hippocampal plasticity and overall brain gene expression in C57BL6 mice. *Front Mol Neurosci* **9**, 62 (2016).
187. Veyrac, A. *et al.* Novelty determines the effects of olfactory enrichment on memory and neurogenesis through noradrenergic mechanisms. *Neuropsychopharmacology* **34**, 786–795 (2009).
188. Godoy, L. D., Rossignoli, M. T., Delfino-Pereira, P., Garcia-Cairasco, N. & de Lima Umeoka, E. H. A comprehensive overview on stress neurobiology: basic concepts and clinical implications. *Front Behav Neurosci* 127 (2018).

189. Stanton, M. E., Gutierrez, Y. R. & Levine, S. Maternal deprivation potentiates pituitary-adrenal stress responses in infant rats. *Behavioral neuroscience* **102**, 692 (1988).
190. Laryea, G., Arnett, M. G. & Muglia, L. J. Behavioral studies and genetic alterations in corticotropin-releasing hormone (CRH) neurocircuitry: insights into human psychiatric disorders. *Behavioral sciences* **2**, 135–171 (2012).
191. Ehrlich, D. E., Ryan, S. J. & Rainnie, D. G. Postnatal development of electrophysiological properties of principal neurons in the rat basolateral amygdala. *J Physiol* **590**, 4819–4838 (2012).
192. Nieves, G. M., Bravo, M., Baskoylu, S. & Bath, K. G. Early life adversity decreases pre-adolescent fear expression by accelerating amygdala PV cell development. *Elife* **9**, e55263 (2020).
193. Ohta, K. *et al.* The effects of early life stress on the excitatory/inhibitory balance of the medial prefrontal cortex. *Behavioural Brain Research* **379**, 112306 (2020).
194. Chen, Y. *et al.* Early Life Stress Induces Different Behaviors in Adolescence and Adulthood May Related With Abnormal Medial Prefrontal Cortex Excitation/Inhibition Balance. *Frontiers in Neuroscience* **15**, (2021).
195. Martisova, E. *et al.* Long lasting effects of early-life stress on glutamatergic/GABAergic circuitry in the rat hippocampus. *Neuropharmacology* **62**, 1944–1953 (2012).
196. Perry-Paldi, A. *et al.* Early environments shape neuropeptide function: the case of oxytocin and vasopressin. *Frontiers in Psychology* **10**, 581 (2019).
197. Alviña, K., Jodeiri Farshbaf, M. & Mondal, A. K. Long term effects of stress on hippocampal function: emphasis on early life stress paradigms and potential involvement of neuropeptide Y. *Journal of Neuroscience Research* **99**, 57–66 (2021).
198. Heinrichs, M., Baumgartner, T., Kirschbaum, C. & Ehlert, U. Social support and oxytocin interact to suppress cortisol and subjective responses to psychosocial stress. *Biol Psychiatry* **54**, 1389–1398 (2003).
199. Grimm, S. *et al.* Early life stress modulates oxytocin effects on limbic system during acute psychosocial stress. *Soc Cogn Affect Neurosci* **9**, 1828–1835 (2014).
200. Englund, J. *et al.* Downregulation of kainate receptors regulating GABAergic transmission in amygdala after early life stress is associated with anxiety-like behavior in rodents. *Transl Psychiatry* **11**, 1–15 (2021).
201. Murthy, S. *et al.* Perineuronal nets, inhibitory interneurons, and anxiety-related ventral hippocampal neuronal oscillations are altered by early life adversity. *Biol Psychiatry* **85**, 1011–1020 (2019).
202. Liguz-Leczna, M., Dobrzanski, G. & Kossut, M. Somatostatin and Somatostatin-Containing Interneurons—From Plasticity to Pathology. *Biomolecules* **12**, 312 (2022).
203. Guilloux, J.-P. *et al.* Molecular evidence for BDNF-and GABA-related dysfunctions in the amygdala of female subjects with major depression. *Mol Psychiatry* **17**, 1130–1142 (2012).
204. Fee, C., Banasr, M. & Sibille, E. Somatostatin-positive gamma-aminobutyric acid interneuron deficits in depression: cortical microcircuit and therapeutic perspectives. *Biol Psychiatry* **82**, 549–559 (2017).
205. Ågren, H. & Lundqvist, G. Low levels of somatostatin in human CSF mark depressive episodes. *Psychoneuroendocrinology* **9**, 233–248 (1984).
206. Tripp, A., Kota, R. S., Lewis, D. A. & Sibille, E. Reduced somatostatin in subgenual anterior cingulate cortex in major depression. *Neurobiol Dis* **42**, 116–124 (2011).

207. Lin, L. C. & Sibille, E. Somatostatin, neuronal vulnerability and behavioral emotionality. *Mol Psychiatry* **20**, 377–387 (2015).
208. Ma, T. *et al.* Suppression of eIF2 α kinases alleviates Alzheimer's disease--related plasticity and memory deficits. *Nat Neurosci* **16**, 1299–1305 (2013).
209. Soumier, A. & Sibille, E. Opposing effects of acute versus chronic blockade of frontal cortex somatostatin-positive inhibitory neurons on behavioral emotionality in mice. *Neuropsychopharmacology* **39**, 2252–2262 (2014).
210. Strowski, M. Z. *et al.* Somatostatin receptor subtypes 2 and 5 inhibit corticotropin-releasing hormone-stimulated adrenocorticotropin secretion from AtT-20 cells. *Neuroendocrinology* **75**, 339–346 (2002).
211. Saiz-Sanchez, D. *et al.* Somatostatin, olfaction, and neurodegeneration. *Frontiers in Neuroscience* **14**, 96 (2020).
212. Johansson, O., Hökfelt, T. & Elde, R. P. Immunohistochemical distribution of somatostatin-like immunoreactivity in the central nervous system of the adult rat. *Neuroscience* **13**, 265–IN2 (1984).
213. Nocera, S. *et al.* Somatostatin serves a modulatory role in the mouse olfactory bulb: neuroanatomical and behavioral evidence. *Front Behav Neurosci* **13**, 61 (2019).
214. Lepousez, G., Mouret, A., Loudes, C., Epelbaum, J. & Viollet, C. Somatostatin contributes to in vivo gamma oscillation modulation and odor discrimination in the olfactory bulb. *Journal of Neuroscience* **30**, 870–875 (2010).
215. Bernstein, J. G. & Boyden, E. S. Optogenetic tools for analyzing the neural circuits of behavior. *Trends Cogn Sci* **15**, 592–600 (2011).
216. Josh Huang, Z. & Zeng, H. Genetic approaches to neural circuits in the mouse. *Annu Rev Neurosci* **36**, 183–215 (2013).
217. Lo, L. & Anderson, D. J. A Cre-dependent, anterograde transsynaptic viral tracer for mapping output pathways of genetically marked neurons. *Neuron* **72**, 938–950 (2011).
218. Nagel, G. *et al.* Channelrhodopsin-2, a directly light-gated cation-selective membrane channel. *Proceedings of the National Academy of Sciences* **100**, 13940–13945 (2003).
219. Gunaydin, L. A. *et al.* Ultrafast optogenetic control. *Nat Neurosci* **13**, 387–392 (2010).
220. Chow, B. Y., Han, X. & Boyden, E. S. Genetically encoded molecular tools for light-driven silencing of targeted neurons. *Prog Brain Res* **196**, 49–61 (2012).
221. Liu, Q., Zhang, Z. & Zhang, W. Optogenetic dissection of neural circuits underlying stress-induced mood disorders. *Frontiers in Psychology* **12**, 1249 (2021).
222. Nagai, Y., Sano, H. & Yokoi, M. Transgenic expression of Cre recombinase in mitral/tufted cells of the olfactory bulb. *genesis* **43**, 12–16 (2005).
223. Mitsui, S., Igarashi, K. M., Mori, K. & Yoshihara, Y. Genetic visualization of the secondary olfactory pathway in Tbx21 transgenic mice. *Neural systems & circuits* **1**, 1–14 (2011).
224. Koldaeva, A. *et al.* Generation and Characterization of a Cell Type-Specific, Inducible Cre-Driver Line to Study Olfactory Processing. *Journal of Neuroscience* **41**, 6449–6467 (2021).
225. Takahashi, H., Yoshihara, S. & Tsuboi, A. The functional role of olfactory bulb granule cell subtypes derived from embryonic and postnatal neurogenesis. *Frontiers in Molecular Neuroscience* **11**, 229 (2018).
226. Alonso, M. *et al.* Activation of adult-born neurons facilitates learning and memory. *Nat Neurosci* **15**, 897–904 (2012).

227. Garcia, I. *et al.* Local CRH signaling promotes synaptogenesis and circuit integration of adult-born neurons. *Dev Cell* **30**, 645–659 (2014).
228. Thiebaud, N., Gribble, F., Reimann, F., Trapp, S. & Fadool, D. A. A unique olfactory bulb microcircuit driven by neurons expressing the precursor to glucagon-like peptide 1. *Sci Rep* **9**, 1–16 (2019).
229. Dao, N. C., Brockway, D. F. & Crowley, N. A. In vitro optogenetic characterization of neuropeptide release from prefrontal cortical somatostatin neurons. *Neuroscience* **419**, 1–4 (2019).
230. Abraham, N. M., Guerin, D., Bhaukaurally, K. & Carleton, A. Similar odor discrimination behavior in head-restrained and freely moving mice. *PLoS One* **7**, e51789 (2012).
231. Wang, D. *et al.* VIP interneurons regulate olfactory bulb output and contribute to odor detection and discrimination. *Cell Reports* **38**, 110383 (2022).
232. Boyden, E. S., Zhang, F., Bamberg, E., Nagel, G. & Deisseroth, K. Millisecond-timescale, genetically targeted optical control of neural activity. *Nat Neurosci* **8**, 1263–1268 (2005).
233. Arrigoni, E. & Saper, C. B. What optogenetic stimulation is telling us (and failing to tell us) about fast neurotransmitters and neuromodulators in brain circuits for wake–sleep regulation. *Curr Opin Neurobiol* **29**, 165–171 (2014).
234. Schöne, C. *et al.* Optogenetic probing of fast glutamatergic transmission from hypocretin/orexin to histamine neurons in situ. *Journal of Neuroscience* **32**, 12437–12443 (2012).
235. Liu, A. *et al.* Mouse navigation strategies for odor source localization. *Front Neurosci* **14**, 218 (2020).
236. Brennan, P., Kaba, H. & Keverne, E. B. Olfactory recognition: a simple memory system. *Science (1979)* **250**, 1223–1226 (1990).
237. Roberts, S. A. *et al.* Darcin: a male pheromone that stimulates female memory and sexual attraction to an individual male’s odour. *BMC Biol* **8**, 1–21 (2010).
238. Wilson, E. O. Pheromones. *Sci Am* **208**, 100–115 (1963).
239. Stowers, L. & Marton, T. F. What is a pheromone? Mammalian pheromones reconsidered. *Neuron* **46**, 699–702 (2005).
240. Luo, M., Fee, M. S. & Katz, L. C. Encoding pheromonal signals in the accessory olfactory bulb of behaving mice. *Science (1979)* **299**, 1196–1201 (2003).
241. Liberles, S. D. Mammalian pheromones. *Annu Rev Physiol* **76**, 151–175 (2014).
242. Albone, E. S. Mammalian semiochemistry. *The investigation of chemical signals between mammals* 2–5 (1984).
243. Arakawa, H., Blanchard, D. C., Arakawa, K., Dunlap, C. & Blanchard, R. J. Scent marking behavior as an odorant communication in mice. *Neuroscience & Biobehavioral Reviews* **32**, 1236–1248 (2008).
244. Wyatt, T. D. *Pheromones and animal behavior: chemical signals and signatures*. (Cambridge University Press, 2014).
245. Hurst, J. L. The priming effects of urine substrate marks on interactions between male house mice, *Mus musculus domesticus* Schwarz & Schwarz. *Animal Behaviour* **45**, 55–81 (1993).
246. Hurst, J. L. & Beynon, R. J. Scent wars: the chemobiology of competitive signalling in mice. *Bioessays* **26**, 1288–1298 (2004).

247. Ferkin, M. H. The response of rodents to scent marks: four broad hypotheses. *Horm Behav* **68**, 43–52 (2015).
248. Ferkin, M. H. Scent marks of rodents can provide information to conspecifics. *Animal Cognition* **22**, 445–452 (2019).
249. Desjardins, C., Maruniak, J. A. & Bronson, F. H. Social rank in house mice: differentiation revealed by ultraviolet visualization of urinary marking patterns. *Science (1979)* **182**, 939–941 (1973).
250. Kimura, T. & Hagiwara, Y. Regulation of urine marking in male and female mice: effects of sex steroids. *Horm Behav* **19**, 64–70 (1985).
251. Ferkin, M. H. & Johnston, R. E. Meadow voles, *Microtus pennsylvanicus*, use multiple sources of scent for sex recognition. *Animal Behaviour* **49**, 37–44 (1995).
252. Whitten, W. K. Modification of the oestrous cycle of the mouse by external stimuli associated with the male. *Journal of Endocrinology* **13**, 399–404 (1956).
253. Whitten, M. K. Effect of exteroceptive factors on the oestrous cycle of mice. *Nature* **180**, 1436 (1957).
254. Whitten, W. K. Modification of the oestrous cycle of the mouse by external stimuli associated with the male. *Journal of Endocrinology* **17**, 307–313 (1958).
255. Lombardi, J. R. & Vandenberg, J. G. Pheromonally induced sexual maturation in females: regulation by the social environment of the male. *Science (1979)* **196**, 545–546 (1977).
256. Bruce, H. M. An exteroceptive block to pregnancy in the mouse. *Nature* **184**, 105 (1959).
257. Peele, P., Salazar, I., Mimmack, M., Keverne, E. B. & Brennan, P. A. Low molecular weight constituents of male mouse urine mediate the pregnancy block effect and convey information about the identity of the mating male. *European Journal of Neuroscience* **18**, 622–628 (2003).
258. Yamazaki, K. *et al.* Recognition of H-2 types in relation to the blocking of pregnancy in mice. *Science (1979)* **221**, 186–188 (1983).
259. Overath, P., Sturm, T. & Rammensee, H.-G. Of volatiles and peptides: in search for MHC-dependent olfactory signals in social communication. *Cellular and Molecular Life Sciences* **71**, 2429–2442 (2014).
260. Thom, M. D. & Hurst, J. L. Individual recognition by scent. in *Annales Zoologici Fennici* 765–787 (2004).
261. Roberts, S. A. *et al.* Individual odour signatures that mice learn are shaped by involatile major urinary proteins (MUPs). *BMC Biol* **16**, 1–19 (2018).
262. Hastie, N. D., Held, W. A. & Toole, J. J. Multiple genes coding for the androgen-regulated major urinary proteins of the mouse. *Cell* **17**, 449–457 (1979).
263. Schwende, F. J., Wiesler, D., Jorgenson, J. W., Carmack, M. & Novotny, M. Urinary volatile constituents of the house mouse, *Mus musculus*, and their endocrine dependency. *J Chem Ecol* **12**, 277–296 (1986).
264. Zhou, Y. & Rui, L. Major urinary protein regulation of chemical communication and nutrient metabolism. *Vitamins & Hormones* **83**, 151–163 (2010).
265. Johnson, D., Al-Shawi, R. & Bishop, J. O. Sexual dimorphism and growth hormone induction of murine pheromone-binding proteins. *J Mol Endocrinol* **14**, 21–34 (1995).
266. Ma, M. Encoding olfactory signals via multiple chemosensory systems. *Crit Rev Biochem Mol Biol* **42**, 463–480 (2007).

267. Meredith, M. & O'Connell, R. J. Efferent control of stimulus access to the hamster vomeronasal organ. *J Physiol* **286**, 301–316 (1979).
268. Meredith, M., Marques, D. M., O'Connell, R. J. & Stern, F. L. Vomeronasal pump: significance for male hamster sexual behavior. *Science (1979)* **207**, 1224–1226 (1980).
269. Meredith, M. Chronic recording of vomeronasal pump activation in awake behaving hamsters. *Physiology & behavior* **56**, 345–354 (1994).
270. Holy, T. E. The accessory olfactory system: innately specialized or microcosm of mammalian circuitry? *Annu Rev Neurosci* **41**, 501–525 (2018).
271. Dulac, C. & Torello, A. T. Molecular detection of pheromone signals in mammals: from genes to behaviour. *Nature Reviews Neuroscience* **4**, 551–562 (2003).
272. Dulac, C. & Axel, R. A novel family of genes encoding putative pheromone receptors in mammals. *Cell* **83**, 195–206 (1995).
273. Pantages, E. & Dulac, C. A novel family of candidate pheromone receptors in mammals. *Neuron* **28**, 835–845 (2000).
274. Boschat, C. *et al.* Pheromone detection mediated by a V1r vomeronasal receptor. *Nat Neurosci* **5**, 1261–1262 (2002).
275. Zhang, X., Marcucci, F. & Firestein, S. High-throughput microarray detection of vomeronasal receptor gene expression in rodents. *Frontiers in Neuroscience* **4**, 164 (2010).
276. Liberles, S. D. *et al.* Formyl peptide receptors are candidate chemosensory receptors in the vomeronasal organ. *Proceedings of the National Academy of Sciences* **106**, 9842–9847 (2009).
277. Riviere, S., Challet, L., Fluegge, D., Spehr, M. & Rodriguez, I. Formyl peptide receptor-like proteins are a novel family of vomeronasal chemosensors. *Nature* **459**, 574–577 (2009).
278. Asaba, A., Hattori, T., Mogi, K. & Kikusui, T. Sexual attractiveness of male chemicals and vocalizations in mice. *Front Neurosci* **8**, 231 (2014).
279. Jia, C. & Halpern, M. Subclasses of vomeronasal receptor neurons: differential expression of G proteins (G α 2 and G α) and segregated projections to the accessory olfactory bulb. *Brain Res* **719**, 117–128 (1996).
280. Isogai, Y. *et al.* Molecular organization of vomeronasal chemoreception. *Nature* **478**, 241–245 (2011).
281. Dulac, C. & Wagner, S. Genetic analysis of brain circuits underlying pheromone signaling. *Annu. Rev. Genet.* **40**, 449–467 (2006).
282. Lin, D. *et al.* Functional identification of an aggression locus in the mouse hypothalamus. *Nature* **470**, 221–226 (2011).
283. Yang, C. F. *et al.* Sexually dimorphic neurons in the ventromedial hypothalamus govern mating in both sexes and aggression in males. *Cell* **153**, 896–909 (2013).
284. Lee, H. *et al.* Scalable control of mounting and attack by Esr1+ neurons in the ventromedial hypothalamus. *Nature* **509**, 627–632 (2014).
285. Haga, S. *et al.* The male mouse pheromone ESP1 enhances female sexual receptive behaviour through a specific vomeronasal receptor. *Nature* **466**, 118–122 (2010).
286. Ishii, K. K. *et al.* A labeled-line neural circuit for pheromone-mediated sexual behaviors in mice. *Neuron* **95**, 123–137 (2017).
287. Ma, M. Multiple olfactory subsystems convey various sensory signals. *The neurobiology of olfaction* 225–240 (2010).

288. Bepari, A. K., Watanabe, K., Yamaguchi, M., Tamamaki, N. & Takebayashi, H. Visualization of odor-induced neuronal activity by immediate early gene expression. *BMC Neurosci* **13**, 1–17 (2012).
289. Lin, D. Y., Zhang, S.-Z., Block, E. & Katz, L. C. Encoding social signals in the mouse main olfactory bulb. *Nature* **434**, 470–477 (2005).
290. Yoon, H., Enquist, L. W. & Dulac, C. Olfactory inputs to hypothalamic neurons controlling reproduction and fertility. *Cell* **123**, 669–682 (2005).
291. Kang, N., Baum, M. J. & Cherry, J. A. A direct main olfactory bulb projection to the ‘vomeronasal’ amygdala in female mice selectively responds to volatile pheromones from males. *European Journal of Neuroscience* **29**, 624–634 (2009).
292. Matsuo, T. *et al.* Genetic dissection of pheromone processing reveals main olfactory system-mediated social behaviors in mice. *Proceedings of the National Academy of Sciences* **112**, E311–E320 (2015).
293. Danchin, E., Giraldeau, L.-A., Valone, T. J. & Wagner, R. H. Public information: from nosy neighbors to cultural evolution. *Science (1979)* **305**, 487–491 (2004).
294. Edward, D. A. The description of mate choice. *Behavioral Ecology* **26**, 301–310 (2015).
295. Seyfarth, R. M. & Cheney, D. L. Social cognition. *Animal Behaviour* **103**, 191–202 (2015).
296. Ferkin, M. H. Odor communication and mate choice in rodents. *Biology (Basel)* **7**, 13 (2018).
297. Beach, F. A. Analysis of the stimuli adequate to elicit mating behavior in the sexually inexperienced rat. *Journal of Comparative Psychology* **33**, 163 (1942).
298. Chung, M., Wang, M.-Y., Huang, Z. & Okuyama, T. Diverse sensory cues for individual recognition. *Development, Growth & Differentiation* **62**, 507–515 (2020).
299. Maggio, J. C., Maggio, J. H. & Whitney, G. Experience-based vocalization of male mice to female chemosignals. *Physiology & behavior* **31**, 269–272 (1983).
300. Premoli, M., Memo, M. & Bonini, S. A. Ultrasonic vocalizations in mice: relevance for ethologic and neurodevelopmental disorders studies. *Neural Regeneration Research* **16**, 1158 (2021).
301. Kavaliers, M., Choleris, E., Ågmo, A. & Pfaff, D. W. Olfactory-mediated parasite recognition and avoidance: linking genes to behavior. *Hormones and Behavior* **46**, 272–283 (2004).
302. Arakawa, H., Arakawa, K. & Deak, T. Oxytocin and vasopressin in the medial amygdala differentially modulate approach and avoidance behavior toward illness-related social odor. *Neuroscience* **171**, 1141–1151 (2010).
303. Beltran-Bech, S. & Richard, F.-J. Impact of infection on mate choice. *Animal Behaviour* **90**, 159–170 (2014).
304. Valzelli, L. The “isolation syndrome” in mice. *Psychopharmacologia* **31**, 305–320 (1973).
305. Beery, A. K. & Kaufer, D. Stress, social behavior, and resilience: insights from rodents. *Neurobiol Stress* **1**, 116–127 (2015).
306. Haller, J., Fuchs, E., Halasz, J. & Makara, G. B. Defeat is a major stressor in males while social instability is stressful mainly in females: towards the development of a social stress model in female rats. *Brain Res Bull* **50**, 33–39 (1999).
307. Herzog, C. J. *et al.* Chronic social instability stress in female rats: a potential animal model for female depression. *Neuroscience* **159**, 982–992 (2009).

308. Dugatkin, L. A. Sexual selection and imitation: females copy the mate choice of others. *The American Naturalist* **139**, 1384–1389 (1992).
309. Kavaliers, M. *et al.* Inadvertent social information and the avoidance of parasitized male mice: a role for oxytocin. *Proceedings of the National Academy of Sciences* **103**, 4293–4298 (2006).
310. Kavaliers, M., Matta, R. & Choleris, E. Mate-choice copying, social information processing, and the roles of oxytocin. *Neuroscience & Biobehavioral Reviews* **72**, 232–242 (2017).
311. Goodson, J. L. Deconstructing sociality, social evolution and relevant nonapeptide functions. *Psychoneuroendocrinology* **38**, 465–478 (2013).
312. Choleris, E. *et al.* An estrogen-dependent four-gene micronet regulating social recognition: a study with oxytocin and estrogen receptor- α and- β knockout mice. *Proceedings of the National Academy of Sciences* **100**, 6192–6197 (2003).
313. Welker, W. I. Analysis of sniffing of the albino rat 1. *Behaviour* **22**, 223–244 (1964).
314. Wesson, D. W., Donahou, T. N., Johnson, M. O. & Wachowiak, M. Sniffing behavior of mice during performance in odor-guided tasks. *Chem Senses* **33**, 581–596 (2008).
315. Khan, A. G., Sarangi, M. & Bhalla, U. S. Rats track odour trails accurately using a multi-layered strategy with near-optimal sampling. *Nat Commun* **3**, 1–10 (2012).
316. Ranade, S., Hangya, B. & Kepecs, A. Multiple modes of phase locking between sniffing and whisking during active exploration. *Journal of Neuroscience* **33**, 8250–8256 (2013).
317. Calvert, G. A. & Thesen, T. Multisensory integration: methodological approaches and emerging principles in the human brain. *Journal of Physiology-Paris* **98**, 191–205 (2004).
318. Carandini, M. & Churchland, A. K. Probing perceptual decisions in rodents. *Nat Neurosci* **16**, 824–831 (2013).
319. Meredith, M. A., Nemitz, J. W. & Stein, B. E. Determinants of multisensory integration in superior colliculus neurons. I. Temporal factors. *Journal of Neuroscience* **7**, 3215–3229 (1987).
320. Burr, D., Silva, O., Cicchini, G. M., Banks, M. S. & Morrone, M. C. Temporal mechanisms of multimodal binding. *Proceedings of the Royal Society B: Biological Sciences* **276**, 1761–1769 (2009).
321. Wallace, M. T. & Stevenson, R. A. The construct of the multisensory temporal binding window and its dysregulation in developmental disabilities. *Neuropsychologia* **64**, 105–123 (2014).
322. Siemann, J. K. *et al.* A novel behavioral paradigm to assess multisensory processing in mice. *Front Behav Neurosci* **8**, 456 (2015).
323. Raposo, D., Sheppard, J. P., Schrater, P. R. & Churchland, A. K. Multisensory decision-making in rats and humans. *Journal of neuroscience* **32**, 3726–3735 (2012).
324. Sheppard, J. P., Raposo, D. & Churchland, A. K. Dynamic weighting of multisensory stimuli shapes decision-making in rats and humans. *J Vis* **13**, 4 (2013).
325. Ghazanfar, A. A. & Schroeder, C. E. Is neocortex essentially multisensory? *Trends Cogn Sci* **10**, 278–285 (2006).
326. Holmes, N. P. & Spence, C. Multisensory integration: space, time and superadditivity. *Current Biology* **15**, R762–R764 (2005).

327. Wang, D. *et al.* Neurons in the barrel cortex turn into processing whisker and odor signals: a cellular mechanism for the storage and retrieval of associative signals. *Frontiers in Cellular Neuroscience* **9**, 320 (2015).
328. Lei, Z. *et al.* Synapse innervation and associative memory cell are recruited for integrative storage of whisker and odor signals in the barrel cortex through miRNA-mediated processes. *Front Cell Neurosci* **11**, 316 (2017).
329. O'Connor, D. H., Peron, S. P., Huber, D. & Svoboda, K. Neural activity in barrel cortex underlying vibrissa-based object localization in mice. *Neuron* **67**, 1048–1061 (2010).
330. Quak, M., London, R. E. & Talsma, D. A multisensory perspective of working memory. *Front Hum Neurosci* **9**, 197 (2015).
331. Boisselier, L., Ferry, B. & Gervais, R. Involvement of the lateral entorhinal cortex for the formation of cross-modal olfactory-tactile associations in the rat. *Hippocampus* **24**, 877–891 (2014).
332. Matthies, H. In search of cellular mechanisms of memory. *Prog Neurobiol* **32**, 277–349 (1989).
333. Sheng, M. & Greenberg, M. E. The regulation and function of c-fos and other immediate early genes in the nervous system. *Neuron* **4**, 477–485 (1990).
334. Robertson, H. A. Immediate-early genes, neuronal plasticity, and memory. *Biochemistry and Cell Biology* **70**, 729–737 (1992).
335. Tischmeyer, W. & Grimm, R. Activation of immediate early genes and memory formation. *Cellular and Molecular Life Sciences CMLS* **55**, 564–574 (1999).
336. Freeman, F. M., Rose, S. P. R. & Scholey, A. B. Two time windows of anisomycin-induced amnesia for passive avoidance training in the day-old chick. *Neurobiol Learn Mem* **63**, 291–295 (1995).
337. Nikolaev, E., Kaminska, B., Tischmeyer, W., Matthies, H. & Kaczmarek, L. Induction of expression of genes encoding transcription factors in the rat brain elicited by behavioral training. *Brain Res Bull* **28**, 479–484 (1992).
338. Chiu, R. *et al.* The c-fos protein interacts with c-JunAP-1 to stimulate transcription of AP-1 responsive genes. *Cell* **54**, 541–552 (1988).
339. Heurteaux, C., Messier, C., Destrade, C. & Lazdunski, M. Memory processing and apamin induce immediate early gene expression in mouse brain. *Molecular Brain Research* **18**, 17–22 (1993).
340. Herrera, D. G. & Robertson, H. A. Activation of c-fos in the brain. *Prog Neurobiol* **50**, 83–107 (1996).
341. Xie, H. *et al.* In vivo imaging of immediate early gene expression reveals layer-specific memory traces in the mammalian brain. *Proceedings of the National Academy of Sciences* **111**, 2788–2793 (2014).
342. Meenakshi, P., Kumar, S. & Balaji, J. In vivo imaging of immediate early gene expression dynamics segregates neuronal ensemble of memories of dual events. *Mol Brain* **14**, 1–19 (2021).
343. Matchynski, J. I. *et al.* Direct measurement of neuronal ensemble activity using photoacoustic imaging in the stimulated Fos-LacZ transgenic rat brain: a proof-of-principle study. *Photoacoustics* **24**, 100297 (2021).
344. Gonzales, B. J., Mukherjee, D., Ashwal-Fluss, R., Loewenstein, Y. & Citri, A. Subregion-specific rules govern the distribution of neuronal immediate-early gene induction. *Proceedings of the National Academy of Sciences* **117**, 23304–23310 (2020).

345. Guzowski, J. F., Setlow, B., Wagner, E. K. & McGaugh, J. L. Experience-dependent gene expression in the rat hippocampus after spatial learning: a comparison of the immediate-early genes Arc, c-fos, and zif268. *Journal of Neuroscience* **21**, 5089–5098 (2001).
346. Steward, O., Wallace, C. S., Lyford, G. L. & Worley, P. F. Synaptic activation causes the mRNA for the IEG Arc to localize selectively near activated postsynaptic sites on dendrites. *Neuron* **21**, 741–751 (1998).
347. Rao-Ruiz, P. *et al.* Engram-specific transcriptome profiling of contextual memory consolidation. *Nat Commun* **10**, 1–14 (2019).
348. Plath, N. *et al.* Arc/Arg3.1 is essential for the consolidation of synaptic plasticity and memories. *Neuron* **52**, 437–444 (2006).
349. Bramham, C. R. *et al.* The Arc of synaptic memory. *Exp Brain Res* **200**, 125–140 (2010).
350. Shepherd, J. D. *et al.* Arc/Arg3.1 mediates homeostatic synaptic scaling of AMPA receptors. *Neuron* **52**, 475–484 (2006).
351. Bhattacharjee, A. S. *et al.* Similarity and strength of glomerular odor representations define a neural metric of sniff-invariant discrimination time. *Cell Rep* **28**, 2966–2978 (2019).
352. Gratzner, H. G. Monoclonal antibody to 5-bromo- and 5-iododeoxyuridine: a new reagent for detection of DNA replication. *Science* (1979) **218**, 474–475 (1982).
353. Wojtowicz, J. M. & Kee, N. BrdU assay for neurogenesis in rodents. *Nat Protoc* **1**, 1399–1405 (2006).
354. Schindelin, J. *et al.* Fiji: an open-source platform for biological-image analysis. *Nat Methods* **9**, 676–682 (2012).
355. Baum, M. J. Contribution of pheromones processed by the main olfactory system to mate recognition in female mammals. *Front Neuroanat* **6**, 20 (2012).
356. Gener, T., Reig, R. & Sanchez-Vives, M. v. A new paradigm for the reversible blockage of whisker sensory transmission. *Journal of Neuroscience Methods* **176**, 63–67 (2009).
357. Montag-Sallaz, M. & Montag, D. Learning-induced arg 3.1/arc mRNA expression in the mouse brain. *Learning & Memory* **10**, 99–107 (2003).
358. Roberts, S. A., Davidson, A. J., McLean, L., Beynon, R. J. & Hurst, J. L. Pheromonal induction of spatial learning in mice. *science* **338**, 1462–1465 (2012).
359. Brennan, P. A. & Zufall, F. Pheromonal communication in vertebrates. *Nature* **444**, 308–315 (2006).
360. Hurst, J. L. The functions of urine marking in a free-living population of house mice, *Mus domesticus* Ruddy. *Animal Behaviour* **35**, 1433–1442 (1987).
361. Karlson, P. & Lüscher, M. ‘Pheromones’: a new term for a class of biologically active substances. *Nature* **183**, 55–56 (1959).
362. Demir, E. *et al.* The pheromone darcin drives a circuit for innate and reinforced behaviours. *Nature* **578**, 137–141 (2020).
363. Findley, T. M. *et al.* Sniff-synchronized, gradient-guided olfactory search by freely moving mice. *Elife* **10**, e58523 (2021).
364. Reddy, G., Murthy, V. N. & Vergassola, M. Olfactory sensing and navigation in turbulent environments. *Annual Review of Condensed Matter Physics* **13**, (2022).
365. Reddy, G., Shraiman, B. I. & Vergassola, M. Sector search strategies for odor trail tracking. *Proceedings of the National Academy of Sciences* **119**, (2022).

366. Jayakumar, S. & Murthy, V. N. A new angle on odor trail tracking. *Proceedings of the National Academy of Sciences* **119**, (2022).
367. Rigolli, N., Reddy, G., Seminara, A. & Vergassola, M. Alternation emerges as a multi-modal strategy for turbulent odor navigation. *bioRxiv* (2021).
368. Moore, J. D. *et al.* Hierarchy of orofacial rhythms revealed through whisking and breathing. *Nature* **497**, 205–210 (2013).
369. Garcia, J. & Koelling, R. A. Relation of cue to consequence in avoidance learning. *Psychon Sci* **4**, 123–124 (1966).
370. Kim, J., Erskine, A., Cheung, J. A. & Hires, S. A. Behavioral and neural bases of tactile shape discrimination learning in head-fixed mice. *Neuron* **108**, 953–967 (2020).
371. Wolfe, J. *et al.* Texture coding in the rat whisker system: slip-stick versus differential resonance. *PLoS Biol* **6**, e215 (2008).
372. Severson, K. S. & O'Connor, D. H. Active sensing: The rat's nose dances in step with whiskers, head, and breath. *Current Biology* **27**, R183–R185 (2017).
373. Kurnikova, A., Moore, J. D., Liao, S.-M., Deschênes, M. & Kleinfeld, D. Coordination of orofacial motor actions into exploratory behavior by rat. *Current Biology* **27**, 688–696 (2017).
374. Gao, M. *et al.* A specific requirement of Arc/Arg3.1 for visual experience-induced homeostatic synaptic plasticity in mouse primary visual cortex. *Journal of Neuroscience* **30**, 7168–7178 (2010).
375. Guthrie, K., Rayhanabad, J., Kuhl, D. & Gall, C. Odors regulate Arc expression in neuronal ensembles engaged in odor processing. *Neuroreport* **11**, 1809–1813 (2000).
376. Alonso, M. *et al.* Olfactory discrimination learning increases the survival of adult-born neurons in the olfactory bulb. *Journal of Neuroscience* **26**, 10508–10513 (2006).
377. Lledo, P.-M., Alonso, M. & Grubb, M. S. Adult neurogenesis and functional plasticity in neuronal circuits. *Nature Reviews Neuroscience* **7**, 179–193 (2006).
378. Brennan, P. A. & Keverne, E. B. Something in the air? New insights into mammalian pheromones. *Current biology* **14**, R81–R89 (2004).
379. Khodadad, A., Adelson, P. D., Lifshitz, J. & Thomas, T. C. The time course of activity-regulated cytoskeletal (ARC) gene and protein expression in the whisker-barrel circuit using two paradigms of whisker stimulation. *Behavioural brain research* **284**, 249–256 (2015).
380. Bellistri, E., Aguilar, J., Brotons-Mas, J. R., Foffani, G. & la Prida, L. M. Basic properties of somatosensory-evoked responses in the dorsal hippocampus of the rat. *The Journal of Physiology* **591**, 2667–2686 (2013).
381. Pereira, A. *et al.* Processing of tactile information by the hippocampus. *Proceedings of the National Academy of Sciences* **104**, 18286–18291 (2007).
382. Hainmueller, T. & Bartos, M. Dentate gyrus circuits for encoding, retrieval and discrimination of episodic memories. *Nature Reviews Neuroscience* **21**, 153–168 (2020).
383. Zong, W. *et al.* Large-scale two-photon calcium imaging in freely moving mice. *bioRxiv* (2021).
384. Ferris, C. F. *et al.* Distinct BOLD activation profiles following central and peripheral oxytocin administration in awake rats. *Front Behav Neurosci* **9**, 245 (2015).
385. Mitre, M. *et al.* A distributed network for social cognition enriched for oxytocin receptors. *Journal of Neuroscience* **36**, 2517–2535 (2016).

386. Oettl, L.-L. *et al.* Oxytocin enhances social recognition by modulating cortical control of early olfactory processing. *Neuron* **90**, 609–621 (2016).
387. Choe, H. K. *et al.* Oxytocin mediates entrainment of sensory stimuli to social cues of opposing valence. *Neuron* **87**, 152–163 (2015).
388. Ye, B. *et al.* The functional upregulation of piriform cortex is associated with cross-modal plasticity in loss of whisker tactile inputs. (2012).